The University Of Sheffield.

Characterising and Improving the Switchable Adhesion between Two Oppositely Charged Polyelectrolytes

By

Latifah Hamad Alfhaid

A thesis submitted for the degree of Doctor of Philosophy
Department of Physics and Astronomy

March 2016

Contents

Abstract vi

Acknowledgements viii

Presented Works and Publications ix

Nomenclature x

List of Figures xi

List of Tables xxi

I Introduction and Background 1

1 Introduction 2
1.1 Introduction to Adhesion Science . . . 2
1.2 Introduction to Switchable Adhesion . . . 3
1.2.1 A Synthetic Switchable Adhesive System . . . 5
1.2.2 Scope of this Study . . . 22

2 Adhesion Theories 24
2.1 Introduction . . . 24
2.2 Contact Mechanisms and Adhesion Theories . . . 25
2.2.1 Role of the Interface and Surface Energy . . . 25
2.2.2 Hertz Theory . . . 27
2.2.3 JKR Theory . . . 28
2.2.4 DMT Theory . . . 30
2.3 Stress Distribution . . . 31

3 Polyelectrolytes: Polymer Brushes and Hydrogels 34
3.1 Introduction . . . 34
3.1.1 The Conformation of a Polyelectrolyte Chain in Solution . . . 35
3.1.2 The Debye-Hückel Theory of Charge Screening . . . 35
3.1.3 Osmotic Pressure . . . 36
3.1.4 Charged Polyelectrolytes . . . 38
3.1.4.1 Strong Polyelectrolytes . . . 38

3.1.4.2 Weak Polyelectrolytes . . . 38
3.1.4.3 Acids and Bases . . . 39
3.1.4.4 Strong and Weak Acids or Bases . . . 40
3.1.5 Stimuli-Responsive Polyelectrolytes . . . 42
3.2 Polyelectrolyte Brushes . . . 43
3.2.1 General Features of Polymer Brushes . . . 43
3.2.2 Strong Polyelectrolyte Brushes . . . 45
3.2.3 Weak Polyelectrolyte Brushes . . . 46
3.2.4 Polymer Brush Synthesis . . . 49
3.2.4.1 Physisorption . . . 49
3.2.4.2 Chemisorption . . . 50
3.2.4.2.1 '*Grafting-From*' . . . 50
3.2.4.2.2 '*Grafting-To*' . . . 51
3.2.4.3 Synthesis of Polymer Brush Via SI-ATRP . . . 51
3.3 Polyelectrolyte Hydrogels . . . 54
3.3.1 Physical Gels (Reversible) . . . 55
3.3.2 Chemical Gels (Irreversible) . . . 56
3.3.3 Swelling Behaviour of Polyelectrolyte Networks . . . 56
3.3.4 Free Radical Polymerisation . . . 59
3.3.5 Classification of Hydrogels . . . 60
3.3.5.1 Soft Hydrogels . . . 61
3.3.5.2 Tough Hydrogels . . . 61
3.3.5.2.1 Topological Hydrogels . . . 62
3.3.5.2.2 Nano-Composite Hydrogels . . . 63
3.3.5.2.3 Double-Network Hydrogels . . . 64

II Experimental **68**

4 Experimental Methods **69**
4.1 Introduction . . . 69
4.2 Sample Preparation . . . 70
4.2.1 Single-Network Hydrogel Synthesis . . . 70
4.2.1.1 Synthesis of the Poly(Methacrylic Acid) Hydrogel . . . 70
4.2.1.2 Synthesis of the Poly [2-(Diethyl Amino)Ethyl Methacrylate] Hydrogel . . . 72
4.2.2 Double-Network Hydrogel Synthesis . . . 73
4.2.2.1 Poly[Oligo(Ethylene Glycol)Methyl Ether Methacrylate]–Poly (Methacrylic Acid) Hydrogel . . . 75
4.2.2.2 Poly(Methacrylic Acid)–Poly[Oligo(Ethylene Glycol)Methyl Ether Methacrylate] Hydrogel . . . 76
4.2.3 Polymer Brush Synthesis . . . 78
4.2.3.1 The Initiator Deposition on a Silicon Substrate . . . 79
4.2.3.1.1 Preparation of Self-Assembled Monolayer . . . 79
4.2.3.1.2 Preparation of Initiator Functionalised Surfaces . . . 80

4.2.3.2 Synthesis of the Poly(Methacrylic Acid) Brush 80
4.2.3.3 Synthesis of the Poly[2-(Diethyl Amino)Ethyl Methacrylate] Brush 83
4.3 Experimental Techniques 84
4.3.1 Spectroscopic Ellipsometry 85
4.3.2 Contact Angle Measurements 86
4.4 Switchable Adhesion Experiments 87

5 Polymer Brush Adhesion With A Single–Network Hydrogel 89
5.1 Introduction 90
5.2 pH Behaviour of Hydrogels and Brushes 92
5.2.1 Swelling Behaviours of Polyelectrolyte Brushes 92
5.2.2 Swelling Ratios of Hydrogels 94
5.2.3 Elastic Modulus of Single-Network Hydrogels 97
5.2.3.1 Elastic Moduli of PDEAEMA Hydrogels 98
5.2.3.2 Elastic Moduli of PMAA Hydrogels 99
5.3 Adhesion Measurements of Single-Network Hydrogels 102
5.3.1 Adhesion of Polyacid and Polybase Hydrogels 102
5.3.2 Effect of Hydrogel's Crosslinking Concentration on Adhesion 106
5.3.3 Effect of Brush Thickness on Adhesion 108
5.3.4 The Effect of Other Parameters on the Hydrogel-Brush Adhesion . . . 109
5.3.4.1 Equilibrium Effect on the Interfacial Adhesion 109
5.3.4.2 Effect of Debonding Speed on the Intefacial Adhesion 111
5.3.4.3 Applied Force Effect on the Interfacial Adhesion 113
5.4 The Thermodynamic Work of Adhesion 115
5.5 Conclusion 117

6 Switchable and Repeatable Adhesion of A Double–Network Hydrogel 119
6.1 Introduction 120
6.2 Adhesion of Single-Network and Double-Network Hydrogels 123
6.3 The Effect of the Second Network's Monomer Concentration on the Adhesion of Double-Network Hydrogels 127
6.3.1 Adhesion of POEGMA–PMAA Hydrogels 129
6.3.2 Adhesion of PMAA–POEGMA Hydrogels 131
6.4 The Effect of the Crosslinker Concentraion of the First Network on the Adhesion of Double-Network Hydrogels 133
6.5 The Repeatable Adhesion of Double-Network Hydrogel 138
6.6 The Thermodynamic Work of Adhesion 143
6.7 The Elastic Modulus of Double-Network Hydrogel 146
6.8 The Swelling Ratio of Hydrogels 148
6.9 Laser Scanning Confocal Microscopy 149
6.10 Adhesion Switchability at the Gel-Brush Interface 151
6.11 Conclusion 159

7 Switchable Adhesion in Salt Solutions **161**
7.1 Introduction 161
7.2 The Effect of Salt Solutions on Switchable Adhesion 163
7.2.1 Swelling Ratios of Hydrogels in Salt Solutions 163
7.2.2 Switchable Adhesion Inside Salt Solutions 165
7.3 Comparing the Effect of Salt and pH Solutions on Switchable Adhesion 171
7.4 Conclusion 173

8 Summary and Future Work **175**
8.1 Summary 175
8.2 Future Work 178

References **180**

Abstract

This study develops and evaluates switchable adhesion between two oppositely charged polyelectrolytes: a hydrogel and a grafted polymer brush layer. A mechanical tester, called a Stable Micro Systems TA.XT Plus, is used to perform adhesion experiments underwater and to measure the adhesion at the hydrogel-brush interface as a function of pH. Force-distance curves of adhesion tests serve to give a better understanding of the switchable adhesion at the hydrogel-brush interface when it is stimulated by varying the pH value of the surrounding water.

This work confirms that the adhesion at the hydrogel-brush interface is tuned and strongly increased inside deionised water at pH $\sim$ 6, but becomes less strong at pH values above 8 and below 3. The adhesion becomes very weak at the hydrogel-brush interface at a strong acidic or basic pH value (pH $\sim$ 1 or 12) as a result of the polymer chains collapsing due to the neutralisation of the electrostatic charges of anionic (at pH 1) or the cationic (at pH 12) polyelectrolytes.

Two types of hydrogels are used: 1) a single-network (SN) hydrogel, which consists of a single polymeric network, and 2) a double-network (DN) hydrogel, which consists of two polymeric networks. The difference between the SN and DN hydrogels is that the DN hydrogel has a much stronger mechanical strength than the SN hydrogel (i.e. the elastic modulus of the DN hydrogel is 1.0 MPa that is five times higher than that of the SN hydrogel). Both of the SN and DN hydrogels have a high water content of 90 wt%, however, and both are pH-stimuli responsive materials.

This study finds that the strength of underwater adhesion between the polyacid hydrogel and polybase brush is increased five-fold at pH $\sim$ 6 when using the DN hydrogel, compared to the adhesion of the SN hydrogel. The significant contribution of the adhesion of the DN hydrogel is that it can be repeated up to four times inside water at pH $\sim$ 6 (attaching to and detaching from the same location on the brush surface), without changing the pH value. This is due to the adhesive failure of the DN hydrogel, which always occurs at the DN hydrogel-brush interface, when it is detached from the brush surface. The adhesion of the SN hydrogel, in contrast, always ends with a cohesive failure due to the softness of this gel when it is fully swollen inside water. Furthermore, the '*on–off*' cycle of the switchable adhesion at the (SN and DN) hydrogel-brush interface is successfully achieved by oscillating the pH value between pH $\sim$ 6 and pH $\sim$ 1. After seven cycles of switching the adhesion at the hydrogel-brush interface *on* and *off*, both the SN and DN hydrogels are still able to re-adhere strongly to the brush surface at pH $\sim$ 6 in the eighth cycle of the repeated adhesion.

Moreover, the adhesion at the hydrogel-brush interface is examined as a function of increasing the salt concentration inside the surrounding water (at a fixed pH value of water). Sodium chloride is used at different concentrations due to the fact that salt ions screen the electrostatic

charges of the weakly charged polyelectrolytes causing them to become neutral and collapse. The obtained results confirm that the adhesion at the (SN and DN) hydrogel-brush interface can be eliminated inside highly concentrated salt solutions above 1 M.

Acknowledgements

The work in this thesis would not have been possible without the support from many people. First and foremost I would like to express my sincere thanks to my supervisor, Prof. Mark Geoghegan, for his trust in me, support and encouragement over the last four years. Mark has provided me continuous encouragement and guidance during my PhD journey while giving me the freedom that allows me to work independently.

My thanks also go to all the people in the Department of Chemistry for helping me out. I would like to thank my second supervisor, Prof. Nicholas H. Williams, for his support and his valuable suggestions during our monthly meetings. I also would like thank William D Seddon, who is also doing a PhD project in 'the switchable adhesion' in the Department of Chemistry, for his help while working together in the lab. Prof. Graham Leggett is also acknowledged for kindly allowing me to use some facilities of his group's lab. I am very grateful and thankful to Dr Abdullah Alswieleh for his kind help and support during the lab work. Thank goes to Mr. Daniel Jackson in the Chemistry Glass Workshop for preparing the glassware that I needed.

My appreciation also goes to Dr Rita La Spina, who also did the switchable adhesion project in 2010, for her useful discussions and interesting conversations on Skype!

My colleagues in polymer physics groups are acknowledged too for their helps and supports: Dr Ana Lorena Morales-García, Dr Youmna Mouhamad, Dr Chris Clarkson, Dr Amy Hall, Dr Zhenyu (Jason) Zhang, Dr Andy Parnell, Alessandra Petroli, Tom Kennelly, Eleanor Dougherty, Fabio Pontecchiani and Lamiaa Alharbe. I would like to thank all people in the workshops in the Department of Physics and Astronomy for preparing the components of the experimental setup.

Thanks go to my sponsor, University of Hail, represented by the Saudi Arabian Cultural Bureau in London for funding me to complete my postgraduate studies in the UK.

Special thanks go to my beloved husband, Ziyad Alateeq, who has provided a huge amount of help, patience, encouragement and support during my PhD journey. I am also grateful and thankful for my lovely little sons; Tariq and Abdulaziz, who are the pride and joy of my life, for their patience and love.

Last, but not least, I would like to thank my family in Saudi; my parents, Hamad and Mona, and my sisters and brothers, for their love and support throughout this PhD journey.

Presented Works and Publications

Conferences

- Poster presentation, the One-Day-Away Department Meeting for postgraduate students on September 2012 in the Millennium Gallery, The Physics and Astronomy Department at Sheffield University.
- Poster presentation, the Physical Aspects of Polymer Science, Institute of Physics (IOP) conference, in Sheffield, 9–11 September 2013.
- Oral presentation, the Department Postgraduate Presentations on the 8$^{\text{th}}$ March 2014, The Physics and Astronomy Department at Sheffield University.
- Oral presentation, the American Physical Society Meeting (APS) in San Antonio in Texas in the USA, on the 4$^{\text{th}}$ March 2015.
- Poster presentation, the Structured Soft and Biological Matter, Durham University, on the 9$^{\text{th}}$ June 2015, Durham.
- Poster presentation, Physical Aspects of Polymer Science, Institute of Physics (IOP) conference, in Manchester, 8–10 September 2015.

Publications and Prize

- Double-network hydrogels improve pH-switchable adhesion. Paper submitted.
- Adhesion between oppositely-charged polyelectrolytes. Paper in preparation.
- Switchable adhesion between oppositely-charged polyelectrolytes in salt solutions. Paper in preparation.
- A poster prize winner for best poster, Royal Society of Chemistry (RSC), the Structured Soft and Biological at Durham University, on the 9$^{\text{th}}$ June 2015, Durham.

Nomenclature

k_{B}	Boltzmann constant
δ	Displacement
χ	Flory-Huggins interaction parameter
Π	Osmotic pressure
ν	Poisson's ratio of the surface
ε	Strain
σ	Stress
γ	Surface energy
λ	Transition parameter
$2a$	The contact diameter
A	The contact area
AFM	Atomic force microscope
ATRP	Atom transfer radical polymerization
DMT	Derjaguin, Muller, and Toporov adhesion model
f	Degree of dissociation of a charged polymer
F	Maximum adhesion force
G	Gibbs free energy
h	Brush thickness
N_{A}	Avogadro's constant, $= 6.02 \times 10^{23}\,\mathrm{mol}^{-1}$
JKR	Johnson, Kendall and Roberts model
K	Elastic modulus
L	The length of a polymeric chain
N	Number average degree of polymerization
M_{n}	Molecular number
M_{w}	Weight average molecular weight
P	The applied force

PDEAEMA	Poly[2-(diethyl amino)ethyl methacrylate]
PDMAEMA	Poly[2-(dimethyl amino)ethyl methacrylate]
PDMS	Poly(dimethylsiloxane)
PMAA	Poly(methacrylic acid)
POEGMA	Poly[oligo(ethylene glycol)methyl ether methacrylate]
RCA	Radio Corporation of America Cleaning Treatment
R	The radius of a hemispherical body
W_{adh}	Thermodynamic work of adhesion
W	Work done of adhesion

List of Figures

1.1 The fibrillar switchable adhesive surface of a thermoplastic elastomer, switching from adhesive to non-adhesive states and vice versa. Image adapted with permission of . Copyright (2007) John Wiley and Sons. 6

1.2 A schematic diagram of the contact between the hemispherical probe with (a) a large diameter pancake and (b) small diameter post. Image used with permission from . Copyright (2005) American Chemical Society. 8

1.3 The work of adhesion (W_{adh}) as a function of varying the post radius (r_{p}). Two differently spaced patterns were used: $L = 500$ μm (the maximum contact area images of which are shown on the top) and $L = 50$ μm (maximum contact area images shown on the bottom line). Image taken with permission from . Copyright (2005) American Chemical Society. 9

1.4 The synthetic design of wet/dry hybrid nanoadhesive. An array of holes in a PMMA thin film supported on silicon (PMMA/Si) was created by electron-beam lithography. This was followed by PDMS casting onto the PMMA/Si, resulting in gecko-mimetic nanopillars. Finally, the mussel-mimetic polymer was dip-coated onto the nanopillars. Image taken with permission from . Copyright (2007) Nature Publishing Group. 11

1.5 A comparison between the adhesion forces per pillar in air (black columns) and in water (red columns) for gecko and geckel adhesive structures. Image adapted from . Copyright (2007) Nature Publishing Group. 12

1.6 Underwater adhesion tests of the flat-flat contact between the hydrogel and the surface of the polymer brush. Image taken with permission from . Copyright (2012) Royal Society of Chemistry. 13

1.7 Energy of adhesion of a PAM hydrogel and a PDMA hydrogel with a PAA brush as a function of varying the pH value. Image adapted with permission of . Copyright (2012) Royal Society of Chemistry. 15
1.8 An illustrative diagram of the JKR experimental setup between a hemispherical hydrogel and the surface of the polymer brush underwater. The contact diameter ($2a$) was 0.93 mm after applying a load (P). Image taken with permission from . Copyright (2007) John Wiley and Sons. 16
1.9 The work of adhesion (G) as a function of the compressive stress (i.e. the pressure) (σ) for two different loads of 32 and 60 mN at three pH values. Image taken with permission from . Copyright (2007) John Wiley and Sons. . 16
1.10 A schematic diagram (on the top) shows the process of attaching and detaching the oppositely charged surfaces of polymer brushes. The substrates of the poly(SPMK) and poly(MTAC) brushes were bonded together after injecting 2 μL of DI water into their interface. The graph shows the lap shear adhesion strength of repeating the adhesion of the brush substrates after (a) testing it in air and (b) exfoliation in a 0.5 M aqueous NaCl solution. After detaching the adhered brush surfaces inside NaCl solutions, they were washed with water before bonding them again. Image adapted with permission of . Copyright (2011) Royal Society of Chemistry. 18
1.11 The brush-brush adhesion interactions when they were induced by adding a few drops of water (on the left-hand side) or interrupted by the salt ions of the NaCl solution (on the right-hand side). Image adapted with permission of . Copyright (2011) Royal Society of Chemistry. 19
1.12 The retention time (h) of the adhered poly(MAPS) brush substrates inside water as a function of different temperatures. Image taken with permission from . Copyright (2013) Royal Society of Chemistry. 20
1.13 (a) The lap shear adhesion strength of the rebonded PMAPS brushes in hot water at 333 K with subsequent repeated adhesions by immersing them in water again and then allowing them to dry for 3 h. (b) The lap shear adhesion strength of the PSPMK–PMTAC brushes after debonding them in a 0.5 M aqueous NaCl solution, which were added here to make an adhesion comparison with the adhesion of the PMAPS brush in (a). Image adapted with permission of . Copyright (2013) Royal Society of Chemistry. 21

2.1 A schematic diagram of a liquid drop (L) on a solid surface (S) for contact angle experiments. 26
2.2 The interfacial contact ($2a$) between two hemispherical bodies resulting from pressing them together by a compressive force ($P_{\perp}$). 27
2.3 A schematic diagram shows a comparison between the contact radius a_0 predicted by Hertz (the solid line) and a_1 predicted by JKR (the dotted line). The difference in the value of the contact radii, a_0 and a_1, is that a_1 is affected by the attractive force at the interface of the two elastic solids 29
2.4 A schematic diagram showing a comparison between the contact radius in different adhesion theories. Image adapted with permission from . Copyright (2013) John Wiley and Sons. 32

3.1 A schematic diagram of polymer chains anchored on a surface, the stretching conformation in (a) is called the 'mushroom conformation' and in (b) the 'brush conformation' . Where R is the gyration radius of the chains and d is the distance between adjacent anchor points. The chains take a mushroom conformation if $d > R$, while chains will stretch vertically, with a height h, and repel each other when $d < R$. 44
3.2 A schematic diagram of the physisorption approach of two block copolymers, which are represented by two different colours of chains. The red chains represent the adsorbed 'anchor' block to a substrate, while the blue chains represent the floating chains in a solvent that stretch away from the surface. 50
3.3 A representation of: (a) the '*grafting-from*' and (b) the '*grafting-to*' techniques. 51
3.4 Free radical polymerisation mechanism, where R means the radical, M is the monomer and P is the polymer. 59
3.5 A schematic diagram for the TP gel, where the figure-of-eight crosslinkers are trapping polymer chains. The figure was used with permission from . Copyright (2005) Elsevier. 62
3.6 The polyrotaxane (TP) gel in (a) as-prepared, (b) dried, and (c) fully swollen states. Taken from with permission. Copyright (2005) Elsevier. 63
3.7 A schematic diagram for the network structure of NC gels. Taken with permission from . Copyright (2005) Elsevier. 64

3.8 Photograph for (a) a single-network (SN) gel of the PAMPS and (b) a DN gel of the PAMPS-PAAm under a compression test. Taken from with permission. Copyright (2003) John Wiley and Sons. 65
3.9 Stress-strain curves for the PAMPS–PAAm (DN) hydrogel and the SN gels of the PAMPS and PAAm. Taken with permission from . Copyright (2003) John Wiley and Sons. 66

4.1 (a) The glass container used to prepare the hemispherical pieces of a hydrogel. (b) The removable mould inside the glass container used for making hemispherical pieces of hydrogel. 71
4.2 A hemispherical piece of a just-prepared PMAA hydrogel with a diameter of 4 mm. 72
4.3 The preparation process for a double-network (DN) gel. 74
4.4 A swollen POEGMA hydrogel (on the left-hand side) and a non-swollen (just-prepared) POEGMA hydrogel (on the right-hand side). 75
4.5 A swollen PMAA hydrogel (on the left-hand side) and a non-swollen (just-prepared) PMAA hydrogel (on the right-hand side). 77
4.6 Silicon surface functionalisation with silane initiator 80
4.7 An illustration of the sealed round-bottom flask used for preparing the polymer brush solution. 81
4.8 An illustrative diagram of the glass cell within which the polymerisation reaction for the polymer brush took place. 82
4.9 The synthesis of the PMAA brush. 82
4.10 The synthesis of the PDEAEMA brush. 84
4.11 Photograph of the Stable Micro Systems TA.XT Plus Texture Analyser (TA), (Sheffield University, UK). 87
4.12 A hydrogel attached to the TA's probe (a) before and (b) after bringing it in contact with the brush surface. 87
4.13 Raw data obtained from the adhesion test using the TA mechanical tester. (a) A force-distance curve and (b) a force-time curve for an adhesion test between the PMAA hydrogel and PDEAEMA brush underwater at pH 5.8 with an applied force (P) of 0.5 N and a contact time (t) of 2 min. 88

5.1 Ellipsometric characterisation of the PMAA and PDEAEMA brush thicknesses as a function of pH. 93
5.2 The swelling ratios of the polybase, PDEAEMA, gel (blue symbols) and polyacid, PMAA, gel (red symbols) as a function of the pH levels. 95
5.3 The behaviour of PMAA gel in response to the pH changes. At a low pH, the PMAA becomes uncharged and hydrophobic, while it becomes charged and hydrophilic at a high pH. 96
5.4 The behaviour of the PDEAEMA gel in the response to the pH changes. At a high pH, the PDEAEMA becomes uncharged and hydrophobic, while it becomes charged and hydrophilic at a low pH. 96
5.5 The elastic modulus of PDEAEMA gels at pH 5.8. 98
5.6 The elastic modulus of PMAA gels at pH 5.8. 99
5.7 The relationship between the elastic moduli of PDEAEMA and PMAA hydrogels with the %crosslinker concentration in their total solutions. 100
5.8 The elastic modulus of the (0.18 mol%)–PMAA gel at pH 1, 5.8 and 12. . . . 101
5.9 The maximum adhesion forces (F) and work done (W) for the adhesion tests of (i) (0.18 mol%)–PMAA gel adhering to the PDEAEMA brush and (ii) (3.9 mol%)–PDEAEMA gel adhering to the PMAA brush as a function of pH. The closed blue symbols indicate the values of the maximum adhesion force at the gel-brush interface. The open red symbols indicate the work done (calculated from the area under force-distance curves) to detach the gel from the brush surface. 102
5.10 Optical microscope images for the cohesive failures of: (a) the PDEAEMA gel on the PMAA brush surface and (b) the PMAA gel on the PDEAEMA brush surface inside DI water at pH 5.8. 104
5.11 The presence of the necking and stretching behaviours in the PMAA gel: image 1 (a), 2 (a) and 3 (a) and their absence in the PDEAEMA gel: image 1 (b), 2 (b) and 3 (b). A source of light was used with the PMAA gel to take images since it is transparent and has a similar reflective index to water. 105
5.12 The effect of the crosslinking density of the PMAA, polyacid, and the PDEAEMA, polybase, hydrogels on their adhesion force and work done as a function of pH. 107
5.13 An illustrative diagram showing the cohesive failure of a hemispherical hydrogel on a brush-coated surface inside DI water. 108

5.14 The adhesion force (blue symbols) and work done (red symbols) of the PMAA gel adhering to the PDEAEMA brush with different thicknesses as a function of pH. 109
5.15 The effect of equilibrium time on the adhesion force between the PMAA gel and PDEAEMA brush at different pH values. The open symbols show the results of the 2 min contact time and the filled symbols are for the 10 min contact time between the gel and the polymer brush underwater. 111
5.16 The effect of separation speed on the interfacial adhesion measurements of the PMAA gel adhering to the PDEAEMA brush. 112
5.17 The effect of the separation speed on the size of the occurred cohesive failures. 113
5.18 An illustrative diagram of the JKR setup adhesion experiment between a hemispherical hydrogel and the surface of the polymer brush underwater. The contact diameter ($2a$) was created after applying a load (P). Image taken with permission from . Copyright (2007) John Wiley and Sons. 114
5.19 The effect of applied force on the gel-brush adhesion underwater at pH 5.8. . 114
5.20 Variation of a^3 as a function of W_{adh} at pH 1 , 5.8 and 12. 116

6.1 Adhesion measurements of the (DN) hydrogels of the PMAA–POEGMA (red symbols) and POEGMA–PMAA (green symbols), and also the PMAA (SN) hydrogel (blue symbols) as a function of pH. 124
6.2 Optical microscope images for the PDEAEMA brush surfaces after being in contact with (a) the PMAA–POEGMA (DN) hydrogel, (b) POEGMA–PMAA (DN) hydrogel and (c) PMAA (SN) hydrogel at pH 5.8 in DI water. These images were taken using a 5× objective. 126
6.3 POEGMA–PMAA (DN) hydrogels are presented in the top row images: (i), (ii) and (iii), while PMAA–POEGMA (DN) hydrogels are presented in the bottom row images: (iv), (v) and (vi). 128
6.4 The adhesion force and work done for the three POEGMA–PMAA (DN) hydrogels that were made with different amounts of the MAA monomer in the second network. 130
6.5 The adhesion measurements of three PMAA–POEGMA (DN) hydrogels made with differing OEGMA concentrations in the solutions of their second network. 132

6.6 The effect of the molar ratio of the second network to the first network on the mechanical strength of a DN hydrogel. The numbers on the curve indicate the monomer concentration value in the solution of the second network. Figure reproduced with permission from . Copyright (2003) John Wiley and Sons. . 133
6.7 The adhesion force and work done of the PMAA–POEGMA-1 (DN) hydrogel, PMAA–POEGMA-2 (DN) hydrogel and PMAA (SN) hydrogel underwater at pH 5.8. 134
6.8 The detaching process of (a) the PMAA–POEGMA-1 (DN) hydrogel, (b) PMAA–POEGMA-2 (DN) hydrogel and (c) PMAA (SN) hydrogel from the PDEAEMA brush surface in DI water. The diameter of the black probe is 10 mm 135
6.9 Force-distance curves of adhesion tests of the PMAA (SN) hydrogel (red line), PMAA–POEGMA-1 (DN) hydrogel (blue line) and PMAA–POEGMA-2 (DN) hydrogel (black line) underwater at pH 5.8. 137
6.10 Strain-stress curves of the PMAA (SN) hydrogel (red line), PMAA–POEGMA-1 (DN) hydrogel (blue line) and PMAA–POEGMA-2 (DN) hydrogel (black line) underwater. 138
6.11 The adhesion repeatability test of the PMAA–POEGMA (DN) (red symbols) and PMAA (SN) (blue symbols) hydrogels underwater at pH $\sim$ 6. 139
6.12 Force-distance curves of the repeatable adhesion test for the PMAA–POEGMA (DN) hydrogel. 140
6.13 Force-distance curves of the non-repeatable adhesion of the PMAA (SN) hydrogel. 141
6.14 AFM images for the PDEAEMA brush surface (a) before and (b) after the initial adhesion test underwater at pH 5.8. Representative cross-sectional images (height profiles) of the PDEAMEA brush (c) before and (d) after the adhesion test, which were taken from the white line on each image. This data was analysed using Image SXM 198. 142
6.15 (a) A thin scratch was made on the PDEAEMA brush surface after running the initial adhesion measurement. (b) The corresponding cross-sectional scratch on the PDEAMEA brush. 143

6.16 The work of adhesion, W_{adh}, of the PMAA–POEGMA (DN) and PMAA (SN) gels vs. the change in the a^3_{JKR} as a function of pH using four different applied forces. The symbols in the red colour indicate the measurements at pH 1, the green colour symbols indicate the measurement in pH 5.8 and the blue colour symbols indicate the measurement in pH 12. 145
6.17 An image of a PMAA–POEGMA (DN) gel brought into contact by the TA mechanical probe and pressed against a silicon surface. 146
6.18 Variation of PR as a function of a^3 at pH 1, 5.8 and 12. The elastic modulus, K, was calculated from the gradient of linear fits to the data. 147
6.19 The effect of the pH value of the surrounding water on the swelling ratio of the PMAA (SN) (blue symbols), POEGMA (SN) (black symbols) and PMAA–POEGMA (DN) (red symbols) hydrogels. 148
6.20 A CLSM image of the PMAA (SN) hydrogel immersed in rhodamine B water-based solution. 150
6.21 A CLSM image of the PMAA–POEGMA (DN) hydrogel immersed in rhodamine B water-based solution. 150
6.22 An illustration of the experimental procedure for removing the adhesion at the hydrogel-brush interface by either decreasing the pH 5.8 to 1 or increasing it from pH 5.8 to 12. 152
6.23 Adhesion switchability of DN (red columns) and SN (blue columns) hydrogels at pH 1 and pH 12. The measurements at pH 5.8 show the actual initial adhesion at the gel-brush interface (without adding HCl (at pH 1) or NaOH (at pH 12)). The filled columns indicate the maximum adhesive force, while the dotted columns indicate the work done values. 153
6.24 The adhesion switchability of DN and SN hydrogels at pH 1 and 5.8 with an applied force of 0.1 N. Cycles 1 to 7 were conducted at pH 1, while cycles 1.5, 2.5, 3.5, 4.5, 5.5 and 6.5 were related to the reattaching process of the hydrogel to the brush surface inside DI water at pH $\sim$ 6. Cycle 8 was carried out by attaching the hydrogel to an uncoated silicon surface to confirm the absence of the adhesive interaction. In cycle 9, a final adhesion test was conducted between the hydrogels with the PDEAEMA brush surface in DI water at pH $\sim$ 6 (without changing the pH). 155

6.25 Force-distance curves of the adhesion measurements for both SN and DN gels in test cycles number 7 (at pH 1), 8 (with a blank silicon surface at pH 5.8) and 9 (with PDEAEMA brushes at pH 5.8). 156
6.26 Post-detachment images were recoded by a side-view camera for the changes in the contact diameter, $2a$, of the SN gel at pH 1 after cycle 1 (a), cycle 3 (b), cycle 5 (c), and cycle 7 (d) in Figure 6.24. While the unchanged contact diameter of the DN gel is showing in (e) after cycle 1 and (f) cycle 7. 158
6.27 The measured contact diameter of the SN (blue symbols) and DN (red symbols) gels after detachment cycles 1, 3, 5 and 7 at pH 1. 158

7.1 The swelling ratio (Q) of the PMAA (SN) hydrogel (blue symbols) and the PMAA–POEGMA (DN) hydrogel (red symbols) inside NaCl solutions of different concentrations between 0.001 M to $\sim$ 5 M. 164
7.2 The adhesion experiments for the PMAA (SN) hydrogel (blue symbols) and the PMAA–POEGMA (DN) hydrogel (red symbols) after adding the NaCl solution into their surrounding water at different concentrations. The filled symbols are related to the maximum adhesion forces while the crossed symbols refer to the work done, which were collected from force-distance curves. 167
7.3 The detaching process for the hydrogel-brush interfaces after adding the 5 M NaCl solution into their surrounding water: (a) PMAA (SN) hydrogel and (b) PMAA–POEGMA (DN) hydrogel. A cohesive failure was still obtained with the SN hydrogel, while an adhesive failure occurred with the DN hydrogel. The black dashed arrow indicates the diameter length of the mechanical probe of 10 mm. 170
7.4 Maximum adhesion force and work done measurements at interfaces between the SN (blue columns) and DN (red columns) hydrogels and the polybase brushes inside pH solutions (on the left-hand side) and inside NaCl solutions (on the right-hand side). The filled columns indicate the measurement of the maximum adhesive force, while the dotted columns indicate the work done. . 172

List of Tables

4.1 Chemicals used to make the PMAA hydrogel. 71
4.2 Chemicals used to make the PDEAEMA hydrogel. 72
4.3 Chemicals used to make the first POEGMA network of the POEGMA–PMAA (DN) hydrogel. 75
4.4 Chemicals used to make the second PMAA network of the POEGMA–PMAA (DN) hydrogel. 76
4.5 Chemicals used to make the first network PMAA network of the PMAA–POEGMA (DN) hydrogel. 77
4.6 Chemicals used to make the second POEGMA network of the PMAA–POEGMA (DN) hydrogel. 78
4.7 Chemicals used to make the solution of the PMAA brush. 81
4.8 Chemicals used to make the PDEAEMA solution. 83
4.9 Contact angle measurements for different surfaces. 86

5.1 The double-crosslinked (X2 CL), normal-crosslinked (X1 CL) and half-crosslinked (X0.5 CL) single-network gels of the PMAA and PDEAEMA are presented with their crosslinker% concentration in the total solution. 94
5.2 The elastic moduli of PDEAEMA hydrogels in DI water as a function of the crosslinking densities. 98
5.3 The elastic moduli of PMAA hydrogels in DI water as a function of the crosslinking densities. 99
5.4 The elastic moduli of the (0.18 mol%)–PMAA hydrogel as a function of pH. . 101

6.1 The POEGMA–PMAA and PMAA–POEGMA (DN) hydrogels and the amount of the monomer and its concentration in the total solutions for their second networks. 127

6.2 The used hydrogels and their crosslinker/monomer ratios 134
6.3 The elastic modulus of the DN and SN hydrogels as a function of pH. 147

Part I

Introduction and Background

Chapter 1

Introduction

1.1 Introduction to Adhesion Science

Adhesion is a word used to describe the process of adhering two surfaces together via strong bonds that resist separation [1]. The word 'adhesion' is derived from the Latin word *adhaerere*, which is used by Lucretius to describe the adhesion of iron to a magnet [2]. The term adhesive is therefore usually used to refer to a type of material that induces an adhesion phenomenon between two surfaces, such as glue, epoxy and cement [3]. Throughout history, humans have used adhesives for different purposes. For example, the ancient Egyptians used glues in veneering their treasures [4]. In the 19^{th} century, glues were made from mammalian collagen and from the starches and dextrins of plants, however these were replaced when synthetic chemical glues and adhesives were introduced in the 20^{th} century [5]. A wide variety of glues have been prepared and used in many different applications to create strong bonds between different surfaces and materials. For instance, a solvent based polyurethane is used in the attachment of soles to shoes, and book binding is achieved by the use of hot melted adhesives [6].

Adhesion science does not only consider adhesion in the sense of sticking two surfaces together, but also studies surface coating, sealants and printing inks. The adhesion mechanism is, therefore, classified as a multidisciplinary subject because it involves physics, surface chemistry, rheology, stress analysis and polymer physics and chemistry [1, 7]. The importance of under-

standing the adhesion mechanism is primarily associated with the fast growth of, and strong demand for, the use of adhesives in many types of manufacturing, such as packaging, furniture, footwear, tile flooring, bookbinding, and automotive and aircraft manufacture. Nowadays, adhesives are mainly made from polymers since they give a good adhesive strength [6] due to their strong mechanical properties. The intensive use of polymers as adhesives in manufacturing is also due to their low cost [7].

Many studies have described adhesion phenomena on the basis of two mechanisms, namely interatomic and intermolecular interactions between the atoms at the interface between two adhered surfaces [1,7]. The type of adhesion is also recognised by the type of the bonds at the interface between the adhered surfaces, whether they be physical, chemical and/or mechanical bonds. Physical bonds are weaker than chemical and mechanical bonds and exhibit various forms, including van der Waals forces, hydrogen bonds and dipole-dipole interactions. An example of a physical bond is when a water droplet is put between two glass slides, hydrogen bonds form at their interface allowing them to adhere to each other. Chemical bonds, in contrast, last for a longer time than physical bonds and their forms are metallic, ionic and covalent. An example of a chemical bond is when two gold surfaces stick to each other after a cohesion process, allowing them to create a new area of interface that eventually disappears due to the surface atoms becoming bonded. Mechanical bonds, meanwhile, are considered to be a strong interlocking mechanism between surfaces, such as the Velcro closure of some dental materials that are mechanically interlocked to some extent. Adhesion science and research are now focusing on understanding the formation of the adhesive interface between surfaces by characterising the interface before the adhesion and after adhesion failure in order to detect its capabilities in a range of potential applications [1,6,8].

1.2 Introduction to Switchable Adhesion

The switchable adhesion has inspired much research into the development of an artificial switchable adhesive structure, since this kind of controllable adhesion is efficient for some potential applications [7,9]. This is due to the fact that dismantling and re-assembling adhered surfaces or structures would remove the obstacles to recycling many modern-day products and thus promote sustainability and waste minimisation; and consequently protect the environ-

ment [10]. For example, '*smart*' switchable adhesion technology is promising for 'End-of-Life' recycling scheme initiatives and the EU end-of-life Vehicles Directive (2000/53/EC), which demands that 85% of car parts by weight should be recycled [11]. Also, a four-year Cooperation in Science and Technology programme called 'Biological Adhesive: From Biology To Biomimetics' was co-ordinated between 16 countries in Europe aiming to analyse the natural adhesion system and to determine its main molecular and structural components in order to synthesise a biomimetic adhesive structure for specific applications. For instance, smart dry adhesives will contribute to produce climbing robots that can create a temporary controlled adhesion with surfaces. While smart wet adhesives will contribute to improved recycling and disassembly in the packaging and automotive industries, and has also been proposed for several medical applications, such as wound care and dressing tapes. In addition, most of the adhesives that are being used nowadays to bond surfaces together are irreversible, such as the glue that is used to adhere carpet tiles to the floor. Some 70 million kg of carpet tile waste is sent to landfill in Europe every year [12, 13] and, as a consequence, these adhesives represent an obstacle to the recycling process since the adhered surfaces resist separation. Hence, the developments of reversible adhesives or glues will be a step towards recyclable and environmentally friendly real-world applications [10, 12, 13].

A synthetic responsively switchable glue is required in order to control the adhesion between surfaces and to switch their adhesion to a non-adhesive state. Most switchable adhesion research has used stimuli-responsive materials, such as polyelectrolytes, since these polymers can show different responses to various stimuli, including pH, thermal, mechanical and light switching [10, 14, 15]. This is due to the fact that polyelectrolytes are charged polymers that can become uncharged when they undergo a change in their surrounding environment. It is therefore possible to control the charge density of the polyelectrolytes by applying an external environmental stimulus, with the high adhesion force contributing to the interactions of the high charge density polyelectrolytes. In other words, polyelectrolytes are suitable for use within switchable adhesive structures due to their ability to become charged or uncharged (i.e. their chains extend or collapse) under a known introduced trigger. A considerable amount of literature has been published on using polymers as adhesion modifiers for potential switchable adhesive applications [16, 17]; some of this literature is discussed in the following

section.

1.2.1 A Synthetic Switchable Adhesive System

Although the rapid growth in adhesion technology in the last few decades has led to a huge improvement in making strong mechanical adhesive bonds, developing adhesive bonds that attach and/or detach on demand remains challenging. A common example for a switchable adhesive structure from nature is gecko feet, which consist of hundreds of thin and short fibrils that terminate in 200 – 500 nm spatula-shaped structures that exhibit adhesion switchability with smooth and rough surfaces [12, 18]. These adhesive fibrillar structures in nature have inspired several recent studies investigating how to create similar artificial adhesive structures [19].

In the literature, the developments in switchable adhesion technology can be divided into two separated research areas that induce switchable adhesion by: 1) the topography and/or 2) the chemical functionality of the adhesive structures. Topographical adhesion studies are devoted to creating a polymeric adhesive structure with a high adhesion strength, which concentrates on the maximisation and minimisation of the contact area and its relationship with the enhancement of the adhesion level. Controlling the switchable adhesion by using chemical functionality, however, is implemented by using types of polymers with stimuli-responsive properties that initiate adhesion upon changes to the pH level or temperature, by the addition of salt or by applying an electric or mechanical field [16].

Some of the switchable adhesion studies on topography have relied on finding the relationship between the geometry of the adhesive structure and the type of material used. For example, a study by Reddy *et al.* [20] was inspired by the design of the attachment pads in some animals, such as gecko feet and their ability to stick strongly to, and detach easily from, different surfaces. This is due to the fact that animal adhesive setae are oblique and all the tips are tilted and pointing to one particular direction. The tilted position in the animal feet is responsible for the '*on-off*' adhesion process. In this work, therefore, the adhesive structure of micropillars was fabricated with shape memory thermoplastic elastomers. The micropatterned surfaces were made using a thermedics polymer called Tecoflex, which is a cycloaliphatic polyetherurethane block copolymer made of two phase segregated glassy components: hard

segments (containing methylene bis(*p*-cyclohexyl isocyanate) and 1,4-butanediol) and soft segments containing poly(tetramethylene glycol). These shape memory polymers (SMPs) are known for their ability to return to their original shape when they are exposed to an external thermal trigger. The micropatterned surfaces were designed with arrays of vertical micropillars with diameters of 0.5 – 50 μm and heights of 10 – 100 μm by soft molding the material at its highest transition temperature (T_{perm}) T= 120 – 140 °C, with the structure subsequently stabilising into its permanent shape.

The micropatterned pillars were deformed from an upright position to a tilted position by using a glass slide and applying mechanical deformation. In order to make the micropatterned tilt similar to the tilted bio-adhesive structure, the glass slide was pulled horizontally in one direction while heating the Tecoflex surface at T= 70 °C. The angle of the tilted micropatterned pillars was typically around 54°, and they maintained their tilted position as the polymer structure was cooled below its lower transition temperature $\left(T_{\text{trans}} = 50\ ^{\circ}\text{C}\right)$. The pillars were switched to the original upright position after they were reheated above their T_{trans}, however, since the physical crosslinks are cleaved this forces the material to return to its permanent shape (Figure 1.1).

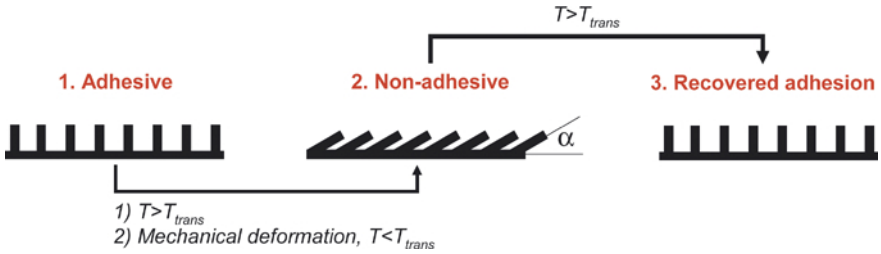

Figure 1.1: The fibrillar switchable adhesive surface of a thermoplastic elastomer, switching from adhesive to non-adhesive states and vice versa. Image adapted with permission of [20]. Copyright (2007) John Wiley and Sons.

The adhesion of the micropattern surface was measured by using a piece of home-built indentation equipment that recorded the load-displacement curves. This equipment consisted of a spherical probe, with a diameter of 5 mm, made of a piezoelectric crystal. Pull-off adhesion experiments were conducted by fixing the patterned sample on a stable stage and then the probe was brought into contact with the sample. The adhesion of the original vertical pillar (before deformation), and also of the tilted pillar (after deformation), was assessed after

retracting the compressive sphere, by finding the maximum vertical displacement of the piezoelectric sphere. The load-displacement curves obtained show that the adhesion was higher with the upright pillars while that of the tilted pillar was negligible. The adhesion of the tilted pillars was restored by reheating them, however, since they became able once again to make a good contact with the spherical indenter.

The pull-off force (P_c) determined the adhesive strength of the original pillar to be 29.7 kPa, which is roughly equal to a third of the value achieved by a typical gecko, whereas the adhesion strength of the recovered upright state of the tilted pillar amounted to 11.8 kPa. The reason that the adhesion value of the recovered pillar was reduced to nearly half the initial value was because some of the pillars remained in a slightly tilted position. This result was attributed to the high aspect ratio of the tilted pillars, which allows them to bend under the compressive force, thus resulting in a higher compliance. The heating and cooling transitions of micropatterned surfaces can therefore mimic to an extent biological attachment pads that attach firmly and/or detach easily from surfaces (i.e. by switching from tilted to non-tilted state). These shape memory polymer micropatterns have been found to be efficient for use in some reversible adhesion applications, such as medical tapes.

Natural models, such as gecko feet, provide a guide to the specific topographic patterning that can be used not only to enhance the adhesion of the artificial adhesive structure, but also, and more importantly, to tune the adhesion. Another topographical pattern study [21] has investigated the effect of the low-aspect-ratio cylindrical pillars, called '*pancakes*', of patterned surfaces made by poly(dimethylsiloane) (PDMS) on enhancing the adhesion with a smooth silica hemisphere. The micropillar dimensions play an important role in the aspect ratio and the tilting position of the pillar. This study used the Johnson, Kendall and Roberts (JKR) model to predict the thermodynamic work of adhesion (W_{adh}) in order to investigate the relationship between the pattern dimensions (length scales) and the adhesion interactions that are governed by the material properties. The imprint lithography technique was used to create topographical polymer patterns that consisted of cylindrical posts with a radius (r_p) ranging from 25 to 250 μm and height (h) equal to 4 μm, arranged in square arrays (edge-to-edge spacing (L) ranging from 50 to 500 μm).

The contact adhesion tests were conducted on custom-designed equipment consisting of a

force transducer, a hemispherical probe $\left(\text{with a radius of } 5\ \mu\text{m}\right)$ attached to a sub-nanometre precision inchworm actuator, and a fully automated inverted optical microscope. The hemispherical probe was attached to, but separated from, the patterned elastomer layer and, during this process, the displacement (δ), contact area $\left(A = \pi a^2\right)$, and the resulting force (P) were recorded. The glass elastomer interface was assessed by the results of the noncovalent adhesion mechanism, and confirmed the effect of the pattern feature diameter (r_{p}) on the local separation process at the interfacial adhesion (Figure 1.2).

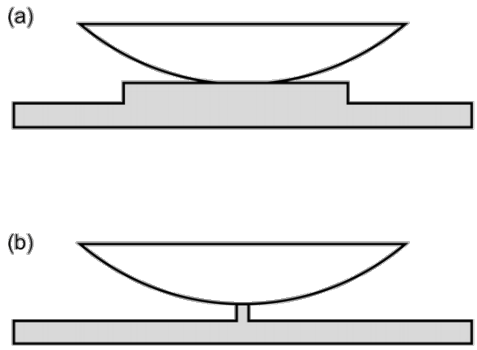

Figure 1.2: A schematic diagram of the contact between the hemispherical probe with (a) a large diameter pancake and (b) small diameter post. Image used with permission from [21]. Copyright (2005) American Chemical Society.

It was observed that there were different local separation process at the interfaces depending on the size of the pillar radius and also the edge-to-edge spacing. The value of conventional adhesion descriptors for nonpatterned interfaces was increased from 20% to 400% by using the low-aspect-ratio posts $\left(\text{where } h/r_{\mathrm{p}} \ll 1\right)$. This adhesion enhancement was not caused by the magnitude of the interfacial area but by changing the local separation process at the interface (Figure 1.3).

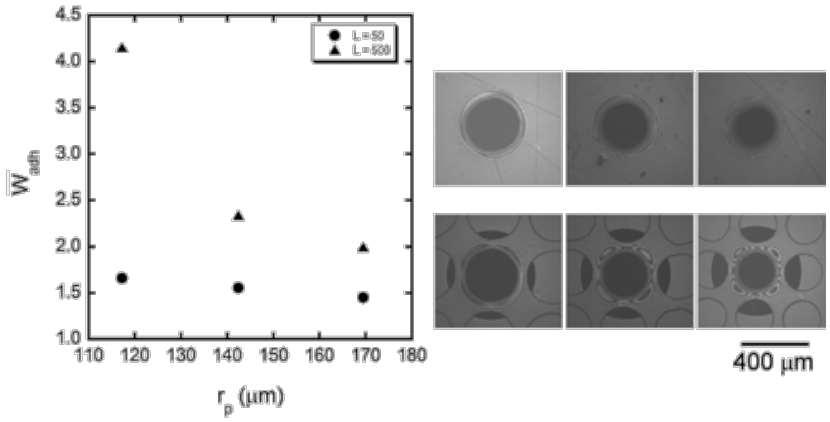

Figure 1.3: The work of adhesion (W_{adh}) as a function of varying the post radius (r_{p}). Two differently spaced patterns were used: $L = 500$ μm (the maximum contact area images of which are shown on the top) and $L = 50$ μm (maximum contact area images shown on the bottom line). Image taken with permission from [21]. Copyright (2005) American Chemical Society.

It was found that the W_{adh} increased when the r_{p} decreased until the critical radius (a_{c}) is reached $\left(a_{\mathrm{c}} = 160\ \mu\mathrm{m}\right)$. If r_{p} was larger than a_{c}, then the maximum separation force was no longer increased since the stress distribution was imposed by the influence of the separation process, and so it behaved like a nonpatterned surface. In other words, the radius of the hemispherical probe is infinite relative to the post radius, and so the posts are considered to be a flat surface. Controlling the geometric structure adjusts the energy required to separate an interface. Accordingly, this geometrical control is critical for the future development of smart adhesion, and also for understanding adhesion in natural systems.

Another study, reported by Lamblet *et al.* [22], confirmed the importance of the low-aspect-ratio posts and showed the relationship between elastic (soft) micrometric patterns and high adhesion levels. The imprint lithography technique was therefore used to prepare micropatterned soft and rigid PDMS substrates with high-aspect-ratio and also low-aspect-ratio posts. The peel test technique was used with a homemade apparatus for testing the adhesion between the microposts and a commercial acrylic adhesive tape in 90° geometry at a chosen velocity (V) between 500 nm/s and 1 mm/s. The peel energy (G) was calculated by dividing the peel force (F) over the width (b) of the acrylic tape. The results showed that the low-aspect-ratio posts were more efficient at increasing the adhesion when they were made of deformable soft patterned substrates. In contrast, the soft high-aspect-ratio posts lost their adhesive efficiency

since some pillars were more likely to stick to each other when they were irreversibly bent. The ability of the patterned pillars to be elastic (deformable) played an important role in tuning the adhesion level at the PDMS-acrylic interface. In other words, the adhesion was improved as the pillar height was increased until the height reached a limit where it gets very long. Whereas, the non-deformable pillars did not enhance the adhesion due to their lower elastic contribution. Although PDMS has a low surface energy and weak chemical reactivity that make it a suitable choice for antiadhesive coatings, it is also a commonly used biomaterial for medical devices and microfluidic systems [23]. Creating an adhesive structure by using PDMS with smart adhesive properties remains a real technical challenge, therefore a common path to enhance the adhesive properties of PDMS is to use chemical modification. Microstructuration is an alternative technique that has been extensively investigated recently, however, and used to build a structure inspired by some insects. Independently of the chemical details of an adhesive, the level of the adhesion at the PDMS/acrylic interface can be tuned by controlling: i) the pattern size and ii) the mechanical properties of the substrate [22].

One of the main drawbacks of the switchable adhesive system of the gecko is that it exhibits dry reversible adhesion only, the performance adhesion of gecko feet is affected by exposure to humidity and also becomes very weak underwater since it is formed by weak secondary bond forces such as Van der Waals. As a consequence of this, another study, reported by Lee. H *et al.* [24], was conducted to achieve a switchable dry/wet adhesive structure, which was inspired by both gecko dry adhesion and mussel wet adhesion. The mussel is a renowned biological example of wet adhesion since it can cling powerfully to surfaces underwater. Mussel adhesive is made up of proteins that contain a high content of the catecholic amino acid 3,4-dihydroxy-L-phenylalanine (L-DOPA). The mussel's unique characteristic is that the chemical basis for L-DOPA has the ability to adhere to underwater surfaces by high-strength reversible bonds. Although it has been suggested that the L-DOPA adhesion mechanism is not driven by the hydrogen bond formation, the adhesion mechanism of mussels underwater has never been fully explained [25].

As a consequence, the task of designing a synthetic mussel adhesive protein was initiated by choosing a polymer with a high catecholic content, since L-DOPA accounts for as much as 27% of amino acids. Additionally, wet adhesion requires a polymer with low water solubil-

ity in order to prevent its loss into the aqueous medium. A synthetic adhesive structure was therefore demonstrated, consisting of an array of nanofabricated polymer pillars coated with a thin layer of poly(dopamine methacrylamide-co-methoxyethyl acrylate) (p(DMA-co-MEA)). The arrays of the hybrid adhesive structure were fabricated by using electron-beam lithography to make pillars that were 400 nm in diameter and 600 nm in height in poly(methyl methacrylate) (PMMA) film on a silicon substrate (Figure 1.4). Then, the sol phase of poly(dimethylsiloxane) (PDMS) was cast onto the PMMA film, thermally solidified and then moved up from the silicon substrate. Finally, a thin layer of the mussel-mimetic polymer of p(DMA-co-MEA) was added to the pillar by the dip-coating technique $(< 20$ nm$)$.

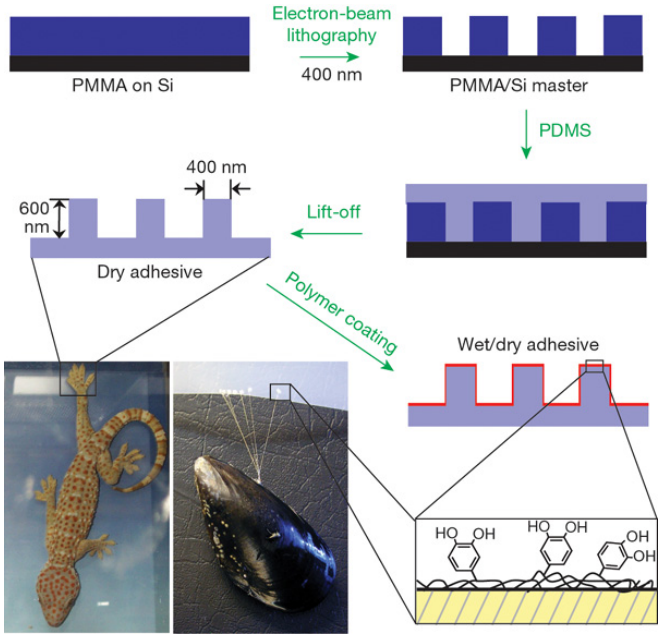

Figure 1.4: The synthetic design of wet/dry hybrid nanoadhesive. An array of holes in a PMMA thin film supported on silicon (PMMA/Si) was created by electron-beam lithography. This was followed by PDMS casting onto the PMMA/Si, resulting in gecko-mimetic nanopillars. Finally, the mussel-mimetic polymer was dip-coated onto the nanopillars. Image taken with permission from [24]. Copyright (2007) Nature Publishing Group.

The adhesion experiments of this hybrid adhesive system were performed in air, and also underwater, using atomic force microscopy (AFM) to bring the pillars into contact with a tipless cantilever made out of silicon nitride (Si_3N_4). The adhesive contact force of a single pillar with a clear nanoscale contact area of the AFM tip was measured upon a retraction force that was consumed in separating the cantilever from the pillar. The adhesion of the

uncoated pillars (i.e. without the mussel-mimetic polymer p(DMA-co-MEA) layer) that are called 'gecko' , were compared with the adhesion of the p(DMA-co-MEA) coated pillars that are called 'geckel' . The typical force-distance curves showed that the adhesion force per individual pillar in air equalled 39.8 ± 2 nN for the uncoated pillar and 120 ± 6 nN for the p(DMA-co-MEA) coated pillar, whereas underwater it equalled 5.9 ± 0.2 nN for the uncoated pillar and 86.3 ± 5 nN for the p(DMA-co-MEA) coated pillar (Figure 1.5). A dramatic enhancement in the wet adhesion measurements was therefore obtained with the p(DMA-co-MEA) coated pillars, meaning that the mussel-mimetic polymer increased the underwater adhesion of the pillars significantly.

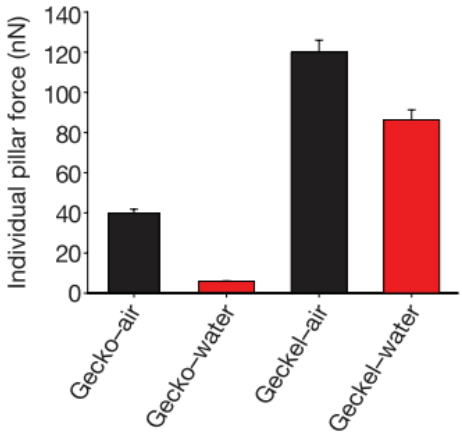

Figure 1.5: A comparison between the adhesion forces per pillar in air (black columns) and in water (red columns) for gecko and geckel adhesive structures. Image adapted from [24]. Copyright (2007) Nature Publishing Group.

The multiple contact cycles for both wet and dry adhesion for the p(DMA-co-MEA) coated pillars showed that the adhesion was slightly reduced after 1,100 adhesion test cycles. Further refinement of these hybrid adhesive nanofabricated polymer pillars could lead to a huge improvement in the performance of switchable adhesion technology sufficient for use in medical and industrial applications [24]. Overall, it is evident that although the details of the animal switchable adhesion mechanisms remain difficult and complex to copy directly, translating some of their functional adhesion principles to the materials world is possible [9].

In the field of chemically induced switchable adhesion, there has been a growing interest in the use of stimuli-responsive materials, such as polyelectrolytes, to make switchable adhesive

structures. Polyelectrolytes are a class of macromolecule that consist of positive or negative ionisable groups inside polar solutions, such as water. There are two types of polyelectrolytes - weak and strong - with the difference between them being that the ionisable groups in weak polyelectrolytes have an unfixed degree of association (f) that allows the control of their electrostatic charges by varying the environmental conditions [17, 26, 27]. In other words, the adhesion of the stimuli-responsive weak polyelectrolytes is controlled by their molecular interactions such as electrostatics, hydrophobic interactions or hydrogen bonding [16, 28].

A model of a reversible adhesion system between hydrogels and polymer brushes was investigated under a fully immersed condition as a function of pH. In this study, adhesion was demonstrated between a poly(*N,N*-dimethylacrylamide) (PDMA) and polyacrylamide (PAM) as polymer gels and a poly(acrylic acid) (PAA) as the pH-sensitive polymer brush [29]. Polymer brushes refer to the polymer chains that are chemically grafted onto a planar surface by anchor points with a defined grafting density that allows them to stretch away from the surface in a 'brush-like' conformation [30, 31]. While a hydrogel is a three-dimensional crosslinked network that is commonly made from water-soluble polymers where their chains are connected and linked together via physical or chemical crosslinking points [32, 33].

Pull-off experiments were performed between the hydrogel and PAA brush, and were set up on a flat-flat contact underwater (Figure 1.6) by using a commercial Instron machine (for tensile and compression tests) fitted with a load cell of 10 N for all adhesion experiments. The contact area at the gel-brush interface was observed underwater using a camera from below at 45° due to the similarity in the reflective indices of hydrogels and water.

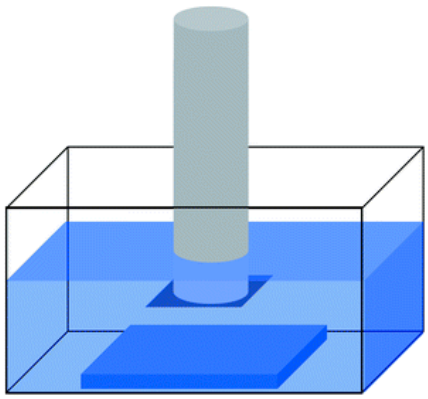

Figure 1.6: Underwater adhesion tests of the flat-flat contact between the hydrogel and the surface of the polymer brush. Image taken with permission from [29]. Copyright (2012) Royal Society of Chemistry.

The PAA brushes were grafted on a planar silicon substrate and the flat polymer gels were covalently attached to flat quartz substrates. The hydrogels used were hydrophilic networks and so they swell in water to an equilibrium volume that is reached by achieving a balance between the entropy of mixing and the conformational entropy that leads to hydrogels behaving like an elastic rubber. These neutral hydrogels were chosen for their dimensional stability and relatively low sensitivity when the pH level of water is changed. These chosen networks made the pH-sensitive macroscopic adhesion tunable by creating a short-range adhesion interaction with the pH-sensitive brushes (i.e, by forming hydrogen bonds at the hydrogel-brush interface). As a consequence, the interaction potential between the hydrogel and the brush surface was variable, meaning that both interaction and macroscopic adhesion were switchable. The flat-flat contact test was used in order to gain information regarding adhesion energy that can then be adapted in many switchable adhesive systems. The energy of adhesion (W_{adh}) of the flat-flat system was calculated by

$$W_{\mathrm{adh}} = l_0 \int_0^{+\infty} \sigma \, \mathrm{d}\varepsilon. \tag{1.1}$$

where l_0 is the initial thickness of the flat gel, σ is the stress that is obtained by dividing the force by the punch area, and ε is the strain.

The contact mechanism of the gel-brush adhesive interface provided quantitative data on the work of adhesion (W_{adh}). The effect of changing the pH level, contact time and the debonding speed on the adhesion interactions were also investigated. Here, it was found that the adhesion force increased as the pH value of the surrounding water decreased (at pH 2), due to an increase in the formation of hydrogen bonds at the gel-brush interface as the brush surface became protonated at low pH. As the pH level of water was increased (to pH $\geq$ 4), the adhesion strength was dramatically reduced. The adhesion of the PAM gel with the PAA brush was significantly larger than that of the PDMA hydrogel with the PAA brush but this adhesion result remained unexplained (Figure 1.7).

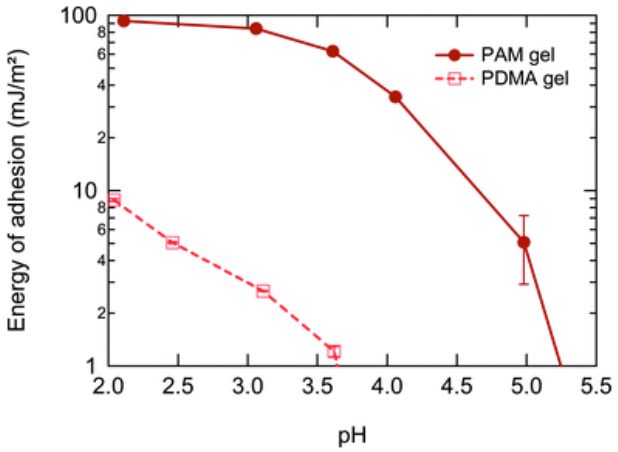

Figure 1.7: Energy of adhesion of a PAM hydrogel and a PDMA hydrogel with a PAA brush as a function of varying the pH value. Image adapted with permission of [29]. Copyright (2012) Royal Society of Chemistry.

The work of adhesion of the flat-flat contact between the hydrogel and polymer brush was also measured as a function of varying the contact time of bringing the hydrogel into contact with the brush surface. It was found that the adhesion increased with longer contact times, suggesting that the longer contact time would allow the reorganisation of the interaction at the interface since the H-bond formation process was very slow [29].

Another hydrogel-brush switchable adhesion study was reported by La Spina *et al.* [10, 34], with adhesion demonstrated between two types of oppositely charged polyelectrolytes; poly(methacrylic acid) (PMAA, a hemispherical polyacid gel) and poly[2-(dimethyl amino)ethyl methacrylate] (PDMAEMA, a polybase brush). Although both the hydrogel and polymer brush are sensitive to changes in the environmental pH value, each polymer has an opposite type of electrostatic charge. The PMAA hydrogel, which has a negatively charged carboxylic end-group, was prepared in a hemispherical shape by free radical polymerisation, while the PDMAEMA brushes, which have positively charged amine groups, were grafted onto a silicon substrate via the '*grafting-from*' technique. The work of adhesion (G) was estimated by measuring the contact diameter ($2a$) at the adhesive gel-brush interface underwater by a side-view camera using the Johnson-Kendall-Roberts (JKR) model (Figure 1.8). So, the pH-sensitive adhesion of the PMAA gel-PDMAEMA brushes was studied by finding the work of adhesion, G, as a function of varying the pH value, using the JKR equation,

$$a^3 = \frac{R}{K}\left(P + 3\pi GR + \sqrt{\left(6\pi GRP + (3\pi GR)^2\right)}\right). \tag{1.2}$$

where R is the radius of the hemispherical gel, K is the modulus of the gel and P is the applied load used to adhere the gel to the brush layer [35].

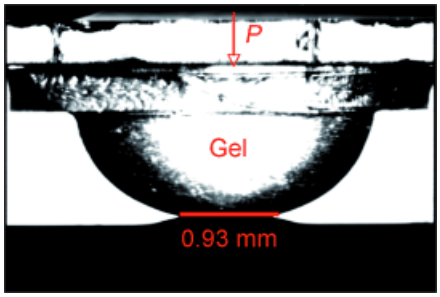

Figure 1.8: An illustrative diagram of the JKR experimental setup between a hemispherical hydrogel and the surface of the polymer brush underwater. The contact diameter ($2a$) was 0.93 mm after applying a load (P). Image taken with permission from [34]. Copyright (2007) John Wiley and Sons.

The work of adhesion, G, between the polyacid gel and polybase brushes was measured at different pH values, and the JKR experimental setup showed that the adhesion strength was higher underwater at a neutral pH level (pH $\sim$ 5.8) and poorer at a very strong acid level (pH $\sim$ 2.4) after adding a few drops of hydrochloric acid (HCl) (Figure 1.9).

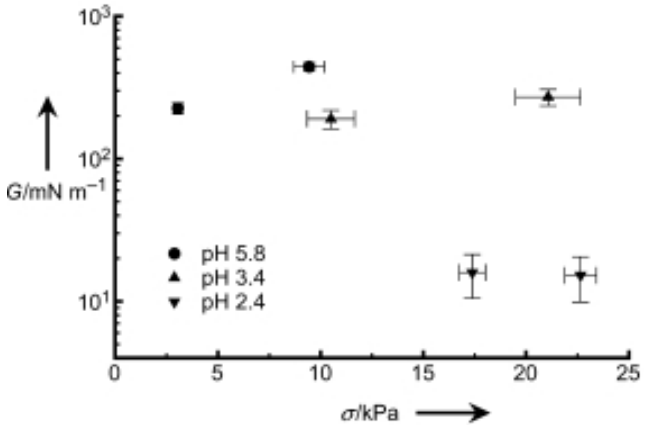

Figure 1.9: The work of adhesion (G) as a function of the compressive stress (i.e. the pressure) (σ) for two different loads of 32 and 60 mN at three pH values. Image taken with permission from [34]. Copyright (2007) John Wiley and Sons.

The contact diameter, $2a$, was also varied by changing the applied force, P. In other words, a increased by increasing P, suggesting that this pH-reversible adhesion was a pressure-sensitive adhesion. Increasing the contact diameter, $2a$, at the hydrogel-brush interface also resulted in an increase in the work of adhesion, G. The switchability of the adhesion at the gel-brush interface was confirmed by the decrease in the contact diameter at their interface when the pH value was varied from basic to acidic. One major criticism of this system is that detaching the gel from the brush surface took a long time ($\sim$ 7 h) inside the strong acidic pH level for a small applied load of 32 mN, which could increase to as much as a number of days for larger applied loads [34]. Although the weakly charged polyelectrolytes are sensitive to the salt concentration as the salt ions screen their electrostatic charges [36, 37], the switchability of the adhesion at the gel-brush interface was not examined as a function of adding salt to their surrounding water.

The effect of the salt concentration on the adhesion strength between two oppositely charged polyelectrolytes was, however, examined within the study of a brush-brush adhesive system [38]. Here, the two surfaces of the polymer brushes were cationic and anionic polymers of poly[2-(methacryloyloxy)ethyl trimethylammonium chloride] (PMTAC) and poly(3-sulfopropyl methacrylate potassium salt) (PSPMK). The high-density polyelectrolyte brushes were prepared with a thickness of 100 nm using surface-initiated atom transfer radical polymerization (SI-ATRP) and grafted onto silicon substrates. Both polymer brushes were adhered to each other with a small amount of deionized (DI) water (i.e. 2 μL of water) that was injected into a brush surface and then the second brush surface was pressed into it with a load of 4.9 N. The rectangular contact area between the two brush substrates was 5 $\times$10 mm^2, and the drying time of the injected water was 2 h at room temperature and 55% relative humidity.

The adhesive strength between the two surfaces of polymer brushes was examined with a tensile tester (Shimadzu EZ-Graph) in an ambient atmosphere by measuring the lap shear strength. The lap shear (tensile) is a method for testing the adhesion between two adhered surfaces by pulling bonded layers apart in opposite directions in order to determine the bond strength and efficiency at their interface (N/mm^2). Both brush samples were thus held at their ends with mechanical chucks connected to a load cell and a tester base anchor. The lap

shear strength was tested with a speed of 1 mm/min and defined by the force corresponding to the breaking point divided by 50 mm^2 of the contact area. The obtained results of the lap shear showed that the bond strength between the strongly adhered surfaces of the polymer brushes was 1.52 ± 0.43 MPa. The switchability of the polyelectrolyte brush-brush adhesion, however, was achieved after immersing the two adhered surfaces inside a 0.5 M aqueous solution of sodium chloride (NaCl) at room temperature (Figure 1.10).

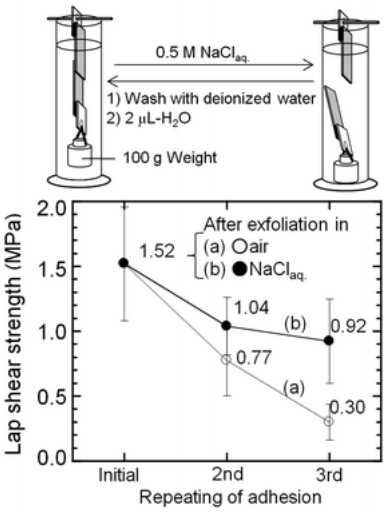

Figure 1.10: A schematic diagram (on the top) shows the process of attaching and detaching the oppositely charged surfaces of polymer brushes. The substrates of the poly(SPMK) and poly(MTAC) brushes were bonded together after injecting 2 μL of DI water into their interface. The graph shows the lap shear adhesion strength of repeating the adhesion of the brush substrates after (a) testing it in air and (b) exfoliation in a 0.5 M aqueous NaCl solution. After detaching the adhered brush surfaces inside NaCl solutions, they were washed with water before bonding them again. Image adapted with permission of [38]. Copyright (2011) Royal Society of Chemistry.

It was found that the adhering substrates were debonded inside the NaCl solution as a result of screening the electrostatic interactions on the brush surfaces by the hydrated salt ions (Figure 1.11). In contrast, the adhered surfaces did not come apart when they were immersed inside DI water. Also, the adhesion strength was lower than 0.01 MPa when the brushes were very thin ($\sim$ 10 – 20 nm thick), since the two surfaces of the polymer brushes were hardly attach to each other. This result, therefore, suggested that the brush-brush adhesion was affected by the chain length and the molecular weight of the brushes .

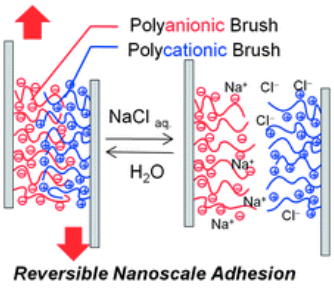

Figure 1.11: The brush-brush adhesion interactions when they were induced by adding a few drops of water (on the left-hand side) or interrupted by the salt ions of the NaCl solution (on the right-hand side). Image adapted with permission of [38]. Copyright (2011) Royal Society of Chemistry.

Although adhesion repeatability was achieved using the NaCl solution to remove the brush-brush adhesive interaction up to three times, the adhesive strength decreased to 0.30 ± 0.13 MPa by the third occasion (see Figure 1.10). The reason for the reducing adhesive strength was unclear since both polymer brushes were still attached on each substrate under the AFM after detaching them. It is possible that the adsorption of contamination from the atmosphere probably affected the repeatability of the brush-brush adhesion. These switchable bonding and debonding processes of the brush-brush adhesive system can be used in clean, nontoxic and environmentally friendly nano-devices.

One of the weaknesses of eliminating the adhesion between the oppositely charged polyelectrolyte brushes of poly(SPMK)-poly(MTAC) by using salt solutions was the formation of an inorganic salt at the adhesion interface, as was observed by the same authors in a follow-up study. The salt ions of the NaCl solutions could affect the adhesion repeatability of the brush-brush adhesive system and disrupt their attractive electrostatic interactions, since the potassium counterion of poly(SPMK) and the chloride of poly(MTAC) produced potassium chloride. The brush-brush adhesion was therefore developed and carried out by using a zwitterionic poly[3-(*N*-2-methacryloyloxyethyl-*N,N*-dimethyl) ammonato propane sulfonate] (poly(MAPS)) brush grafted onto two silicon substrates [39]. Using a thermo-sensitive zwitterionic brush that contains an ammonium cation and a sulfonic anion in the same monomer unit was able to enhance the adhesion strength and achieve switchable adhesion by changing the temperature of water without the formation of an inorganic salt due to the control the dipole-dipole interaction between the sulfobetaine units of the thermo-sensitive poly(MAPS) brush.

The poly(MAPS) brushes were grafted onto silicon substrates via SI-ATRP with a thickness of 100 nm. The attachment process of adhering two substrates of poly(MAPS) brushes together entailed by applying a contact area of 5 $\times$10 mm^2 and then placing them inside a Petri dish in hot water at 333 K under a constant load of 4.9 N using a 500 g weight for 1 min. After that, the water was removed and the adhered brush surfaces were allowed to stand at room temperature in ambient air (55% relative humidity) and dried for 3 h. Then, the adhesion strength was measured by using a tensile tester (Shimazdu EZ-Graph) at room temperature in ambient atmosphere.

It was found that the lap shear adhesion strength for the brush surfaces that were attached in water at 333 K was 2.05 $\pm$ 0.43 MPa, whereas it dramatically decreased to 0.1 MPa when the brush surfaces were attached in cold water at 298 K. In addition, the retention time (h) of the adhered substrates was examined inside water as a function of varying water temperature by attaching a 100 g weight to the bottom of one brush surface (see Figure 1.12). It was found that the adhered substrates were debonded after 12 h of immersing them in water below 280 K, while the retention time was reduced to 1 h after increasing the temperature of water to 333 K. This was because the poly(MAPS) brushes are temperature sensitive and so their adhesion behaviour was controlled by the upper critical solution temperature (UCST), which allowed the MAPS brushed to exhibit a phase separation in water above the UCST. The UCST of the poly(MAPS) is approximately 298 – 303 K (25 – 30 °C). It was suggested that the greater adhesion strength was driven by the extension of the brushes above the UCST, which allowed the formation of a rough interface, promoting the intermixing of the opposing polymer brushes and increasing the number of sulfobetaine pairs with a sufficiently close distance.

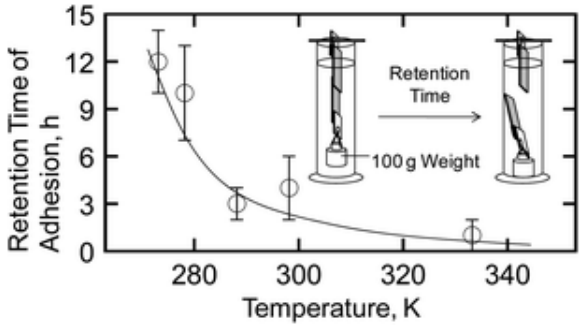

Figure 1.12: The retention time (h) of the adhered poly(MAPS) brush substrates inside water as a function of different temperatures. Image taken with permission from [39]. Copyright (2013) Royal Society of Chemistry.

The repeatability of this thermo-sensitive adhesion between the zwitterionic brushes was examined and controlled by immersing the adhered surfaces in hot water at 333 K in order to detach them apart, and then re-adhering them a number of times (Figure 1.13). It was found that the swelling behaviour of the poly(MAPS) brushes in hot water at 333 K was useful for separating them successfully without causing damage to brushes. The separation process of adhered brushes was induced by placing a 100 g weight to a bottom of one of these brush substrates while the other substrate was attached vertically to a holder. Atomic force microscopy (AFM) was used to examine the presence of polymer brushes on the silicon surface after the detaching process and it was found that the brushes remained on the silicon surface, which confirmed that the adhesive failure occurred at the brush interface. As a consequence, the adhesion of zwitterionic brushes was repeated several times, and the lap shear adhesion strength was slightly reduced from 2.05 MPa to 1.92 MPa in test cycle number 4.

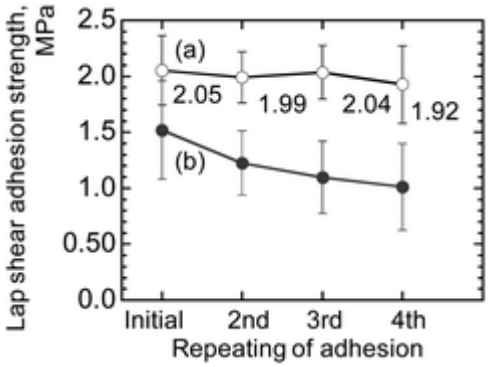

Figure 1.13: (a) The lap shear adhesion strength of the rebonded PMAPS brushes in hot water at 333 K with subsequent repeated adhesions by immersing them in water again and then allowing them to dry for 3 h. (b) The lap shear adhesion strength of the PSPMK–PMTAC brushes after debonding them in a 0.5 M aqueous NaCl solution, which were added here to make an adhesion comparison with the adhesion of the PMAPS brush in (a). Image adapted with permission of [39]. Copyright (2013) Royal Society of Chemistry.

The switchable repeatable zwitterionic brushes system, which strongly attaches and smoothly detaches by controlling the temperature of water, was compared to the oppositely charged cationic poly(MTAC) and anionic poly(SPMK) brushes, which attach by water and detach in NaCl solution (Figure 1.13). The adhesion strength in the zwitterionic brush system was stronger than the adhesion of the cationic-anionic brushes (2.05 MPa and 1.52 MPa,

respectively). Also, the adhesion of the zwitterionic brushes system was able to sustain its repeatability up to four times as a result of the attractive dipole-dipole interactions. The adhesion of cationic-anionic brushes, in contrast, decreased after repeating the adhesion test four times, which was probably due to the inorganic salt residues that remained on the brush layer after detachment, even after washing with large amounts of water.

1.2.2 Scope of this Study

The work presented in this PhD thesis studies the switchable adhesion between two oppositely charged polyelectrolytes underwater; a hemispherical hydrogel and a polymer brush. This study, therefore, aimed to quantify and evaluate the adhesion strength at the gel-brush interface underwater using a mechanical tester called a Stable Micro Systems TA.XT Plus Texture Analyser (TA). The mechanical tester (TA) was used to perform the pull-off adhesion experiments by attaching the hemispherical hydrogel onto the surface of the polymer brush and then detaching them apart in order to measure the adhesion at their interface.

This work focused on characterising the real adhesion features at the gel-brush interface by finding the maximum adhesive force (F) and the work done (W), which were calculated from the force-distance curves obtained by the TA tester. Two types of weakly charged polyelectrolytes were used in this study: i) a poly(methacrylic acid) (PMAA, polyacid) and ii) poly[2-(diethyl amino)ethyl methacrylate] (PDEAEMA, polybase) to make both hydrogels and polymer brushes.

The adhesion experiments were carried out between: 1) the PMAA hydrogel and PDEAEMA brush and 2) the PDEAEMA hydrogel and PMAA brush as a function of varying the pH value of their surrounding water. The influence of other controlled parameters on the adhesion strength at the gel-brush interface were also examined, such as: the thickness of the polymer brush and the crosslinking density of the hydrogel.

This study also compared the switchable adhesion of two different types of polyelectrolyte hydrogels, namely: 1) a *soft* gel called a single-network (SN) hydrogel and also 2) a *robust* gel called a double-network (DN) hydrogel. The main difference between the SN gels, which were made out of a single polymeric network, and the DN gels, which were made out of two polymeric networks, is that the DN gels have a higher mechanical strength and elastic

modulus than SN gels. Furthermore, the switchability and reuseability of the adhesion at the (SN/DN) hydrogel-brush interface were investigated using pH 1–pH 6 oscillating cycles. In addition, the effect of adding sodium chloride (NaCl) salt into the surrounding water (at a fixed pH value of DI water) on the hydrogel-brush adhesion was examined.

While this chapter 1 has provided an introduction to adhesion science and an overview of all the relevant switchable adhesion studies, chapters 2 and 3 review the adhesion mechanisms and theories and also present a literature review of polyelectrolytes; hydrogels and polymer brushes. Chapter 4 presents the preparation details of the polyelectrolyte hydrogels and brushes and also highlights the experimental techniques that were used in this PhD work. The obtained results and main findings of the gel-brush switchable adhesion are presented in chapter 5, 6 and 7. Finally, chapter 8 is a brief summary with some suggestions for future work.

Chapter 2

Adhesion Theories

2.1 Introduction

Most scientific research on adhesion phenomena has focused on understanding contact mechanisms and enhancing the joint strength of adhesives, as a result of the increasing demands placed on adhesives in industrial applications such as automobile manufacturing and the aeronautical and space industries [40, 41]. In 1882, a study of the contact mechanism was made by Hertz [42], who reported the importance of understanding the contact mechanism of two surfaces in contact with each other. The Hertz model of the contact mechanism was applied in the context of industrial development that needed to overcome some deformation problems such as the contact of train wheels on the steel rails, however, the Hertz model neglected adhesion forces. The role of adhesion forces was introduced later by Johnson, Kendall and Roberts (JKR) in 1971 [35]. The JKR model extended the Hertz model by introducing the relationship of the interactive adhesive forces at the interface between two spheres in contact and the adhesion energy at their interface. Recently, JKR adhesion theory has been considered in many adhesion studies due to its importance in understanding the adhesive joints and strength.

This chapter will present and discuss the contact mechanisms and adhesion theories so as to give a better understanding of the measurement of adhesive forces and the characterisation of two surfaces in contact.

2.2 Contact Mechanisms and Adhesion Theories

Classical theoretical models for the adhesive contact between two elastic surfaces are commonly known as contact mechanics theories. These models of the contact mechanism are used to evaluate the thermodynamic work of adhesion between two surfaces in contact, their surface deformation and stress distribution. The most important term in these contact mechanism models, however, is the work of adhesion since it identifies the required energy to separate the adhesive interfaces between two bodies, whether the type of the adhesive bond formed is physical or due to intermolecular forces, or electrostatic forces [43].
This section reviews classical theoretical models for the adhesion phenomenon between two surfaces in contact with each other.

2.2.1 Role of the Interface and Surface Energy

The adhesion process is an interfacial phenomenon that results from the atoms or molecules interacting at the adhesive interface. The adhesion interactions are controlled by the surface energies of the two attached bodies. The surface energy (γ) is defined as the energy that is consumed to create a new unit area (a) of an adhesive interface. The value of the surface energy (γ) depends on the type of bonds that must be broken and it was given by Fowkes as following

$$\gamma = \gamma_{\mathrm{d}} + \gamma_{\mathrm{p}} + \gamma_{\mathrm{h}} \,. \tag{2.1}$$

where γ_{d} is dispersion force, γ_{p} is polar force, and γ_{h} is hydrogen bonding. Therefore, the surface energy can also be given by

$$\gamma = \left(\frac{\partial G}{\partial A}\right). \tag{2.2}$$

where G is the surface Gibbs free energy and A is the created area.
The surface energy helps to find the work of adhesion (W_{adh}) at the adhesive interface. The work of adhesion, W_{adh} , is the free energy per unit area when two surfaces are separated and is given by

$$W_{adh} = \gamma_1 + \gamma_2 - \gamma_{12}\,. \tag{2.3}$$

where, γ_1 and γ_2 are the surface energies of the two interacting surfaces in phases 1 and 2 and γ_{12} is the interfacial energy.

The work of adhesion and the equilibrium of the liquid/solid interface, in Figure 2.1, can be obtained by Young's equation. Young's equation shows the relationship between the surface and interfacial energies as

$$\gamma_{\mathrm{L}} \cos\theta = \gamma_{\mathrm{S}} - \gamma_{\mathrm{SL}}\,, \tag{2.4}$$

where, γ_{L}, γ_{S} and γ_{SL} are the surface energies of the liquid/air, solid/air and solid/liquid interfaces, respectively [7, 8].

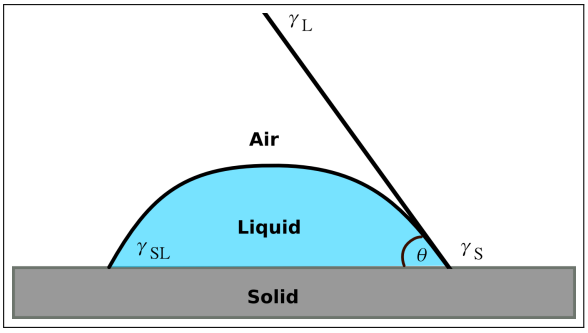

Figure 2.1: A schematic diagram of a liquid drop (L) on a solid surface (S) for contact angle experiments.

When the interfacial energy γ_{12} in equation (2.3) equals zero and the energy in phases 1 and 2 are identical, the work of cohesion W_{coh} is given by

$$W_{\mathrm{coh}} = 2\,\gamma\,. \tag{2.5}$$

The work of cohesion W_{coh} is the free energy required to separate the adhered surfaces mechanically from contact to infinity. The liquid drop does spread if the the work of adhesion is larger [44, 45].

2.2.2 Hertz Theory

In 1882, Hertz [42] conducted the first study of the contact mechanism, exploring deformation at a non-adhesive interface between two bodies. By that time, the industrial interest was focused on an understanding of contact deformation to solve problems such as the contact between a train's wheels and the steel rails. The Hertz model takes into consideration deformation rather than adhesive interactions between the surfaces in contact because the deformation force is much larger than the adhesive force [46].

Figure 2.2 represents the non-adhesive contact diameter ($2a$) between two sphere surfaces, whose radii are R_1 and R_2 and whose Young's moduli are E_1 and E_2, respectively. The interfacial contact diameter, $2a$, is created by pressing the sphere bodies against each other by an applied force ($P_\perp$).

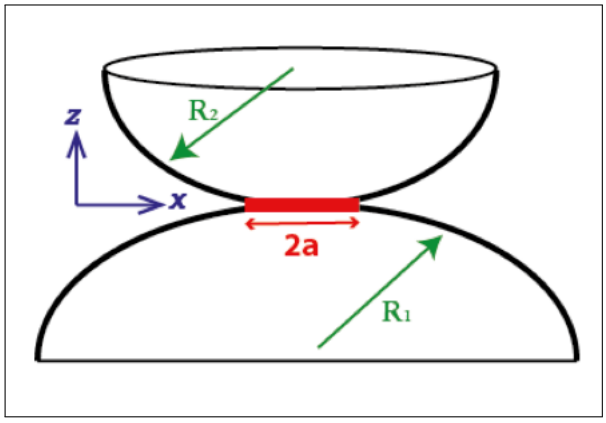

Figure 2.2: The interfacial contact ($2a$) between two hemispherical bodies resulting from pressing them together by a compressive force ($P_\perp$).

The contact diameter between these two bodies depends on the elastic deformation of both surfaces. The Hertz equation can also be used to study a contact radius between a hemispherical body and a flat surface, assuming that the flat surface is a sphere of infinite radius. The radius of the contact area (a_0) under the compressive load is given by the following equation

$$a_0^3 = \frac{PR}{K}\,. \tag{2.6}$$

where the equivalent radius (R) and the equivalent elastic modulus (K) are given by

$$\frac{1}{R} = \frac{1}{R_1} + \frac{1}{R_2}\,. \tag{2.7}$$

$$\frac{1}{K} = \frac{3}{4}\left(\frac{1-\nu_1^2}{E_1} + \frac{1-\nu_1^2}{E_2}\right). \tag{2.8}$$

where ν_1 and ν_2 give the Poisson's ratio of the two surfaces.

The movement (displacement) (δ) of the applied force (P) is given by

$$\delta = \frac{a_0^2}{R}\,. \tag{2.9}$$

The Hertz model is not suitable for adhesion experiments since it assumed that there was no adhesion interaction at the interface of two bodies in contact [47, 48]. Therefore, Johnson, Kendall and Roberts (JKR) developed the Hertz equation by introducing an interfacial attractive effect on the contact radius between the two spheres because the contact radius between two bodies at a low load is larger than predicted in the Hertz model [35].

2.2.3 JKR Theory

Understanding the thermodynamic aspect of adhesion is vital in order to determine and evaluate the adhesive force at the interface between two surfaces [49, 50]. Johnson, Kendall and Roberts [35] published the JKR theory in 1971 that describes how the surface energy influences the contact between solids. The JKR hypothesis was derived from the Hertz theory, but takes into consideration that there are attractive forces increasing the contact diameter between solids, which are short-range interactions just at the interface between these two bodies [51, 52].

The JKR theory states that when a load ($P_\perp$) is applied on two elastic spheres in contact, a new unit area of radius (a) is created at their interface, which is given by

$$a^3 = \frac{R}{K}\left(P + 3\pi W_{adh}R + \sqrt{6\pi W_{adh}RP + (3\pi W_{adh}R)^2}\right), \tag{2.10}$$

where W_{adh} is the work of adhesion at the interfacial contact between these two bodies.

The value of the new unit area of radius, a, depends on how strong the attractive force is. In other words, the interfacial radius, a, between two bodies in contact with each other increases when the adhesive forces at their interface are very strong (Figure 2.3).

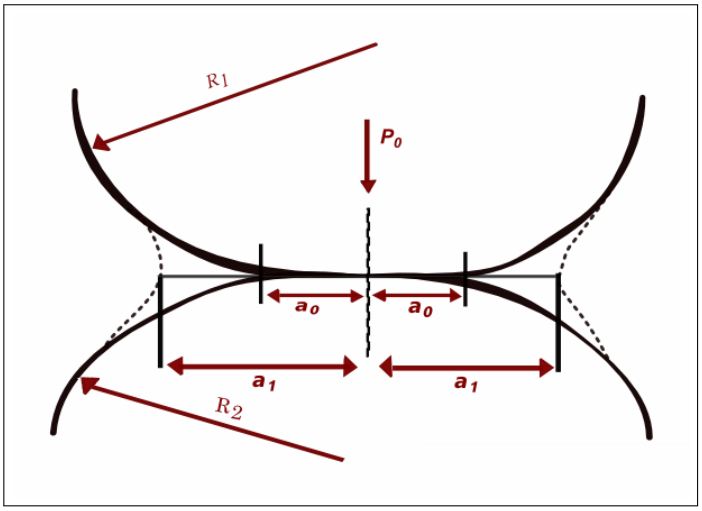

Figure 2.3: A schematic diagram shows a comparison between the contact radius a_0 predicted by Hertz (the solid line) and a_1 predicted by JKR (the dotted line). The difference in the value of the contact radii, a_0 and a_1, is that a_1 is affected by the attractive force at the interface of the two elastic solids [35].

Accordingly, equation (2.10) reverts to the Hertz equation (2.6) when W_{adh} equals zero. Consequently, the contact radius, a_{JKR}, becomes finite when the load ($P_{\perp}$) in the JKR model is zero, and so equation (2.10) becomes

$$a_{\text{JKR}} = \left(\frac{6\,\pi\, W_{adh}\, R^2}{K} \right)^{\frac{1}{3}}. \tag{2.11}$$

In order to separate two adhered surfaces, a pull-off force ($P_{\text{pull-off}}$) must be applied, which must be negative in order to overcome the adhesive force. When the pull-off force, $P_{\text{pull-off}}$, is applied, the contact diameter, $2a$, at the interface decreases and so as to allow the separation to take place. The pull-off force is given by

$$P_{\text{pull-off}} = -\frac{3}{2}\,\pi\, W_{\text{adh}}\, R\,. \tag{2.12}$$

Stronger adhesion at the interface between two surfaces requires a larger pull-off force to detach them. The JKR model, therefore, supplies a new experimental technique to measure the W_{adh} at the interface between two elastic surfaces. Since its publication, therefore, the JKR model has been used extensively in studies of adhesion contact mechanisms, since it is able to show mathematically the dependency of the contact radius at the adhesive interface, applied force and their elastic moduli on the adhesion force [34, 46, 50].

2.2.4 DMT Theory

Another model for the contact mechanism between two spherical bodies under a load was proposed by Derjaguin, Muller, and Toporov (DMT) in 1975 [53]. The DMT theory assumes that the adhesion between the spheres originates from long-ranged attractive forces, although the spheres shape outside the interface is assumed to be Hertzian, and is hence not deformed by these attractive forces. The DMT theory is applicable for small spherical bodies with small radii, low adhesion and high elastic modulus. The DMT contact radius (a_{DMT}) is given by

$$a_{\mathrm{DMT}}^3 = \frac{R}{K}\Big(P + 2\,\pi\,W_{\mathrm{adh}}\,R\Big). \tag{2.13}$$

The DMT pull-off force ($P_{\mathrm{c(DMT)}}$), therefore, is a critical force required to detach the adhered surfaces when a negative load is applied [47, 54], and is given by

$$P_{\mathrm{c(DMT)}} = -2\,\pi\,W_{\mathrm{adh}}\,R. \tag{2.14}$$

So, the contact radius, $a_{0(\mathrm{DMT})}$, at zero load is given by

$$a_{0(\mathrm{DMT})} = \left(\frac{2\,\pi\,W_{\mathrm{adh}}\,R^2}{K}\right)^{\frac{1}{3}}. \tag{2.15}$$

The pull-off force equations (2.14) and (2.12) of the DMT and JKR models give different values since they describe two different extreme situations. As a consequence of this, much debate has raged which model is the correct one to use in studying the contact mechanism. In this regard, Tabor proved that both the DMT and JKR models are valid for the contact mechanism, but that each one describes the opposite extremes of the same phenomenon [55]. Hence, Tabor established a dimensionless parameter (μ) given by

$$\mu = \left(\frac{R\, W_{\text{adh}}^2}{K^2\, \varepsilon^3} \right)^{\frac{1}{3}}, \tag{2.16}$$

where ε is the equilibrium distance in the Lennard-Jones potential.

The JKR model is applicable to elastic spheres with large radii, where $\mu > 5$. In contrast, the DMT model is applicable to rigid spheres with small radii, where $\mu < 0.1$.
As the debate has continued about choosing a suitable theory (JKR or DMT) to explain the contact mechanise between two adhering surfaces, another dimensionless parameter was also introduced by Maugis-Dugdale (MD), called the transition parameter (λ). The λ is related to (μ) by the following equation

$$\lambda = 1.16\, \mu. \tag{2.17}$$

The MD model is built on a numerical calculation for the DMT and JKR theories and consequently it is close to the DMT curve when $\lambda < 0.1$, while it is closer to the JKR curve when $\lambda > 5$ [43, 46, 47].

2.3 Stress Distribution

When two bodies are in contact with each other under a vertical load ($P_{\perp}$), there is another important parameter in their contact mechanism must be taken into consideration that is the stress distribution (σ). In the Hertz model, there is no attractive force at the interface between two bodies in contact and as a consequence of this the stress distribution is given by

$$\sigma_{\text{H}} = -\frac{3P_{\text{H}}}{2\pi a^2} \sqrt{1 - \left(\frac{r^2}{a^2} \right)}, \tag{2.18}$$

where r is the radial distance from the axis of symmetry of the contact, a is the contact radius and P_{H} is the applied load. The negative sign refers to the fact that the stress is compressive. The stress distribution in the Hertz model, therefore, is larger at the central area of the contact radius, but it decreases towards the edge.
In the case that there are adhesive forces at the interface between two bodies in contact, a tensile force (P) is introduced that is less than the applied load (P_{H}). The system of the two

adhering surfaces will undergoes a tensile stress that is given by

$$\sigma_{\text{adh}} = -\frac{3P_{\text{H}} - P}{2\pi a^2}\sqrt{1-\left(\frac{r^2}{a^2}\right)}\,, \tag{2.19}$$

The stress distribution is small at the contact area making an infinite stress at the interface in the presence of adhesive forces [47,54]. Whereas, the stress distribution in the JKR model, which combines between the Hertz model and the adhesion force, can be given by

$$\sigma_{\text{JKR}} = \sigma_{\text{H}} + \sigma_{\text{adh}}\,. \tag{2.20}$$

Figure 2.4 compares the previously mentioned classical contact mechanics theories in terms of the stress distribution and shape profiles.

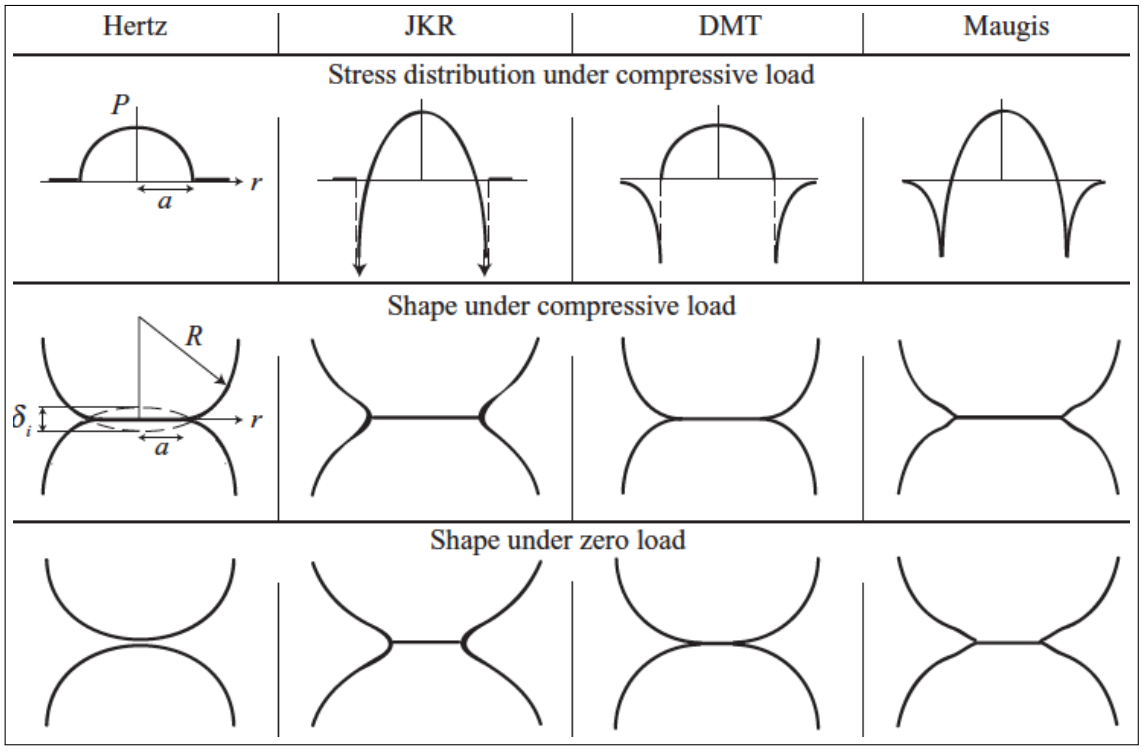

Figure 2.4: A schematic diagram showing a comparison between the contact radius in different adhesion theories. Image adapted with permission from [54]. Copyright (2013) John Wiley and Sons.

A summary can therefore be provided for all the above mentioned adhesion contact models:

- In the Hertz model, no surface forces are considered at the interface of the two rigid

spheres and they are separated under zero load since they are rigid, frictionless and smooth bodies. Also, the Hertz stress distribution under a normal compressive load is greater at the centre of the contact area of the spheres, but lower at the edges [47].

- In the JKR model, short-range adhesion forces are considered at the interface of the contact area and it is functionalised with the work of adhesion. Hence, the contact area in the JKR model is greater than in the Hertz model under a normal compressive load. These adhesive forces are limited to the contact area only, however, and are not present at the edges [47].

- In the DMT model, long-range surface forces are acting outside the radius of the contact area. The DMT assumes a Hertzian shape but with no interaction inside the contact radius at the interface [47].

- In the MD model, an approximation was built that defines if the adhesion between surfaces is based on either the DMT model (for $\lambda < 0.1$) or the JKR model (for $\lambda > 5$). Meaning that the MD contact mechanism is in-between the DMT and JKR when the λ value is between 0.1 and 5 [47].

Chapter 3

Polyelectrolytes: Polymer Brushes and Hydrogels

3.1 Introduction

Polyelectrolytes (PEs) are a class of polymers whose monomers become charged when they dissolve and dissociate in solution. There are many examples of PEs found in nature such as DNA, proteins and cellulose [56]. The polyelectrolytes are classified into two types depending on the strength of the charges on their polymeric chains: *strong* and *weak* polyelectrolytes. The difference between strong and weak PEs is that the degree of association (f) of the ionisable groups of the strong PEs is fixed and not affected by environmental changes. In contrast, the charges on the ionisable group of the weak PEs are not fixed and thus are controllable by applying an external environmental change, such as changing the pH level, temperature degree or by adding salt [57, 58].

Generally speaking, weak PEs, consisting of monomers carrying negative charges, are known as polyacids (polyanions), while those carrying positive charges are known as polybasics (polycations). When the ionisable end-group of the weak PEs becomes charged in a solution, the chain stretches away (self-repelling) as a result of Coulombic interactions, which can act over a long distance. The chain of a weakly charged PE collapses, however, when it becomes neutral as a result of the hydrophobicity in some solutions [27, 59].

This chapter will discuss the polyelectrolyte conformation inside solutions and the charging mechanisms of the weak and strong polyelectrolytes. The general features of the polyelectrolyte brush and hydrogel, their types, their preparation techniques and also their applications will be reviewed.

3.1.1 The Conformation of a Polyelectrolyte Chain in Solution

Polymers consist of monomers with high molar mass linked together via covalent bonds. The molar mass (M_{m}) of a polymer is determined by the number of monomers (N) on the chain, where the length (L) of the chain is given by

$$L = Na, \tag{3.1}$$

where a is the effective monomer size.

Since the chains can rotate freely in space as each link between monomers has a different orientation, the path of a polymer chain is a random walk. This means that when the polymer chain is an ideal random walk in a theta solvent, the end-to-end distance (R) of a polymer is given by [60]

$$R = aN^{\frac{1}{2}}. \tag{3.2}$$

The expanding (swollen) conformation of polymer chain is governed by the Coulomb interactions between their monomers, although the chain cannot intersect itself. The expanding conformation of a polymer chain that has already been diluted in a good solvent can, therefore, be given by a scaling law

$$R = aN^{\frac{3}{5}}. \tag{3.3}$$

3.1.2 The Debye-Hückel Theory of Charge Screening

The presence of free ionic charges in a PE system can have an effect on the swelling behaviour of the polymeric chains, since the counterions can be trapped and prevented from diffusing along the chain as a result of the high osmotic pressure. The Bjerrum length (ℓ_{B}) is used to

estimate the distance at which the Coulombic interactions between two units of charges are equivalent to their thermal energy ($k_{\mathrm{B}}T$), and is given by

$$\ell_{\mathrm{B}} = \frac{e^2}{4\pi\epsilon k_{\mathrm{B}}\, T}\,, \tag{3.4}$$

where e represents the single electronic charge (1.6022×10^{-19} C), ϵ is the medium dielectric constant, given by $\epsilon = \epsilon_0\, \epsilon_{\mathrm{r}}$ (ϵ_0 is the permittivity in free space and ϵ_{r} is the medium relative dielectric constant), k_{B} is the Boltzmann constant, and T is the absolute temperature.

Peter Debye and Erich Hückel made an important assumption about ionic solutions that contribute to the distribution of the counterions in electrolyte systems. The Debye-Hückel theory describes the potential distribution of electrolyte solutions and it assumes that Coulombic (repulsive and attractive) interactions are responsible for the ions' deviation from ideal behaviour in solutions [27, 59].

When salt is added to a PE system, the Coulombic interactions of the charged monomers are screened by salt ions. The Debye screening length (ζ_{D}) can therefore be used to assume the distance between the ionisable groups and the counterions that have been affected by the disappearance of the repulsive forces. Hence, the electrostatic potential (V) of the polymer chains in this system is given by

$$V(r) = \frac{e}{4\pi\epsilon\epsilon_0 r} \exp - \frac{r}{\zeta_{\mathrm{D}}}, \tag{3.5}$$

When the distance between two electric charges r is $\ll \zeta_{\mathrm{D}}$, the charges are not screened and the potential V is active. Whereas, the Debye screening length ζ_{D} decreases when ($r \gg \zeta_{\mathrm{D}}$) since the salt ions are copiously added to the system, ultimately causing the Coulombic forces to disappear [26, 27, 59].

3.1.3 Osmotic Pressure

Osmotic pressure (Π) is defined as the minimum pressure required to prevent the diffusion of the inward flow of water across a semi-permeable membrane. The osmotic pressure is developed in a system as a result of the large molecules that cannot diffuse through the semi-permeable membrane. The osmotic pressure of a neutral polymer at a low concentration in a

diluted solution is controlled by the polymer density (c_{p}), and this is given by

$$\Pi = k_{\mathrm{B}}\, T\, \frac{c_{\mathrm{m}}}{N}\,, \tag{3.6}$$

where c_{m} is the polymer concentration in a dilute solution that is given by

$$c_{\mathrm{m}} = N\, c_{\mathrm{p}}. \tag{3.7}$$

The osmotic pressure is usually observed when the larger molecules get trapped and are not able to diffuse into a semi-permeable membrane. If the polymer is a polyelectrolyte, however, this observation will be different since the counterions are small enough to diffuse through, which leads to an increase in the volume of the polymer until it reaches an equilibrium. The osmotic pressure is given by

$$\frac{\Pi}{k_{\mathrm{B}}\, T} = \frac{c_{\mathrm{m}}}{N} + \phi_{\mathrm{i}0}\, c_{\mathrm{m}}\,, \tag{3.8}$$

where $\phi_{\mathrm{i}0}$ is the fraction of the charged polymer.

When the counterions are dominated by the attractive force of the polymer charged groups and thus condense on the polymer chains, the second term for a dilute polyelectrolyte solution is given by

$$\frac{\Pi}{k_{\mathrm{B}}\, T} \approx \phi_{\mathrm{i}0}\, c_{\mathrm{m}}\,. \tag{3.9}$$

After adding salt into a PE system, the counterions start to condense on the charged chains until the system reaches neutrality. This allows an equal number of both negative and positive charges to move in all directions at equilibrium, and this phenomenon is called the Donnan effect [59, 61].

3.1.4 Charged Polyelectrolytes

Polyelectrolytes become charged when they are dissolved inside an appropriate solvent and their charges are carried on their monomers [56]. The association-dissociation equilibrium of a PE, however, determines if it is considered as a strong or weak polyelectrolyte.

3.1.4.1 Strong Polyelectrolytes

As mentioned at the beginning of this chapter, strong polyelectrolytes have charges that are fixed to a particular chemical group and are not affected by external triggers such as pH or salt concentration. Strong PEs, therefore, dissociate completely inside favourable solutions by donating (or accepting) a proton immediately and permanently, thus becoming fully charged. Hence, strong PEs are not affected by any change in their environmental parameters. In other words, strong PEs will become, and remain, fully charged when they dissolve in water [59].

3.1.4.2 Weak Polyelectrolytes

In contrast, the charges of weak PEs are unfixed and thus they can be influenced by changes in their environment. The degree of the dissociation (f) of weak polyelectrolytes can therefore be controlled (i.e. whether they become charged or uncharged) by varying the environmental parameters such as pH, ionic strength, or temperature. The electrostatic charges of weak polyelectrolytes are directed by an equilibrium between association and dissociation and, because of this, each monomer has the ability to be charged at a given instant, and its charge is free to move, as long as the overall equilibrium charge fraction is conserved [62].
Weak PEs are called '*stimuli-responsive*' polymers since their charges can be switched on or off by (being charged or uncharged) inside their controlled environment. This characteristic, along with their high biocompatibility, is why stimuli-sensitive PEs are used extensively within numerous technological applications such as drug delivery systems, artificial muscles and biomaterials, and they have also been used for surface coating, printing and adhesion [54, 63, 64]. Polyelectrolytes are sorted into two classes: weak polyacids and weak polybases.

3.1.4.3 Acids and Bases

The acid and base components are called electrolytes since they form ions after dissolving in water. In 1884, Arrhenius introduced the definition of acid and base substances and linked it to the chemical reaction output. A substance is called an acid when it dissolves in water and releases H^+ ions and a base when it dissolves in water and releases OH^- ions [65]. For example, hydrochloric acid (HCl) is a strong acid and, when it dissolves in water, it will donate a proton H^+ to a water molecule, as is shown by

$$HCl + H_2O \longrightarrow H_3O^+ + Cl^- . \tag{3.10}$$

Arrhenius' definition for acid and base was considered to be restrictive because there are some chemical reactions that combine both acid and base reactions, such as when HCl reacts with ammonia, NH_3. Another definition of acids and bases was therefore introduced by Johannes Brønsted and Thomas Martin Lowry in 1923, called the Brønsted-Lowry model. This model classified the components of a reaction into either acids or bases based upon their chemical reactions by

$$HB + A^- \rightleftharpoons HA + B^- , \tag{3.11}$$

where the species in the forward and backward reactions of HB and HA are Brønsted-Lowry acids, while A^- and B^- are Brønsted-Lowry bases.

The rules of the Brønsted-Lowry model can be summarised as follows:

- An acid is a proton donor, and is called a Brønsted acid.
- A base is a proton acceptor, and is called a Brønsted base.
- When a proton is transferred between an acid and a base, it is called a Brønsted acid-base reaction.

Since the Brønsted-Lowry model was limited for some chemical reactions that do not involve proton transfer, in the same year that it was originally proposed, Gilbert Lewis extended it [66, 67]. A Lewis acid is defined as the species that can accept a pair of electrons and then

form a new covalent bond. A Lewis base is the species that can donate a pair of electrons and then form a new covalent bond [65].

3.1.4.4 Strong and Weak Acids or Bases

Acids and bases are divided into strong and weak depending on their ionisation range when they dissolve in water. When a strong acid (or a strong base) is dissolved in water, it becomes totally ionised. In contrast, a weak acid (or a weak base) is partially ionised when it dissolves in water. An example of a strong acid is hydrochloric acid (HCl), since when it dissolves in water it forms (H^+) ions and (Cl^-) anions and undergoes dissociation [66]:

$$HCl \longrightarrow H^+ + Cl^- . \tag{3.12}$$

A weak acid, such as acetic acid ($CH_3\,COOH$), will dissolve partially in water and form hydronium acetate ions, but this reaction does not go to completion, as shown by the double arrows in the reaction [68]

$$CH_3\,COOH + H_2O \rightleftharpoons CH_3\,COO^- + H_3O^+ . \tag{3.13}$$

Bases, like acids, are also sorted into weak and strong, but they form OH^- ions and cations when they dissolve in water. Sodium hydroxide (NaOH), for example, is a strong base and its dissociation in water can be given by

$$NaOH \longrightarrow Na^+ + OH^- . \tag{3.14}$$

Weak bases differ from strong bases in their reaction with water. A weak base gains protons after it dissolves in water and leaves OH^- ions behind, such as ammonia's (NH_3) reaction with water [66]

$$NH_3 + H_2O \rightleftharpoons NH_4^+ + OH^- . \tag{3.15}$$

Overall, the ionisation reaction of acids and bases is detected by an ionisation constant (K_a) for acids or (K_b) for bases, which are used to find the values of the conjugate acid or base concentrations. The dissociation constant (K_a) of a weak acid (HA) is, therefore, given by

$$K_{\mathrm{a}} = \frac{\left[\mathrm{H}^{+}\right]\left[\mathrm{A}^{-}\right]}{\left[\mathrm{HA}\right]}\,, \tag{3.16}$$

where $\left[\mathrm{HA}\right]$ is the weak acid concentration, $\left[\mathrm{H}^{+}\right]$ is the conjugate acid concentration and $\left[\mathrm{A}^{-}\right]$ is the conjugate base, as shown in the reaction

$$\mathrm{HA} \rightleftharpoons \mathrm{H}^{+} + \mathrm{A}^{-}\,. \tag{3.17}$$

In the case of a weak base (B), the dissociation constant (K_{b}) is given by

$$K_{\mathrm{b}} = \frac{\left[\mathrm{BH}^{+}\right]\left[\mathrm{OH}^{-}\right]}{\left[\mathrm{B}\right]}\,, \tag{3.18}$$

where $\left[\mathrm{B}\right]$ is the weak base concentration, $\left[\mathrm{BH}^{+}\right]$ is the conjugate acid concentration and $\left[\mathrm{OH}^{-}\right]$ is the conjugate base, as shown in the reaction

$$\mathrm{B} + \mathrm{H_2O} \rightleftharpoons \mathrm{BH}^{+} + \mathrm{OH}^{-}\,. \tag{3.19}$$

The ratio of the the conjugate acid or base concentrations can be found by knowing the pH value and the (K_{a}) for the acid or (K_{b}) for the base by using

$$\left[\mathrm{H}^{+}\right] = K_{\mathrm{a}} \times \frac{\left[\mathrm{HA}\right]}{\left[\mathrm{A}^{-}\right]}\,. \tag{3.20}$$

By taking the negative logarithm for both sides

$$\mathrm{pH} = pK_{\mathrm{a}} - \log\frac{\left[\mathrm{A}^{-}\right]}{\left[\mathrm{HA}\right]}\,. \tag{3.21}$$

where pH is the negative logarithm of $\left[\mathrm{H}^{+}\right]$, which is the concentration of the H^{+} ions that have been released from the acid. In the case of a weak base

$$\mathrm{pOH} = pK_b + \log\frac{\left[\mathrm{BH}^{+}\right]}{\left[\mathrm{B}\right]}\,, \tag{3.22}$$

where $\left[\mathrm{BH}^{+}\right]$ is the concentration of the conjugate acid. The values of K_{a} and K_{b} can therefore be given by

$$pK_{\mathrm{a}} = -\log\left(K_{\mathrm{a}}\right), \tag{3.23}$$

or by

$$pK_{\mathrm{b}} = -\log\left(K_{\mathrm{b}}\right). \tag{3.24}$$

An acid can be defined as weak or strong depending on the value of the acid ionisation constant (pK_{a}) :

1) It is a weak acid when pK_{a} is > 3 $\left(K_{\mathrm{a}} < 10^{-3}\right)$.

2) It is a strong acid when $\mathrm{p}K_{\mathrm{a}}$ is < 1 $\left(K_{\mathrm{a}} > 10^{-1}\right)$.

3) It is a moderate acid when pK_{a} is $1 < \mathrm{p}K_{\mathrm{a}} < 3$ $\left(K_{\mathrm{a}} = 10^{-1} \text{ to } 10^{-3}\right)$ [69].

3.1.5 Stimuli-Responsive Polyelectrolytes

'*Smart-responsive*' PEs are an important class of polymers that are able to change their physical, chemical, optical, mechanical, wettability, adsorptive and adhesive properties after applying an environmental trigger, such as changing the pH level or alternating ionic strength. Stimuli-responsive polymers are described as '*smart*' reconstructable materials, due to their ability to switch between the charged and uncharged state, and thus these materials have become of great significance in a diverse range of applications across materials science, biotechnology and nanotechnology [15, 54].

Responsive polymer materials can be formed in two different architectures that are either

1) two-dimensional systems (2D) of thin polymer films such as polymer brushes, or

2) three-dimensional (3D) systems such as polymer gels [16, 30, 70, 71].

Since polymer brushes and gels were mainly used in this PhD project; the following sections (3.2) and (3.3) review their features, behaviours in solution and their applications.

3.2 Polyelectrolyte Brushes

During the past fifty years, researchers have showed an increased interest in studying polymer brushes in a vast variety of different high-tech areas. In the 1950s, polymer brushes received attention after it was discovered that flocculation of colloidal particles was prevented by grafting polymer molecules to the colloidal particles so as to suspend them in solvent, achieving their stabilisation, and preventing their overlapping [72]. Subsequently, many theoretical approaches were introduced to study and understand the behaviour of polymer brushes. These studies were limited, however, by an inability to characterise the grafted layers of polymer brushes accurately [73].

In recent years, there has been an increasing development in polymer brushes using surface-grafted architectures as '*soft*' building blocks at the nanoscale that enable practical nanotechnology with highly tailored structures. The chemical composition, thickness and grafting density of polymer brushes allows the control of their swelling behaviour and electrostatic interactions in many potential applications [74].

3.2.1 General Features of Polymer Brushes

Polymer brushes refer to the polymer chains that are grafted onto a planar surface and attached by anchor points with a defined grafting density that allows them to stretch away from the surface. The stretching behaviour of the polyelectrolyte brushes is caused by the segment-segment interactions between the polymer molecules, which leads to a strong loss of the conformational entropy. These polymeric brushes can be synthesised either by a single homopolymer component or by several different block copolymers. Nevertheless, it has been found that mixed polymer brushes (at least two types of polymers grafted on the same substrate) can have a broadening range of switching properties [30, 31].

Weak PE brushes are usually described as '*smart-responsive*' layers since they respond to different external triggers, such as temperature, pH, light, voltage and pressure [75, 76]. The structural conformation of the polymer brushes is controlled by two parameters: the number of monomers in the chain (N) and the average distance between the polymer chains (d). Hence, the brush conformation is affected by the grafting density (σ) of the brush system, which is defined as the number of grafted chains in a square area of the segment size (a^2),

given by

$$\sigma = \frac{a^2}{d^2}\,. \tag{3.25}$$

When polymer brushes are placed inside a solvent, their responsive behaviours have different observations. In a good solvent, the polymer chains expand as a result of the dominance of the interaction between monomer and solvent molecules. In a poor solvent, in contrast, the polymer chains are collapsed due to the entropy that minimises the chains' contact with the solvent. There is also an intermediate polymer brush conformation for a neutral solvent, which lies between the case of the good solvent and the poor solvent, and which is called the theta solvent. Here, the interactions between the chains and solvent are equal to monomer-monomer interactions and so the chains are effectively inert to the surrounding solvent and to themselves.

There are, therefore, two basic conformations for the grafting density of the attached chains of polymer brushes:

1) A low grafting density, where $d > R$, and where the chains form a 'mushroom conformation' since they are far from each other and there is no interaction between them and the surface (as shown in Figure 3.1 (a)).

2) A high grafting density, where $d < R$, and where the chains form a 'brush conformation' since they expand in order to avoid each other (as shown in Figure 3.1 (b)).

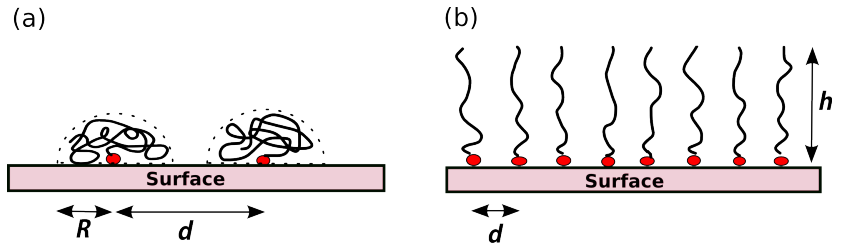

Figure 3.1: A schematic diagram of polymer chains anchored on a surface, the stretching conformation in (a) is called the 'mushroom conformation' and in (b) the 'brush conformation'. Where R is the gyration radius of the chains and d is the distance between adjacent anchor points. The chains take a mushroom conformation if $d > R$, while chains will stretch vertically, with a height h, and repel each other when $d < R$.

The gyration radius (R) of a polymer chain in a good solvent is given by the Flory equation (3.3). The swelling behaviour of the charged PE brushes results from the balance between the electrostatic interaction and the osmotic pressure of the counterions inside the brush. The PE brushes are therefore divided into strong or weak types, with each type being governed by a specific swelling model [75, 77].

3.2.2 Strong Polyelectrolyte Brushes

The strong PE brushes are called 'quenched brushes' since the charge numbers and their positions on the chains are fixed and are not affected by changes in the environment [77]. The scaling theories for the swelling behaviour of the strong PE brushes were introduced to understand the behaviour of such systems since they exhibit different structural conformations depending on the degree of dissociation (f) and grafting density of the brushes (σ) and also the ionic strength of their surrounding solution. In the case of a dense and thick system, quenched brushes undergo osmotic pressure leading to the trapping of the counterions inside the brushes.

Pincus [78] introduced a scaling theory for strong PE brushes, called osmotic brushes (OB), in a salt-free good solvent. The height (h) of the strong polyelectrolyte brushes can be calculated by the balance between the osmotic pressure of the counterions and the restoring force of the stretched chains. This means that the brush height (h_{OsB}) of the swollen surface-attached brush in a good solvent is given by

$$h_{\mathrm{OsB}} \approx N.a.f^{1/3}\,. \tag{3.26}$$

where N is the degree of polymerization and a is the segment length.

The osmotic pressure of such a system can be calculated by

$$P_{\mathrm{osm}} = \frac{1}{2}\,v\,c^2\,k_{\mathrm{B}}\,T\,. \tag{3.27}$$

where v is the excluded volume and c is the segment concentration.

This theory was also applied for poor or theta solvents for strong polyelectrolyte brushes where the excluded volume interactions are not neglected. The excluded volume is the space

occupied by a macromolecule that cannot be used by another molecule in the same dilute solution. The excluded volume is a function of the solvent quality since it is affected by the energy of mixing the solvent and the polymer. This theory of quenched brushes, however, is considered simpler than the theory of weak PE brushes since the charges are fixed. The height of strong polyelectrolyte brushes in poor solvents is given by

$$h_p \approx N.a.f, \tag{3.28}$$

While in the case of theta solvents, the brush height is given by

$$h_\theta \approx N.a.f^{1/2}\,. \tag{3.29}$$

The height of strong PE brushes decreases with the addition of salt since the increasing concentration of salt ions screen the charges on the chains [77, 79]. This behaviour of strong PE brushes is called 'salted brushes' and thus their length (h_{salt}) becomes a function of the concentration of the added salt ions (c_{s}) as

$$h_{\text{salt}} \approx N.a.c_{\text{s}}^{-1/3}.\sigma^{1/3}\,. \tag{3.30}$$

3.2.3 Weak Polyelectrolyte Brushes

The scaling theory for the swelling behaviour of weak PE brushes is more complex than strong PE brushes due to their charge switchability (i.e. instability) when the environmental condition is changed [80]. The swelling behaviour of weak PE brushes can, however, be said to be controlled by their charge density since the charges are not fixed and ions can move freely along the chains. The first theoretical descriptions to understand the behaviour of weak PE brushes appeared in the 1990s [78, 79], although little progress in their synthesis had been achieved.

The behaviour of the equilibrated weak PE brushes is described according to their presence in two different types of solutions: 1) in a *salt-free* solution, and in this case the brushes are called 'osmotic brushes' (OsB); and 2) in *a salt* solution, whereupon the brushes are called 'salted brushes' (SB).

An example of the swelling behaviour of weak PE brushes is weak acid polyacid brushes (e.g. carboxylic groups) where the proton dissociation yields chain end-groups of a carboxylic group with negative charges [81]. This means that the charge density in this system is governed by the acid-base equilibrium, which was given previously in equation (3.16).
Thus, the degree of the dissociation (α) is given as a function of the local concentration by

$$\alpha = \frac{\left[\mathrm{A}^-\right]}{\left[\mathrm{A}^-\right] + \left[\mathrm{HA}\right]} \,. \tag{3.31}$$

A numerical self-consistent-field (SCF) model [82,83] is used to analyse the swelling of polymer brushes and assumes that the half-space next to a surface can be divided into parallel layers of thickness d and numbers $z = 1, 2, ..., M$ $\big($where M is sufficiently large$\big)$. In order to define the statistical weight of a free segment (A) that is in a specific layer z, a new parameter is introduced, called the effective weighting $\big(G_{\mathrm{A}}(z)\big)$, which is given by

$$G_{\mathrm{A}}(z) = e^{-U_{\mathrm{A}}(z)/k_{\mathrm{B}}\,T} \,. \tag{3.32}$$

As a consideration of this acid-base equilibrium in each layer, the effective weighting $G_{\mathrm{A}}(z)$ for A segments that can be introduced in two states is given by

$$G_{\mathrm{A}}(z) = \alpha^{\mathrm{b}} G_{\mathrm{A}\text{-}}(z) + \big(1 - \alpha^{\mathrm{b}}\big) G_{\mathrm{HA}}(z) \,, \tag{3.33}$$

where $\big(G_{\mathrm{HA}}(z)\big)$ is the true weighting for the (HA) segment and $\big(G_{\mathrm{A}\text{-}}(z)\big)$ is that for the (A^-) segment. Hence, the degree of dissociation of a polyacid segment in the bulk (α^{b}) can be given by

$$\alpha^{\mathrm{b}} = \frac{K_{\mathrm{a}}}{K_{\mathrm{a}} + \left[\mathrm{H}^+\right]} = \frac{\left[\mathrm{A}^-\right]}{\left[\mathrm{A}^-\right] + \left[\mathrm{HA}\right]} \,. \tag{3.34}$$

The weighting of A^- and HA segments are expressed by

$$G_{\mathrm{A}}(z) = \frac{\left[\mathrm{A}^-\right](z)}{\left[\mathrm{A}\right](b)} \quad \text{and} \quad G_{\mathrm{HA}}(z) = \frac{\left[\mathrm{HA}\right](z)}{\left[\mathrm{HA}\right](b)} \,. \tag{3.35}$$

Therefore, the dissociation α in layer z in equation (3.31) can be written as

$$\alpha(z) = \frac{\alpha^{\mathrm{b}} G_{\mathrm{A}^-}(z)}{G_{\mathrm{A}}(z)}\,, \tag{3.36}$$

By combining equations (3.33) and (3.36), α can be written as

$$\alpha = \frac{\alpha^{\mathrm{b}}}{\alpha^{\mathrm{b}} + \left(1 - \alpha^{\mathrm{b}}\right) e^{-\mathrm{y}}}\,, \tag{3.37}$$

where $e^{-\mathrm{y}}$ is defined as the Boltzmann factor of the local electrostatic potential ($y(\mathrm{z})$) and is given by

$$e^{-\mathrm{y}}(z) = \frac{G_{\mathrm{A}^-}(z)}{G_{\mathrm{HA}}(z)}\,. \tag{3.38}$$

For weak PE brushes, the local electrostatic potential $y(z)$ is negative and $G_{\mathrm{HA}}(z)$ is larger than $G_{\mathrm{A}^-}(z)$, and so equation (3.36) can be re-written by substituting it into equations (3.34) to obtain

$$\alpha(z) = \frac{K_{\mathrm{a}}}{K_{\mathrm{a}} + \left[\mathrm{H}^+\right] e^{-\mathrm{y(z)}}}\,. \tag{3.39}$$

Since the height (h) of the weak PE brushes is proportional to the charge density and the length of the chain in the salt-free solutions (OsB), which swells by the osmotic pressure, the thickness h scales on

$$h \approx N\alpha_0{}^{1/2}\,. \tag{3.40}$$

In contrast, the height of the PE brushes in the salt solutions $\big($the salted brushes (SB)$\big)$ depends on the salt concentration (n_{s}) and observes the following rules [77, 78, 81]:

- At high salt concentrations, weak PE brushes behave in a similar way to the strong brushes. As long as the salt concentration is increased, the height of the brushes decreases, and so the scaling behaviour for the salted brushes can be given by

$$h_{\text{salted}} \approx N(\alpha^{\text{b}})^{2/3}\sigma^{1/3}n_{\text{s}}^{-1/3}\,. \tag{3.41}$$

- At low salt concentrations, weak PE brushes are in the OB regime and their height can be given by

$$h_{\text{osmotic}} \approx N\sigma^{-1/3}n_{\text{s}}^{1/3}\,. \tag{3.42}$$

The last equation (3.42) shows that increasing the salt concentration will increase the brush height as a result of the osmotic pressure that leads to stretching of the chains. Adding more salt will increase the degree of the dissociation of the acidic groups of the weak PE brushes and results in increased stretching of the chains [77, 81].

As in the case of polyacid brushes considered previously, polybase brushes can be treated equivalently to what has been presented here. In that case, however, the equilibrium constant will be K_{b} and the uncharged brush segment will be B. The polybase brushes will become positively charged as a result of the dissociation of an OH^- group and yields HB^+ ions.

3.2.4 Polymer Brush Synthesis

Generally speaking, forcing polymer molecules to form into 'brush-like' conformations requires a sufficiently high strength anchoring of the molecules to connect the polymer brush irreversibly to a substrate. The grafted brushes on a substrate stretch when their grafting density is so high due to the sufficient repulsive monomer-monomer interactions on the chains. The synthesis of the end-grafted polymer brush layer is achieved experimentally by two main approaches: 1) by the physical adsorption of a polymer into a substrate; called 'physisorption' , or 2) by the chemical adsorption of a polymer into a substrate; called 'chemisorption' [31, 75, 77, 84, 85].

3.2.4.1 Physisorption

Polymer brushes that are made using a physisorption approach usually consist of two block copolymers, where one part can strongly attach to the interface, acting like an 'anchor', while the other part extends to generate the polymer layer, since it has stronger interactions with

the solvent than with the surface (Figure 3.2). Block copolymers are made up of blocks of different polymerised monomers.

The main drawbacks of this approach is that there is poor control of the grafting density of the brush layer when polymer brushes exhibit thermal and solvolytic instability. Furthermore, the interaction of physisorpted brushes with the surface is based on long range and weak Van der Waals interactions, which are weaker than the covalently bonded brushes.

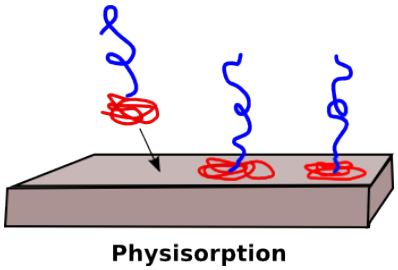

Figure 3.2: A schematic diagram of the physisorption approach of two block copolymers, which are represented by two different colours of chains. The red chains represent the adsorbed 'anchor' block to a substrate, while the blue chains represent the floating chains in a solvent that stretch away from the surface.

3.2.4.2 Chemisorption

The approach of chemisorption refers to the covalently bonded chain to a planar substrate and it can be achieved with either '*grafting-from*' or '*grafting-to*' techniques, although both these chemisorption approaches serve to provide strong bonding between polymer brushes and their substrate [31, 75, 84, 85].

3.2.4.2.1 '*Grafting-From*'

The '*grafting-from*' technique allows for a higher grafting density of the polymer brush layer comparing to the '*grafting-to*' technique. This technique is widely used for making both neutral and charged PE brushes. The polymerisation of the polymer chains via the '*grafting-from*' requires a prior surface functionalising process, with an initiator molecule, in order to grow the polymer brush on it. The initiator points are made by a self-assembled monolayer (SAM) followed by *in-situ* surface initiated polymerisation to generate the tethered polymer brush (Figure 3.3 (a)). The '*grafting-from*' technique is, therefore, called surface-initiated

polymerisations (SI-ATRP), and this type of polymerisations will be reviewed in more detail in Section 3.2.4.3.

3.2.4.2.2 '*Grafting-To*'

The '*grafting-to*' technique is used to attach polymer chains with defined functionalised end-groups to a surface under appropriate conditions. In order to allow the polymer film to reach the reactive sites on the surface, its chain must diffuse through, and hence the barrier becomes more pronounced after increasing the film thickness (Figure 3.3 (b)). This technique therefore has more limited applications since it produces a brush layer with a very low grafting density and low film thickness [15, 31, 75, 75, 85].

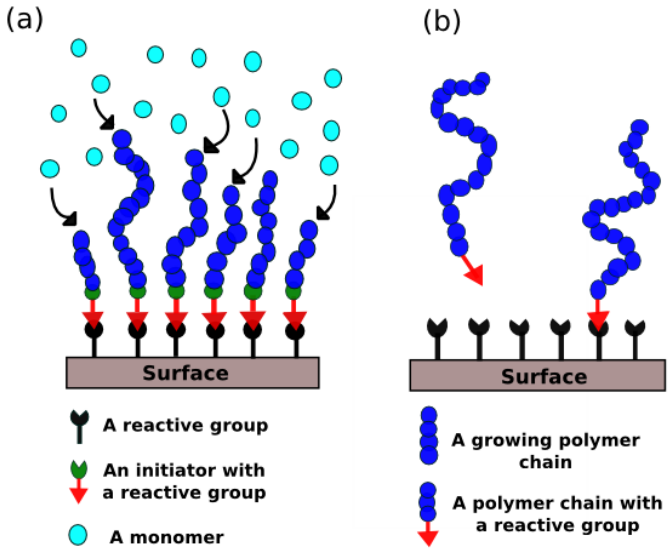

Figure 3.3: A representation of: (a) the '*grafting-from*' and (b) the '*grafting-to*' techniques.

3.2.4.3 Synthesis of Polymer Brush Via SI-ATRP

In 1956, 'living' or 'controlled' polymerisation was discovered by Szwarc [86–88], providing a route to synthesise a polymer brush where the chain termination step and the chain transfer reaction are not present in a given location. Living polymerisation can give a wide range of polymer topologies with the possibility of a low dispersity and a pre-determined molecular

weight. A wide range of monomers can be used to synthesise different polymer structures with special functional groups through living polymerisation.

Living polymerisation has an advantage in respect to producing well-defined polymer structures since it is an inexpensive method that provides an essential control in their production. On the other hand, living polymerisation has disadvantages including a limitation in the number of monomers, high sensitivity to impurities and also the presence of water and long reaction times [89].

The most commonly used technique of controlled polymerisation to produce polymer brushes is atom transfer radical polymerisation (ATRP), which is a relatively modern technique developed in the 1990s [90, 91]. ATRP can produce well-controlled and low dispersity polymer brushes over large areas and is tolerant to a wide range of monomer functionalities. The ATRP polymerisation is a '*grafting-from*' technique used for making polymer brushes where the polymer chains are grown monomer by monomer [15, 31, 75, 75, 85].

The ATRP reaction requires a substrate covered by a self-assembled monolayer of initiator molecules to use as anchoring points in order to grow an individual polymer chain. The grafting density of polymer brushes that are grown by ATRP can therefore be controlled and tuned by mixing initiator molecules with a proportion of an inactive species prior to their deposition. A copper/ligand complex allows a monomer to react at that site by removing the bromine. The equilibrium highly favours the dormant chain at a given time, where a radical is generated by an electron transfer process after activating the dormant species.

The ATRP reaction has been the source of much academic attention due to the simplicity of its setup, relatively inexpensive products, a low concentration of catalysts and its suitability for use with various types of polymers, such as styrenes, methacrylates, acrylates and acrylamides. The initiation and propagation mechanism in the ATRP are described by the following strategies [92]:

Initiation (halogen exchange):

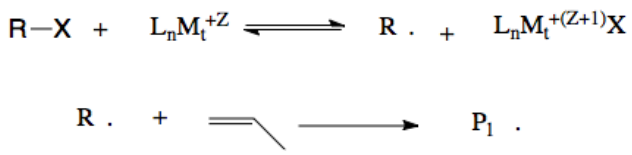

Controlled propagation:

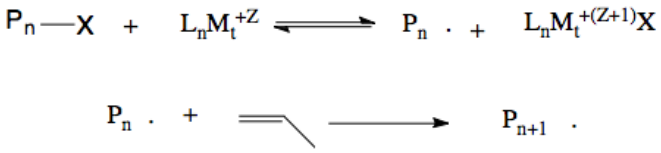

Termination:

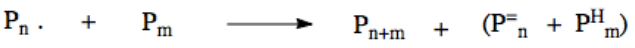

Since the propagation step is much faster than the initiation step in a classical radical polymerisation, the polymer has a wide dispersity. In the initiation step, a monomer is bound to a halogen species that keeps the inactive species P-X mostly in a dormant state. When a transition metal (M) and the catalyst, in the lower oxidation state are added, it reacts with a ligand (L) to form a stable complex. The catalyst is oxidised in the initiation stage, forming a complex with a co-ordinated halide ligand. The propagation radicals (R) result from exchange of the halogen between the dormant species and the transition metal in the higher state of oxidation.

The atom transfer equilibrium constant (K_{ATRP}) is given by

$$K_{\mathrm{ATRP}} = \frac{k_{\mathrm{act}}}{k_{\mathrm{edact}}} \,. \tag{3.43}$$

The kinetics of an ATRP polymerisation is controlled by the rate of polymerisation (v_{p}), which is given by

$$v_{\mathrm{p}} = k_{\mathrm{p}} \frac{k_{\mathrm{act}}}{k_{\mathrm{edact}}} \left[\mathrm{R\text{-}X}\right] \left[\mathrm{M}\right] \frac{\left[\mathrm{CuX}\right]}{\left[\mathrm{CuX_2}\right]} \,, \tag{3.44}$$

where k_{p} is the rate constant for propagation, [R–X] is the concentration of the growing ends, [M] is the concentration of the free monomer in the solution, and [CuX] and [CuX_2] are the concentrations of CuX and CuX_2 , respectively.

The dry thickness (h) of a polymer on the substrate is related to the molecular weight (M_{w}) of the polymer and it is given by

$$h = M_{\mathrm{w}} \frac{\sigma}{\rho \, N_{\mathrm{A}}} \,, \tag{3.45}$$

where σ is the grafting density of polymer, ρ is the density of the polymer, and N_{A} is the Avogadro number [75, 90, 93–95].

3.3 Polyelectrolyte Hydrogels

A polyelectrolyte hydrogel is a three-dimensional crosslinked network that is commonly made from water-soluble polymers where their chains are connected and linked together via physical or chemical crosslinking points. Polymer gels are known as hydrogels when the solvent used is water [32, 33]. Hydrogels have attracted researchers' attention because many are biocompatible, especially after Wichterle and Lim used hydrophilic networks of the poly(2-hydroxyethyl methacrylate) (PHEMA) to make contact lenses in 1960. Since that time, hydrogels have been intensively used in the field of 'tissue engineering' for different pharmaceutical and biomedical applications [81, 96–98].

The most important characteristic of hydrogels is their tunable swelling and de-swelling behaviour inside an aqueous environment. Depending on the chemical structure, most hydrogels are able to respond to different environmental stimuli, such as temperature, pH level, light or the ionic strength [99, 100]. Due to the hydrophilic groups of the polymer network, hydrogels can absorb water, or other favourable solvents, causing swelling and an increase in the network volume. The response of weak PE hydrogels to external stimuli is usually quite clear due to the hydrophobicity and hydrophilicity of the ionic groups on their polymeric backbones, i.e. a reversible swelling and de-swelling behaviour, and therefore they are called *'smart'* materials [14].

Hydrogels are able to absorb a large amount of water without being dissolved, from 10 – 20% up to thousands of times their dry weight [97]. This occurs as a result of the decrease in entropy of mixing of the entire system, which leads to thermodynamically favourable counterions being able to move freely in a solution. The swelling process of the hydrogel is controlled by the osmotic pressure caused by the counterions inside the network, which it terminates by an equilibrium swelling resulting from a balance between the gel elastic energy and the osmotic

pressure of the ions.

The formation process of hydrogels involves crosslinking macromolecular chains together, which is called the gelation process. Gelation leads to progressively larger branched soluble polymers that are called '*sol*' . Sol is defined as a stable suspension of colloidal solid particles in a liquid. As the chain linking process continues, the size of the resulting branched polymer increases with decreasing solubility. This leads to an 'infinite polymer network' and is called a *'gel'*. A gel forms when the homogeneous dispersion in the initial sol rigidifies. The transition from a finite branched polymer to infinite molecules is called the *'sol-gel'* transition [101–103]. In general, hydrogels are classified as *uncharged* (neutral) and *charged* (polyelectrolyte) networks, which vary in their swelling properties. The swelling of neutral hydrogels results from the osmotic pressure that is caused by the solvent-polymer interaction and also by the elastic contribution of the crosslinked chains. In contrast, the swelling behaviour of the charged hydrogels is more complex than the uncharged gels due to the electrostatic interactions on the chains that are induced by an external stimulus, such as the pH, in addition to the effect of the osmotic pressure [99].

Furthermore, hydrogels are subdivided into two types of networks depending on the nature of the crosslinks used in making the polymer gels: *'physical'* and *'chemical'* gels [101].

3.3.1 Physical Gels (Reversible)

A hydrogel is called a physical gel when its polymeric chains are connected together via physical links (bonds) that can be removed or broken by applying an external factor such as heating the system, which is called thermoreversible gel. In such physically crosslinked gels, polymer chains are linked and connected together by non-covalent bonds, such as secondary forces including ionic, hydrogen bonding or hydrophobic interactions, or by molecular entanglements.

The crosslinking mechanisms of the physical gels involve the following:

- **The microcrystalline regions** where more than one chain meet together and form a small crystalline region. The crosslinks of the system are broken when they are heated above their melting point, but can be reformed when they cool down. A typical example of such a physical gel is the jelly that is made from gelatin.

- **Microphase separation** when the gel is made out of a block copolymer consisting of hydrophilic and hydrophobic parts. An example is the polystyrene blocks that can microphase separate into spherical areas, since polystyrene is glassy at room temperature and so the rubbery chain ends are anchored into the domain acting as a crosslinker. The ends of the polystyrene will separate inside the domain, however, as a result of the melting process when it is heated above its glass transition temperature. This type of polymer is known as a thermoplastic elastomer and is used commercially for making products such as shoe soles [60, 101].

3.3.2 Chemical Gels (Irreversible)

Chemical gels are made by crosslinking the polymeric chains using chemical bonds, such as covalent bonds. This type of gel is a three-dimensional network that can be made by a straightforward chemical reaction, such as free radical polymerisation, radiative crosslinking using electron beams or X-rays, or in the presence of UV light. Many water-soluble polymers can be prepared as a chemical gel by using a crosslinking agent or by carrying out a crosslinking reaction in a solution of the polymer. The mechanical and physical properties of the gel can be determined by the degree of the crosslinking. Different examples for this type of gel include:

- **Thermosetting resin**. Such as epoxy resins that are made from a *short* polymer with a reactive endgroup and a hardener with a multi-functional molecule. After mixing the resin and the hardener together, a hard and stiff three-dimensional network is formed by linking their chains together.
- **Vulcanised rubbers**. Long polymer chains are used to make a rubber, where the polymeric chains are randomly crosslinked together. The elastic modulus of the rubber increases as the crosslinking density increases and the material become a glassy when the concentration of the crosslinks is very high [60].

3.3.3 Swelling Behaviour of Polyelectrolyte Networks

A polymer gel swells without being dissolved inside a good solvent when the gel is thermodynamically compatible with this surrounding solvent. The swelling behaviour results from the

electrostatic interactions between the network and the solvent that make the chains charged so that they repel each other. Polymer gels can also show a reversible response to the swelling behaviour, that is shrinking behaviour, when they become uncharged inside a solvent so as to make the chains collapse. Thus, polyelectrolyte hydrogels are called *'smart'* or *'stimuli-responsive'* hydrogels since they can swell and shrink in a reversible way as they react to an external stimulus such as changes in the pH level or the temperature. Hydrogels have therefore been considered for use in some industrial applications such as intelligent sensors, as mechanical actuators, or as controlled delivery devices [104–107].

Understanding the transition behaviours of hydrogel systems, from swelling to de-swelling, is therefore vital to characterise their properties and define their structures. The total free energy is used to understand and express the swelling mechanism of the hydrogels inside their favourable solvents when they reach their thermodynamic equilibrium. Equilibrium is reached when the elastic contributions due to the stretching energy of the polymer chains balances the osmotic pressure due to the polymer-solvent interaction, and this is given by the total Gibbs free energy (ΔG_{total}) as follows

$$\Delta G_{\text{total}} = \Delta G_{\text{mixture}} + \Delta G_{\text{elastic}} \,. \tag{3.46}$$

where $\Delta G_{\text{mixture}}$ is the thermodynamic compatibility of the swollen gel inside the solvent and $\Delta G_{\text{elastic}}$ is the contribution of the elastic relative force [108, 109].

The chemical potential (μ) per chain, in units of ($k_{\text{B}}\,T$), is then used to express the change in the mixing and elastic contributions of water during the swelling process of hydrogel, which is expressed by

$$\mu_1 - \mu_{1,0} = \Delta\mu_{\text{mixture}} + \Delta\mu_{\text{elastic}} \,, \tag{3.47}$$

where μ_1 is the chemical potential of the water within the gel and $\mu_{1,0}$ is the chemical potential of pure water.

When the system reaches equilibrium, the chemical potential of the water inside and outside of the gel are equal, and so the elastic and the mixing contributions balance each other. The

change in the chemical potential during the mixing that resulted from the heating and the entropy of mixing can therefore be expressed by the Flory [110] and Huggins theory,

$$\Delta\mu_{\text{mixture}} = RT\Big[\ln\left(1-\nu_2\right) + \nu_2 + \chi\,\nu_2^2\Big]\,, \tag{3.48}$$

where ν_2 is the volume fraction of the hydrogel, χ is known as the Flory-Huggins interaction parameter between the gel and water, R is the gas constant, and T is the absolute temperature [111].

The thermodynamic swelling, which is counterbalanced by the elastic contribution of the polymer network, is given by

$$\Delta\mu_{\text{elastic}} = \frac{RT\varphi 1 N_c^{\text{gel}}}{V_0}\left(\nu_2^{1/3} - \frac{\nu_2}{2}\right), \tag{3.49}$$

where φ_1 is the molar volume of the solvent, $N_{\text{c}}^{\text{gel}}$ is the number of monomers among the crosslink points and V_0 is the total volume of the gel.

After the hydrogel reaches equilibrium and swells, the overall chemical potential change can be given by

$$\mu_1 - \mu_{1,0} = \Delta\mu_{mixture} + \Delta\mu_{elastic} = 0\,, \tag{3.50}$$

$$\mu_1 - \mu_{1,0} = \left[RT(\ln\left(1-\nu_2\right) + \nu_2 + \chi\,\nu_2^2\right] + \left[\frac{RT\,\varphi_1\,N_{\text{c}}^{\text{gel}}}{V_0}\Big(\nu_2^{1/3} - \frac{\nu_2}{2}\Big)\right] = 0\,, \tag{3.51}$$

and

$$\Big[\ln\left(1-\nu_2\right) + \nu_2 + \chi\,\nu_2^2\Big) = -\,\frac{\varphi_1 N_{\text{c}}^{\text{gel}}}{V_0}\left(\nu_2^{1/3} - \frac{\nu_2}{2}\right). \tag{3.52}$$

Equation (3.52) is used to describe ideal polymer networks, and so the term on the left-hand side indicates that the chemical potential increases due to the thermodynamic interactions between the solvent and the polymer; while the right-hand side suggests a decrease in the chemical potential given by the elastic force of the network.

The equilibrium swelling ratio (Q) of the polymer gels can be defined by the ratio of the swollen weight (V) and the unswollen/dry weight (V_0) of a gel and is given by

$$Q = \frac{V}{V_0}\,. \tag{3.53}$$

Since the swelling ratio of the polymer gels is a function of the quality of the solvent χ and the crosslinker density, the maximum swelling ratio (Q_{m}) of the polymer networks can be shown to be [61, 96, 112, 113]

$$Q_{\mathrm{m}}^{\frac{3}{5}} \cong \frac{V_0}{N_0^{\mathrm{gel}}\,\varphi_1}\left(\frac{1}{2} - \chi\right). \tag{3.54}$$

3.3.4 Free Radical Polymerisation

Free radical polymerisation (FRP) is a type of polymerisation method in which polymer chains are grown by three fundamental steps: initiation, propagation and termination [114] (as shown in Figure 3.4).

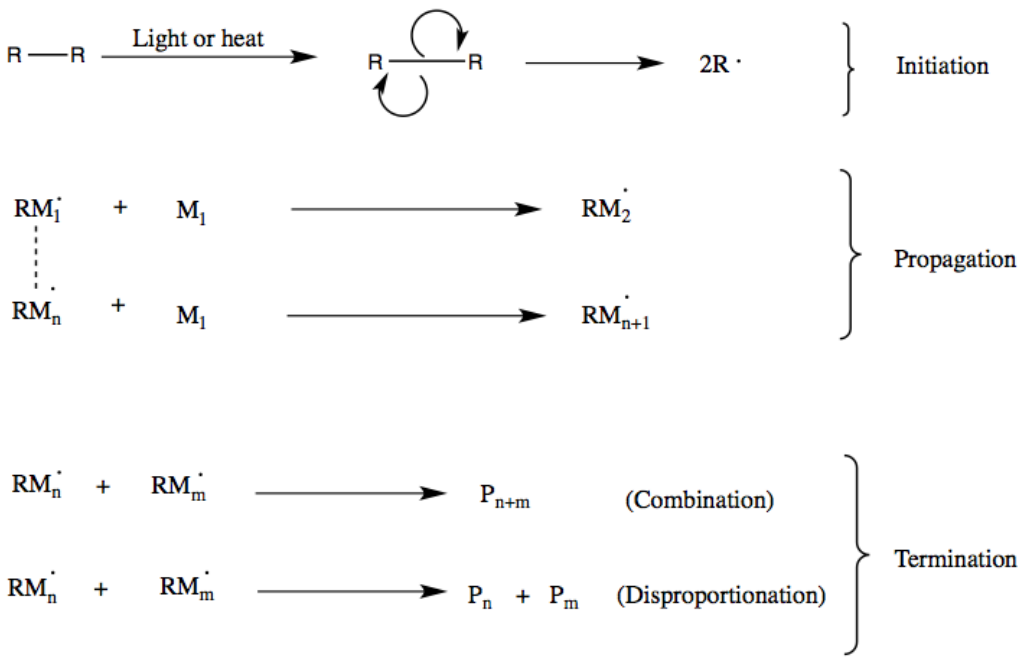

Figure 3.4: Free radical polymerisation mechanism, where R means the radical, M is the monomer and P is the polymer.

The initiation stage is where the polymerisation starts after the initiator molecules (atoms or molecules with unpaired electrons) break down under a condition of heat or electromagnetic radiation. In the propagation stage, the free radicals react with the monomers and so produce other active centres out of these monomers. The growth of the chains continues until all the monomers are consumed, which is called the termination stage. The polymer chains can be connected to each other in the termination stage by two methods: 1) combination, in which one long chain is formed by bonding two radicals from a single chain, and 2) disproportionation, in which a chain is formed by connecting two individual chains to each other after moving a hydrogen atom from one active end to another [115, 116].

3.3.5 Classification of Hydrogels

Hydrogels are found widely both in nature and industry with variable mechanical and physical properties. In nature, for example, hydrogels are found in some water-soluble proteins such as collagen [117]. While in the industrial sector, synthetic hydrogels have become very attractive due to their unique 'stimuli-responsive' properties, biocompatibility and water solubility, which make them suitable for use with different applications in the industrial and medical fields [118, 119]. For instance, hydrogels have been used in applications, such as biosensors, microfluidic devices, drug delivery and tissue implants, and engineering [107, 120–122].
Generally speaking, hydrogels are subdivided into different classifications. For example, hydrogels can be either neutral or charged according to their functional groups (i.e. anion, cation or zwitterion). Also, hydrogels can be referred to as either homopolymer, copolymer or multipolymer networks, depending on the number of polymers used during the gel preparations. In addition, hydrogels can be sorted into *soft* or *tough* gels according to their mechanical strengths and structural features, which can be controlled by changing the crosslinking degree. In other words, soft hydrogels can become solid by increasing the crosslink concentration during the gel synthesis. The disadvantage of this, however, is that they also become very brittle [123, 124]. In order to overcome this brittleness issue, and to improve the strength of soft hydrogels, some new types of tough gels have emerged with significantly improved mechanical properties, such as the topological (TP) hydrogels, nano-composite (NC) hydrogels and double-network (DN) hydrogels [125].

The properties of *soft* and *tough* hydrogels are discussed in more detail in the following sections, and their fundamental applications are also reviewed.

3.3.5.1 Soft Hydrogels

Hydrogels are networks of hydrophilic polymers that can swell to a high water content ($>$ 80 wt %) without dissolving in water, since their polymer chains are chemically joined together by crosslink points. There is a type of hydrogels called '*smart*' gels that are prepared by '*stimuli-responsive*' polyelectrolytes. PE hydrogels are able to change their mechanical or physical properties upon chemical or physical triggers, such as changes in pH, ionic strength, temperature, solvent, light, electric or magnetic fields, and mechanical stress. These changes in properties are reversible when the stimulus is reversed [14,63,126–128]. As a result, hydrogel scientists have found that the soft three-dimensional networks can mimic the natural tissue due to their higher content of water and thus have used them in a range of applications [129]. For example, the soft hydrogels have been considered for use in cell encapsulation technology which promises to treat diseases, such as cancer [28, 130]. In addition, hydrogels, such as the hydrophilic soft network of poly(2-hydroxyethyl methacrylate) (PHEMA), have been found to be suitable for use in contact lens applications when the refractive power of the cornea is compromised since the softness of the hydrogels helps oxygen to diffuse to the corona [97, 112, 126]. Also, hydrogels, such as the hydrophilic acrylate derivatives, have been used in making skin adhesive gels and for wound and burn dressings [99].

A critical disadvantage of soft hydrogels is that they are generally weak, fragile and soft materials due to their low fracture strength and elastic modulus. The use of such hydrogels is therefore limited by their weak mechanical properties and so restricted to use with applications that require no or little mechanical force so that mechanical failure is neglected or unlikely [129].

3.3.5.2 Tough Hydrogels

There are some load-bearing applications, such as in tissue engineering, where the mechanical strength of the hydrogels is essential. An articular cartilage, for example, is an amorphous tissue that contains a good amount of water, however, it exhibits low wear under high loading

due to its high mechanical strength. A tough gel was needed in this kind of tissue engineering due to the difficulty of using soft biological gels to fill the gaps between cartilage [125,131,132]. Tough hydrogels that are able to resist an applied force or deformation without a failure have recently been developed in a number of studies [132–134].

Tough hydrogels are able to swell and absorb large amounts of water, and they are extremely stretchable with a low flow frictional coefficient, while maintaining their significant mechanical properties and large elastic modulus. There are three types of tough hydrogels: 1) topological (TP) hydrogels, 2) nano-composite (NC) hydrogels and 3) double-network (DN) hydrogels, each of which will be reviewed in the following section.

3.3.5.2.1 Topological Hydrogels

Topological (TP) hydrogels can stretch without having any fracture while absorbing a large amount of water as a result of the junctions of their figure-of-eight crosslinkers. The figure-of-eight crosslinker is a sliding double ring crosslinking agent that traps the polymer chains, while remaining able to move and slide along them (Figure 3.5).

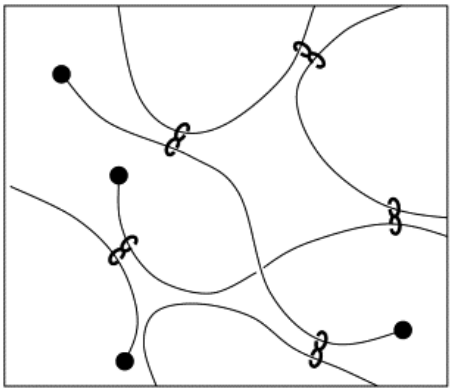

Figure 3.5: A schematic diagram for the TP gel, where the figure-of-eight crosslinkers are trapping polymer chains. The figure was used with permission from [125]. Copyright (2005) Elsevier.

Polyrotaxane gel, which is shown in Figure 3.6, is a good example of a TP hydrogel and is made up of poly(ethylene glycol) (PEG) chains trapped by α-cyclodextrin (α-CD) circles threaded. This TP gel can swell with water by up to 500 times its as-prepared weight and it can also stretch 20 times more than its original length. The discoverers of this TP gel,

Okumura and Ito [135], refer to the sliding of the crosslinks as a 'pulley effect' that is driven by the large water absorbance [33, 125].

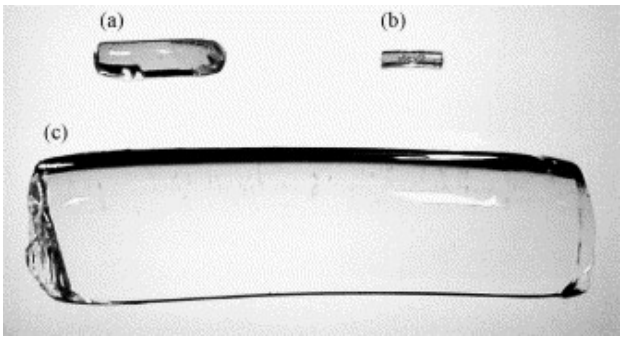

Figure 3.6: The polyrotaxane (TP) gel in (a) as-prepared, (b) dried, and (c) fully swollen states. Taken from [125] with permission. Copyright (2005) Elsevier.

3.3.5.2.2 Nano-Composite Hydrogels

The nano-composite (NC) (clay-filled) hydrogels are another type of tough hydrogels that are also extremely stretchable because they are crosslinked by inorganic clay slabs on the scale of several tens of nanometers (Figure 3.7). The NC gel was designed by Haraguchi and Takehisa [136] using inorganic clay slabs and potassium peroxodisulfate (KPS) as a radical initiator to make the NC poly(*N*-isopropyl acrylamide) (PNIPA) gel. It is essential that during the preparation stage of the NC gels, the monomer of NIPA must be mixed with the clay slabs, in addition to a radical initiator that can ionically absorb to the clay surface by radical polymerisation.

NC gels have the ability to stretch to about 10 times their original lengths due to the fact that the clay slabs are able to rotate during the deformation of NC gels. NC gels are useful in biomedical tissue engineering such as artificial muscles [33, 125, 136].

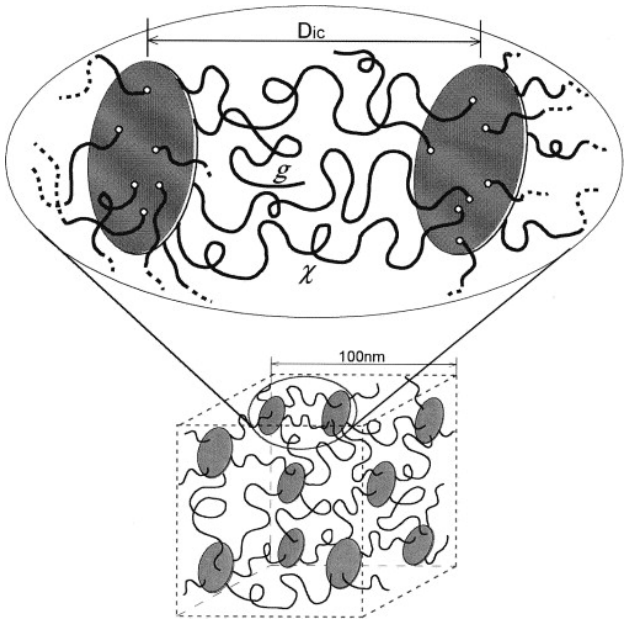

Figure 3.7: A schematic diagram for the network structure of NC gels.
Taken with permission from [125]. Copyright (2005) Elsevier.

3.3.5.2.3 Double-Network Hydrogels

A double-network (DN) hydrogel was introduced by Gong *et al.* [131] in 2003, who obtained a strong hydrogel by combining between two hydrophilic polymers *via* a two-step network formation. The first network of a DN hydrogel must be a highly crosslinked since it is responsible for the highest elastic modulus ($\sim$ 1.0 MPa), while the second network must be a loosely crosslinked since it is responsible for dissipating the stress and enhancing the mechanical strength of the DN hydrogel. A double-network (DN) hydrogel provides a combination of hardness and toughness, although it contains 60 – 90 wt% of water. The mechanical strength of a robust DN hydrogel is significantly higher than that of SN hydrogels, which prepared from its individual networks. The excellent mechanical property of DN hydrogels results both from the high degree of chemical crosslinkage in the first network of a DN hydrogel and from the physical entanglements that are accrued between the first and second networks [131,137,138]. It has been emphasised that when the crosslinking density of a DN hydrogel was 4 mol% for the first network and 1.0 mol% for the second network, the DN gel exhibited a high mechanical strength. In other words, if the crosslinker density of the first network was decreased while

that of the second was increased then the DN gel exhibited a similar brittle behaviour to that of a single-network (SN) gel.

Gong *et al.* [131,139] demonstrated a DN hydrogel prepared from poly(2-acrylamido-2-methyl-1-propanesulfonic acid) (PAMPS) and poly(acrylamide) (PAAm). Both the first, PAMPS, and second, PAAm, networks of the PAMPS–PAAm (DN) hydrogel are crosslinked by *N,N'*-methylenebis (acrylamide) (MBAA), however, 4 mol% of the MBAA was used in the PAMPS network and 0.1 mol% of the MBAA was used in the PAAm network. It was found that the mechanical strength of the AMPS–PAAm (DN) hydrogel was able to sustain a higher compression load than the PAMPS single-network hydrogel, as presented in Figure 3.8.

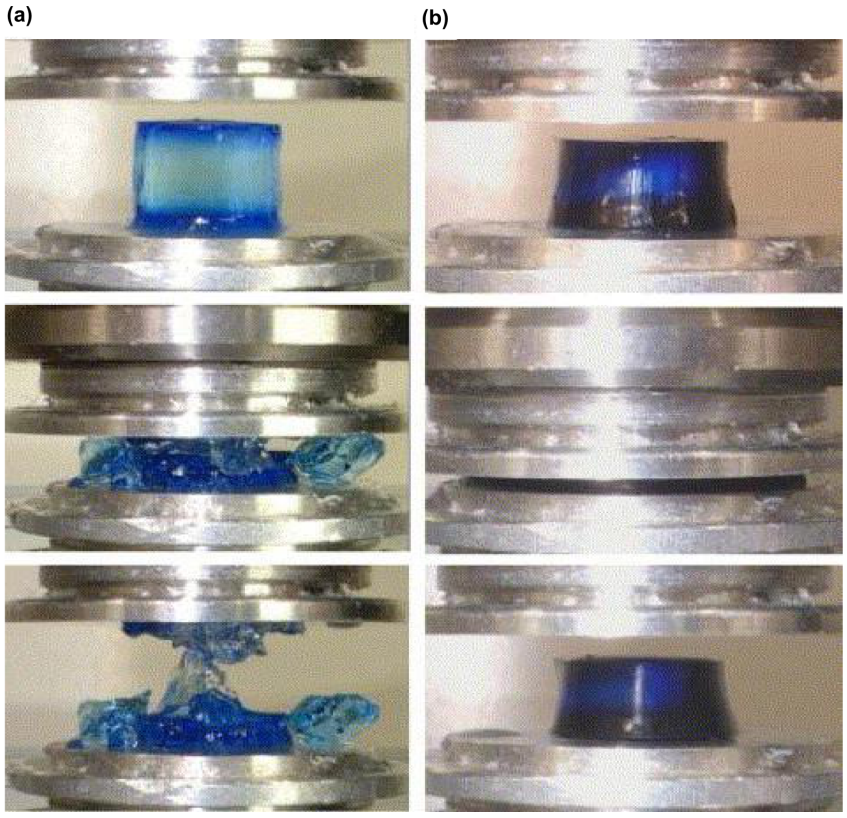

Figure 3.8: Photograph for (a) a single-network (SN) gel of the PAMPS and (b) a DN gel of the PAMPS-PAAm under a compression test. Taken from [131] with permission. Copyright (2003) John Wiley and Sons.

Figure 3.9 presents strain-stress curves of the PAMPS-PAAm (DN) hydrogel and SN gels of the PAMPS and PAAm networks. The DN gel sustained a stress of 17.2 MPa, while the SN gels broke at a stress of 0.4 MPa for the PAMPS gel and 0.8 MPa for the PAAm gel.

This result suggested that the contribution of the loosely crosslinked second network helps to dissipate the energy of the (compressive) load that initiate the crack and prevents it from growing so as to deform the network, and also to allow the physical entanglement points to slide along the chains at the interface with the highly crosslinked first network [33, 125, 131].

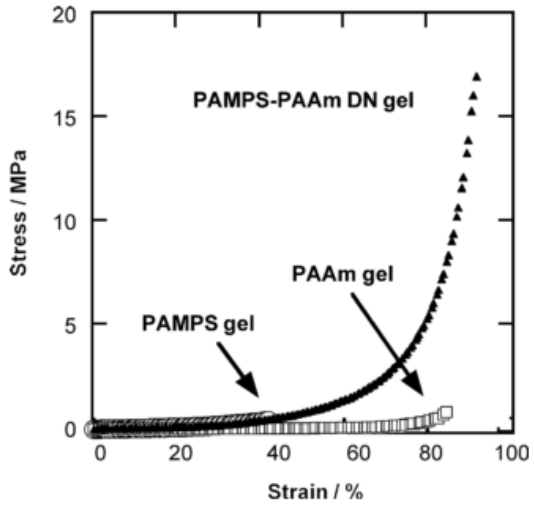

Figure 3.9: Stress-strain curves for the PAMPS–PAAm (DN) hydrogel and the SN gels of the PAMPS and PAAm. Taken with permission from [131]. Copyright (2003) John Wiley and Sons.

Furthermore, DN hydrogels can be responsive to the pH changes if one of their networks is made from a weakly charged polyelectrolyte. For example, a pH-sensitive DN hydrogel was prepared by two polymers: a poly[oligo(ethylene glycol)methyl ether methacrylate] (POEGMA) and a poly(acrylic acid) (PAA) [140]. It was found that the mechanical strength of the POEGMA–PAA (DN) hydrogel was 14 times higher comparing to the SN hydrogels of the POEGMA and PAA. The mechanical strength of the POEGMA–PAA (DN) was ~ 1 MPa at a pH > 4, however, it increased to ~ 8 MPa at a pH below ~ 4. The POEGMA–PAA (DN) hydrogel had a higher mechanical strength and lower swelling ratio at pH < 4 since the DN gel shrunk and became opaque as a result of the hydrogen bond interactions between their two networks, where these interactions occurred between the non-ionised carboxylic acid groups on PAA and PEG. Hence, a reduction in the DN gel swelling at pH below 4 was taken as evidence of the complex formation of the strong hydrogen bonds that exist between PAA and PEG. At pH values above 4, in contrast, the DN gel swelled to a limit size imposed by the

more tightly crosslinked first network after disrupting the hydrogen bonding between the two networks. As a result of their high pH responsiveness and the excellent mechanical properties, DN hydrogels could open a new era for tissue engineering and medical applications, such as for artificial muscles or controlled release devices [131, 140].

Part II

Experimental

Chapter 4

Experimental Methods

4.1 Introduction

This chapter is divided into two sections. The first section presents in details the sample preparations of weakly charged polyelectrolytes; i.e. hydrogels and polymer brushes, while the second section presents all the main experimental techniques that were used in this study to either characterise the hydrogel and polymer brush samples or to measure their adhesion force at the hydrogel-brush interface underwater.

A hydrogel is defined as a three-dimensional crosslinked hydrophilic network and is prepared using free radical polymerisation (FRP) [32,33]. Two types of polymer hydrogels were used in this study: 1) a single-network (SN) hydrogel and 2) a double-network (DN) hydrogel. The difference between the SN and DN hydrogels is that the SN hydrogel is made straightforwardly using just one type of a polymer, while the DN hydrogel is prepared using two different types of polymers. In other words, a DN hydrogel is made by a two-step formation method that starts by: i) making the first network of a hydrogel, and then ii) forming the second network that reinforces the first network [131,137,139,140]. Whereas, a polymer brush is a chemically grafted polymer layer on a planar surface, which is formed by attaching a polymer chain to an anchor point that allows the chain to stretch away from the surface in a 'brush-like' conformation [30,31]. The polymer brush is synthesised using surface-initiated atom transfer radical polymerisation (SI-ATRP).

In this work presented in this thesis, the **SN hydrogels** used are: **i)** a poly(methacrylic acid) (PMAA, polyacid) hydrogel and **ii)** a poly[2-(diethyl amino)ethyl methacrylate] (PDEAEMA, polybase) hydrogel. The **DN hydrogels** used are: **i)** a poly(methacrylic acid)–poly[oligo(ethylene glycol)methyl ether methacrylate] (PMAA–POEGMA) hydrogel and **ii)** poly[oligo(ethylene glycol)methyl ether methacrylate]–poly(methacrylic acid) (POEGMA–PMAA) hydrogel. Whereas, the **polyelectrolyte brush** samples are: **i)** a poly(methacrylic acid) (PMAA) brush and **ii)** a poly[2-(diethyl amino)ethyl methacrylate] (PDEAEMA) brush.

4.2 Sample Preparation

This switchable adhesion study was carried out between two types of oppositely charged polyelectrolytes; one being a hydrogel and the other a polymer brush, underwater. The preparation methods of hydrogels and polymer brushes are presented in the following section.

4.2.1 Single-Network Hydrogel Synthesis

A single-network (SN) hydrogel consists of polymer chains that are chemically crosslinked together [141]. A weakly charged polyelectrolyte (PE) hydrogel is a class of polymer gels that is able to respond to external environmental changes. The unique characteristic of PE hydrogels is that the monomer units can be switched from charged to uncharged by an appropriate stimulation. The stimuli-responsive networks of PE hydrogels are capable of responding to various stimuli such as pH, ionic, temperature, magnetic and electric fields [71]. These '*smart–responsive*' PE hydrogels exhibit controllable and reversible changes in their chemical and physical properties when they undergo changes upon external stimulus. PE gels have received considerable attention as a results of their remarkable mechanical properties that make them ideal materials for certain niche applications [14]. The next section describes the preparation method used for the PMAA and PDEAEMA (SN) hydrogels.

4.2.1.1 Synthesis of the Poly(Methacrylic Acid) Hydrogel

The poly(methacrylic acid) (PMAA, polyacid) hydrogel was prepared using free radical polymerisation (FRP) [142] using water as a solvent, methacrylic acid (MAA) (Aldrich, 98%) as a monomer, 2,2'-azobis(2-methylpropionamidine) dihydrochloride (Aldrich, 98%) (AMPA) as

an initiator and *N,N'*-methylenebisacrylamide (MBAA) (Aldrich, 99%) as a crosslinker. Table 4.1 shows the quantities of chemicals used to prepare the solution of the PMAA gel.

Table 4.1: Chemicals used to make the PMAA hydrogel.

Reagents	Quantities
H_2O	100 mL, 5.5 mol.
MAA	20 mL, 0.23 mol.
AMPA	0.03 g, 0.1 mmol.
MBAA	0.06 g, 0.4 mmol.

These chemicals were mixed together until they completely dissolved. The PMAA solution was then stirred using a magnetic stirrer and degassed under nitrogen (N_2) for about 20 min and subsequently transferred by a purged syringe into a glass container (see Figure 4.1 (a)). The glass container was also degassed with N_2 for a while before transferring the polymer solution into it. The glass container consists of a removable glass mould that containing a number of hemispherical holes with a diameter of 4 mm (Figure 4.1 (b)). Afterwards, the glass container was placed inside an oven at 80 °C for 2 h in order to polymerise the PMAA solution and then obtain the hydrogel.

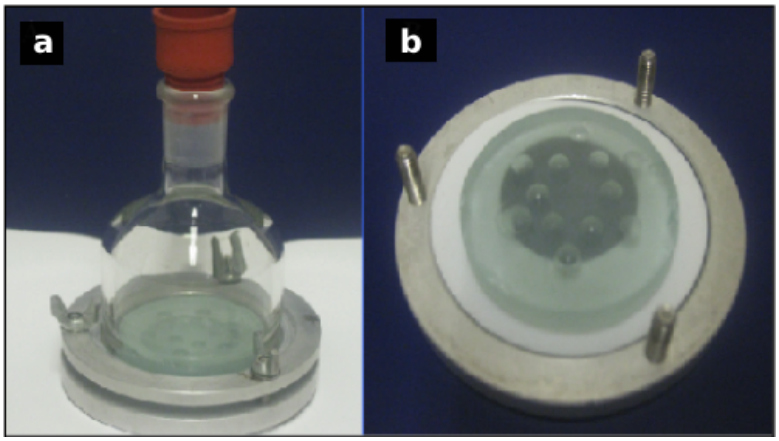

Figure 4.1: (a) The glass container used to prepare the hemispherical pieces of a hydrogel. (b) The removable mould inside the glass container used for making hemispherical pieces of hydrogel.

After the hydrogel was formed, the glass container was taken out of the oven and left to cool at room temperature for a few minutes. The hemispherical pieces of hydrogel formed on the glass mould were then cut with a hollow metallic tube (a cutter). Finally, the hemispherical pieces of the PMAA hydrogel (see Figure 4.2) were kept inside deionised (DI) water in order to remove the unreacted residues, and also to prevent dryness, and for use later in the adhesion experiments.

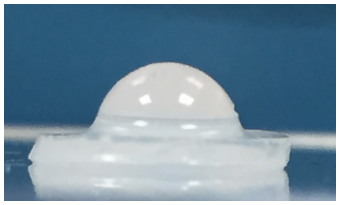

Figure 4.2: A hemispherical piece of a just-prepared PMAA hydrogel with a diameter of 4 mm.

4.2.1.2 Synthesis of the Poly [2-(Diethyl Amino)Ethyl Methacrylate] Hydrogel

The poly[2-(diethyl amino)ethyl methacrylate] (PDEAEMA, polybase) hydrogel was synthesised by free radical polymerisation using 2,2'-azobis(2-methylpropionamidine) dihydrochloride (Aldrich, 98%) (AMPA) as an initiator, ethylene glycol dimethacrylate (EGDMA) (Aldrich, 98%) as a crosslinker, 2-(diethyl amino)ethyl methacrylate (Aldrich, 99%) (DEA) as a monomer and methanol and water as a solvent. Table 4.2 shows the chemical quantities that were used to prepare the PDEAEMA solution.

Table 4.2: Chemicals used to make the PDEAEMA hydrogel.

Reagents	Quantities
CH_4O	50 mL, 1.2 mol.
H_2O	30 mL, 1.7 mol.
DEA	40 mL, 0.2 mol.
AMPA	0.8 g, 2.9 mmol.
EGDMA	1.5 mL, 7.9 mmol.

The PDEAEMA solution was stirred and degassed with N_2 for about 20 min before being transferred into the degassed glass container. Then, the PDEAEMA solution inside the glass container was placed in an oven at 70 °C for 2 h. The PDEAEMA gel was then cut and kept inside DI water for use later with the adhesion experiments.

4.2.2 Double-Network Hydrogel Synthesis

A double-network (DN) hydrogel is a robust gel that has a higher mechanical strength compared to the SN hydrogels that are apart of its individual networks. A double-network (DN) hydrogel is prepared by a two-step formation method using two different polymers to make its two networks. The first network of a DN hydrogel must be highly crosslinked since it is responsible for giving the hydrogel its higher elastic modulus, while the second network must be loosely crosslinked since it is responsible for supporting the first network and so dissipating the energy during the compressive or tensile tests. The excellent mechanical properties of DN hydrogels do not just result from the high degree of chemical crosslinkage but also from the physical entanglements between their two networks [131, 137, 138].

Two types of DN hydrogels were prepared and used here in this study of the switchable adhesion with a polymer brush in order to compare their adhesion with that of SN hydrogels. DN hydrogels were therefore made using: i) a poly(methacrylic acid) (PMAA) and ii) poly[oligo(ethylene glycol)methyl ether methacrylate] (POEGMA). These two DN hydrogels are: 1) a POEGMA–PMAA (DN) hydrogel and 2) a PMAA–POEGMA (DN) hydrogel, and with these being prepared as follows:

1) The POEGMA–PMAA (DN) hydrogel was prepared by making the first, POEGMA, network and then strengthening it by making a second, PMAA, network.

2) The PMAA–POEGMA (DN) hydrogel was made the other way around: the PMAA network was made first and then strengthened it by making the POEGMA network around it.

Figure 4.3 presents an illustrative diagram outlining the preparation stages for making a double-network (DN) hydrogel:

1) The first network of the highly crosslinked hydrogel is made into a hemispherical shape using the glass mould (as shown in Figure 4.1).

2) A polymer solution of the loosely crosslinked second network is then prepared.

3) The hemispherical pieces of the first network are then immersed inside the second network solution for five days.

4) Subsequently, the immersed hemispherical pieces of the hydrogel are taken out of the second network solution (after 5 days) and placed inside an oven at 60 °C for 6 hours.

5) Finally, the hemispherical pieces of the prepared DN hydrogel are then washed and kept inside DI water.

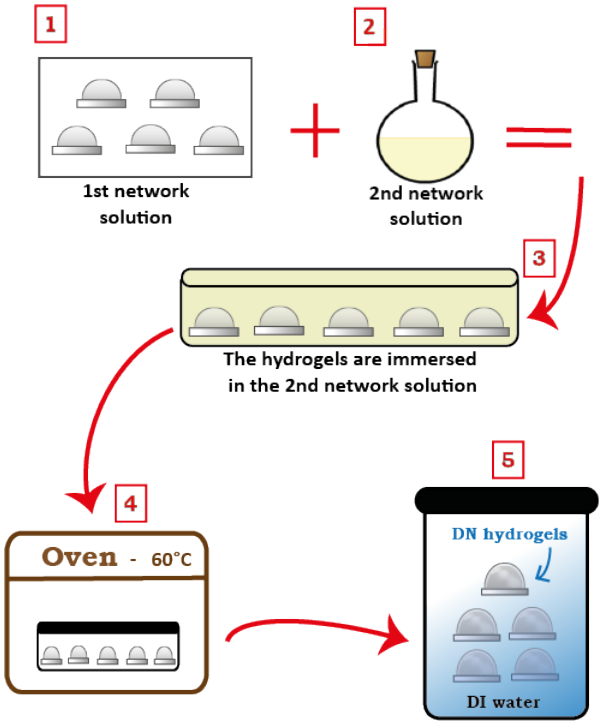

Figure 4.3: The preparation process for a double-network (DN) gel.

The preparation details of the POEGMA–PMAA and PMAA–POEGMA (DN) hydrogels are presented in the following section.

4.2.2.1 Poly[Oligo(Ethylene Glycol)Methyl Ether Methacrylate]–Poly (Methacrylic Acid) Hydrogel

To make the POEGMA–PMAA (DN) hydrogel, the POEGMA gel was prepared first using oligo(ethylene glycol) methyl ether methacrylate, [average M_n 950] (Aldrich) as a monomer, water as a solvent, potassium persulfate (KPS) (Aldrich, 99%) as an initiator and *N,N'*-methylenebisacrylamide (MBAA) (Aldrich, 99%) as a crosslinker. The chemical quantities used for making the POEGMA solution are shown below in Table 4.3.

Table 4.3: Chemicals used to make the first POEGMA network of the POEGMA–PMAA (DN) hydrogel.

Reagents	Quantities	
POEGMA	12 g,	0.013 mol.
H_2O	50 mL,	2.8 mol.
KPS	0.2 g,	0.74 mmol.
MBAA	0.1 g,	0.65 mmol.

The POEGMA solution was stirred and degassed under N_2 for 20 min until the mixture was completely dissolved. Then, the POEGMA solution was transferred by a purged syringe into a degassed sealed container and placed inside an oven at 60 °C for 6 hours. After the POEGMA gel was formed, the glass container was taken out of the oven and left to cool at room temperature for a few minutes. Subsequently, the gel was cut into the hemispherical pieces and put inside the DI water to remove the unreacted residues. The POEGMA gel was kept inside the DI water for three days and the water was changed at least twice during these three days. The POEGMA gel swelled after it was allowed to equilibrate inside the DI water, and it maintained its transparent colour (Figure 4.4).

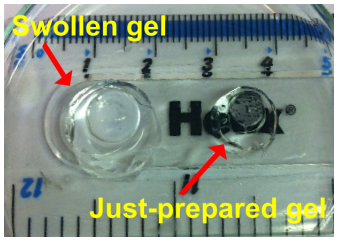

Figure 4.4: A swollen POEGMA hydrogel (on the left-hand side) and a non-swollen (just-prepared) POEGMA hydrogel (on the right-hand side).

The solution for the second, PMAA, network was then prepared as shown below in Table 4.4.

Table 4.4: Chemicals used to make the second PMAA network of the POEGMA–PMAA (DN) hydrogel.

Reagents	Quantities
MAA	6 mL, 0.07 mol.
H_2O	60 mL, 3.3 mol.
KPS	0.04 g, 0.15 mmol.
MBAA	0.1 g, 0.65 mmol.

The hemispherical pieces of the POEGMA gel, which had been kept in DI water for three days, were then immersed inside this PMAA solution for five days. Thereafter, the gel pieces were taken out of the PMAA solution, put inside a sealed glass cell and placed in an oven at 60 °C for 6 h. Finally, the robust POEGMA–PMAA (DN) hydrogel was formed and its colour transferred to white, and so it was kept inside DI water for later use within the adhesion experiments.

4.2.2.2 Poly(Methacrylic Acid)–Poly[Oligo(Ethylene Glycol)Methyl Ether Methacrylate] Hydrogel

The PMAA–POEGMA (DN) hydrogel was made in a very similar way to the previously mentioned POEGMA–PMAA (DN) hydrogel but with the PMAA gel being made as the first network and the POEGMA network made as the second network.

The PMAA gel was made by mixing methacrylic acid (MAA) (Aldrich, 98%) as a monomer, water as a solvent, *N,N'*-methylenebisacrylamide (MBAA) (Aldrich, 99%) as a crosslinker, and potassium persulfate (KPS) (Aldrich, 99%) as an initiator. The chemical quantities are shown in Table 4.5.

Table 4.5: Chemicals used to make the first network PMAA network of the PMAA–POEGMA (DN) hydrogel.

Reagents	Quantities	
MAA	10 mL,	0.12 mol.
H_2O	50 mL,	2.8 mol.
KPS	0.13 g,	0.48 mmol.
MBAA	0.94 g,	0.006 mol.

The PMAA solution was stirred and degassed with N_2 for 20 min, then this solutions was transferred by a purged syringe into the degassed glass container and finally placed inside an oven at 60 °C for 6 h. After the required period, the glass container was taken out of the oven and left to cool at room temperature. Subsequently, the gel was cut into hemispherical pieces and put inside DI water to remove the unreacted residues. The PMAA gel pieces were kept inside the DI water for three days and the water was changed at least twice during this period. The PMAA gel swelled after it was allowed to equilibrate inside the DI water (Figure 4.5).

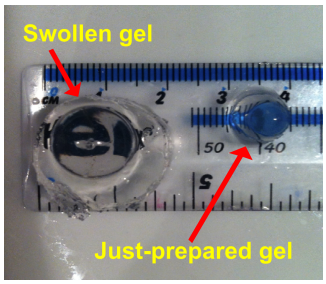

Figure 4.5: A swollen PMAA hydrogel (on the left-hand side) and a non-swollen (just-prepared) PMAA hydrogel (on the right-hand side).

Following this, the solution for the second network, POEGMA, was prepared as shown in Table 4.6. The hemispherical pieces of the PMAA gel, which were kept in DI water for three days, were immersed inside this POEGMA solution for five days. Thereafter, the gel pieces were taken out of the POEGMA solution, put inside a sealed glass cell and then placed in an oven at 60 °C for 6 h. Finally, the robust DN gel was formed and kept inside DI water for later use within the adhesion experiments.

Table 4.6: Chemicals used to make the second POEGMA network of the PMAA–POEGMA (DN) hydrogel.

Reagents	Quantities	
POEGMA	12 g,	0.013 mol.
H_2O	60 mL,	3.3 mol.
KPS	0.04 g,	0.15 mmol.
MBAA	0.02 g,	0.13 mmol.

4.2.3 Polymer Brush Synthesis

Surface-initiated atom transfer radical polymerisation (SI-ATRP) is described as a functional technique used to grow polymer brushes on a substrate from surface-bound initiators through covalent bonds [31, 84]. The polymer brush is attached to the surface by one end, and so the other end of the chain is free to either collapse (in a poor solvent) or extend (in a good solvent) [31, 75, 84]. The conformation of end-grafted polymer chains in a good solvent is controlled by the degree of polymerisation (N) and also by the chains' grafting density on the surface (σ). The covalently attached polymer brushes can be synthesised by chemisorption process in two different methods; which are either the '*grafting-from*' or '*grafting-to*' techniques [143]. The '*grafting-from*' method ensures a highly dense structure for the polymer brush and was therefore adopted for use in this project. This technique, however, it requires initiator-bearing self-assembled monolayers (SAMs) before growing the polymer brushes on the surface [143].

In this project, two types of polyelectrolyte brushes were prepared using the '*grafting-from*' technique by growing them on a silicon substrate: 1) poly(methacrylic acid) (PMAA) and 2) poly(2-(diethyl amino)ethyl methacrylate) (PDEAEMA). Both of the polyelectrolyte, PMAA and PDEAEMA, brushes are pH-stimulus responsive polymers, however, each one has an opposite response to pH changes. The carboxylic acid groups in PMAA brushes become dissociated at a high pH leading to repulsive electrostatic interactions between the negatively charged carboxylic groups, causing the brush to swell. In contrast, the amino groups of PDEAEMA brushes gain protons at low pH, allowing the positively charged brush to swell. While the amino groups of PDEAEMA brushes release protons at a high pH, causing the brushes to become uncharged and collapse [56, 144].

4.2.3.1 The Initiator Deposition on a Silicon Substrate

Making an initiator functionalised layer on a silicon surface in order to grow polymer brushes on it is required prior to the polymerisation of brushes. Silicon substrates were purchased from Prolog Semicor and used to grow polymer brushes, which have the following characteristics: diameter 50 mm, dopant *p*-type boron, orientation (100) $\pm\,1^\circ$ and thickness $4000 \pm 50\ \mu$m. In order to insure a high standard of cleaning for the silicon substrates, the RCA Standard Clean method was employed to remove organic contaminations on their surfaces [145]. Accordingly, the silicon substrates and the glassware were cleaned separately by immersing them inside a solution of hydrogen peroxide (35 wt%), ammonia (30 wt%), and deionized water in a volume ratio of 1:1:5, respectively. This solution was heated up to 80 °C, and the silicon wafers and the glassware were immersed in for 10 min. After that, the silicon substrates were rinsed with copious amounts of water, dried under nitrogen and then transferred to a refluxing environment in order to make the initiator functionalised surfaces. The glassware were also washed repeatedly with clean water, dried under nitrogen, covered with foil and placed inside a hot oven for a few hours to remove all traces of water [146].

Later on, the clean hydrophilic silicon substrates were prepared for the initiator functionalised process in order to grow the polymer brush. The initiating reaction allows a transformable halogen to be deposited on the silicon surface that later reacts with a double bond of a monomer. The polymerisation reaction stops when all the monomers are consumed in making the chains of the polymer brush. The cleaned silicon substrates were initiated following two steps; firstly by making the self-assembled monolayer (SAM) and secondly by preparing the initiator functionalised surface [147] as follows:

4.2.3.1.1 Preparation of Self-Assembled Monolayer

In order to make the SAM, a silicon substrate was immersed in a solution of ethanol and 3-aminopropyltriethoxysilane (APTES) (Aldrich, 98%) 2% (v/v) for 10 min. Afterwards, the silicon substrate was rinsed with ethanol, dried by nitrogen and lastly annealed inside a vacuum oven at 120 °C for 30 min (Figure 4.6).

4.2.3.1.2 Preparation of Initiator Functionalised Surfaces

A final step for the initiator deposition on the silicon substrate was done by immersing the silicon substrate inside a solution of α-bromoisobutyryl bromide (Aldrich, 98%) (0.37 ml, 3 mmol), triethylamine (Aldrich, 99%) (0.41 ml, 3 mmol) and dichloromethane (DCM) (Aldrich, 99%) (100 mL, 1.4 mol) for 30 min (Figure 4.6). Lastly, the silicon substrate was rinsed with dichloromethane and ethanol and then dried under nitrogen to be ready for the polymer brush polymerisation.

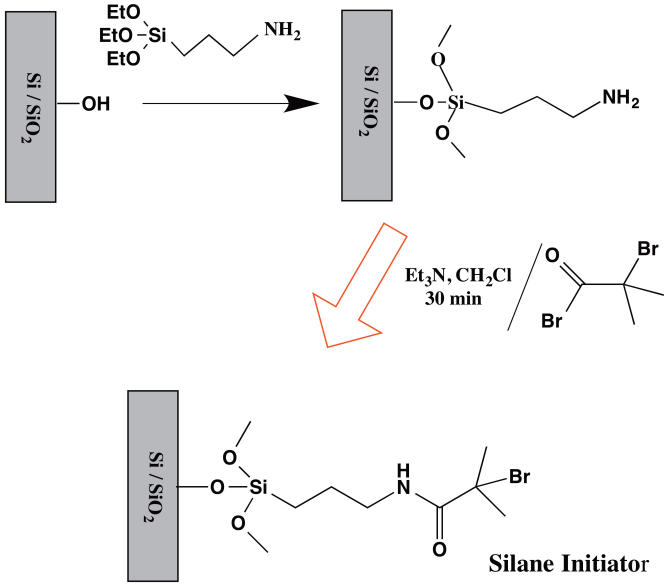

Figure 4.6: Silicon surface functionalisation with silane initiator

The formation of the initiator layer on the surface of the silicon substrate was confirmed using ellipsometry (contact angle and this step is described later in Section 4.3).

4.2.3.2 Synthesis of the Poly(Methacrylic Acid) Brush

The poly(methacrylic acid) (PMAA, a weak polyacid) brush was synthesised by the atom transfer radical polymerisation (ATRP) reaction using the '*grafting-from*' method [58]. The PMAA brush was grown on a cleaned silicon substrate (i.e. planer surface) after the initiation process described above (Figure 4.6). The polyacid brush was synthesised by hydrolysing the poly(*tert*-butyl methacrylate) (P*t*BMA) brush to obtain the poly(methacrylic acid) (PMAA) brush.

The chemicals employed in the PMAA brush synthesis were: copper(I) chloride (CuCl) (Aldrich, 99%), 1,4-dioxane ($C_4H_8O_2$) (Aldrich, 98%), *tert*-butyl methacrylate (*t*BMA) (Aldrich, 98%) and *N,N,N',N″,N″*-pentamethyldiethylenetriamine (PMDETA) (Aldrich, 99%), as given in Table 4.7.

Table 4.7: Chemicals used to make the solution of the PMAA brush.

Reagents	Quantities
$(t\text{BMA})_l$	10 mL, 0.061 mol.
$(C_4H_8O_2)_l$	5 mL, 0.059 mol.
$(\text{PMDETA})_l$	0.1 mL, 0.479 mmol.
$(\text{CuCl})_s$	0.05 g, 0.050 mmol.

The PMAA solution was prepared by mixing the three liquids, *t*BMA, $C_4H_8O_2$, and PMDETA, inside a sealed round-bottom flask under N_2 since this reaction required an inert (reduced) oxygen environment (Figure 4.7). The PMAA solution was stirred under N_2 for 30 min before the copper(I) chloride (CuCl) was added to this mixture and then degassed again under N_2 and stirred for another 30 min. A purged syringe was then used to transfer the PMAA solution and injected via the Suba-Seal to a custom glass cell containing the initiated silicon substrates (see Figure 4.8).

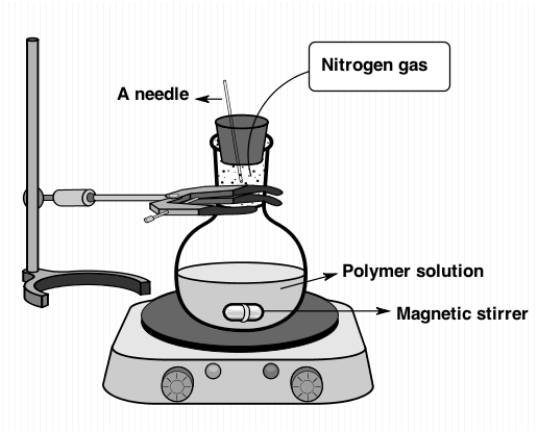

Figure 4.7: An illustration of the sealed round-bottom flask used for preparing the polymer brush solution.

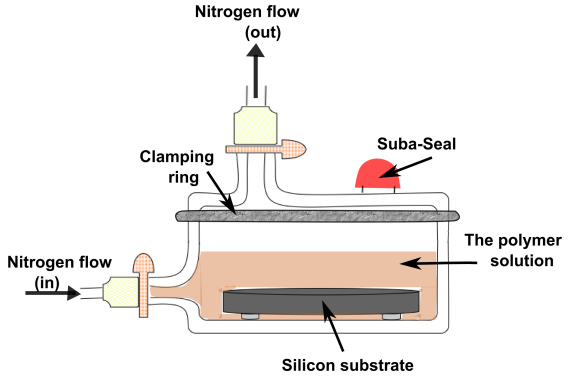

Figure 4.8: An illustrative diagram of the glass cell within which the polymerisation reaction for the polymer brush took place.

After injecting the polymer solution into the glass cell, the nitrogen flow was stopped and the glass cell was then submerged inside a heat bath pre-heated to 50 °C and then left there overnight (Figure 4.9 (a)). Once the silicon substrate was taken outside the glass cell, the sample was washed with 1,4-dioxane and ethanol and then dried under nitrogen (Figure 4.9 (b)). The final step in making the PMAA brush involved hydrolysing the poly(*tert*-butyl methacrylate) (P*t*BMA) brush to the poly(methacrylic acid) (PMAA) brush. This step was undertaken by immersing the P*t*BMA brushes in a mixture of 1,4-dioxane (10 mL) and *p*-toluenesulfonic acid (PTSA) (0.38 g) inside the glass cell, which was then submerged in a heat bath pre-heated to 100 °C for 24 h (Figure 4.9 (c)). Finally, the sample of the PMAA brush was washed with 1,4-dioxane and ethanol and was subsequently dried under nitrogen. The layer of the PMAA brush was characterised by the contact angle and its thickness was measured by ellipsometry, as will be presented later, in Section 4.3.

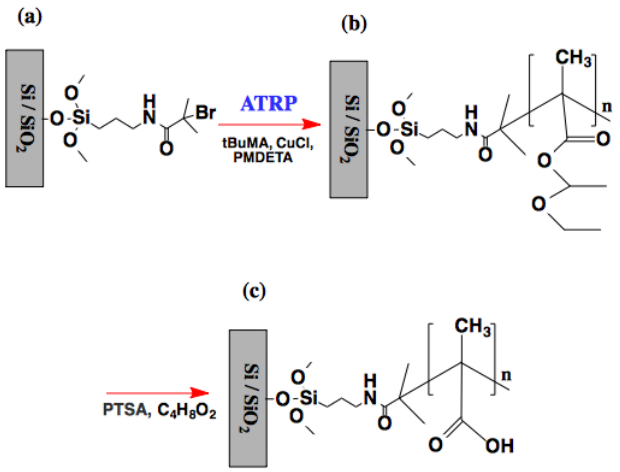

Figure 4.9: The synthesis of the PMAA brush.

4.2.3.3 Synthesis of the Poly[2-(Diethyl Amino)Ethyl Methacrylate] Brush

The poly[2-(diethyl amino)ethyl methacrylate] (PDEAEMA, a weak polybase) brush was synthesised via the ATRP reaction using the '*grafting-from*' method [148]. The silicon substrate was first functionalised and initiated using the method mentioned previously in section 4.2.3.1. The PDEAEMA solution was prepared from the following chemicals: 2-(diethyl amino)ethyl methacrylate (DEA) (Aldrich, 99%), 2,2'-bipyridine (bipy) (Aldrich, 99%), copper(I) bromide ($CuBr_1$) (Aldrich, 99%), copper(II) bromide ($CuBr_2$) (Aldrich, 99%), methanol and de-ionised water. All water used during the synthesis was $> 15\ \Omega$ DI filtered water. The chemicals quantities are shown below in Table 4.8.

Table 4.8: Chemicals used to make the PDEAEMA solution.

Reagents	Quantities	
$(CH_4O)_l$	8 mL	0.20 mol.
$(H_2O)_l$	2 mL	0.11 mol.
$(DEA)_l$	10.84 mL	54.0 mmol.
$(bipy)_s$	0.39 g	2.5 mmol.
$(CuBr_1)_s$	0.12 g	0.9 mml.
$(CuBr_2)_s$	0.06 g	0.3 mml.

First, the three liquids, methanol, water and DEA monomer, were degassed separately under nitrogen inside sealed round-bottom flasks for 30 min. The methanol and water were then transferred by a purged syringe into the DEA monomer's flask and stirred together under nitrogen. Next, bipy, $CuBr_2$ and $CuBr_1$ were added quickly to this mixture inside the sealed flask, and then degassed and stirred again for another 30 min. Subsequently, the PDEAEMA solution was transferred by a purged syringe into the degassed glass cell that contained the initiated silicon substrate and was then left at room temperature (22 °C) for 24 h (Figure 4.10). Once the sample of the PDEAEMA brush was taken out of the glass cell, it was washed with methanol and ethanol and then dried under N_2. The thickness of the PDEAEMA brush was measured and characterised by the contact angle and by ellipsometry, as will be presented in Section 4.3.

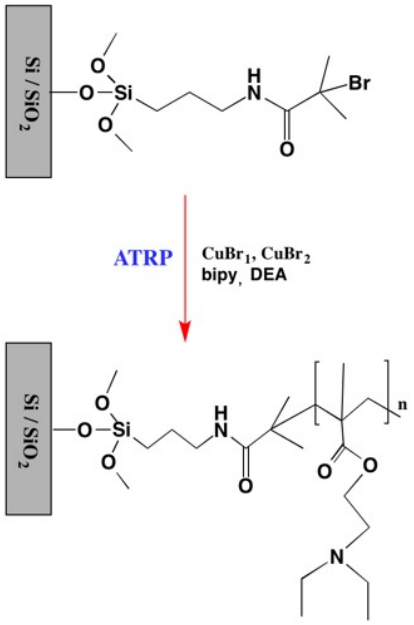

Figure 4.10: The synthesis of the PDEAEMA brush.

4.3 Experimental Techniques

This section presents the experimental techniques that were used in the work presented in this thesis. Ellipsometry and the contact angle were used to measure the thickness of the polymer brush and to confirm the formation of both the initiated layer and the polymer brush on silicon substrates. A mechanical tester, called a Stable Micro Systems TA.XT Plus Texture Analyser (TA), was also used to carry out the adhesion experiments between the hydrogels and polymer brushes underwater as a function of either changing the pH or adding salt to the surrounding water. A few drops of sodium hydroxide (NaOH) or hydrochloric acid (HCl) were used to adjust the pH value of the water, and the pH was measured by the Mettler Toledo pH/mV/temperature meter SevenEasy S20. Sodium chloride (NaCl) was used at various concentrations to investigate the salt effect on the interfacial adhesion between a hydrogel and polymer brush underwater.

The switchable adhesion experiments were then conducted as follows:

1) Single-network (SN) hydrogel adhesion experiments:

   - Adhesion test between the PMAA gel and PDEAEMA brush.

- Adhesion test between the PDEAEMA gel and PMAA brush.

2) Double-network (DN) hydrogel adhesion experiments:

- Adhesion test between the PMAA–POEGMA gel and PDEAEMA brush.
- Adhesion test between the POEGMA–PMAA gel and PDEAEMA brush.

4.3.1 Spectroscopic Ellipsometry

Ellipsometry is an optical technique that is commonly used for surface analysis to measure the thickness of thin films from a few angstroms up to tens of microns. This technique is widely used in scientific research as a result of its ability to give accurate information about sample properties, such as the roughness and the thickness (depth). Ellipsometry measures the changes in the polarisation (amplitude ratio Ψ and phase difference Δ) of a reflected beam of the light source from a surface of interest, depending on the layer material and its thickness [149].

The spectroscopic ellipsometer that was employed in this study was a M-2000V rotating compensator ellipsometer (J. A. Woollam Co. Inc, USA). A fixed angle of incidence of 70 ° was taken with all measurements using CompleteEASE analysis software. The thickness measurements of the PMAA and PDEAEMA brush on a silicon substrate were carried out in a dry conditions. The samples were modelled with a multilayer model of Si layer, native layer (2 nm) and a generic Cauchy layer. The Cauchy layer was fitted to allow dry thickness that represented the thickness of the polymer brush. The thickness results were obtained from an average of three different positions on the surface of the polymer brush.

The measured thickness of the initiator layer was 1 – 2 nm, which was fitted with the same Cauchy model. Whereas, the thickness of the polymer brush after 24 h polymerisation time was $\sim$ 90 nm for the PMAA brush and $\sim$ 80 nm for the PDEAEMA brush.

In addition, ellipsometry was used to measure the conformational changes (collapsing and extending states) of the polymer brush under wet conditions as a function of varying the pH value by using a fitted EMA model consisting of the two adjustable parameters of the pure polymer and water. These data will be presented and discussed later in Chapter 5.

4.3.2 Contact Angle Measurements

In order to quantify the hydrophobicity/hydrophilicity of the silicon surface and brush samples, the surface tension between the surface of a polymer brush and a droplet of pure water was measured prior and after growing the polymer brushes by using a contact angle. The contact angle was measured with a Theta optical tensiometer (Attension, Biolin Scientific, Espoo, Finland) that equipped with a high contrast camera to capture images of the drop of water on the surface. The drop of water was dispensed from a syringe using water (15 MΩ).

The contact angle is a straightforward technique that gives information about the balance between the three phases boundaries, air, liquid and the solid surface, and represents it through Young's equation

$$\gamma_L \, cos\, \theta = \gamma_{\mathrm{S}} - \gamma_{\mathrm{SL}} \, . \tag{4.1}$$

where, γ_{L}, γ_{S} and γ_{SL} are the surface energies of the liquid/air, solid/air and solid/liquid interfaces, respectively [7, 8].

The contact angle was therefore measured before and after preparing the polymer brush on a silicon surface and the obtained results of the average water contact angle with: APTES, initiated and polymer brush layers are presented in Table 4.9 below.

Table 4.9: Contact angle measurements for different surfaces.

Surface type	Contact angles
APTES layer on silicon surface	50° – 70°
Intiated silicon surface	60° – 80°
PDEAEMA brush	45° – 60°
PMAA brush	30° – 50°

4.4 Switchable Adhesion Experiments

The switchable adhesion experiments between the oppositely charged polyelectrolytes; hydrogel and polymer brush, were carried out underwater using a mechanical tester called a Stable Micro Systems TA.XT Plus Texture Analyser (TA) (shown in Figure 4.11). The mechanical tester (TA) has a mobile probe that consists of a plastic jacket, which is used to insert and fix a hemispherical piece of a hydrogel inside it (Figure 4.12 (a)). The TA mechanical probe moves vertically down and brings the hydrogel in contact with the polymer brush surface underwater, and then it applies a certain pressure (an applied force) on the hydrogel to ensure the formation of an interfacial adhesive contact with the polymer brush (Figure 4.12 (b)).

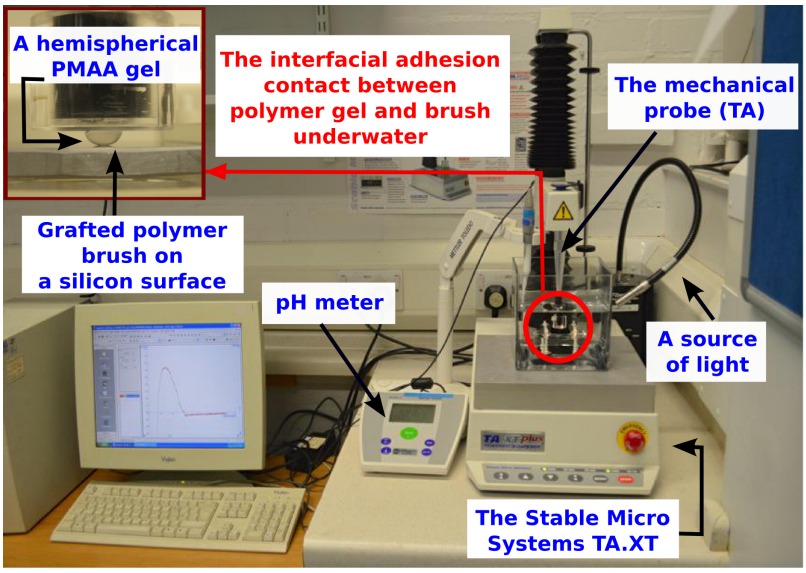

Figure 4.11: Photograph of the Stable Micro Systems TA.XT Plus Texture Analyser (TA), (Sheffield University, UK).

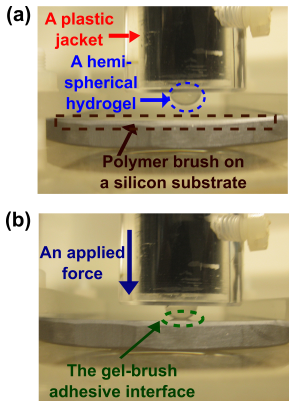

Figure 4.12: A hydrogel attached to the TA's probe (a) before and (b) after bringing it in contact with the brush surface.

The coated surface of a polymer brush was secured to heavy Perspex and fixed by plastic screws and nuts in order to prevent it moving during the attaching–detaching process of the adhesion test. The surface of a polymer brush was then placed inside a glass dish containing DI water. Pull-off experiments were thereafter conducted to measure the adhesion between the hydrogel and polymer brush underwater as a function of the pH value or salt concentration.

When the mechanical probe brings the hydrogel into contact with the surface of the polymer brush underwater, it leaves them in contact with each other for 2 min before pulling them apart with a speed of 50 mm/min. The pull-off adhesion tests with the TA mechanical tester help to provide information about how strong the adhesion is at the hydrogel-brush interface by presenting either force-distance curves (Figure 4.13 (a)) or force-time curves (Figure 4.13 (b)). The force-distance (time) curve helps to find the maximum adhesive force (F) at the hydrogel-brush interface and also to calculate the work done (W), i.e. to detach the hydrogel from the brush surface.

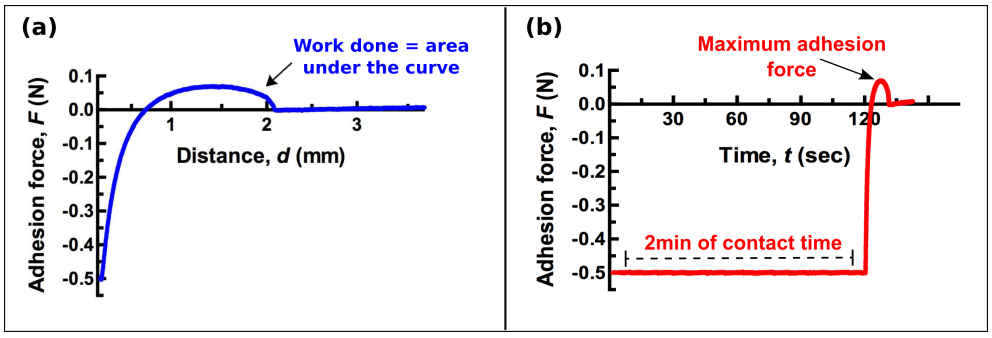

Figure 4.13: Raw data obtained from the adhesion test using the TA mechanical tester. (a) A force-distance curve and (b) a force-time curve for an adhesion test between the PMAA hydrogel and PDEAEMA brush underwater at pH 5.8 with an applied force (P) of 0.5 N and a contact time (t) of 2 min.

The obtained results of the switchable adhesion between different types of hydrogels (both SN hydrogel and DN hydrogel) with the surface of a polymer brush will be presented and discussed later in Chapter 5, 6 and 7.

Chapter 5

Polymer Brush Adhesion With A Single–Network Hydrogel

Abstract. Adhesion experiments were conducted between two oppositely charged polyelectrolytes: a single-network hydrogel and a polymer brush, to assess their interfacial adhesive interactions underwater as a function of pH. A polyacid of the poly(methacrylic acid) and a polybase of the poly[2-(diethyl amino)ethyl methacrylate] were used to prepare the hydrogels and brushes. It was found that the adhesion between oppositely charged hydrogels and brushes was stronger inside water at pH $\sim$ 6, while it became very low and weak inside water at pH 12 or pH 1. The reduction in the adhesion at the hydrogel-brush interface inside a strong basic or acidic pH level was because there was no significant interaction between the hydrogel and brush due to the dissipation of hydrogen bonding as well as the electrostatic interaction (as the chain collapse) of either the polyacid (at pH 1) or the polybase (at pH 12). Since single-network hydrogels are quite soft when they are fully swollen in water, their adhesion with the surface of polymer brushes always ends with a cohesive failure after their detachment (damage occurred to the hydrogel). The adhesion of single-network hydrogels was, however, a pH-switchable and controllable process since it showed an '*on-off*' oscillation by changing the pH value of water from pH $\sim$ 6 to either pH 1 or pH 12.

5.1 Introduction

Adhesion between polymer/polymer and polymer/solid interfaces has attracted considerable interest due to its industrial importance. For example, the automotive and aerospace industries have directed much attention towards the use of epoxy resins and polymers in manufacturing their products (adhering the surfaces together) due to their lower cost, strong adhesion and good mechanical properties [7]. Recently, '*smart*' adhesive technology has provided a new approach to achieve switchable and controllable adhesion between two surfaces that are simultaneously responsive to the change in the environmental condition, such as pH, salt or temperature. Succeeding in producing such dual-responsive adhesion that allows surfaces to adhere together and detach '*on-demand*' would be a further step towards recyclable and environmentally friendly real-world applications [10, 13, 34].

Weakly charged polyelectrolytes (PEs) are promising candidates as reversible adhesives since they have stimuli-responsive groups that are able to switch their electrostatic charges *on* (when their chains expand) and *off* (when their chains collapse) in response to an environmental trigger [13, 28]. PEs are a class of macromolecules that dissociate into positive or negative ionisable groups inside a polar solution, such as water. In general, there are two types of polyelectrolytes, weak and strong, with the difference between them being that the ionisable groups in weak polyelectrolytes have an unfixed degree of association (f) that allows their electrostatic charges to be controlled by varying the environmental conditions. Whereas, in contrast, strong polyelectrolytes have a fixed degree of association that makes their charges fixed and uncontrollable [17, 26–28].

Switchable adhesion was recently demonstrated between two oppositely charged polyelectrolytes: a poly(methacrylic acid) (PMAA, a polyacid *single-network* (SN) hydrogel) and a poly[2-(dimethyl amino)ethyl methacrylate] (PDMAEMA, a polybase brush-coated surface). By changing the pH value of the surrounding water and using a modified Johnson-Kendall-Roberts (JKR) experiment [10, 34], it was found that the work of adhesion (W_{adh}) at the interface between the polyacid hydrogel and polybase brush was higher underwater at a neutral pH value (pH 5.8) and weaker at a very strong acid value (pH < 3). The work of adhesion was assessed by measuring the adhesive contact diameter ($2a$) at the hydrogel-brush interface using a side-view camera. The increase in the contact radius at the hydrogel-brush inter-

face in deionised (DI) water indicated that adhesion was stronger, while the decrease in the interfacial radius (at low pH) indicated that the adhesion force was very weak [150].

The work in this thesis studies the switchable adhesion between two oppositely charged polyelectrolytes (a SN hydrogel and polymer brush) underwater, as a function of pH using a mechanical tester called Stable Micro Systems (TA). This mechanical tester has a mobile probe that moves vertically down to attach the hydrogel to the surface of the polymer brush (for 2 min by an applied force of 0.5 N) and then detaches them apart (by a debonding speed of 50 mm/min) in order to measure their adhesion at their interface. Pull-off adhesion experiments were carried out between a hemispherical hydrogel and a flat surface of a polymer brush underwater as a function of pH. The hemispherical hydrogel was inserted and fixed inside the plastic jacket of the mobile probe of the mechanical tester, while the coated-brush surface was attached to a heavy perspex block and placed inside a beaker glass of 2L capacity filled with DI water. The force-distance curve was subsequently collected by the TA mechanical tester after completing attaching and detaching process. Force-distance curves were then used to characterise the real adhesion features by finding: (1) the maximum adhesion force (F) at the gel-brush interface, which was collected from the highest point on the peak of the force-distance curve, and also (2) the work done (W) in separating the gel from the brush surface, which was collected from the area under the force-distance curve.

Two types of weak polyelectrolytes were therefore used here to synthesise the hemispherical SN hydrogels and brush-coated surfaces: i) poly(methacrylic acid) (PMAA, polyacid) and ii) poly[2-(diethyl amino)ethyl methacrylate] (PDEAEMA, polybase). The pH-adhesion experiments were accordingly divided into two parts: (1) the adhesion between a polyacid gel with a polybase brush (the PMAA gel–PDEAEMA brush), and (2) the adhesion between a polybase gel with a polyacid brush (the PDEAEMA gel–PMAA brush). This chapter first discusses the pH-induced swelling behaviours of i) polymer brushes and ii) the SN hydrogels of the PMAA and PDEAEMA. The results of the switchable adhesion of (i) the PMAA gel–PDEAEMA brush and also (ii) the PDEAEMA gel–PMAA brush are then presented as a function of pH. The effect of varying some physical or chemical parameters on the gel-brush adhesion was investigated, such as: the crosslinker density of the hydrogel, the thickness of the polymer brush, the applied force needed to attach and press the hydrogel onto the brush surface in

order to create their adhesive interface, and also the debonding speed of the pull-off adhesion experiment.

5.2 pH Behaviour of Hydrogels and Brushes

Before presenting the results of the pull-off experiments, the swelling properties of both PMAA and PDEAEMA hydrogels and polymer brushes, and also the elastic modulus of the hydrogels, are discussed in order to understand their physical and chemical changes as a function of pH.

5.2.1 Swelling Behaviours of Polyelectrolyte Brushes

The structural (conformational) changes evident in weak PE brushes, PMAA and PDEAEMA, were characterised as a function of pH by using a spectroscopic ellipsometer. An effective medium approximation (EMA) model was applied to equilibrated ellipsometry data in order to measure the wet thickness of the polymer brush layer. This EMA model consisted of two adjustable parameters for the pure polymer and water. A square PTFE liquid cell, made with two quartz windows at 70 ° on opposite sides, was used to measure the thickness of the polymer brush inside water at different pHs. The light beam of the ellipsometer was transmitted into the liquid in such a way that the quartz windows minimised refraction and so the beam was wholly reflected from the sample surface into the detector through the second window. The process of measuring the brush thickness in a wet condition (inside water) was carried out by sticking the brush-coated surface to the base of the liquid cell using a double-side adhesive tape, and water was then added. The brush sample was allow to equilibrate inside water at a known pH for an hour before taking the thickness measurement.

Figure 5.1 illustrates the swelling and collapsing behaviours of the polybase and polyacid brushes inside water at different pHs, and the solid lines are fitted to

$$h = h_2 + \frac{h_1 - h_2}{2}\sqrt{\left(1 + \tanh\left(\frac{\mathrm{pH}_1 - \Delta_1}{\sigma_1}\right)\right)\left(1 + \tanh\left(\frac{\mathrm{pH}_2 - \Delta_2}{\sigma_2}\right)\right)}, \qquad (5.1)$$

where h_1, h_2, Δ_1, Δ_2, σ_1 and σ_2 are fitting parameters. The equation is used to fit an approximate form of the ellipsometry data, which then allows an accurate determination of

the pK_a of PE brushes after setting its second derivative to zero [151].

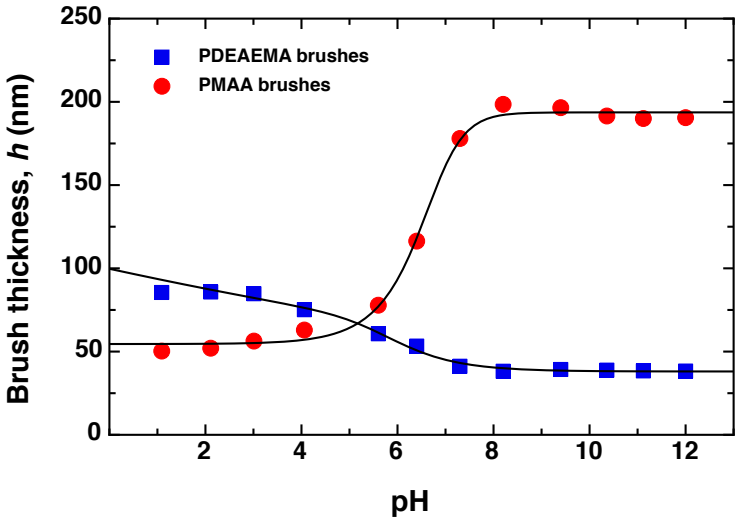

Figure 5.1: Ellipsometric characterisation of the PMAA and PDEAEMA brush thicknesses as a function of pH.

The pH value of DI water was adjusted to alkaline or acidic by adding a few drops of sodium hydroxide (NaOH) or hydrochloric acid (HCl). The Mettler Toledo pH/mV/temperature meter SevenEasy S20 was used to measure the controlled pH of the surrounding water inside the PTFE liquid cell. The dry thickness (in air) for PMAA and PDEAEMA brushes, in Figure 5.1, after 9 h of polymerisation were 32.2 ± 0.2 and 28.8 ± 0.1 nm, respectively. Whereas, the wet thickness was measured from three different points on the surface of polymer brushes. The *in situ* ellipsometry data show that thickness transition (brush expanded) for both the PMAA and PDEAEMA polymer brushes took place at a medium pH value of between pH 5.8 and 7. The PMAA brush was vertically extended at a pH $>$ 5.8 due to the negative charges on the polyacid brush, which caused a stronger electrostatic repulsion between the carboxylic groups, and also due to the high osmotic pressure of counterions within the brush. In contrast, the PDEAEMA brush was extended at pH $<$ 5.8 for the same reason of the repulsive interaction between the positively charged amino groups on the polybase brush [148, 152].

Thus, the pK_a of the PMAA and PDEAEMA brushes were calculated from these data and found to be 6.4 and 5.3, respectively. The PMAA brush became charged at a constant pH above their pK_a, while the PDEAEMA did so below their pK_a [147, 148, 153]. The pH-

transition of the weak polyelectrolyte brush from uncharged to charged is a consequence of the increase in the inter-chain repulsion and the condensation of the counterions around the brush that caused an increase in the osmotic pressure, allowing the brush to extend and absorb more water. When the weakly charged polyelectrolyte brushes become hydrophobic in a solution, the brushes collapse and become uncharged as a result of screening of the electrostatic interactions [58, 142, 152].

5.2.2 Swelling Ratios of Hydrogels

The swelling ratio (Q) of single-network gels, PMAA and PDEAEMA, was calculated as a function of pH value using different crosslinker densities. Both PMAA and PDEAEMA hydrogels were therefore made with three different crosslinker densities in order to examine the impact of the crosslinker density of the hydrogels on their adhesion with the oppositely charged polymer brushes. Accordingly, flat circular sheets of both PMAA and PDEAEMA gels (with a diameter of 5 cm and a width of 5 mm) were made with three different crosslinker quantities. The amount of the normal crosslinker in the regular hydrogel (called X1 CL gel) was doubled (called X2 CL gel) and also halved (called X0.5 CL gel) (see Table. 5.1) in order to allow a comparison between them according to their swelling ratios and also their adhesion performances with the polymer brushes.

Table 5.1: The double-crosslinked (X2 CL), normal-crosslinked (X1 CL) and half-crosslinked (X0.5 CL) single-network gels of the PMAA and PDEAEMA are presented with their crosslinker% concentration in the total solution.

Hydrogels	Crosslinker%
X2 CL PMAA	0.38 mol %
X1 CL PMAA	0.18 mol %
X0.5 CL PMAA	0.08 mol %
X2 CL PDEAEMA	7.2 mol %
X1 CL PDEAEMA	3.9 mol %
X0.5 CL PDEAEMA	1.9 mol %

After synthesising these gels, each one was dried in a vacuum oven at 50 °C for 5 h and then the weight of the dried gel (W_{dry}) was measured and recorded. Thereafter, the dried flat gel was placed inside water at a chosen pH value to equilibrate for 5 days. A while later, the weight of the swollen gel (W_{swollen}) was measured and recorded. The swelling ratios of both the PMAA and PDEAEMA hydrogels, with each of the different crosslink concentrations, were calculated at various pH values using the following equation

$$Q = \frac{W_{\text{swollen}}}{W_{dry}} . \tag{5.2}$$

Figure 5.2 presents the pH-sensitive swelling and de-swelling behaviours of both the PMAA and PDEAEMA gels at different pH value. The polyacid, PMAA, gels had an opposite response to the polybase, PDEAEMA, gels. At a high pH level (above pH $>$ 5.8), the anionic hydrogels (PMAA gels) were ionised and swollen above their pK_a as a result of their carboxylic groups being negatively charged (see Figure 5.3). As a consequence, the chains were extended due to the electrostatic repulsion between neighbouring chains that were induced by the charge condensations on the chains themselves. In other words, the carboxylic endgroups of PMAA gel dissociated in water at neutral or high pH (above pH 5) and so became negatively charged, causing a repulsion between the chains and allowing the gel to absorb more water and swell.

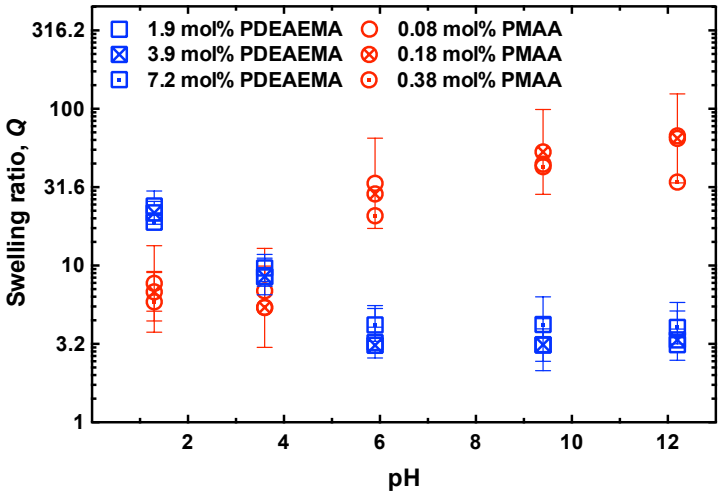

Figure 5.2: The swelling ratios of the polybase, PDEAEMA, gel (blue symbols) and polyacid, PMAA, gel (red symbols) as a function of the pH levels.

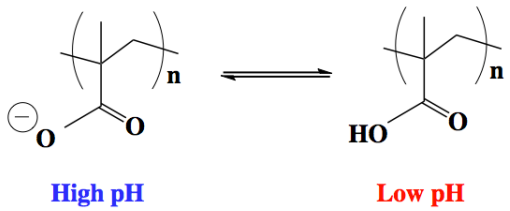

Figure 5.3: The behaviour of PMAA gel in response to the pH changes. At a low pH, the PMAA becomes uncharged and hydrophobic, while it becomes charged and hydrophilic at a high pH.

The carboxylic groups of PMAA gel were deionised and so collapsed (de-swelled) at a pH below pH 5.8 due to the absence of repulsive forces on the chains [81, 154]. In contrast, the cationic, PDEAEMA, gels became positively charged as their polymer chains accepted protons at a pH below 5.8 allowing them to extend and absorb more water. When the amino groups in the PDEAEMA gels became uncharged at a pH above 5.8, the chains collapsed and so the gels were shrunk (Figure 5.4) [80, 155, 156]. Generally speaking, the swelling ratio of the PMAA gel was larger than that of the PDEAEMA gel as a result of the lower quantity of the crosslinkers used in the PMAA. The amount of crosslinker affects the swelling ratio of the hydrogels, i.e. the polymer chains are elastically stretched at a low crosslinking density and so the gel becomes soft and able to absorb more water, while the gel becomes more stiff and not able to absorb a large amount of water at higher crosslinking densities.

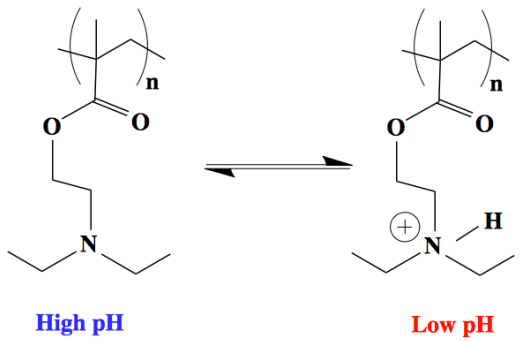

Figure 5.4: The behaviour of the PDEAEMA gel in the response to the pH changes. At a high pH, the PDEAEMA becomes uncharged and hydrophobic, while it becomes charged and hydrophilic at a low pH.

The crosslinking degree influences many of the network properties, such as the swelling ratio and the elastic modulus of the gel. The highly crosslinked hydrogels swell and absorb less water than loosely crosslinked gels. In other words, the polymer chains lose some of their ability to move as individual entities when they are highly crosslinked together and thus the gels swell less [97, 157].

5.2.3 Elastic Modulus of Single-Network Hydrogels

The elastic modulus (K) of all PMAA and PDEAEMA (SN) hydrogels, which were previously presented in Table 5.1, were investigated using the Hertz model. Hertz theory states that when a load (P) is applied on an elastic sphere with a radius (R) and an elastic modulus (K), a new unit area of radius (a) is created at the interface that is given by

$$a^3 = \frac{PR}{K}\,. \tag{5.3}$$

In order to estimate the elastic modulus of both PDEAEMA and PMAA hydrogels, equation (5.3) was used with three different applied forces: 0.5 N, 1 N and 2 N. Since the Hertz model assumes that there are no attractive interactions at the interface between the spherical bodies, it was essential to choose a specific type of surface that did not interact with the hydrogel. The experiments to find the elastic modulus of the PMAA and PDEAEMA gels were conducted by bringing the hydrogel into contact with the chosen surface and then the mechanical probe applied a known force on them for two minutes underwater. Subsequently, the interfacial area (a) between the gel and the substrate was recorded by a camera and measured by ImageJ software.

As a consequence, the elastic moduli of PDEAEMA gels, which were made with different crosslinker densities, were calculated by using an APTES–initiated silicon substrate. Whereas, the elastic moduli of PMAA gels that had different crosslinker densities were obtained by using an uncoated silicon substrate.

5.2.3.1 Elastic Moduli of PDEAEMA Hydrogels

The elastic moduli of the three PDEAEMA hydrogels that were made with different crosslinker amounts were calculated by using the Hertz equation (5.3). Figure 5.5 presents the obtained measurements of the PDEAEMA–APTES interface (a^3) plotted against PR. A straight line of PR vs. a^3 can therefore be used to find the elastic moduli of PDEAEMA gels in DI water.

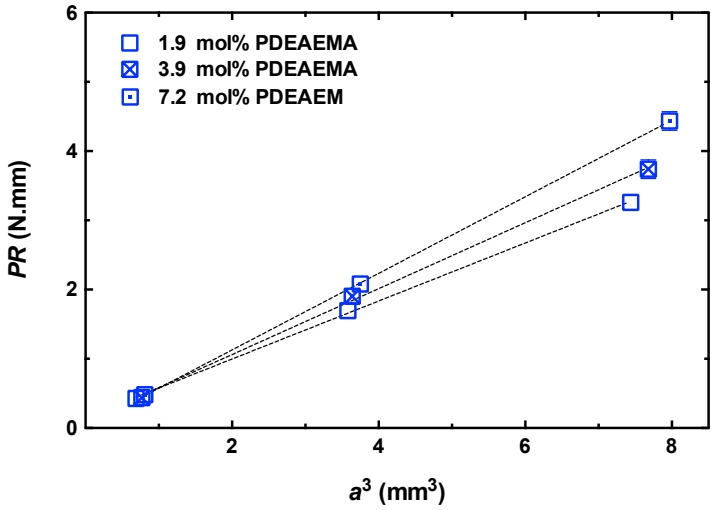

Figure 5.5: The elastic modulus of PDEAEMA gels at pH 5.8.

Table 5.2 presents the elastic moduli of the PDEAEMA hydrogels that were made with three different crosslinker densities inside DI water. The elastic modulus of the PDEAEMA gel was dependent on its swelling degree in water and thus the highly crosslinked hydrogel had a higher elastic modulus (0.55 MPa) since it swelled and absorbed less water, and vice versa for the loosely crosslinked hydrogel.

Table 5.2: The elastic moduli of PDEAEMA hydrogels in DI water as a function of the crosslinking densities.

PDEAEMA hydrogel	Elastic Modulus (MPa)
X0.5 CL PDEAEMA (1.97 mol%)	0.42
X1 CL PDEAEMA (3.88 mol%)	0.48
X2 CL PDEAEMA (7.23 mol%)	0.55

5.2.3.2 Elastic Moduli of PMAA Hydrogels

Changing the crosslinker concentration alters the elastic moduli of the hydrogels, which consequently affects the mechanical strength of the gels. If the gel has a high elastic modulus, the gel is stiff and may resist mechanical deformations, and vice versa [104, 157, 158].

Figure 5.6 presents the obtained measurements of the PMAA–silicon surface interface a^3 plotted against PR. A straight line of PR vs. a^3 can be used to calculate the elastic modulus of PMAA hydrogels in DI water at pH 5.8, and the results obtained for the elastic moduli are presented in Table 5.3.

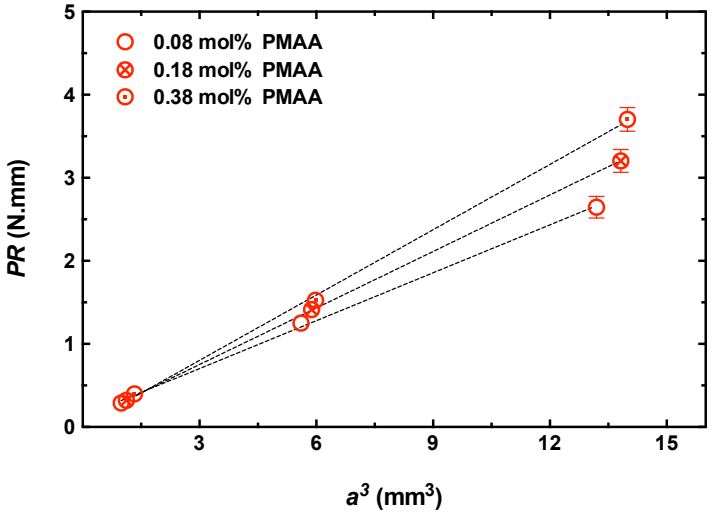

Figure 5.6: The elastic modulus of PMAA gels at pH 5.8.

Table 5.3: The elastic moduli of PMAA hydrogels in DI water as a function of the crosslinking densities.

PMAA hydrogel	Elastic Modulus (MPa)
X0.5 CL PMAA (0.084 mol%)	0.19
X1 CL PMAA (0.18 mol%)	0.30
X2 CL PMAA (0.38 mol%)	0.26

The PMAA gel has a lower elastic modulus than the PDEAEMA gel because it contained a lower amount of crosslinks. It can be concluded that there is a linear relationship between

the elastic modulus of the hydrogel and the amount of crosslinker used in the total solution of hydrogel, as shown in Figure 5.7.

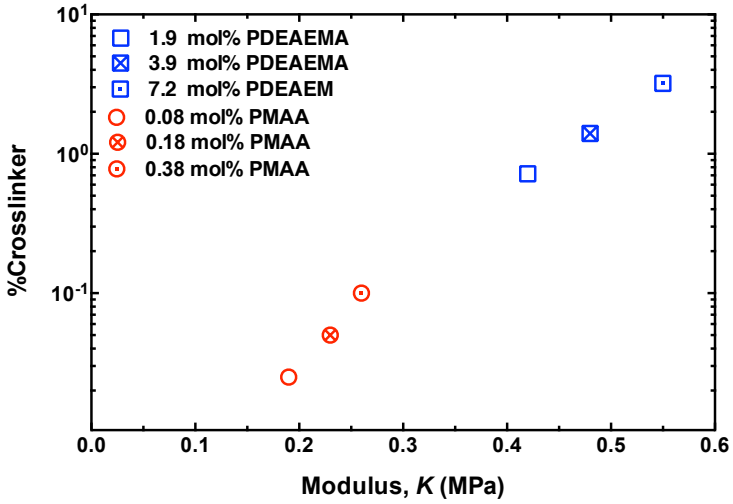

Figure 5.7: The relationship between the elastic moduli of PDEAEMA and PMAA hydrogels with the %crosslinker concentration in their total solutions.

Furthermore, the effect of changing the pH of the surrounding water on the elastic modulus of a PE hydrogel was investigated since the pH controls its swelling ratio. Thus, the elastic modulus of the (0.18 mol%)–PMAA gel was examined at pH 1, 5.8 and 12. Upon analysis of the data collected for estimated elastic moduli, the radius of the PMAA gel was measured as a function of the pH value. A camera setup was used to record side-view images for the interfacial radius ($2a$) of the PMAA gel with an uncoated silicon surface at different pH values using three different applied forces: 0.5, 1 and 2 N. The obtained measurements of the PMAA–silicon interface a^3 were plotted against PR (see Figure 5.8). It became obvious that straight line trends for PR vs. a^3 could be used to find the elastic modulus of (0.18 mol%)–PMAA gel at different pH values by finding the gradient of each linear trend. These elastic moduli calculations of (0.18 mol%)–PMAA gel are presented in Table 5.4.

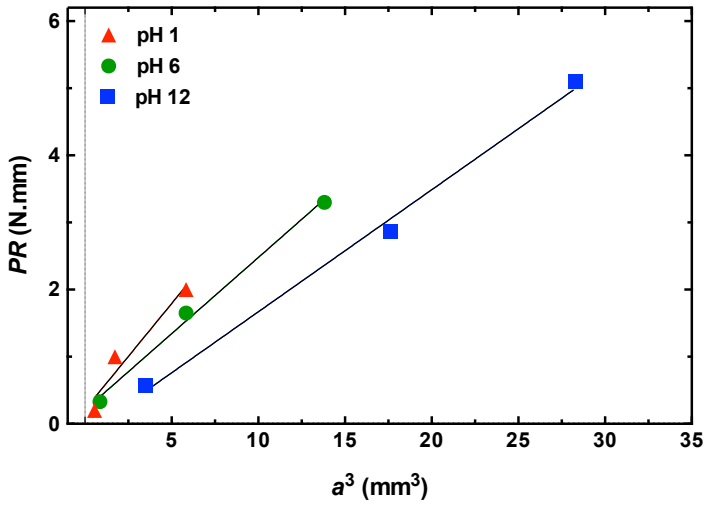

Figure 5.8: The elastic modulus of the (0.18 mol%)–PMAA gel at pH 1, 5.8 and 12.

It was found that the elastic modulus of the (0.18 mol%)–PMAA gel was variable since the swelling ratio of the hydrogel was influenced by the pH value. In other words, the elastic modulus was higher (0.42 MPa) when the PMAA gel was shrunk at pH 1. This was due to the fact that the PMAA gel had a lower swelling ratio at pH 1 since the carboxylic groups were neutralised, and so its elastic modulus consequently increased. Whereas, on the other hand, the elastic modulus of the PMAA gel decreased at a higher pH values (i.e pH 5.8 and 12) due to the increase in its swelling ratio.

Table 5.4: The elastic moduli of the (0.18 mol%)–PMAA hydrogel as a function of pH.

pH level	PMAA elastic Modulus (MPa)
pH 1	0.42
pH 5.8	0.30
pH 12	0.17

5.3 Adhesion Measurements of Single-Network Hydrogels

5.3.1 Adhesion of Polyacid and Polybase Hydrogels

Hydrogels and polymer brushes of PMAA and PDEAEMA were prepared in order to study their adhesion at the gel-brush interface underwater. The adhesion experiments were therefore conducted between two different adhesive gel-brush structures that were: 1) (0.18 mol%)–PMAA gel adhering to PDEAEMA brush and 2) (3.9 mol%)–PDEAEMA gel adhering to PMAA brush as a function of pH. The dry thickness of the PMAA and PDEAEMA brushes were 83.2 ± 0.9 nm and 78.5 ± 0.2 nm, respectively. During the adhesion measurements, the applied force, which was used to attach the hemispherical gel to the surface of the polymer brush in order to create the gel-brush adhesive interface, was 0.5 N, and the contact time for bringing the gel into contact with the brush was 2 min. The applied force, contact time and debonding speed (50 mm/min) of detaching the gel from the brush surface were kept constant in all gel-brush adhesion experiments. Figure 5.9 illustrates the adhesion results of the two adhesive systems: i) PMAA gel–PDEAEMA brush and ii) PDEAEMA gel–PMAA brush, as a function of varying the pH value of their surrounding water.

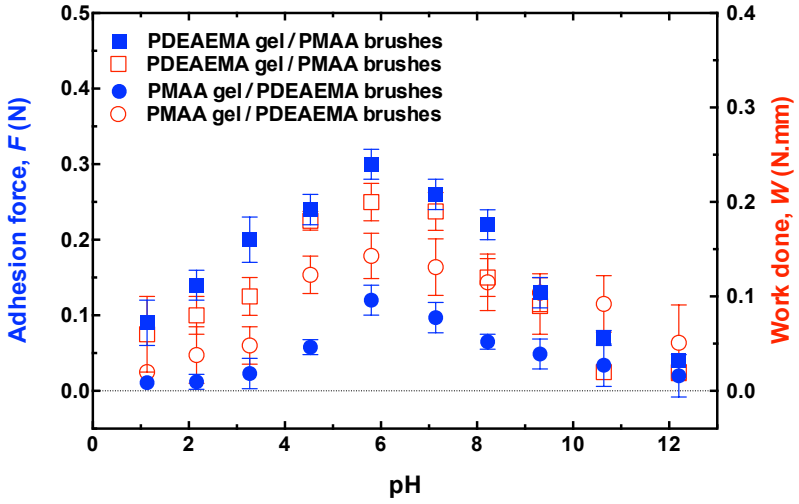

Figure 5.9: The maximum adhesion forces (F) and work done (W) for the adhesion tests of (i) (0.18 mol%)–PMAA gel adhering to the PDEAEMA brush and (ii) (3.9 mol%)–PDEAEMA gel adhering to the PMAA brush as a function of pH. The closed blue symbols indicate the values of the maximum adhesion force at the gel-brush interface. The open red symbols indicate the work done (calculated from the area under force-distance curves) to detach the gel from the brush surface.

It was found that the maximum adhesion force and work done were higher for both adhesive systems, of i) the PMAA gel–PDEAEMA brush and ii) the PDEAEMA gel–PMAA brush, when the pH of the water was between 4 and 8. This was because the two components (the PMAA and PDEAEMA) of both adhesive systems should be oppositely charged at a pH value higher than 4 and lower than 8, which resulted in a good adhesion between the gel and the brush. In contrast, the adhesion started to decrease for both adhesive structures at a pH below 4 and above 8. This was due to the fact that either the polyacid (PMAA) or the polybase (PDEAEMA) became uncharged and collapsed at a pH below and above their pK_a, respectively [34, 58, 147, 148]. Since the adhesion was removed at pH 1 and 12, it was confirmed that the adhesion at the gel-brush interface exhibited switchable behaviour from an adhesive (at a pH $>$ 4 and $<$ 8) to a non-adhesive state (at pH 1 or 12).

The adhesion of the PMAA gel to the PDEAEMA brush was dramatically weaker at pH 1 than at pH 12, while the adhesion of the PDEAEMA gel to the PMAA brush was weaker at pH 12 than pH 1. This result indicated that polymer hydrogels were controlling the adhesion more than the oppositely charged polymer brushes, because the adhesion dropped dramatically resulted from the larger de-swelling ratio of either the PMAA gel at very low pH (below pH 2) and the PDEAEMA gel at a high pH (above pH 10).

Both the PMAA and PDEAEMA (SN) hydrogels exhibited a cohesive failure after detaching from the brush surface inside water at pH 5.8. Failure adhesion mechanisms for a polymer system are either an adhesive failure or a cohesive failure, which are used in adhesion science to explain surface condition after removing the adhesion. The cohesive failure is defined as deformation accrued to the hydrogel, which resulted from the attempt of removing its adhesion with the polymer brush surface. In contrast, the adhesive failure (which is not the case here) is accrued at an interface between two adhered surfaces without deforming them, and it can be used to describe the strength of the adhesive bonds at their interface [1, 7, 159, 160].

Rupturing the cohesive bonds of SN hydrogels left a clear mark on the brush-coated surface causing damage to the gel and also leaving a cohesive failure on the brush surface, and this was observed under the optical microscope for both PDEAEMA and PMAA gels (see Figure 5.10). The cohesive failures occurred within the SN hydrogels since the adhesive bonds at the gel-brush interface were much stronger than the bonds between the macromolecules on the

chains of the SN hydrogels. This was because the polymer gels became softer when they were fully swollen in water and thus they were easily broken when they were forced to detach from the brush surface. Although adhesion was removed at a strong acidic or basic pH, a small trace of the cohesive failure was still found on the brush surface. In other words, the adhesion of the PMAA hydrogel with the PDEAEMA brush ended with a cohesive failure when the PMAA hydrogel was fully swollen at pH 12, however, their adhesion was weak. The reason of this cohesive failure was not clear, but it is most likely resulted from the higher swelling ratio of the PMAA gel at pH 12, which can be 112% larger than its collapsed mass [34]. One solution to overcoming the cohesive failure of SN hydrogels was leaving the gel to detach automatically by itself from the brush surface inside water at either a very high or low pH. The detaching time varies from a few hours to a number of days depending on the applied force that was used to attach the gel to the brush surface [150], however, this detaching time was criticised as the minimum waiting time for the adhesion to fail [29].

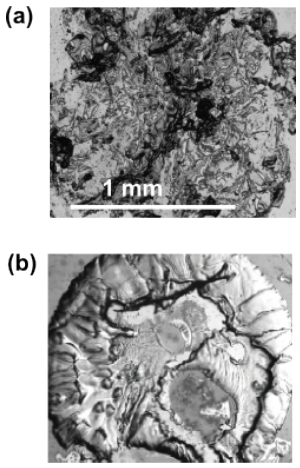

Figure 5.10: Optical microscope images for the cohesive failures of: (a) the PDEAEMA gel on the PMAA brush surface and (b) the PMAA gel on the PDEAEMA brush surface inside DI water at pH 5.8.

Generally speaking, the PDEAEMA gel gave a higher adhesion to the oppositely charged brush than the PMAA gel at pH 5.8. The work done to separate the PDEAEMA gel from the brush surface, however, was close to the work done in detaching the PMAA gel. Comparing the two polymer SN hydrogels in terms of their physical properties, the PMAA gel had a lower elastic modulus than the PDEAEMA gel and so it swelled more and absorbed more water. As

a result of the large swelling ratio and the soft structure of the PMAA gel, it stretched more than the PDEAEMA gel when it was pulled away from the brush surface and so a necking behaviour was observed with the PMAA gel in DI water at pH 5.8, (see Figure 5.11 (a)). The neck served to cause a cohesive mechanism failure since the bonds of the hydrogel were weaker than the adhesive bonds at the interface with the PDEAEMA brush. The stretching behaviour of the PMAA gel therefore consumed more energy in order to detach from the brush surface, which resulted in a larger work done. In addition, the large swelling size of the PMAA hydrogel at pH values above 5 led to an increase in the interfacial contact area with the brush surface, which consequently led to an increase in the adhesive interacting points at the gel-brush interface, resulting in a higher work done.

Since the PDEAMA gel was more crosslinked and also stiffer than the PMAA gel, it gave a higher adhesive force when it was detached from the brush surface underwater. The high adhesive force indicated that the adhesive bonds at the interface were broken suddenly since the highly crosslinked chains of the PDEAEMA gel did not stretch when they were pulled in the opposite direction. As a result, the PDEAEMA gel was promptly detached from the brush surface and therefore no sign of stretching or necking behaviour was observed when it was detached from the PMAA brush surface (see Figure 5.11 (b)). Although the PDEAEMA gel had an elastic modulus (0.48 MPa) twice as high as the PMAA gel (0.30 MPa) in DI water, it was found that adhesion of both the PMAA and PDEAEMA hydrogels ended with cohesive failures, and for this reason the adhesion mechanism of these two (SN) hydrogels was considered to be similar to each other.

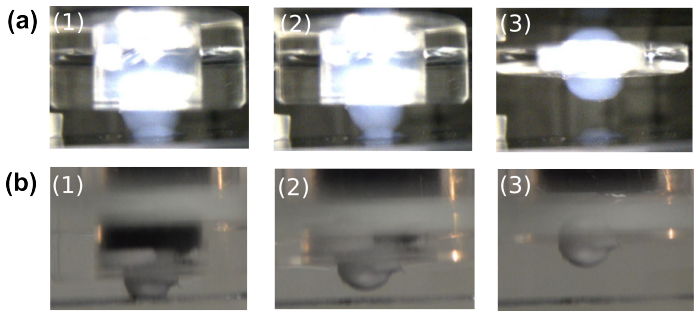

Figure 5.11: The presence of the necking and stretching behaviours in the PMAA gel: image 1 (a), 2 (a) and 3 (a) and their absence in the PDEAEMA gel: image 1 (b), 2 (b) and 3 (b). A source of light was used with the PMAA gel to take images since it is transparent and has a similar reflective index to water.

Single-network hydrogels are soft gels that become brittle when they are either fully swollen or highly crosslinked. The cohesive failures were obtained as the interfacial adhesion between the hydrogel and polymer brush was stronger than the bonds of the chains of the hydrogels. The cohesive failures therefore always occurred within the chains of the hydrogels, especially when the hydrogels were fully swollen in water, which caused a damage to (polyacid and polybase) networks.

5.3.2 Effect of Hydrogel's Crosslinking Concentration on Adhesion

As presented previously, PMAA and PDEAEMA (SN) hydrogels were prepared with three different crosslinker densities (see Table 5.1). The adhesion measurements of these hydrogels were conducted with the mechanical tester (TA) as a function of their crosslinker densities at different pH values: 1.2, 5.8 and 12.7. Figure 5.12 shows the results of the maximum adhesion force (F) and work done (W) in removing i) the PMAA gel from the PDEAEMA brush surface and ii) the PDEAEMA gel from the PMAA brush surface as a function of varying their crosslinker densities. It was found that the loosely crosslinked PMAA and PDEAEMA hydrogels exhibited a larger adhesion force and work done than the highly crosslinked hydrogels. This was due to the loosely crosslinked hydrogel being able to stretch elastically more then the highly crosslinked gel when it was pulled away from the brush surface, and so it produced a higher adhesion force and consequently caused a large work done that was consumed to detach the gel from the brush surface. A loosely crosslinked hydrogel was more elastic and pliable when it became hydrated (swollen) and so it was capable of large deformations. In contrast, a highly crosslinked hydrogel was very stiff and so did not elastically stretch when it was detached from the brush surface. In other words, the adhesion at the hydrogel-brush interface increased when the gel had a lower crosslink density (i.e. a lower elastic modulus), since it was able to stretch and resist the separation.

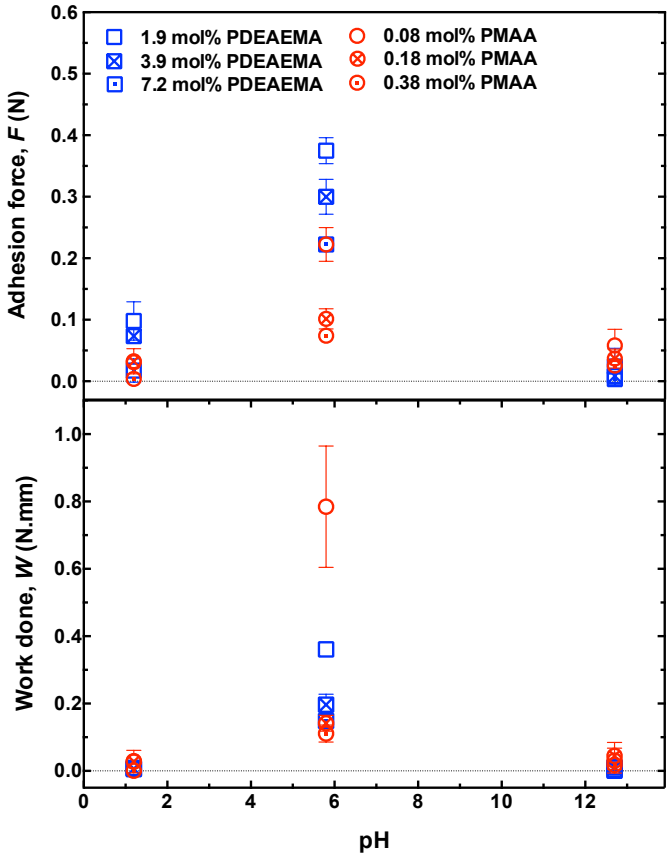

Figure 5.12: The effect of the crosslinking density of the PMAA, polyacid, and the PDEAEMA, polybase, hydrogels on their adhesion force and work done as a function of pH.

The highest crosslinking density influences (restricts) the swelling degree of hydrogels. In other words, the swelling ratio of a hydrogel decreased when its crosslinking density was increased due to the fact that the expanding behaviour of its polymer chains became more restricted by the crosslink points [104]. The highly crosslinked chains of a hydrogel, therefore, had less chance to stretch (and absorb water) and so they required a lower energy to detach when they were adhering to the brush surface. In contrast, at a low crosslink density, the more elastic network stretched and so consumed more energy during the detaching from the brush surface due to the capacity for elongation [161].

It can be deduced that the degree of crosslinking of a hydrogel is critical because it links its swelling ratio and also mechanical strength to the adhesion with the polymer brush [162]. Generally speaking, all these hydrogels, with their different degrees of crosslinking, swelled

inside water when they became hydrophilic (at pH $\sim$ 6), and so cohesive failures were always obtained after detaching them from the brush surface. The cohesive failure caused damage to the network, resulting in a trace from the hydrogel being left on the brush surface (see Figure 5.13). It was therefore suggested that the cohesive failures could be overcome by leaving the attached gel-brush interface to detach by itself for a long time (i.e. either a few hours or days) inside strong acidic or basic pH solutions (i.e. pH 1 or 12).

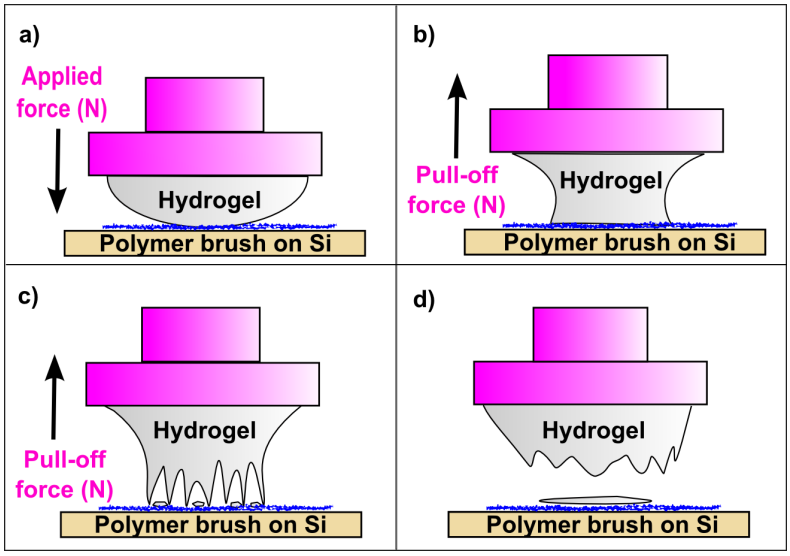

Figure 5.13: An illustrative diagram showing the cohesive failure of a hemispherical hydrogel on a brush-coated surface inside DI water.

5.3.3 Effect of Brush Thickness on Adhesion

The effect of varying the thickness of the polyelectrolyte brush on the relative contribution to the adhesion with the hydrogel was investigated (without varying the crosslinker density of the hydrogel). Three samples of the PDEAEMA brushes were therefore prepared with different brush thicknesses of: 13, 20 and 51 nm in order to test their adhesion with the (0.18 mol%)–PMAA hydrogel. The pull-off adhesion experiments were thus carried out between the (0.18 mol%)–PMAA gel with these three different samples of PDEAEMA brushes as a function of different pH values.

It was found that the adhesion force and the work done between the PMAA gel and PDEAEMA brush increased as the thickness of the brush increased (see Figure 5.14). This was due to the fact that the thicker brush swells more than the thinner one as it extends more, due

to the stronger repulsive interactions between macromolecules on its longer polymer chains. This greater expansion in the length of the PDEAEMA brush could lead to an increase in the contact points with the PMAA hydrogel when they were in contact with each other. Furthermore, for the same grafting density, the thicker brush has a larger molecular weight which consequently leads to an increase in the number of amino groups interacting with the carboxylic groups of the PMAA hydrogel. Thus, the interaction and interpenetration between the amino groups in the PDEAEMA brush and the carboxylic groups of the PMAA gel were larger in the thicker PDEAEMA brush sample (51 nm) than in the thinner one (13 nm), which then resulted in a stronger adhesion force and larger work done.

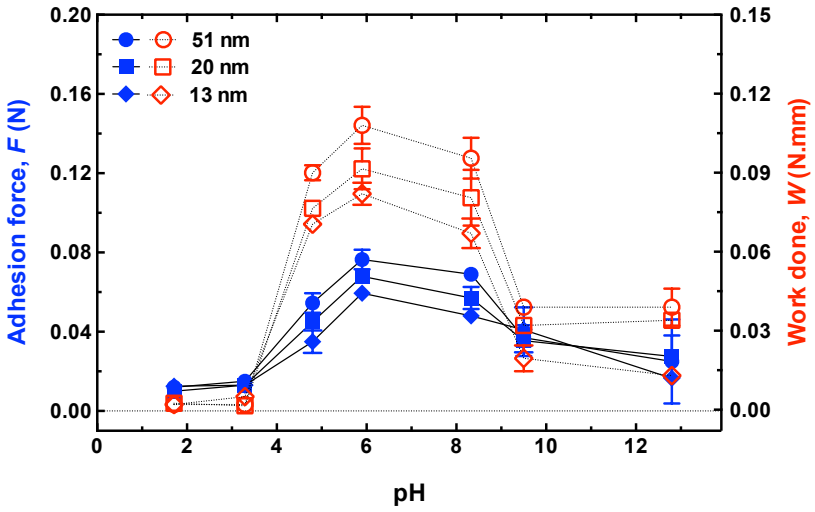

Figure 5.14: The adhesion force (blue symbols) and work done (red symbols) of the PMAA gel adhering to the PDEAEMA brush with different thicknesses as a function of pH.

5.3.4 The Effect of Other Parameters on the Hydrogel-Brush Adhesion

5.3.4.1 Equilibrium Effect on the Interfacial Adhesion

Weak polyelectrolytes undergo association or dissociation during pH changes and thus their polymeric chains are subject to a structural change (expanding or collapsing) when the pH value of their surrounding water becomes equal to their pK_a [163]. It was previously found that an adequate equilibrium contributed to establishing the thermodynamic mechanism of adhesion at the gel-brush interface [150]. The adhesive gel-brush structure, therefore, needs to allow equilibrium to be reached before testing their adhesion inside water at a newly intro-

duced pH. As a consequence, the impact of the equilibration time on adhesion measurements between the (0.18 mol%)–PMAA gel and (43 nm thick)–PDEAEMA brushes was investigated. The adhesion tests were carried out at three different pH values: 1.7, 5.8 and 11.9, as a function of increasing the equilibration time. The equilibration time for the adhesion experiments between the hydrogel and polymer brush, therefore, started at 15 min and then increased progressively until it reached 16 h.

The applied force was 0.5 N, which was kept constant for all of the adhesion experiments. The contact time between the PMAA hydrogel and the PDEAEMA brush was divided into two parts: i) firstly, the PMAA gel was brought into contact with the PDEAEMA brush surface for 2 min before detaching them and then ii) secondly, the test was repeated by bringing the PMAA gel into contact with the PDEAEMA brush surface for 10 min before detaching them. The adhesion tests were therefore conducted between the PMAA gel and the PDEAEMA brush at three pH values with two contact times of 2 min and 10 min as a function of increasing the equilibrium time.

Figure 5.15 shows the maximum adhesion forces at the adhesive gel-brush interface at three pH values as a function of increasing the equilibrium time. It was found that the adhesion force was more affected by increasing the equilibrium time when the pH value was 5.8 (in the green circles), since both the PMAA hydrogel and PDEAEMA brush were electrostatically charged and hence were interacting with each other. In contrast, the adhesion force was not affected at all by increasing the equilibrium time at pH 1.7 (in the red squares) and pH 11.9 (in the blue rhombuses) due to the absence of adhesive interaction at the gel and brush interface.

At pH 5.8, the adhesion force was gradually decreased by increasing the equilibrium time from 15 min until 1 h, at which point it reached a semi-stable value. This implied that the gel and brush needed at least 1 h in order to equilibrate inside the newly introduced pH before running their adhesion measurements. As long as the polymer chain was allowed to equilibrate inside water for enough time, it achieved a balance between the elastic energy and the repulsive interaction. The adhesion force measurements at the PMAA gel–PDEAEMA brush interface were almost the same after an equilibrium time of 8 h or 16 h. In other words, the measurements of the adhesion force remained relatively close after 16 hours as after 1 $\sim$

2 h of equilibration time.

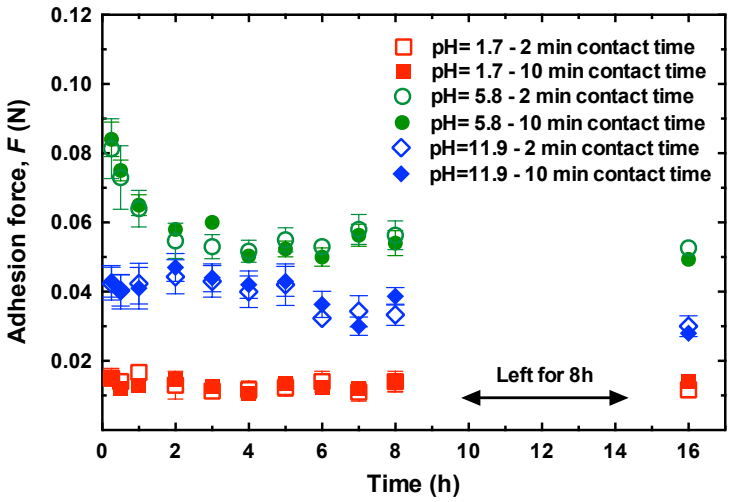

Figure 5.15: The effect of equilibrium time on the adhesion force between the PMAA gel and PDEAEMA brush at different pH values. The open symbols show the results of the 2 min contact time and the filled symbols are for the 10 min contact time between the gel and the polymer brush underwater.

After 15 min of equilibration time, the number of the negative/positive charges on the carboxylic/amino groups was higher since the chains were partially extended due to the slow diffusion of water between the chains. After an hour of the equilibrium, water had diffused completely into the polymer chains and so they became totally expanded due to the strong repulsive interactions between the charges on their macromolecules. As a consequence, the adhesion force was greater when the equilibrium time was less than 1 h. In addition, the change in the contact time between the PMAA gel and the PDEAEMA brush, between 2 min and 10 min, had no significant impact on their interfacial adhesion. This implied that the adhesion interactions at the gel-brush interface are controlled by an equilibrium time that allows both polyelectrolyte structures to reach their equilibrium before adhering them together underwater.

5.3.4.2 Effect of Debonding Speed on the Intefacial Adhesion

During the adhesion measurements, the mobile mechanical probe was attaching the hemispherical hydrogel to the brush surface by an applied force of 0.5 N underwater and leaving them in contact for 2 min before separating them apart with a defined detaching speed.

Varying the separation speed (debonding velocity) of the pull-off adhesion tests gave an idea about how the adhesive bonds at the gel-brush interface were affected by slower and faster separation speeds.

The adhesion of the (0.18 mol%)–PMAA hydrogel was therefore tested with (44 nm thick)–PDEAEMA brush inside DI water at pH 5.8 (without changing the pH). Different separation speeds were chosen ranging from 5 mm/min to 200 mm/min and the obtained results are presented in Figure 5.16. It was found that the adhesion force (in the blue circles) and work done (in the red squares) were stable at a slower separation speed, between 5 $\sim$ 50 mm/min. When the the detaching speed was increased above 60 mm/min, the adhesion measurements suddenly dropped.

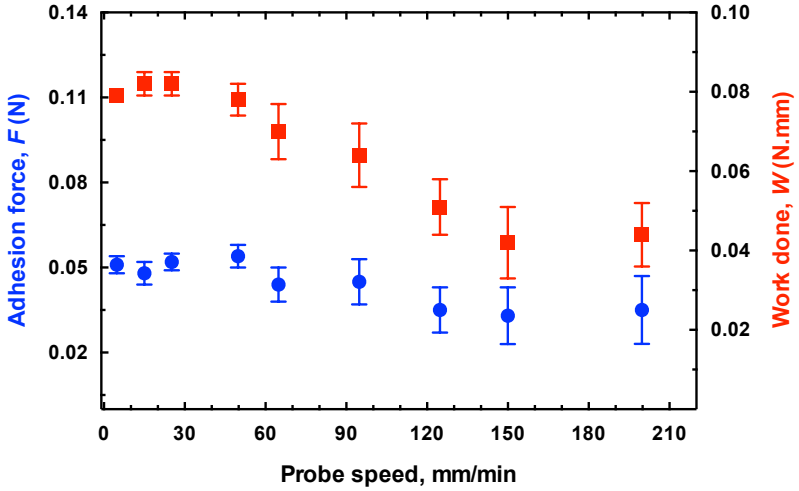

Figure 5.16: The effect of separation speed on the interfacial adhesion measurements of the PMAA gel adhering to the PDEAEMA brush.

At lower retracting speeds, the hydrogel acted as an elastic soft network, since it had enough time to stretch and show its resistance to separation when it was pulled up from the brush surface. As a consequence, the PMAA hydrogel was nearly deformed (cohesive bonds) at the adhesive interfacial area by leaving a cohesive failure on the PDEAEMA brush surface when the separation speed was below 50 mm/min (Figure 5.17 (a)). At higher separation speeds (above $>$ 60 mm/min), in contrast, the PMAA hydrogel was greatly deformed and rapidly broken, and so deformation was accrued at the middle of the hemispherical PMAA network, rather then the area close to the adhesive interface (Figure 5.17 (b)). As a consequence, a

slower separation speed at a constant speed of 50 mm/min was considered as an efficient speed to obtain nearly accurate adhesion measurements, since it allowed to show the viscoelasticity of the formed bonds at the adhesive gel-brush interface.

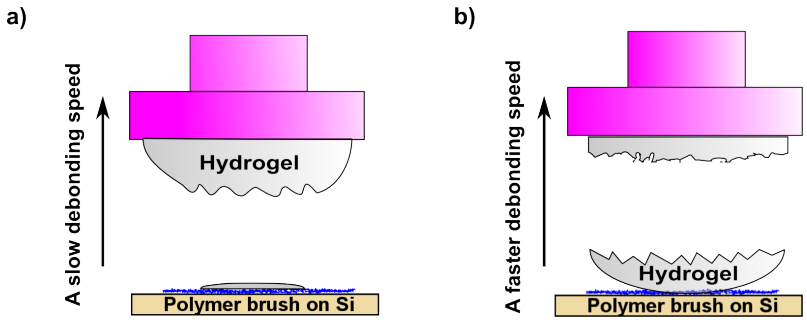

Figure 5.17: The effect of the separation speed on the size of the occurred cohesive failures.

5.3.4.3 Applied Force Effect on the Interfacial Adhesion

When the TA mobile probe was bringing the PMAA gel into contact with the PDEAEMA brush surface underwater, it was applying a specific applied load (P) in order to ensure the formation of the adhesive bonds at the gel-brush interface. Since it was previously found that the adhesive contact diameter ($2a$) at the gel-brush interface increased after increasing the applied force (P) (Figure 5.18) [34, 150], the effect of increasing the applied force on the adhesion force between the PMAA gel and the PDEAEMA brush was therefore investigated. Hence, the applied force was increased progressively from 0.5 N to 15 N and the adhesion of the (0.18 mol%)–PMAA gel was tested with the (75 nm thick)–PDEAEMA brush inside DI water at pH 5.8 (without changing the pH value of water).

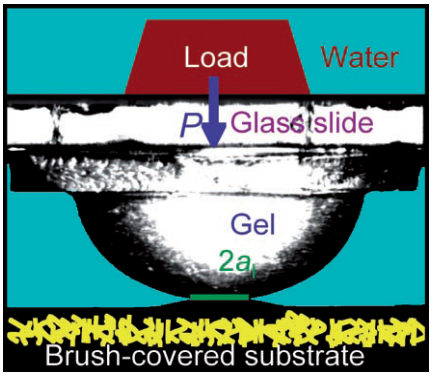

Figure 5.18: An illustrative diagram of the JKR setup adhesion experiment between a hemispherical hydrogel and the surface of the polymer brush underwater. The contact diameter ($2a$) was created after applying a load (P). Image taken with permission from [34]. Copyright (2007) John Wiley and Sons.

Figure 5.19 presents the effect of varying the applied force, P, on the gel-brush adhesion force (F) measurements. It was found that there was a direct relationship between the adhesion force and the applied force, since the gel-brush adhesion force increased as the applied force increased, due to the increase in the contact diameter ($2a$) at their interface. This was because increasing the contact diameter, $2a$, at the gel-brush interface led to an increase in the number of the interacting points (adhesive bonds) between the oppositely charged polymer structures and thus the adhesion force was increased.

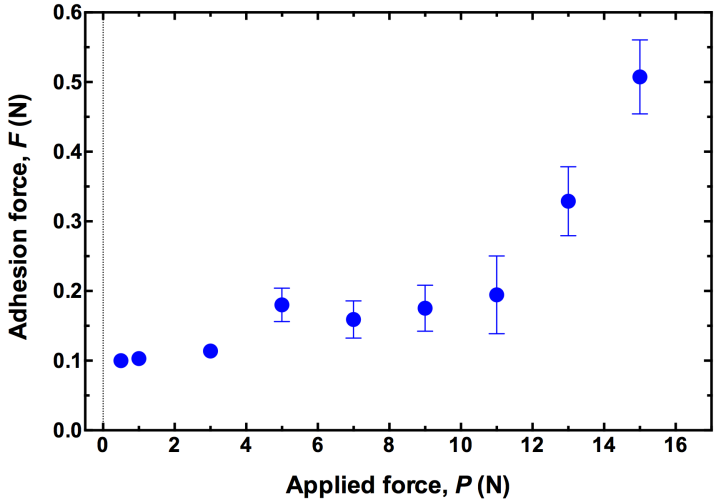

Figure 5.19: The effect of applied force on the gel-brush adhesion underwater at pH 5.8.

This result confirmed that the gel-brush adhesion underwater was a pressure-sensitive adhesion, which also corresponds to the result previously obtained by La Spina *et al.* [34,150]. Two adhesion mechanisms were therefore suggested as serving to control the adhesion interaction at the gel-brush interface that caused it to exhibit pressure-sensitive adhesion that either: 1) interfacial effect or 2) interdigitation effect. The interfacial effect was controlled by the applied force value, since the larger applied forces led to an increase in the contact diameter, $2a$, at the gel-brush interface. This means that the electrostatic or hydrogen interactive points between the carboxylic and amino groups at the gel-brush interface increased once their contact diameter was increased. While the interdigitation effect, meanwhile, refers to the Velcro^{TM} mechanism that involves the interdigitation (entanglement) between carboxylic and amino groups at the gel-brush interface. In this case, however, the interdigitation (entanglement) mechanism was unlikely to occur due to the definite electrostatic interaction at the interface. If the chains at the gel-brush interface were entangled, their adhesion would not be switchable and the only way to detach them apart would be by bond breakage.

Generally speaking, a larger applied force caused more damage to the soft PMAA hydrogel, which was fully swollen inside DI water. The applied force was therefore kept constant at 0.5 N in all the previously mentioned adhesion experiments. At 20 N of applied force, the PMAA gel fractured on the PDEAEMA brush surface as this load was too large for the gel to bear.

5.4 The Thermodynamic Work of Adhesion

The thermodynamic work of adhesion (W_{adh}) was investigated in order to assess the hydrogel-brush adhesion underwater at different pH values by using the pull-off adhesion force (F_{JKR}) based on the JKR model. The pull-off adhesion, F_{JKR}, in the JKR model is defined as the force required to separate two adhered bodies and is given by

$$F_{\mathrm{JKR}} = \frac{3\,\pi\,R\,W_{\mathrm{adh}}}{2}\,, \tag{5.4}$$

where R is the radius of the hemispherical body [54].

When the load (P) in the JKR model is zero, the contact radius (a_{JKR}) becomes finite and is given by

$$a^3_{\mathrm{JKR}} = \left(\frac{6\,\pi\,W_{\mathrm{adh}}\,R^2}{K} \right), \tag{5.5}$$

The adhesion measurements were therefore carried out to estimate the W_{adh} between the (0.18 mol%)–PMAA gel and the (70 nm thick)–PDEAEMA brush at three pH values: 1, 5.8 and 12. Each part of these measurements was repeated with four different applied forces: 0.1, 0.5, 1 and 2 N. The maximum force values were taken by the mechanical tester (TA) and used to calculate the work of adhesion (W_{adh}) using equation 5.4. The contact radius (a^3) and the radius (R) of the hemispherical gel were measured in the unloading regime by using ImageJ software. Figure 5.20 presents the obtained results and shows the linear relationship of the W_{adh} with a^3 .

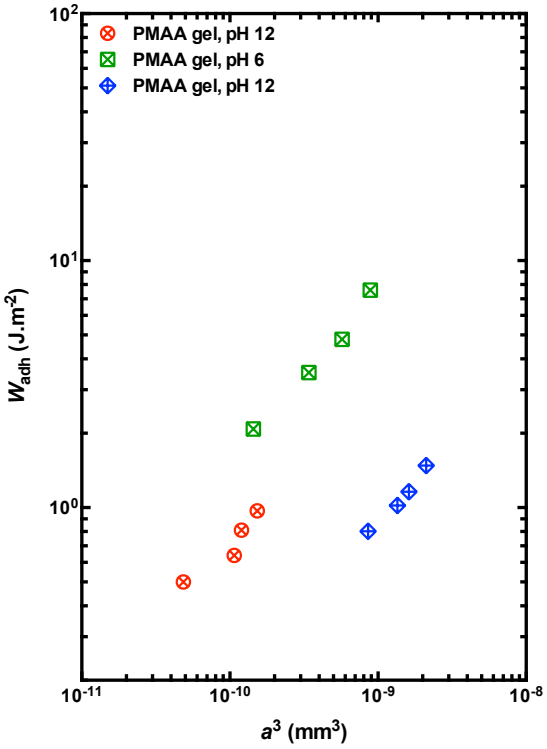

Figure 5.20: Variation of a^3 as a function of W_{adh} at pH 1 , 5.8 and 12.

It was found that the W_{adh} was greater at pH 5.8, compared to pH 1 and pH 12, as a result of the increase in the contact radius and adhesive interactions at the gel-brush interfacial diameter ($2a$), since both polymer structures (hydrogel and brushes) were oppositely charged

at pH 5.8. This result corresponded to the previous result presented in Figure 5.9 that shows that the adhesion force and work done between the PMAA gel and PDEAEMA brush varied strongly between pH 5.8 and pH 1 or pH 12. In other words, the W_{adh} at the PMAA gel–PDEAEMA brush interface was greater in water at pH 5.8 and very low at pH 1 and 12, as a result of the reduction in the contact diameter at the gel-brush interface, $2a$. As long as the applied force, P, was increased, the W_{adh} also increased precisely at pH 5.8, due to increasing the interfacial contact, a^3, between the gel and the brush surface. This result of an increasing the W_{adh} associated with an increasing applied force P also confirmed that the hydrogel-brushes adhesion was a pressure-sensitive adhesion.

5.5 Conclusion

The work presented in this chapter describes the pH-switchable adhesion experiments between two oppositely charged polyelectrolytes, a SN hydrogel and a brush-coated surface, that was conducted underwater using a mechanical tester. Both PMAA and PDEAEMA, hydrogels and brushes, were pH-sensitive polymers and so they both underwent changes of association and dissociation (charged or uncharged) after changing the pH value of their surrounding water. In general, the main findings in respect to this adhesion between two oppositely charged polyelectrolytes confirmed that the adhesion between the hydrogels and polymer brushes was triggered inside neutral water at pH 5.8 (the normal pH value of DI water), whereas the adhesion was removed at a very strong acidic or basic pH value, i.e. pH 1 and 12. This was due to the fact that one of these polyelectrolytes became uncharged at a certain pH value as either PMAA or PDEAEMA become neutral at pH values below or above their pK_a, respectively.

It was also found that the greater adhesion measurements associated with the thicker polymer brush and also with the loosely crosslinked hydrogel. Cohesive failures, however, were always obtained at the hydrogel-brush interface due to the soft texture of SN hydrogels. After applying the JKR model, it was confirmed that the work of adhesion was much larger in water at pH 5.8, while, in contrast, it considerably decreased at pH 1 and 12. Generally speaking, the adhesion of the single-network (SN) hydrogel with oppositely charged polymer brush was

pH-sensitive adhesion that can be easily controlled (i.e. induce or remove the adhesion on-demand). Preventing cohesive failures from occurring and deforming the hydrogel was very difficult due to the soft texture of the SN hydrogels. This problem of cohesive failure was, however, later overcome by using a robust hydrogel called a '*double-network*' (DN) hydrogel, as will be discussed and presented in detail in the following chapter.

Chapter 6

Switchable and Repeatable Adhesion of A Double–Network Hydrogel

Abstract. The switchable adhesion between two oppositely charged polyelectrolytes, (a hydrogel and a polymer brush), was enhanced after converting the soft single-network hydrogel of the poly(methacrylic acid) to a robust gel called a double-network hydrogel by reinforcing it with a second network of the poly[oligo(ethylene glycol)methyl ether methacrylate]. The adhesion at the gel-brush interface was dramatically enhanced by means of the double-network hydrogel since it increased the adhesion with the polybase brush of the poly[2-(diethyl amino)ethyl methacrylate] by five times more than the adhesion of the single-network hydrogel. Furthermore, the adhesion of the double-network gel with the brush surface was repeatable up to four times inside water at pH $\sim$ 6 (without changing the pH). This was due to the adhesive failure obtained after using the double-network gel that made the surface of the polybase brush clean and reusable after detachment. Atomic force microscopy showed that the polymer brush layer remained on the surface after being detached from the double-network hydrogel inside water, since they were covalently bound to the surface. The re-usability of an adhered gel-brush interface therefore was examined a number of times for both the single-network and double-network hydrogels by adding a strong acid to reduce the pH of the water to pH 1. It was found that both the single-network and double-network hydrogels were still capable of adhering efficiently and strongly to the brush surface inside water at pH $\sim$ 6 after seven iterations of the pH 6–pH 1 ('*on-off*') oscillations.

6.1 Introduction

Double-network (DN) hydrogels have recently attracted the attention of researchers in soft and wet materials due to their novel properties of high mechanical toughness, which have been found to outperform the toughness of single-network (SN) hydrogels, and also due to their high water content, which keeps them biocompatible. A DN hydrogel is made out of two polymeric networks via a two-step network formation, where its first network is prepared with a large amount of crosslinks ($\sim$ 4 mol %) and is then reinforced by a loosely crosslinked second network ($\sim$ 0.1 mol %) [131]. By way of illustration, one of the networks of a DN gel is rigid and brittle, such as a highly crosslinked polyelectrolyte gel, while the other network is soft and ductile since it is generally a loosely crosslinked neutral polymer [139].

Due to the fact that a single-network (SN) hydrogel of a hydrophilic polymer is often very soft and brittle, especially when it either absorbs a large amount of water or is highly crosslinked, it has been found that its mechanical performance can be enhanced by bonding it to a second loosely crosslinked network. The second network of such a DN hydrogel makes the first network gel, which is otherwise very brittle, much more robust. A DN hydrogel is therefore a type of interpenetrating network (IPN) that is synthesised by using two different networks that have different distinguishing properties. IPNs are defined as two entangled polymer networks that hold each other together by permanent topological interactions. In other words, the two networks of a DN hydrogel are both chemically crosslinked and they cannot be pulled apart without breaking one or both of the networks [131, 138].

DN hydrogels exhibit a nonlinear enhancement of mechanical strength due to their high fracture strength (up to 17 times greater than that of its individual single component networks) compared to the SN hydrogels [138]. The *first* network in a DN gel is responsible for the greater elastic modulus (of around $\sim$ 1.0 MPa) since it is a very highly crosslinked network; however, it is quite brittle. On other hand, the fluidity (viscosity) of the loosely crosslinked second network is responsible for dissipating the stress and enhancing the mechanical strength of the DN hydrogels. The excellent mechanical performance of the DN gels has also been related to the chemical crosslinkage and physical entanglements, which exist between these, first and second, networks [131, 137].

DN hydrogels can be prepared via two different methods: 1) by using a weakly charged

polyelectrolyte and a neutral polymer (this type of DN gel is called a *charged-neutral* DN hydrogel), or 2) by using two types of neutral polymers (this DN gel is called a *neutral-neutral* DN hydrogel). The charged-neutral DN hydrogels are generally much tougher than the neutral-neutral DN hydrogels. The difference in the synthesis processes can explain the difference between the characteristics of these two DN gels. If a polyelectrolyte monomer is used in synthesising the first gel, a tougher DN hydrogel will be produced, since the weakly charged PE gel will swell more inside the solution of the second neutral monomer. This leads to the high content of the second network in the final DN gel. In contrast, if the first network gel is made using a neutral polymer, the resulting DN gel will be less tough due to the inferior swelling ability in the second network solution. This leads to the lower content of the second network in the final DN gel. Hence, the rigidity of the first network and its swelling ability are hugely important parameters to create a tougher DN hydrogel [137].

Besides their greater mechanical strength and toughness, DN hydrogels can be pH-stimuli responsive materials when one of their two networks is made out of a weakly charged polyelectrolyte. These pH-sensitive DN gels maintain their toughness even when they become fully swollen in water at an appropriate pH value. The swelling ratio (Q) of DN gels is much lower than that of the SN gels, however, due to the higher crosslinking density of the first network of DN gels and also to the formation of complex hydrogen bonds at the interface between the two networks that serve to limit the gel's swelling behaviour [140]. As a result of the novel properties of the DN hydrogels (their toughness and sensitivity to the external stimuli), they were used within this study of pH-switchable adhesion and their adhesion was tested with the PDEAEMA brush underwater.

Due to the brittleness and weak mechanical properties of the SN hydrogels, their adhesion measurements at their interface with the oppositely charged polymer brushes were always accompanied by cohesive failures within the SN gels, especially when the SN gels were fully swollen in water. The cohesive failure was always obtained after pulling the SN hydrogel away from the brush surface, since the gel was easily broken within the hydrophilic network. It was therefore assumed that if the mechanical properties of the used PMAA (SN) hydrogel were enhanced after it was synthesised as a DN hydrogel, the hydrogel would no longer be deformed or damaged after detaching from the brush surface and the adhesion force at the

adhesive gel-brush interface could then be tuned.

Hereafter, this chapter describes a switchable adhesion study between poly[2-(diethyl amino)ethyl methacrylate] (PDEAEMA) brush, which were chemically grafted onto a planar silicon substrate via atom transfer radical polymerisation, with DN hydrogels. The DN hydrogels used were made from two types of polymers: i) poly(methacrylic acid) (PMAA) and ii) poly[oligo(ethylene glycol)methyl ether methacrylate] (POEGMA). The PMAA is a weakly charged polyelectrolyte gel that responds to the pH changes [34]. Whereas, the POEGMA hydrogel is a neutral polymer that has been intensively used in biomedical applications since it is a water-soluble and non-toxic polymer [164]; hence POEGMA was chosen for making the DN hydrogel in this study.

The DN hydrogels were synthesised in two different ways: 1) by making the PMAA gel as the first network and then strengthening it with the POEGMA network and 2) by making the POEGMA gel as the first network and then strengthening it with the PMAA network. This therefore resulted in two distinct DN hydrogels: i) PMAA–POEGMA (DN) gel and ii) POEGMA–PMAA (DN) gel. The adhesion of each of these DN hydrogels with the polybase (PDEAEMA) brushes was investigated as a function of varying the pH value of their surrounding water.

A comparison was also made between the adhesion of the PMAA–POEGMA and POEGMA–PMAA (DN) hydrogels with the adhesion of the PMAA (SN) hydrogel that was previously presented in Chapter 5. The effect of the monomer concentration in the second network of a DN hydrogel, and also the crosslinking density of the first network, on its adhesion performance was examined. The type of failure mechanism (cohesive or adhesive) of the PMAA–POEGMA (DN) and PMAA (SN) hydrogels was investigated after detaching the hydrogels from the brush surface inside DI water at pH 5.8. Furthermore, the repeatability of the adhesion test of the PMAA–POEGMA (DN) and PMAA (SN) hydrogels was examined underwater (without changing the pH value of water), using the same piece of gel and testing the adhesion for few times on the same place on the brush-coated surface. Atomic force microscopy (AFM) was also used to study the status of the polybase brush before and after the initial adhesion test of the PMAA–POEGMA (DN) gel. In addition, the swelling ratio (Q) and elastic modulus (K) of the DN hydrogel were calculated and then compared with those of

the PMAA (SN) hydrogel. Finally, the adhesion switchability of the PMAA–POEGMA (DN) and the PMAA (SN) hydrogels was investigated by using the same piece of gel to switch its adhesion through multiple '*on-off*' cycles by changing the environmental pH. The obtained results are presented and described in this chapter.

6.2 Adhesion of Single-Network and Double-Network Hydrogels

The pH-sensitive adhesion of SN and DN hydrogels with PDEAEMA brushes was studied as a function of varying the pH value of their surrounding water. The hydrogels were prepared as previously described in Section 4.2.2 in Chapter 4. The adhesion measurements between the DN and SN hydrogels with the PDEAEMA brushes were carried out underwater using the mechanical tester (TA).

Figure 6.1 shows the pull-off measurements in respect to the maximum adhesion force (F) and work done (W) for the PMAA–POEGMA (DN), POEGMA–PMAA (DN) and (0.18 %mol)–PMAA (SN) hydrogels with (77 nm thick)–PDEAEMA brushes as a function pH. The maximum adhesion force and work done were extracted from the force-distance curve that was obtained by the mechanical tester.

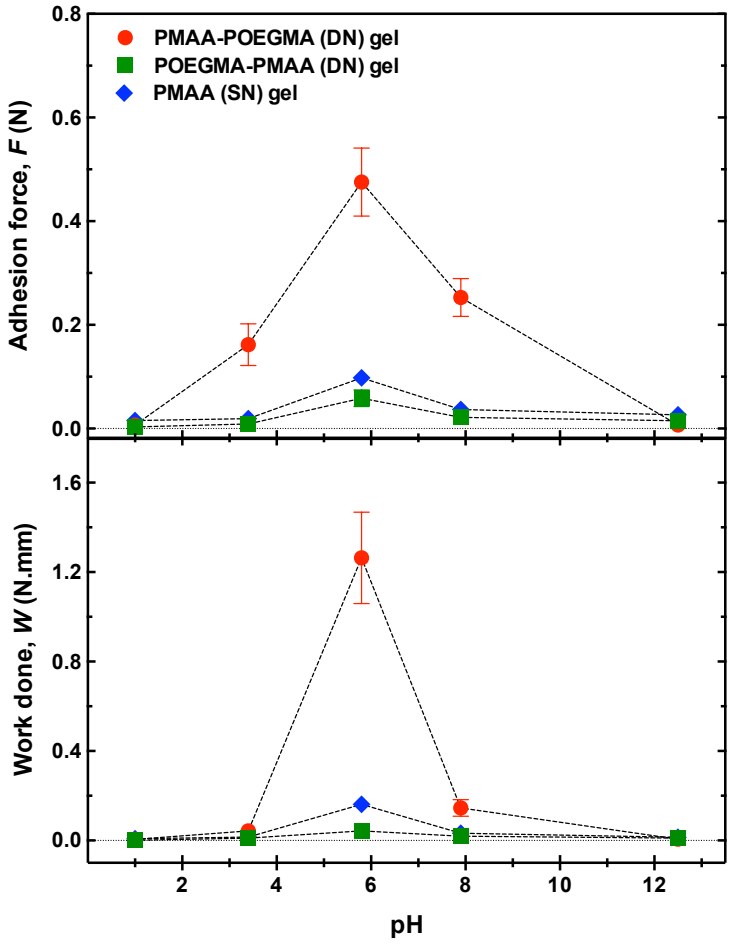

Figure 6.1: Adhesion measurements of the (DN) hydrogels of the PMAA–POEGMA (red symbols) and POEGMA–PMAA (green symbols), and also the PMAA (SN) hydrogel (blue symbols) as a function of pH.

Generally speaking, it was found that all DN and SN hydrogels adhered to the polybase brushes inside DI water at pH 5.8 and then their adhesion was gradually decreased by decreasing the pH value of their surrounding water below 4 or increasing it above 8. Neither the DN gels nor the SN gel adhered to or interacted with the brush-coated silicon surface when they were brought into contact with each other inside strong acidic water at pH 1 or in strong basic water at pH 12, resulting in weak adhesion force and work done. This was due to the disruption of hydrogen bonds and also the attractive interactions at their interface resulting from the loss of the electrostatic charge of either the carboxylic acid groups of the hydrogels (below their pK_a at pH < 5), or the amino group of the PDEAEMA brushes (above their pK_a at pH > 7) [147, 148, 153]. The adhesion of the PMAA–POEGMA gel, however, was much stronger with the polybase brush than it was for the POEGMA–PMAA gel and PMAA gel

underwater at pH 5.8. The adhesion force and work done in respect to the PMAA–POEGMA (DN) gel were almost five times and nine times, respectively, larger than for the POEGMA–PMAA (DN) and PMAA (SN) gels. The combination of the PMAA–POEGMA gel with the PDEAEMA brush was thus considered to give the best adhesion since it gave a much stronger adhesion force and larger work done underwater. In contrast, the adhesion and work done of both the POEGMA–PMAA (DN) and PMAA (SN) gels were comparable, since they both gave similar values of the adhesion force and work done.

Although the POEGMA–PMAA gel was a robust DN hydrogel, its adhesion was not as great as the PMAA–POEGMA (DN) gel, and this was possibly due to the low amount of the solution of the second network absorbed by the POEGMA gel, which might cause a decrease in the number of the carboxylic groups that interact with the amino groups of the polybase brush. The POEGMA gel is a neutral polymer that absorbed a lower amount of water, compared to the PMAA hydrogel (the swelling ratios of these gels are shown in Section 6.8 later in this chapter). In contrast, when the PMAA gel was the first network, as in the PMAA–POEGMA (DN) gel, it absorbed a larger amount of POEGMA solution since the PMAA network is a weakly charged polyelectrolyte network that is very hydrophilic in water-based solutions. The high swelling ratio of the first, PMAA, network resulted from the repulsive interactions between negatively charged carboxylic groups and the osmotic pressure of the counterions that led to a large amount of water being absorbed into the network [165]. Thus, the adhesion of the POEGMA–PMAA gel was affected by the low swelling ratio of its first, POEGMA, network for PMAA solution, which led to a decrease in the amount of the charged carboxylic acid groups within the POEGMA–PMAA (DN) hydrogel. Whereas, the PMAA (SN) hydrogel was quite soft and so its adhesion failed by cohesive bonds within the network reulted in a much lower adhesion than that of the PMAA–POEGMA (DN) gel. Overall, therefore, it was concluded that the adhesion of the PMAA (SN) hydrogel could be dramatically enhanced by: 1) increasing its crosslinking density and then 2) reinforcing it by means of the POEGMA network in order to transfer it to a DN hydrogel.

In adhesive polymer systems, there are two types of adhesion failure mechanisms: cohesive and adhesive failures, which relate to the condition of the adhered surfaces after the detachment [1]. As a consequence of the toughness of the DN gels and the softness of the SN gel, different

failures were observed after detaching them from the brush surface underwater at pH 5.8. Figure 6.2 presents optical microscope images for the PDEAEMA brush surfaces after initial adhesion tests inside DI water (at pH 5.8) with: (a) the PMAA–POEGMA (DN) gel, (b) POEGMA–PMAA (DN) gel and (c) PMAA (SN) gel. A very obvious adhesive failure was found on the brush surface that was tested with PMAA–POEGMA (DN) gel as a result of the higher toughness of this DN gel (see Figure 6.2 (a)). On the other hand, a cohesive failure was obtained with the PMAA (SN) hydrogel (see Figure 6.2 (c)). Whereas, the failure of the POEGMA–PMAA (DN) gel was in-between the adhesive and cohesive failures since this DN gel left a small trace on the brush surface (see Figure 6.2 (b)), which was believed to result from the loosely crosslinked PMAA gel of its second network. This was due to a thin outer layer of the PMAA mesh that was seen to be slightly swollen in the POEGMA–PMAA (DN) gel. In hydrogel-brush adhesive systems, cohesive failures result from the deforming of the hydrogel when it was quite soft since the adhesive bonds at the interface with the polymer brush are stronger than the bonds between the macromolecules on the chains of the hydrogel. Adhesive failure is obtained when the hydrogel is very robust since it resists deformation and so the failure occurs at the adhesive interface rather than within the hydrogel.

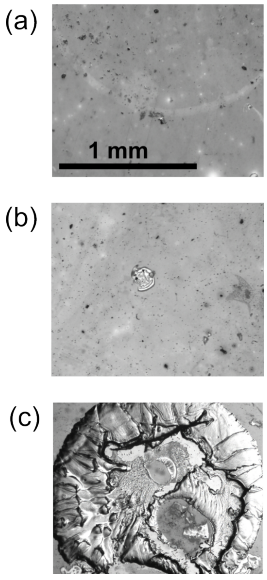

Figure 6.2: Optical microscope images for the PDEAEMA brush surfaces after being in contact with (a) the PMAA–POEGMA (DN) hydrogel, (b) POEGMA–PMAA (DN) hydrogel and (c) PMAA (SN) hydrogel at pH 5.8 in DI water. These images were taken using a 5× objective.

6.3 The Effect of the Second Network's Monomer Concentration on the Adhesion of Double-Network Hydrogels

According to the previous results, and despite the fact that DN hydrogel are both stiff and robust gels, the PMAA–POEGMA (DN) hydrogel gave a better and stronger adhesion than the POEGMA–PMAA gel. Next, therefore, the effect of the monomer concentration in the solution for the second network of the DN hydrogel on their adhesion was examined. Three different monomer concentrations (amounts) were used to make the solution for the second network for the DN hydrogels. In other words, after making the hemispherical gels for the first network, they were divided into three groups and then immersed separately in three solutions of the second network. These three solutions for the second network were made with different concentrations of the monomer but with the same amounts of water, crosslinker and initiator. Table 6.1 presents the amounts of the monomer used in preparing the solution for the second network for both DN hydrogels; the POEGMA–PMAA and PMAA–POEGMA.

Table 6.1: The POEGMA–PMAA and PMAA–POEGMA (DN) hydrogels and the amount of the monomer and its concentration in the total solutions for their second networks.

DN hydrogels	Monomer amounts	Monomer concentration
(i) POEGMA–PMAA	12 mL of MAA	4.07
(ii) POEGMA–PMAA	6 mL of MAA	2.08
(iii) POEGMA–PMAA	3 mL of MAA	1.05
(iv) PMAA–POEGMA	12 g of OEGMA	0.39
(v) PMAA–POEGMA	6 g of OEGMA	0.20
(vi) PMAA–POEGMA	3 g of OEGMA	0.09

Figure 6.3 shows different images of the DN hydrogels described in Table 6.1. POEGMA–PMAA (DN) hydrogels are shown in the first row (i), (ii) and (iii), while PMAA-POEGMA (DN) hydrogels are shown in the bottom row (iv), (v) and (vi). The monomer concentration in the second network of these DN hydrogels decreases from left to right (see Figure 6.3).

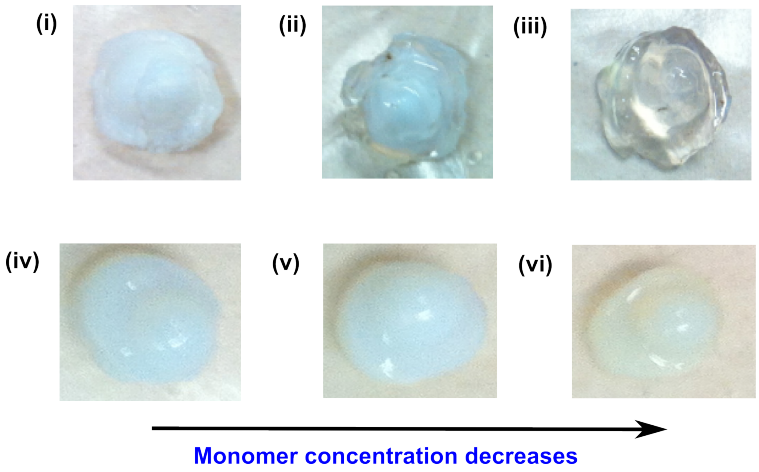

Figure 6.3: POEGMA–PMAA (DN) hydrogels are presented in the top row images: (i), (ii) and (iii), while PMAA–POEGMA (DN) hydrogels are presented in the bottom row images: (iv), (v) and (vi).

It can be clearly seen that the POEGMA–PMAA hydrogel (Figure 6.3 (i), (ii) and (iii)) was more affected by decreasing the MAA monomer concentration in the solution for its second network than the PMAA-POEGMA hydrogel (Figure 6.3 (iv), (v) and (vi)). Both the POEGMA–PMAA and PMAA-POEGMA (DN) hydrogels, however, contained 5 mol% of (MBAA) crosslinker in their first networks and 1 mol% of (MBAA) crosslinker in their second networks. For the POEGMA–PMAA (DN) hydrogels, the POEGMA gel was the first formed network that was more crosslinked than the second network of the PMAA. Thus, the large crosslinking density served to limit the swelling behaviour of the POEGMA gel inside the PMAA solution. The swelling/absorption properties of the POEGMA gel was also quite low compared to the PMAA gel since it is a neutral polymer. The heterogeneous density distribution of the POEGMA to the PMAA solution had an effect on the final formation of the POEGMA–PMAA hydrogel. The absorption of the PMAA solution by the POEGMA gel were decreased when the monomer concentration in the second network PMAA solution was decreased (3 mL of MAA), and so the resulting DN gel was transparent and it did not become a robust gel (Figure 6.3 (iii)). On the other hand, the POEGMA gel became opaque and tough after immersing it in the PMAA solutions with the higher MAA monomer concentrations of 6 and 12 mL (Figure 6.3 (i) and (ii)). This result implied that the lower amount of the MAA monomer in the second network led to a decrease in the absorbed amount of the PMAA solution within the final formed DN hydrogel.

PMAA–POEGMA hydrogels, meanwhile, had a very uniform and stable shape, even after decreasing the amount of the OEGMA in its second network. This result was related to the higher swelling/absorption of the PMAA gel in the POEGMA solution caused by the electrostatic repulsion between the negatively charged carboxylic groups of the PMAA gel. The repulsion between the chains of the PMAA gel served to make them expand and to absorb a large amount of the POEGMA solution. The PMAA–POEGMA (DN) hydrogel was therefore not affected by reducing the amount of the OEGMA in the solution for its second network. In addition, the PMAA gel was a semi-transparent gel that became opaque and robust after polymerising it within the second network of the POEGMA.

After preparing the previously mentioned DN hydrogels (in Table 6.1), their adhesion was tested with the PDEAEMA brush as a function of pH. The pull-off adhesion experiments were carried out by using the mechanical tester (TA), which started the adhesion test by bringing the hemispherical DN hydrogel into contact with the polymer brush-coated surface with an applied a force of 0.5 N. The hemispherical DN gel remained in contact with the brush surface for 2 min before being detached at a speed of 50 mm/min. The adhesion results obtained for both DN hydrogels are presented in the following section.

6.3.1 Adhesion of POEGMA–PMAA Hydrogels

Three POEGMA–PMAA hydrogels were made with three MAA monomer concentrations for their second network solutions (as described in Table 6.1) and their adhesion with the PDEAEMA brush was examined as a function of pH. Figure 6.4 presents the respective adhesion force and work done values of these POEGMA–PMAA (DN) hydrogels.

It was found that the adhesion of all POEGMA–PMAA (DN) hydrogels with the PDEAEMA brush was stronger in water at pH 5.8, but that it became weaker at a very high or low pH (i.e. pH $\sim$ 12 and 1). The adhesion measurements of POEGMA–PMAA hydrogels, however, were affected by changing the monomer amount, MAA, in the solution of the second network. Specifically, the POEGMA–PMAA hydrogel that was prepared in a lower amount of MAA (3 mL) in its second network gave a lower adhesion force and work done compared to the other two POEGMA–PMAA (DN) hydrogels (which were polymerised within the PMAA solutions contained 12 mL and 6 mL of MAA). Decreasing the amount of the MAA monomer in the

second network solution led to a decrease in the concentration of the ionised carboxylic acid groups in the formed DN hydrogel, which probably led to a decrease in the adhesive interaction at the hydrogel-brush interface between the carboxylic acid groups in the DN hydrogel and the amino group in the PDEAEMA brush, resulting in lower adhesion.

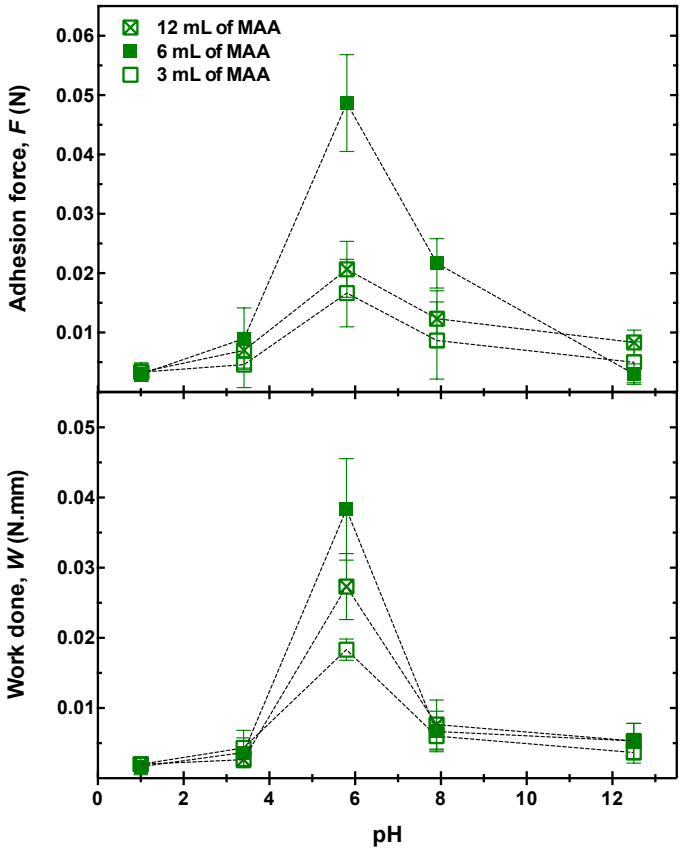

Figure 6.4: The adhesion force and work done for the three POEGMA–PMAA (DN) hydrogels that were made with different amounts of the MAA monomer in the second network.

The adhesion measurements of POEGMA–PMAA hydrogels were enhanced when the MAA monomer in their second network solutions was increased to 6 mL and then to 12 mL, although the (6 mL)-POEGMA–PMAA gel gave a greater adhesion than the (12 mL)-POEGMA–PMAA gel. In both the (6 mL)-POEGMA–PMAA and (12 mL)-POEGMA–PMAA (DN) gels, however, a clear external layer of a swollen PMAA mesh was clearly seen on their top when the gel was fully swollen inside water at pH $\geq$ 5.8, although this PMAA mesh was thinner with the (6 mL)-POEGMA–PMAA gel. In contrast, this outer mesh became thicker

once the MAA monomer in the solution of the second network PMAA was increased to 12 mL. As long as the soft PMAA mesh on the top of the POEGMA–PMAA gel became thicker and swelled clearly, it led to a cohesive failure when detaching the DN gel from the brush surface. In other words, the (12 mL)-POEGMA–PMAA gel gave a clear cohesive failure while the (6 mL)-POEGMA–PMAA gel gave a failure in-between cohesive and adhesive.

6.3.2 Adhesion of PMAA–POEGMA Hydrogels

The effect of the OEGMA concentration in the solution of the second network on the adhesion of PMAA–POEGMA (DN) hydrogel was also investigated. In this case, the three DN hydrogels of the PMAA-POEGMA were made (as described in Table 6.1), and then their adhesion was tested with the PDEAEMA brush as a function of pH. Generally speaking, the obtained results showed that the adhesion force and work done for the three gels were higher and stronger in DI water at pH 5.8, while they gradually decreased as the pH fell below 4 or increased above 8 (see Figure 6.5).

The adhesion of the PMAA–POEGMA (DN) hydrogel was gradually enhanced by increasing the OEGMA concentration in the second network's solution. The (12 g)-PMAA–POEGMA (DN) hydrogel gave a greater adhesion compared to the other gels of the (6 g)-PMAA–POEGMA and (3 g)-PMAA–POEGMA (DN) hydrogels. This might be because the (12 g)-PMAA–POEGMA gel had a broadly higher toughness than the (6 g)-PMAA–POEGMA and (3 g)-PMAA–POEGMA (DN) hydrogels. Overall, all of these PMAA–POEGMA (DN) hydrogels, meanwhile, were opaque and robust and they also did not deform after being detached from the PDEAEMA brush surface, which came about through a cohesive failure at the gel-brush interface underwater.

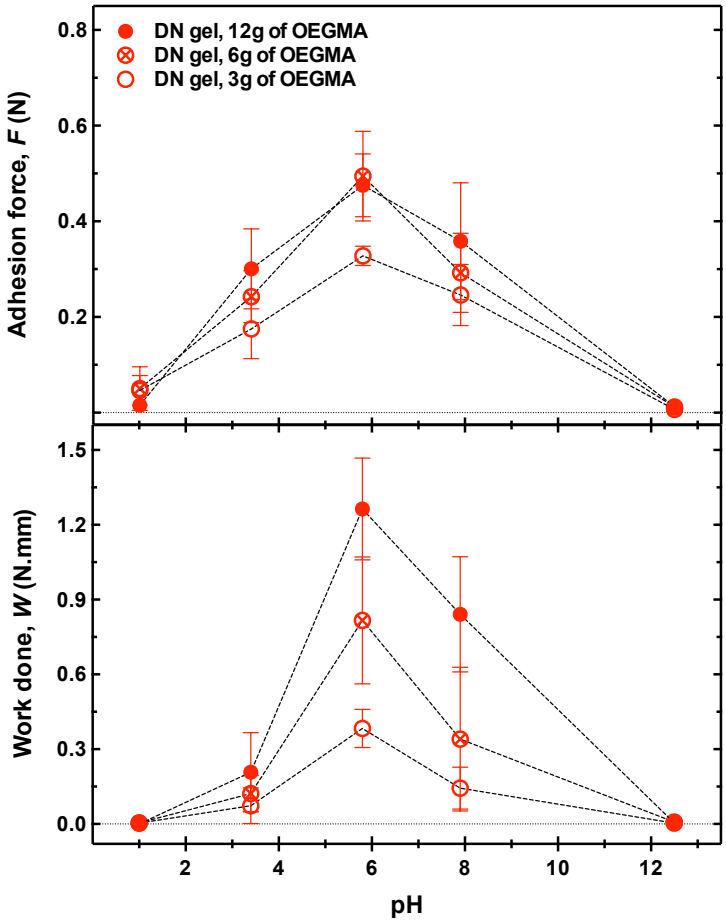

Figure 6.5: The adhesion measurements of three PMAA–POEGMA (DN) hydrogels made with differing OEGMA concentrations in the solutions of their second network.

Generally speaking, there are two important parameters for obtaining a mechanically strong DN hydrogel:

1) The first network must be highly crosslinked and the second network must be loosely crosslinked. Decreasing the crosslinker concentration in the second network (systematically from 2 mol% to $\sim$ 0 mol%), however, did not change the toughness (elastic modulus of the DN hydrogels) if the crosslinking density of the first network was kept very high (at $\sim$ 4 mol%) [131, 139, 140].

2) In addition, the molar ratio of the second network to the first network must be large (i.e. below 30 M) (see Figure 6.6). Hence, using a very high molecular weight for the second polymer is recommended [131, 139].

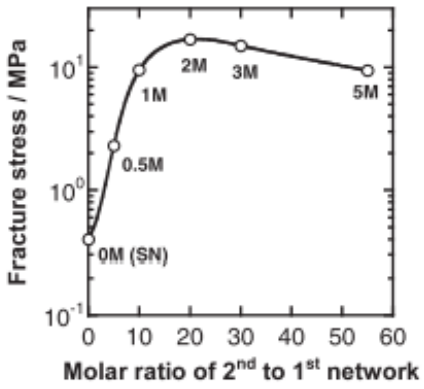

Figure 6.6: The effect of the molar ratio of the second network to the first network on the mechanical strength of a DN hydrogel. The numbers on the curve indicate the monomer concentration value in the solution of the second network. Figure reproduced with permission from [131, 139]. Copyright (2003) John Wiley and Sons.

6.4 The Effect of the Crosslinker Concentraion of the First Network on the Adhesion of Double-Network Hydrogels

Since the first PMAA network of the PMAA–POEGMA (DN) hydrogel was much more highly crosslinked than the single-network of the (SN) PMAA gel (they were compared in Figure 6.1), another PMAA–POEGMA (DN) hydrogel was made containing much less crosslinker (the same as that used in the PMAA (SN) hydrogel). This study was therefore conducted to investigate the affect of the crosslinker concentration used in making the first network of a DN hydrogel on its adhesion with the polybase brush. This comparison was made for the PMAA–POEGMA (DN) hydrogel only, since this hydrogel already gave a better and greater adhesion with the (77 nm thick) PDEAEMA brush underwater than the other POEGMA–PMAA (DN) hydrogel .

Table 6.2 illustrates the three types of hydrogels with their crosslinker/monomer ratios. The highly crosslinked PMAA–POEGMA (DN) hydrogel was therefore called DN gel-1 and the lower crosslinked PMAA–POEGMA (DN) hydrogel was called DN gel-2. The amount of crosslinker was higher by a factor of 25 in the PMAA–POEGMA-1 (DN) hydrogel than the PMAA–POEGMA-2 (DN) hydrogel. The PMAA (SN) hydrogel and PMAA–POEGMA-2 (DN) hydrogels were exactly the same as each other in terms of the amount of water, MAA

monomer and MBAA crosslinker used.

Table 6.2: The used hydrogels and their crosslinker/monomer ratios

Hydrogels	Crosslinker/monomer
PMAA–POEGMA-1 (DN) hydrogel	0.05
PMAA–POEGMA-2 (DN) hydrogel	0.002
PMAA (SN) hydrogel	0.002

The adhesion measurements of the highly crosslinked and loosely crosslinked PMAA–POEGMA (DN) hydrogels were then compared with the adhesion of the PMAA (SN) hydrogel. Figure 6.7 presents the results obtained from the adhesion experiments of these three hydrogels (shown in Table 6.2). It was found that both the PMAA–POEGMA (DN) hydrogels (#1 and #2) gave a much greater adhesion force and work done than the PMAA (SN) hydrogel. The adhesion force was 0.5 N and 0.9 N for the DN hydrogel #1 and #2, respectively. Whereas, the adhesion force of the PMAA (SN) hydrogel with the PDEAEMA brush was 0.09 N in water at pH 5.8. The adhesion force of both DN hydrogels was higher than that of the SN hydrogel because the tougher structures of the DN gels resisted separation from the brush surface underwater, while the soft network of the PMAA (SN) gel was easily deformed during the detachment, resulted in cohesive bonds at the interface and a lower adhesion.

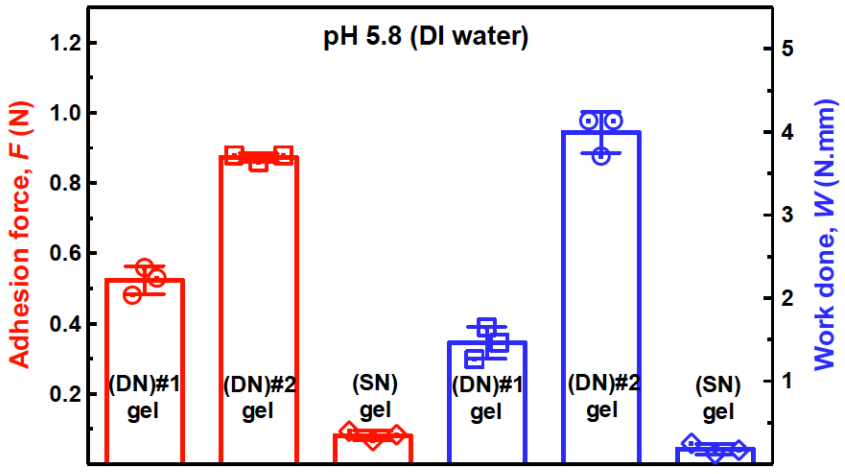

Figure 6.7: The adhesion force and work done of the PMAA–POEGMA-1 (DN) hydrogel, PMAA–POEGMA-2 (DN) hydrogel and PMAA (SN) hydrogel underwater at pH 5.8.

Figure 6.8 shows the different detaching behaviours that were observed using a side-view camera while testing the adhesion of these three, DN and SN, hydrogels with the PDEAEMA brush underwater at pH 5.8.

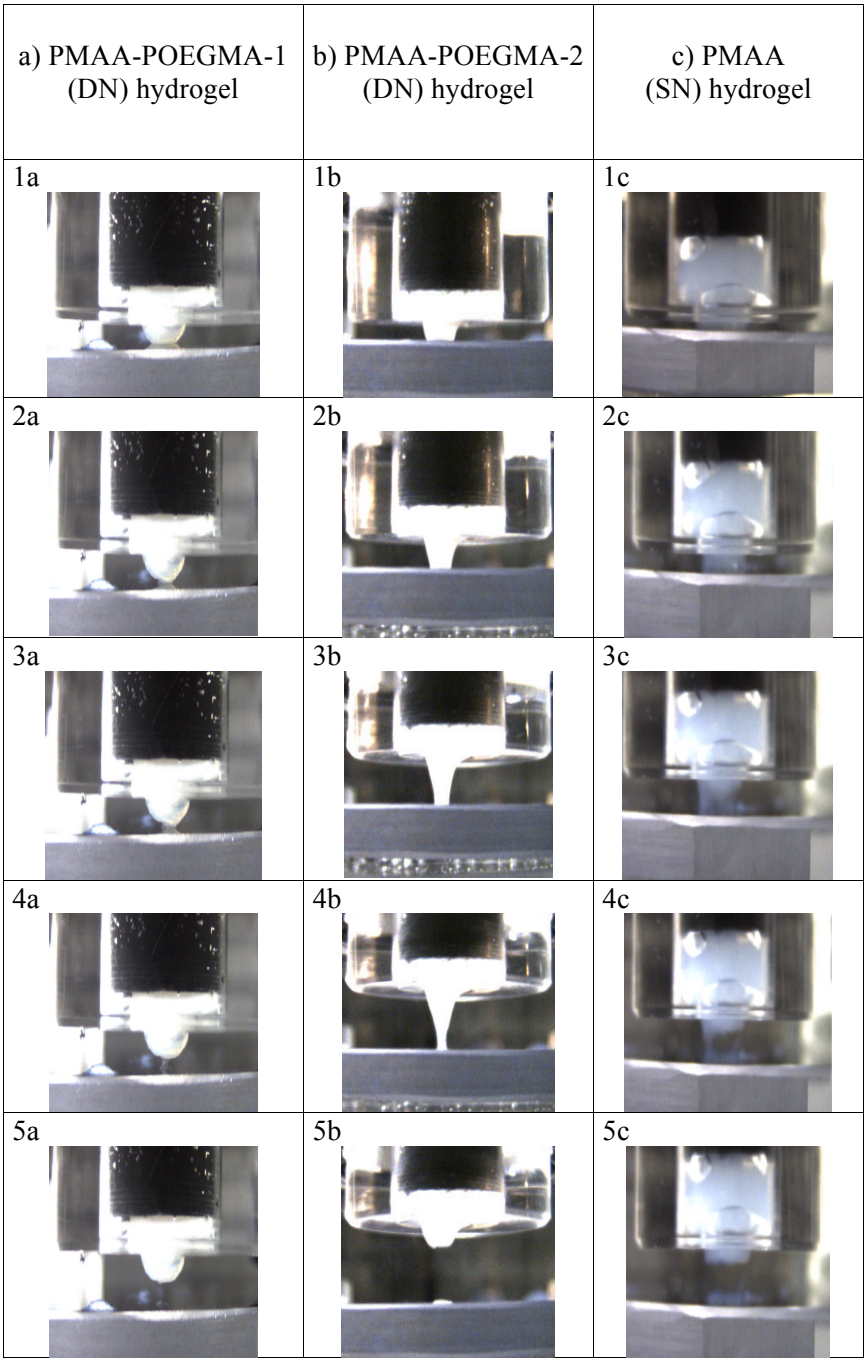

Figure 6.8: The detaching process of (a) the PMAA–POEGMA-1 (DN) hydrogel, (b) PMAA–POEGMA-2 (DN) hydrogel and (c) PMAA (SN) hydrogel from the PDEAEMA brush surface in DI water. The diameter of the black probe is 10 mm

All three gels were adhered to PDEAEMA brushes underwater by an applied force of 0.5 N for 2 min before being removed at a speed of 50 mm/min. The PMAA–POEGMA-1 (DN) hydrogel was found to be much less stretchable (see Figure 6.8 (3a) and (4a)) due to its greater crosslinker density, which made the chains less free to stretch. The adhesive failure was therefore obvious at the interface of the PMAA–POEGMA-1 (DN) hydrogel with the polybase brush, (see Figure 6.8 (5a)), since this DN gel was robust and so was not deformed.

Even though both DN hydrogels were robust gels, the PMAA–POEGMA-2 (DN) hydrogel (the lower crosslinked gel) was able to give a greater adhesion than the PMAA–POEGMA-1 (DN) hydrogel (the highly crosslinked) since it was able to stretch elastically when it was pulled away from the brush surface (Figure 6.8 (2b)). As a consequence of the higher elasticity of the DN-2 gel and its good adhesion with the polybase brush, it was also pulling up the whole brush-coated silicon substrate that weights 18.9 g, even with the heavy Perspex base weights 288 g that holds the PDEAEMA brush sample (see Figure 6.8 (3b) and (4b)). The extensive stretching behaviour of the PMAA–POEGMA-2 (DN) hydrogel led to a cohesive failure on the brush surface, as a result of the sudden break of the DN network due to the large tensile stress that exceeded the elastic limit of this DN gel (see Figure 6.8 (5b)). The PMAA (SN) hydrogel, in contrast, showed cavitation and then fibrillation during its detachment from the PDEAEMA brush surface (see Figure 6.8 (3c) and (4c)), resulted from the soft texture of the hydrogel that caused a cohesive failure (see Figure 6.8 (5c)).

Figure 6.9 represents the raw data for the adhesion experiments of these three hydrogels (in Figure 6.8). It can be clearly seen that the adhesion peaks of these hydrogels were dissimilar as a result of their variation in their stretching ability during detaching. The crooked black curve of the PMAA–POEGMA-2 (DN) hydrogel was caused by the reduction of the gel-brush interfacial area during the pulling-off test, which led to a sudden fracture within the DN network, from one side, as the chains were forced to stretch beyond their elastic limit.

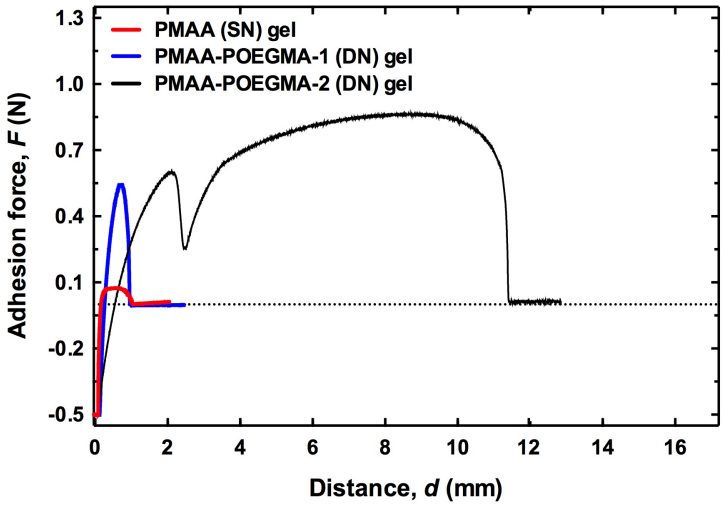

Figure 6.9: Force-distance curves of adhesion tests of the PMAA (SN) hydrogel (red line), PMAA–POEGMA-1 (DN) hydrogel (blue line) and PMAA–POEGMA-2 (DN) hydrogel (black line) underwater at pH 5.8.

In order to extract the stress-strain curve from the force-distance curve in Figure 6.9, the normalised stress (σ) was obtained from the following equation

$$\sigma = \frac{F}{A}\,. \tag{6.1}$$

where F is the adhesion force and A is the contact area of the hemispherical gel ($A = \pi r^2$), and r is the the radius of the hemispherical gel.

In addition, the normalised strain (ε) was obtained from the displacement (the changes in the distance of the pulled gel from the brush surface) by the initial thickness of the hemispherical gel (which was 1.7 mm). Figure 6.10 shows stress-strain curves of the hydrogels' adhesion with the PDEAEMA brush underwater. It was found that the PMAA–POEGMA-2 (DN) hydrogel was able to withstand a larger stress during the detachment, leading to an extension in the gel thickness as it was pulled away from the brush surface. The DN-2 hydrogel, however, experienced irreversible structural change due to its deformation under the larger strain. Although the tougher PMAA–POEGMA-1 (DN) hydrogel underwent a stress level almost the same as that of the an DN-2 hydrogel, this was associated with lower strain, which allowed the structure of the hemispherical gel to remain reversible. The PMAA (SN) hydrogel, meanwhile, had a lower stress value due to its softness, which made it easily deformable.

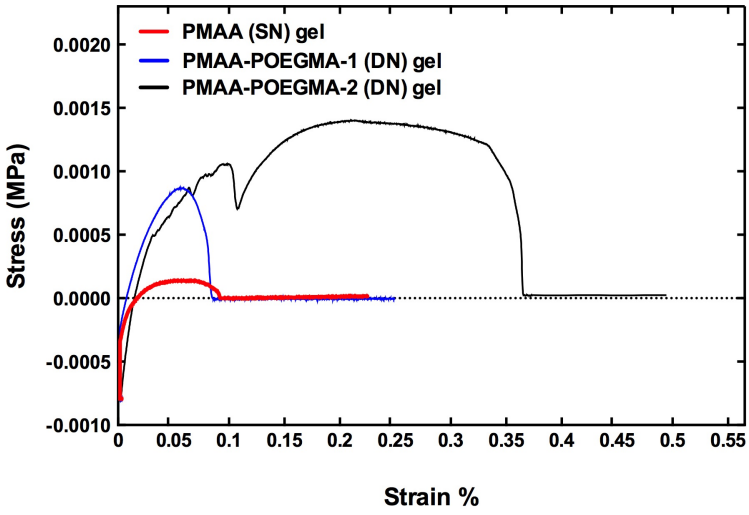

Figure 6.10: Strain-stress curves of the PMAA (SN) hydrogel (red line), PMAA–POEGMA-1 (DN) hydrogel (blue line) and PMAA–POEGMA-2 (DN) hydrogel (black line) underwater.

The above results suggest that adhesive or cohesive failures of hydrogels are largely dependent on their mechanical strengths and viscoelastic behaviours. As long as the DN hydrogel had a large stress distribution at the adhesive contact area, an adhesive failure at the gel-brush interface would occur. Whereas, a cohesive failure was associated with the deformable DN hydrogel since it underwent a greater stress and strain.

6.5 The Repeatable Adhesion of Double-Network Hydrogel

As a result of the adhesive failure associated with the highly crosslinked PMAA–POEGMA (DN) hydrogel in the initial adhesion test and after detaching it from the brush surface (as shown in Figure 6.2 (a)), the quality of the same piece of the PMAA–POEGMA (DN) hydrogel for reuse on the same brush surface was investigated by repeating the adhesion test a few times in DI water (without changing the pH value of water).

To this end, a comparative study of repeated adhesion tests was carried out between the PDEAEMA brush with the PMAA–POEGMA (DN) and PMAA (SN) hydrogels in water at pH 5.8. The hydrogels used were the highly crosslinked PMAA–POEGMA-1 (DN) hydrogel and the (0.18 %mole)–PMAA (SN) hydrogel. The thickness of the PDEAMEA brush was $\sim$ 77 nm. The applied force was 0.5 N and the hydrogels were brought into contact with

the brush surface for 2 min before being retracted at a speed of 50 mm/min. All hydrogels and polymer brush surfaces were left in DI water for 1 h before conducting the adhesion experiments. The same pieces of hydrogel was used to test its adhesion on the same location (± 1 mm) on the PDEAEMA brush surface in DI water. Figure 6.11 shows the results of repeatable adhesion experiments.

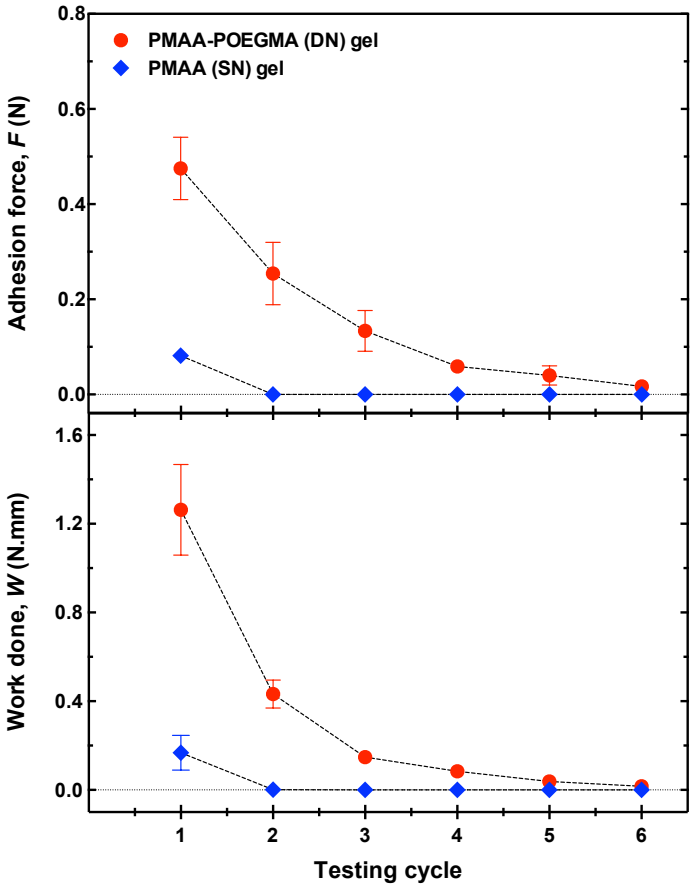

Figure 6.11: The adhesion repeatability test of the PMAA–POEGMA (DN) (red symbols) and PMAA (SN) (blue symbols) hydrogels underwater at pH ∼ 6.

It was found that the adhesion of the PMAA–POEGMA (DN) hydrogel was repeatable up to four times underwater, but that the adhesion force on the second test-cycle decreased to half the value of the first measurement (i.e from 0.5 N to 0.27 N). The calculated work done in respect to the DN adhesion also confirmed that adhesion interactions with the PDEAEMA brush still existed and was 1.4 N.mm (in the first adhesion test), before dramatically dropping to below 0.04 N.mm in the fifth adhesion test-cycle.

The adhesion of the PMAA (SN) gel, on other hand, could not be repeated due to the cohesive failure of the PMAA network (as shown in the optical microscope image in Figure 6.2 (c)). The cohesive failure of the SN gel on the brush-coated surface was therefore affecting the repetition of the adhesion measurement. The adhesion of the PMAA gel was not repeatable because of the like-charged surface of the PMAA trace (the cohesive failure) that remained stuck on the PDEAEMA brush surface.

Figure 6.12 shows force-distance curves of the repeatable adhesion of the DN hydrogel with the PDEAEMA brush underwater (which were presented in Figure 6.11). It can be clearly seen that adhesion curves of the PMAA–POEGMA (DN) hydrogel were gradually decreasing as adhesion tests were repeated at the same point on the PDEAEMA brush in DI water.

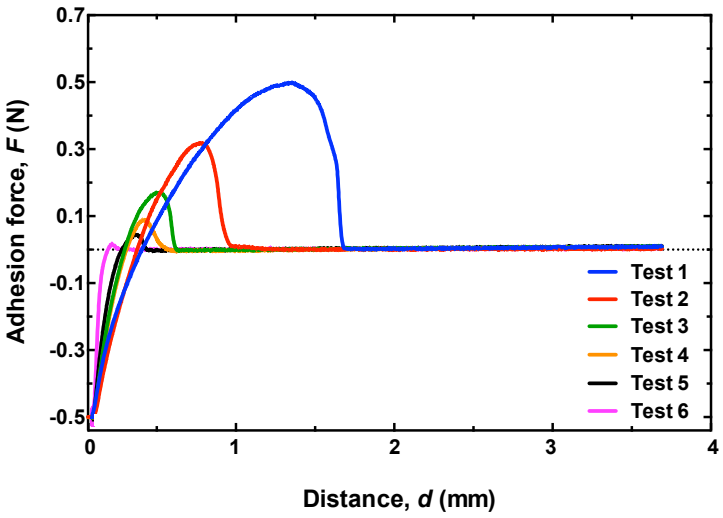

Figure 6.12: Force-distance curves of the repeatable adhesion test for the PMAA–POEGMA (DN) hydrogel.

Although the adhesive failure still existed in all six cycles of repeatable adhesion tests of the DN hydrogel, force-distance curves shifted to the left as a result of the reduction in the adhesive interaction with the brush-coated surface. The reason behind the decrease in the adhesion force in the repeated tests was not clear, although it was most likely that it resulted from the increasing roughness of the surface of the hemispherical DN hydrogel, since the gel was forced to detach from the brush surface while they were strongly interacting (adhering) with each other. In other words, the increasing roughness of the DN hydrogel might lead to a decrease in its adhesive interacting points with the planner surface of the poybase brush.

The adhesion of the PMAA (SN) hydrogel, in contrast, was clearly not repeatable from the second test cycle (see Figure 6.13) since adhesion curves dropped right down to zero after running the initial adhesion test. This was due to the cohesive failure of the PMAA network on the PDEAEMA brush surface that accrued after the initial adhesion test cycle.

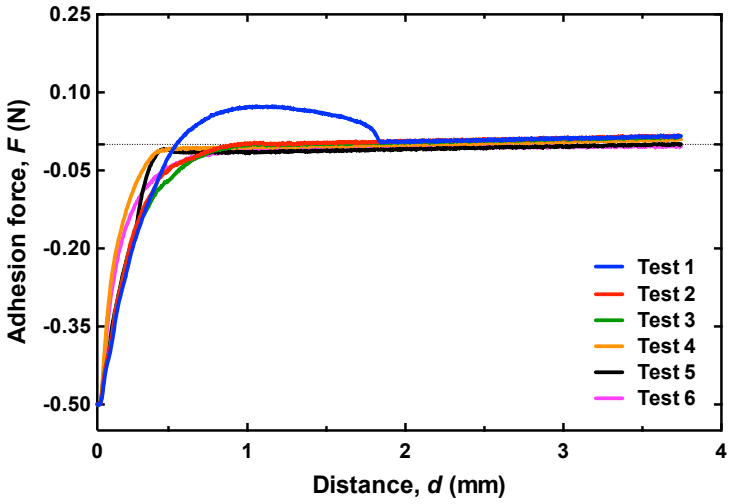

Figure 6.13: Force-distance curves of the non-repeatable adhesion of the PMAA (SN) hydrogel.

The flattened curves of the unrepeated tests (test cycle numbers 2, 3, 4, 5 and 6) confirmed that attractive interactions at the SN hydrogel-brush interface had completely vanished. This was because the PMAA gel on the mechanical probe was not interacting with the like-charged trace of the PMAA network on the brush surface.

As a result of the adhesive failure observed after using the PMAA–POEGMA (DN) hydrogel, atomic force microscopy (AFM) was used to investigate the status of the PDEAEMA brush before and after the initial adhesion test in DI water. In other words, there was a need to check for the presence of the PDEAEMA brush on the silicon surface after it had been detached from the robust DN hydrogel since the adhesion of the DN hydrogel dropped to half the initial value in the second repeated test. A Dimension 3100 AFM (Veeco, UK) and Nanoscope software were therefore used to study the brush status following the pre-adhesion and post-adhesion tests, using tapping mode in ambient conditions.

Figure 6.14 presents AFM images for the PDEAEMA brush surface (a) before and (b) after being detached from the PMAA–POEGMA (DN) hydrogel. It was found that the roughness

of the polymer brush surface was not significantly affected in the post-adhesion test, since it decreased from 9.8 nm to 5.6 nm. The reduction in the surface roughness of the PDEAEMA brush after the initial adhesion test was caused by the 0.5 N applied force that was used to press and adhere the hemispherical hydrogel to the PDEAEMA brush surface. Cross-sectional areas for these AFM images of the PDEAEMA brush surface are presented in Figure 6.14 (c) and (d), which also confirm that the PDEAMEA brush surface was somewhat flattened after being pressed by the DN hydrogel by the 0.5 N applied force.

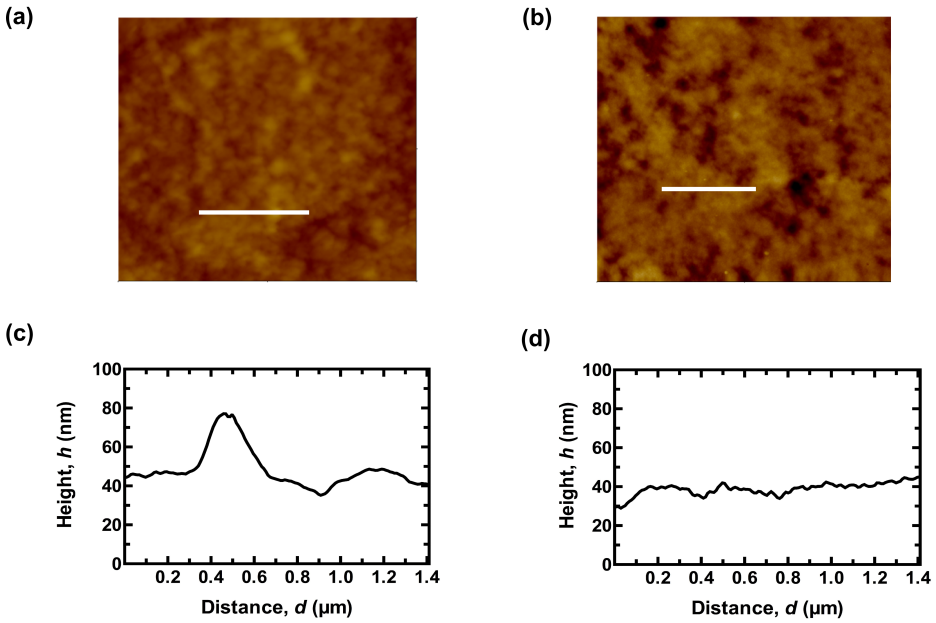

Figure 6.14: AFM images for the PDEAEMA brush surface (a) before and (b) after the initial adhesion test underwater at pH 5.8. Representative cross-sectional images (height profiles) of the PDEAMEA brush (c) before and (d) after the adhesion test, which were taken from the white line on each image. This data was analysed using Image SXM 198.

The result of the repeatable adhesion and adhesive failure of the PMAA–POEGMA (DN) hydrogel was considered as evidence that the types of the bonds formed at the gel-brush interface were physical bonds (i.e. electrostatic interactions and hydrogen bonds) instead of the entanglement between the chains at the interface. Since physical bonds can be easily broken without causing damage to the adhered surface, neither the hydrogel nor the brush were damaged after they were detached; this resulted in an adhesive failure and meant that the adhesion was repeatable.

In addition, the presence of the PDEAEMA brush on the silicon surface was confirmed by measuring the brush thickness before and after the initial adhesion test. The thickness of the PDEAEMA brush was measured by ellipsometry before running the adhesion test, and was found to be around $\sim$ 77 nm. After conducting the initial adhesion test, the thickness of the PDEAEMA brush was measured under the AFM by making a very thin scratch at the same point in the PDEAEMA brush that was used to test the DN hydrogel underwater (see Figure 6.15 (a)). It was found that the thickness of the PDEAEMA brush after conducting the initial adhesion test was still in the same range of $\sim$ 70 nm as before running the adhesion measurement (see Figure 6.15 (b)).

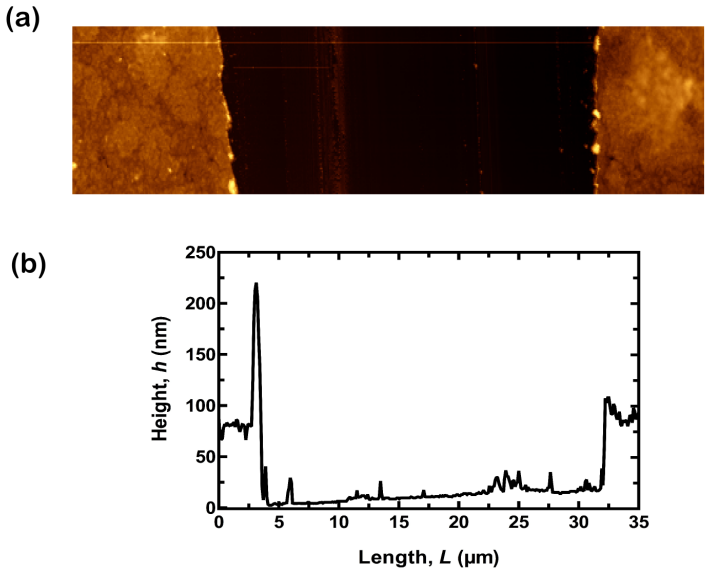

Figure 6.15: (a) A thin scratch was made on the PDEAEMA brush surface after running the initial adhesion measurement. (b) The corresponding cross-sectional scratch on the PDEAMEA brush.

6.6 The Thermodynamic Work of Adhesion

A comparison was made between the thermodynamic work of adhesion (W_{adh}) of the PMAA–POEGMA (DN) and that of the PMAA (SN) hydrogels using the pull-off adhesion measurement. The pull-off adhesion measurements in the JKR model are defined as the forces (F_{JKR}) required to separate an adhesive interfacial contact between two adhered surfaces, which was

then used to calculate the work of adhesion, W_{adh}, of the PMAA (SN) hydrogel (as shown in Section 5.4 in Chapter 5) using the following equation

$$F_{\mathrm{JKR}} = \frac{3\,\pi\,R\,W_{\mathrm{adh}}}{2}\,. \tag{6.2}$$

When a load (P) in the JKR model becomes zero, the contact radius (a_{JKR}) at the interface between two bodies in contact becomes finite and is given by

$$a^3_{\mathrm{JKR}} = \left(\frac{6\,\pi\,W_{\mathrm{adh}}\,R^2}{K}\right). \tag{6.3}$$

The W_{adh} and a_{JKR} of the PMAA–POEGMA (DN) with the PDEAEMA brush were consequently calculated at three pH values (pH 1, 5.8 and 12) using equations (6.2) and (6.3). Each of these measurements was repeated with four different applied forces (0.1, 0.5, 1 and 2 N). The maximum adhesive force values were extracted from force-distance curves obtained by the mechanical tester (TA) and were then used to calculate the work of adhesion, W_{adh}. The contact radius (a_{JKR}) at the adhesive gel-brush interface was then measured from the side-view image taken by a camera during the unloading stage using ImageJ software. Generally speaking, the adhesive contact diameter ($2a$) at the gel-brush adhesive interface increased when the applied force was increased, which then led to an increase in the work of adhesion, W_{adh}. Figure 6.16 shows the results obtained for the contact radius, a, as a function of the W_{adh} at the gel-brush interface of both the PMAA–POEGMA (DN) and PMAA (SN) hydrogels with the (70 nm thick)–PDEAEMA brush.

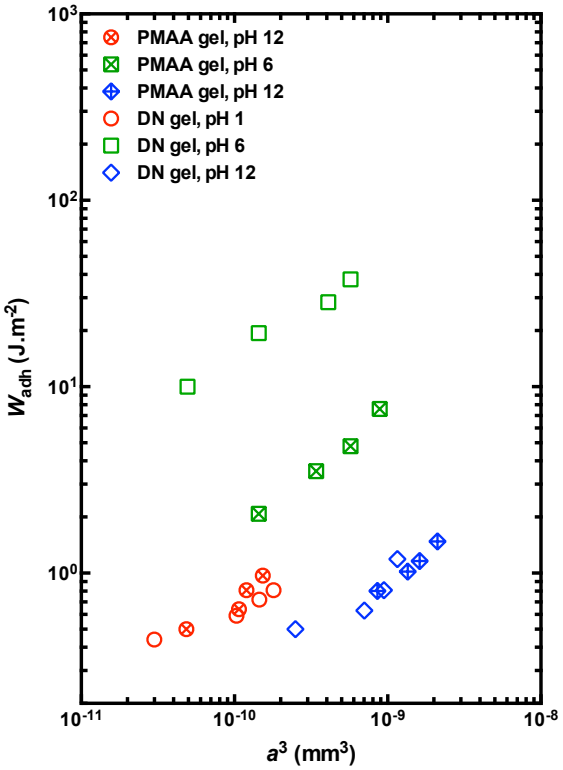

Figure 6.16: The work of adhesion, W_{adh}, of the PMAA–POEGMA (DN) and PMAA (SN) gels vs. the change in the a^3_{JKR} as a function of pH using four different applied forces. The symbols in the red colour indicate the measurements at pH 1, the green colour symbols indicate the measurement in pH 5.8 and the blue colour symbols indicate the measurement in pH 12.

It can be clearly seen that the W_{adh} for both hydrogels, SN and DN, was considerably greater in DI water at pH 5.8, which then decreased at pH 12 and pH 1. The W_{adh} of the DN gel in water was almost five times greater than that of the SN gel, however, due to the fact that the adhesion force of the robust DN hydrogel with the polymer brush surface was found to be five times higher than the adhesion of the soft SN hydrogel (as shown in Figure 6.1). Overall, the W_{adh} for all measurements increased as the applied force at the gel-brush interface was increased, since the finite contact area, a_{JKR} at their adhesive interface was increased in line with the applied force. In contrast, W_{adh} was dramatically decreased at pH 1 and 12 since the adhesive contact radius decreased due to the fact that one of these two polyelectrolytes, either the hydrogel or the brush, became uncharged (neutral) at those pH levels. This also confirmed that the adhesion between the two oppositely charged polyelectrolytes was switchable between pH 5.8 and pH 1/pH 12 since one of these polymers did not electrostatically

interact with the other one (PMAA and PDEAEMA become uncharged (neutral) at pH 1 and 12, respectively).

6.7 The Elastic Modulus of Double-Network Hydrogel

The elastic modulus (K) of the PMAA–POEGMA (DN) hydrogel was calculated (as described previously in section 5.2.3 in Chapter 5 using the Hertz equation (5.3)). According to Hertz theory, when a load (P) is applied to two elastic bodies, a new unit area of radius (a) is created at the interface. The elastic modulus of the PMAA–POEGMA (DN) hydrogel was estimated by measuring the interfacial area of the gel with an uncoated silicon substrate at different pH values (pH 1, 5.8 and 12). In the Hertz model, adhesive interactions are neglected between the two bodies, and so the uncoated silicon substrate was chosen because the silicon surface has negative charges that will not cause adhesive interactions with the negatively charged carboxylic acid groups of the PMAA–POEGMA (DN) hydrogel.

Three different applied forces were used to press the hemispherical hydrogel against the silicon surface (0.5, 1 and 2 N). The estimated calculations of the PMAA–POEGMA (DN) hydrogel for a^3, and PR were calculated after the unloading stage as a function of three different pH values. The DN hydrogel-silicon surface interfaces were recorded by a camera (see Figure 6.17). The interfacial radius, a^3, and radius of the hemispherical gel, R, were measured from the side-view image using ImageJ software. Figure 6.18 shows the variation in the estimated data of the elastic modulus (K) of the PMAA–POEGMA (DN) hydrogel at three different pH values.

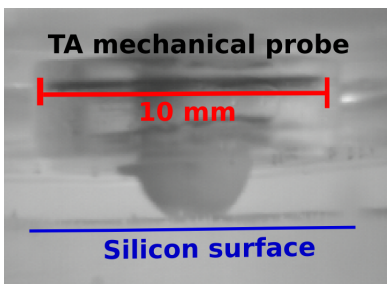

Figure 6.17: An image of a PMAA–POEGMA (DN) gel brought into contact by the TA mechanical probe and pressed against a silicon surface.

It was found that the elastic modulus of the PMAA–POEGMA (DN) hydrogel was 1.18, 1.09 and 1.00 MPa at pH 1, 5.8 and 12, respectively. The DN hydrogel became stiffer at pH 1 due to the hydrophobicity of the carboxylic groups inside the acidic solution, and thus its elastic modulus became slightly larger than it had been at pH 5.8 and 12. In other words, the DN hydrogel became very stiff when it shrank inside strong acidic pH solution (at pH 1), which then led to an increase in its elastic modulus.

Since the swelling ratio of the DN gel increased at pH 12, its elastic modulus decreased due to the larger swelling ratio of the DN gel inside the basic solution. This result corresponded to Gong's report [139] that DN gel possesses an elastic modulus of around $\sim$ 1.0 MPa. The elastic modulus of the DN hydrogel was 4 to 5 times higher than that of the SN hydrogel (see Table 6.3).

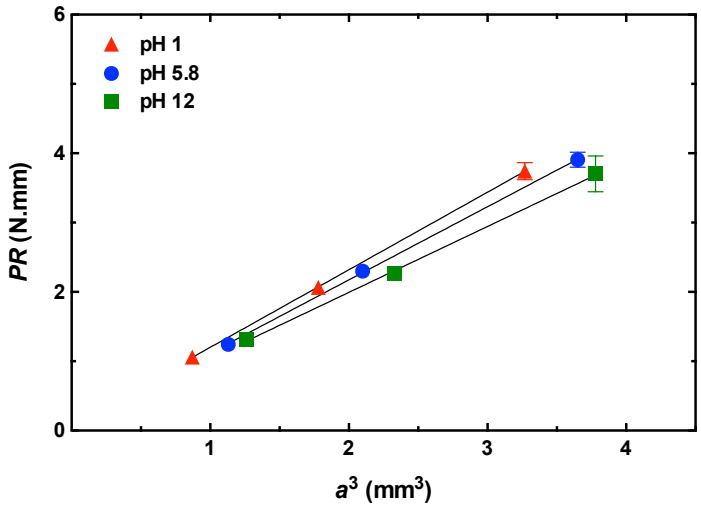

Figure 6.18: Variation of PR as a function of a^3 at pH 1, 5.8 and 12. The elastic modulus, K, was calculated from the gradient of linear fits to the data.

Table 6.3: The elastic modulus of the DN and SN hydrogels as a function of pH.

Hydrogels' elastic moduli (MPa)		
pH level	PMAA–POEGMA (DN) hydrogel	PMAA (SN) hydrogel
pH 1	1.18	0.42
pH 5.8	1.09	0.30
pH 12	1.00	0.17

6.8 The Swelling Ratio of Hydrogels

In order to calculate the swelling ratio (Q) of the PMAA–POEGMA (DN), PMAA (SN) and POEGMA (SN) hydrogels as a function of pH, many circular sheets of hydrogels with a diameter of 5 cm and a width of 5 mm were prepared. After synthesising these gels, each was dried in a vacuum oven at 50 °C for 5 h and then the weight of the dried gel (W_{dry}) was measured and recorded. Thereafter, the dried flat gel was placed inside water at the chosen pH and allow to equilibrate for 5 days. After these 5 days, the weight of the swollen gel (W_{swollen}) was measured and recorded at various pH solutions. The swelling ratio, Q, of all hydrogels was calculated using the following equation

$$Q = \frac{W_{\text{swollen}}}{W_{\text{dry}}} . \tag{6.4}$$

Figure 6.19 presents the swelling ratios (Q) of the PMAA–POEGMA (DN), PMAA (SN) and POEGMA (SN) gels at different pH solutions. Both PMAA–POEGMA (DN) and PMAA (SN) hydrogels showed a pH-responsive swelling behaviour since they both showed an increase in their swelling ratios after increasing the pH value of their surrounded water above pH 5.8 and a decrease in their swelling ratios when they were immersed in water at a pH < 5. In contrast, the swelling ratio of the POEGMA (SN) gel was weakly dependent on pH changes since it is a neutral gel (not a weakly charged polyelectrolyte gel).

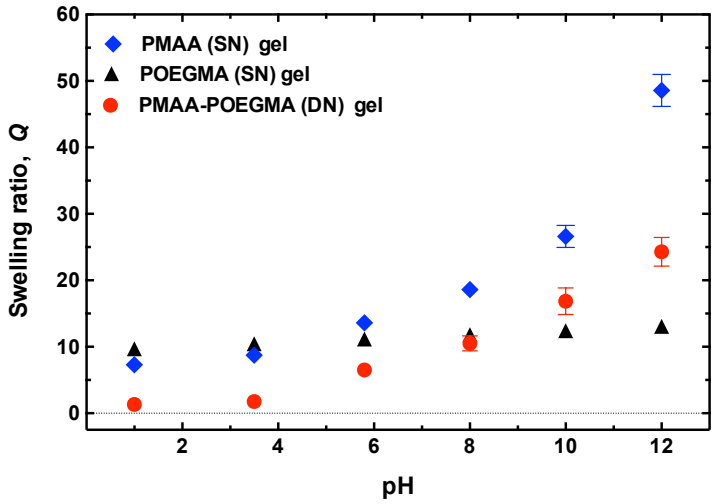

Figure 6.19: The effect of the pH value of the surrounding water on the swelling ratio of the PMAA (SN) (blue symbols), POEGMA (SN) (black symbols) and PMAA–POEGMA (DN) (red symbols) hydrogels.

At a pH < 5.8, the swelling ratio of the PMAA–POEGMA (DN) and PMAA (SN) hydrogels started to decrease, with the DN hydrogel shrinking more than the SN hydrogel. The DN hydrogel de-swelled more than SN hydrogel was due to the interactions of the inter-network hydrogen bonds accrued between the first and second networks of the DN hydrogel. This large reduction in the DN gel's swelling at pH 1 was taken as evidence for the formation of complex hydrogen bonds between the first and second networks. The hydrogen bond interactions between the interpenetrating networks (IPN) are known to be strong with complex formations between POE and the non-ionized carboxylic acid groups of the PMAA gel at pH < 4 [140]. These hydrogen bonds between the DN networks were disrupted when the pH increased above pH 5.8, and so the gel was free to swell. The limitation in the swelling of the DN hydrogel was also imposed by the abundant amount of crossslinkers in the first network, the PMAA. In contrast, the PMAA (SN) hydrogel swelled dramatically at pH 12 since it was less crosslinked than the PMAA–POEGMA (DN) gel.

6.9 Laser Scanning Confocal Microscopy

The swollen wet morphologies of both the PMAA–POEGMA (DN) and PMAA (SN) hydrogels were investigated in DI water at pH 5.8 under a confocal laser scanning microscope (CLSM). An inverted CLSM (Zeiss LSM 510 Meta, with a 63× objective) was used at an excitation wavelength of 543 nm. Rhodamine B (RhB) dye was used as a hydrophilic fluorescent probe to diffuse its water-based solution into the polymeric network of both the SN and DN hydrogels. Hence, RhB was dissolved in DI water at 1 mg/mL and the DN and SN hydrogels were immersed in the solution for 20 min in the dark before being placed under the CLSM. RhB solution was physically absorbed into the polymer network of SN and DN hydrogels by their polymer backbone since both hydrogels were permeable to water-soluble compounds.

Figure 6.20 shows the diffusion of the rhodamine B within the PMAA (SN) hydrogel (shown in red). The resultant homogeneously dispersed network of the PMAA (SN) gel under CLSM was related to its permeability to the water-based rhodamine B solution due to the higher swelling ratio of the PMAA gel in water at pH 5.8. The carboxylic acid groups of the PMAA hydrogel became ionised and negatively charged in water at pH 5.8, which then caused a repulsion between chains allowing them to extend and absorb a larger amount of rhodamine

B water-based solution.

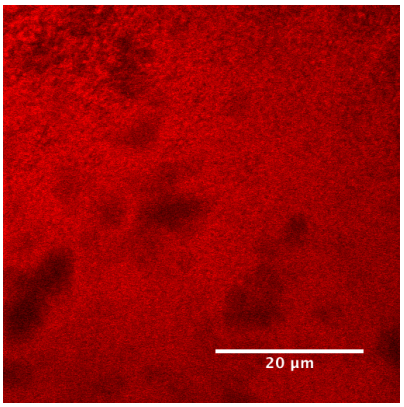

Figure 6.20: A CLSM image of the PMAA (SN) hydrogel immersed in rhodamine B water-based solution.

The permeability of the RhB solution to the PMAA–POEGMA (DN) gel, in contrast, was limited comparing to the SN gel, which was presumably caused by the higher crosslinking density of the PMAA gel (first network of the PMAA–POEGMA (DN) gel), (see Figure 6.21). The fluorescence image indicates the formation of an interconnected structure with networks of the DN hydrogel. The dramatic difference in the permeability of the SN and DN hydrogels to the RhB solution must, therefore, be attributed to the respective toughness of their networks, since the loosely crosslinked structure of the PMAA (SN) gel was more soft and so it absorbed (faster) more dye than the tough PMAA–POEGMA (DN) gel.

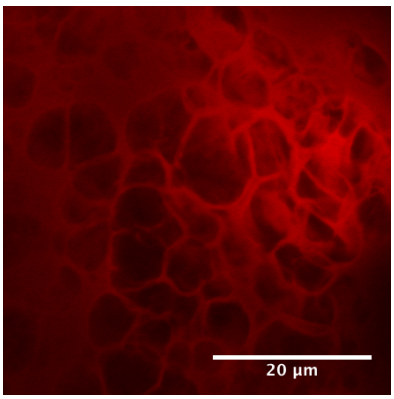

Figure 6.21: A CLSM image of the PMAA–POEGMA (DN) hydrogel immersed in rhodamine B water-based solution.

6.10 Adhesion Switchability at the Gel-Brush Interface

It was previously shown in this chapter that the adhesion was switched on at the interface between the (SN and DN) hydrogels and the PDEAEMA brushes inside DI water at pH 5.8 and off at very high or low pHs, i.e. pH$\sim$ 12 and 1. The adhesion switchability was therefore examined at the hydrogel-brush interface by switching the pH value of DI water from pH 5.8 to pH 12 or from pH 5.8 to pH 1 while the gel was adhering to the brush surface. The switchable adhesion experiments were thus divided into two parts and so were conducted as follows:

1) The first part of the adhesion experiment was conducted by adding a few drops of HCl to switch the adhesion off at the already adhered hydrogel-brush interface by decreasing the pH value of DI water from pH 5.8 to pH 1. This adhesion experiment was carried out (for both the SN and DN gels) by bringing the hemispherical hydrogel into contact with the PDEAEMA brush in DI water. (Both of the hydrogel and coated-brush surfaces were previously placed in DI water at pH 5.8 for at least 1 h before sticking them together.) After sticking the gel to the brush surface, the gel was pressed down on the brush surface by an applied force of 0.5 N for 2 min (see Figure 6.22 (a)). Then, the applied force on the gel-brush interface was removed without pulling them apart. A few drops of HCl were subsequently added to the water that surrounded the adhered gel and brush, in order to reduce the pH of water from 5.8 to 1. A magnetic stirrer was used to stir the water slowly so as to ensure the diffusion of the HCl solution. Both the adhered gel and brush surfaces were left for 1 h inside the pH 1 solution (see Figure 6.22 (b)). Finally, the gel was pulled up from the brush surface (see Figure 6.22 (c)) and the adhesion force (F) and work done (W) at the gel-brush interface were recorded by the TA software of the mechanical tester.

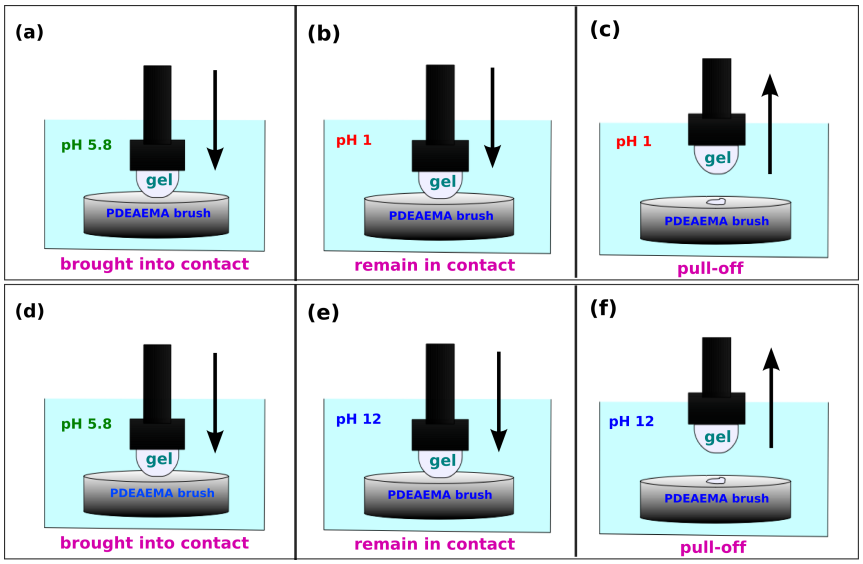

Figure 6.22: An illustration of the experimental procedure for removing the adhesion at the hydrogel-brush interface by either decreasing the pH 5.8 to 1 or increasing it from pH 5.8 to 12.

2) The second part of the experiment was conducted by using a NaOH solution to switch the adhesion off at the gel-brush interface by raising the pH of the water from pH 5.8 to pH 12 (both the hydrogel and coated-brush surfaces were placed in DI water at pH 5.8 for at least 1 h before sticking them together). The hemispherical gel was thereafter brought into contact with the PDEAEMA brush underwater. The gel was then pressed onto the brush surface by an applied force of 0.5 N for 2 min. The applied force was afterwards released without pulling the gel way from the brush surface (see Figure 6.22 (d)). A few drops of NaOH solution were then added into the water in order to raise the pH of water from pH 5.8 to pH 12 (see Figure 6.22 (e)). A magnetic stirrer was used to stir the water slowly so as to ensure the diffusion of the NaOH solution. Finally, the gel was detached from the brush surface (Figure 6.22 (f)) and the adhesion force at their interface was recorded.

The obtained data from these switchable adhesion measurements (the maximum adhesion force and the work done) of PMAA–POEGMA (DN) and PMAA (SN) hydrogels at pH 1 and 12 are presented in Figure 6.23. The initial adhesion measurements for both DN and SN gels at pH 5.8 (in DI water) are also presented in Figure 6.23 so as to illustrate their actual adhesion values without changing the pH of the water in order to compare these with

the pH-switched adhesion values (i.e. at pH 1 and 12). It was found that the adhesion of the PMAA–POEGMA (DN) hydrogel with the polybase brush was noticeably more affected after increasing or decreasing the pH of water, since it was significantly reduced from its actual adhesion value (i.e. the initial test at pH 5.8). However, the adhesion of the PMAA–POEGMA (DN) hydrogel with the polybase brush decreased more after reducing the pH value of the surrounding water to pH 1.

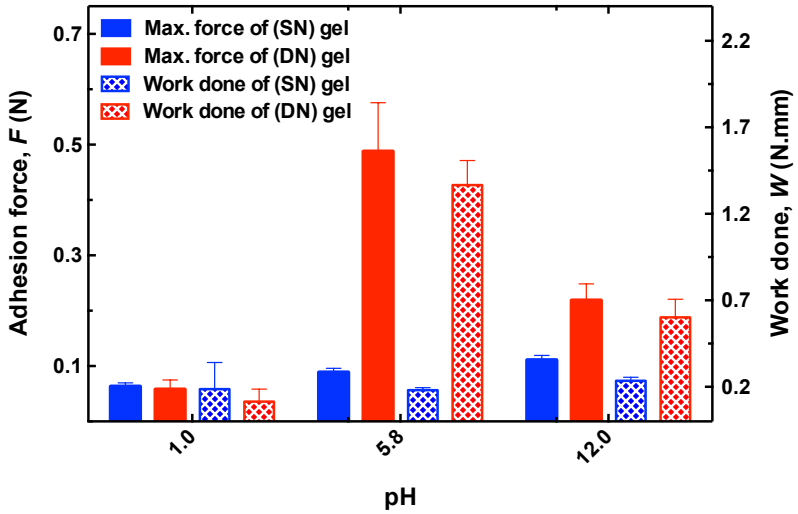

Figure 6.23: Adhesion switchability of DN (red columns) and SN (blue columns) hydrogels at pH 1 and pH 12. The measurements at pH 5.8 show the actual initial adhesion at the gel-brush interface (without adding HCl (at pH 1) or NaOH (at pH 12)). The filled columns indicate the maximum adhesive force, while the dotted columns indicate the work done values.

After reducing the pH value of the water from pH 5.8 to pH 1, the adhesion force and work done in the PMAA–POEGMA (DN) hydrogel's adhesion were reduced from 0.5 N and 1.4 N.mm to 0.06 N and 0.12 N.mm, respectively. After increasing the pH level from 5.8 to 12, however, the adhesion force and work done in the PMAA–POEGMA (DN) hydrogel's adhesion were also reduced from 0.5 N and 1.4 N.mm to 0.23 N and 0.6 N.mm, respectively. On the other hand, the adhesion of the PMAA (SN) hydrogel was only slightly decreased after reducing the pH of the water to pH 1, but it was unexpectedly increased after the pH was increased to pH 12. The reason why the adhesion of the PMAA (SN) hydrogel was increased after the pH level was increased to pH 12 was probably because the highest swelling ratio of the SN hydrogel occurred inside the strong alkaline solution, which led to the gel being

extensively swollen and easily broken when it was pulled up from the brush surface. The swelling ratio of the PMAA was twice higher ($Q = 48.6$) than that of the PMAA–POEGMA (DN) hydrogel at pH 12. In comparison to the PMAA (SN) hydrogel, the PMAA–POEGMA (DN) hydrogel had a lower swelling ratio at pH 12, which meant a less interfacial contact radius with the brush surface, and thus the adhesion of the DN gel was not increased at pH 12 (although the adhesion force and work done remained slightly higher than the adhesion value at pH 1). The lower swelling ratio of the DN hydrogel at a high pH value was related to the higher amount of crosslinkers in the PMAA (of the first) network, allowing the chains to absorb water to a limited extent [140]. It could be that the PMAA (SN) hydrogel needed a longer time to reach equilibrium (more than 1 h) than the DN gel inside the acidic pH in order to reduce its adhesion further, since it swelled significantly more than the DN gel. It was previously shown that the PMAA gel required at least 7 hours to detach from the polybase brush surface by itself at pH 1 after using an applied force of 32 mN, and this self-detachment time increases as long as the applied force increases [29, 150].

At basic pH, the SN gel was very swollen and so was easily deformed and broken when it was pulled up from the brush surface. It could be that the diffusion of HCl or NaOH drops at the interface was very slow since 0.5 N of the applied force led to the creation of a good contact area at the adhesive gel-brush interface. As a consequence, the adhesion test was repeated later by reducing the applied force from 0.5 N to 0.1 N in order to reduce the adhesive contact diameter at the gel-brush interface in order to speed up the time taken to diffuse the acid/basic solution at the gel-brush interface after changing the pH value of their surrounding water. Since the adhesion was remarkably switchable after reducing the pH level of DI water from pH 5.8 to pH 1, the switchable adhesion experiments were conducted again by using an applied force of 0.1 N and also using HCl, only, to reduce the pH of the water to pH 1 to remove the adhesion at the gel-brush interface.

Figure 6.24 shows the results of the adhesion switchability of the DN and SN gels between pH 1 and pH $\sim$ 6 in nine cycles (the same piece of hemispherical hydrogel was used in 9 cycles of adhesion tests with a fresh (new) location on the brush surface). The hydrogel was adhered to the brush surface (with thickness of 76 nm) inside water at pH $\sim$ 6 by an applied force of 0.1 N for 2 min and then the applied force was released and the gel allowed to remain in contact

with the brush. A few drops of HCl solution were consequently added to the water (which was stirred very slowly with a magnetic stirrer) and the adhered gel-brush interface was left for a further hour before conducting the detaching measurement. The adhesion was then measured between the adhered gel and brush surface at pH 1 (cycle 1). Then, the detached gel and brush surface were washed with a copious amount of DI water before being reused in the second test (cycle 2). In cycle number 2, the same gel was brought back into contact with the brush surface in DI water before reducing the pH value of the water to pH 1. After reducing the pH to 1, the gel-brush interface was left for an hour and then the adhesion was measured again. The adhesion switchability cycles were repeated on 7 occasions for both the DN and SN gels with the polybase brushes (the adhesion was measured 7 times at pH 1 using the same piece of hydrogel). In cycle number 8, the adhesion of both the SN and DN gels was tested with a blank clean silicon surface in DI water at pH $\sim$ 6 in order to confirm that they were not interacting with the same-charged surface of the uncoated silicon surface. In the final cycle, test number 9, the adhesion at the gel-brush interface was measured inside DI water at pH $\sim$ 6 (no HCl was added here).

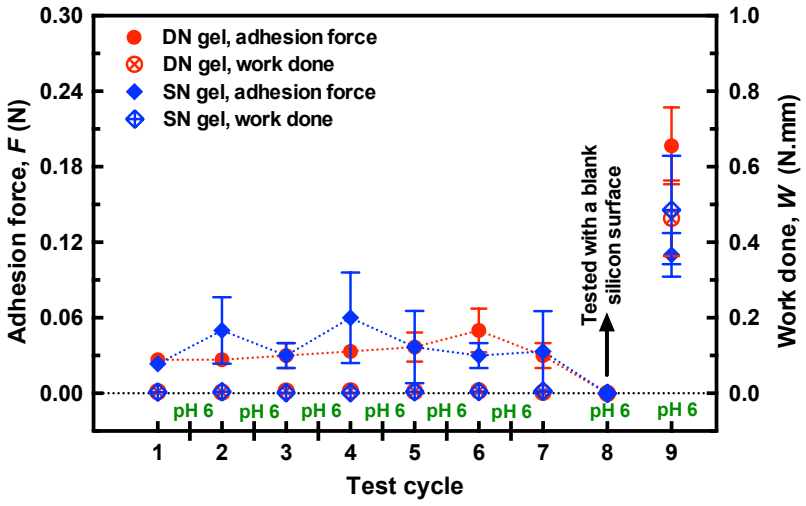

Figure 6.24: The adhesion switchability of DN and SN hydrogels at pH 1 and 5.8 with an applied force of 0.1 N. Cycles 1 to 7 were conducted at pH 1, while cycles 1.5, 2.5, 3.5, 4.5, 5.5 and 6.5 were related to the reattaching process of the hydrogel to the brush surface inside DI water at pH $\sim$ 6. Cycle 8 was carried out by attaching the hydrogel to an uncoated silicon surface to confirm the absence of the adhesive interaction. In cycle 9, a final adhesion test was conducted between the hydrogels with the PDEAEMA brush surface in DI water at pH $\sim$ 6 (without changing the pH).

It was found that the adhesion of both DN and SN gels was switched off after adding HCl to water (cycles 1, 2, 3, 4, 5, 6 and 7) since the work done was very low in each case. The adhesion force was below 0.05 N and the work done was below 0.005 N for both gels. The adhesion force of the PMAA (SN) hydrogel, however, was slightly higher at pH 1 than that for the DN gel as a result of the cohesive failure that was clearly seen on the brush surface after detachment.

Figure 6.25 shows force-distance curves of the adhesion measurements for both SN and DN hydrogels in test cycle number 7 (at pH 1), 8 (with an uncoated silicon surface at pH 5.8) and 9 (with the PDEAEMA brush at pH 5.8). It can be clearly seen that the adhesive interactions had vanished in cycle number 7 for both SN and DN gels after changing the pH of the water to 1 (there was no applied force in cycle 7 at the gel-brush interface because they were already pressed together by 0.1 N applied force before adding HCl, and hence the force-distance curve starts from zero). In test cycle number 8, both the SN and DN gels did not interact at all with the blank silicon surface at pH 5.8 since both gels were negatively charged, as was the silicon surface (although they were pressed together by 0.1 N of applied force). In test cycle number 9, in contrast, both the SN and DN gels adhered strongly to the PDEAEMA brush surface in water at pH 5.8. The force-distance curves in cycle 9 were not very smooth (slightly tortuous), however, possibly because of the increasing roughness at the gel surface due to the previous pulling-off measurements.

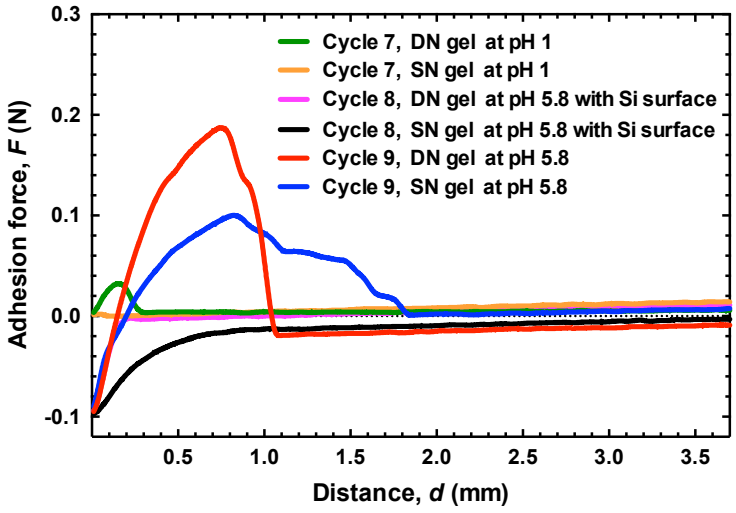

Figure 6.25: Force-distance curves of the adhesion measurements for both SN and DN gels in test cycles number 7 (at pH 1), 8 (with a blank silicon surface at pH 5.8) and 9 (with PDEAEMA brushes at pH 5.8).

Generally speaking, the adhesion measured in the final cycle 9 of the adhesion test of the PMAA–POEGMA (DN) gel was slightly reduced from the initial test, while the adhesion of the PMAA (SN) gel was increased from its initial value. In other words, the adhesion measurements were conducted without changing the pH level of the water in cycle 9 and it was found that the adhesion force values for the SN and DN gels were $\sim$ 0.1 N and $\sim$ 0.2 N, respectively, compared to the actual adhesion force values for the SN and DN gels (after using an applied force of 0.1 N) that were $\sim$ 0.05 N and $\sim$ 0.3 N, respectively. The reason that the adhesion of the PMAA (SN) gel was slightly increased in cycle 9 from its initial value was due to the progressive cohesive failure that had occurred within the PMAA network between cycles 1 and 7, which led to an increase in the adhesive contact diameter of the PMAA gel with the brush surface in the test cycle 9. As a consequence of these adhesive failures, the hemispherical shape of the PMAA (SN) gel was changed to a flat gel.

As a result of the contact diameter ($2a$) of the PMAA (SN) hydrogel being increased after repeated cycles, its adhesion force also increased. In contrast, the PMAA–POEGMA (DN) hydrogel kept its hemispherical shape during all nine adhesion cycles, even though the adhesion had decreased by the final cycle number 9, the reasons for which were unclear. It could be that the surface of the hemispherical PMAA–POEGMA (DN) hydrogel became slightly rough due to the previous attachment–detachment process during the pulling-off measurements. If the gel surface became rough, it would not have a good contact with the brush surface during their attachment process, which would decrease the adhesive interactive point at their interface, and then lead to a decrease in the adhesion force and work done measurements.

Figure 6.26 shows optical images for the PMAA (SN) gel after being detached from the PDEAEMA brush in test cycle 1 (a), cycle 3 (b), cycle 5 (c) and cycle 7 (d), while the PMAA–POEGMA (DN) gel is shown in image (e) after cycle 1 and (f) after cycle 7 at pH 1. The SN gel was easily deformed from cycle 1 to cycle 7 due to its lower elastic modulus, which made the gel quite soft. The contact diameter, $2a$, of the SN gel increased as a result of the cohesive failures and thus its adhesion with the PDEAEMA brush increased in cycle 9 at pH 5.8. In contrast, the DN hydrogels maintained their hemispherical shape after seven cycles of detachment at pH 1 due to their higher elastic moduli that kept the DN from being

deformed.

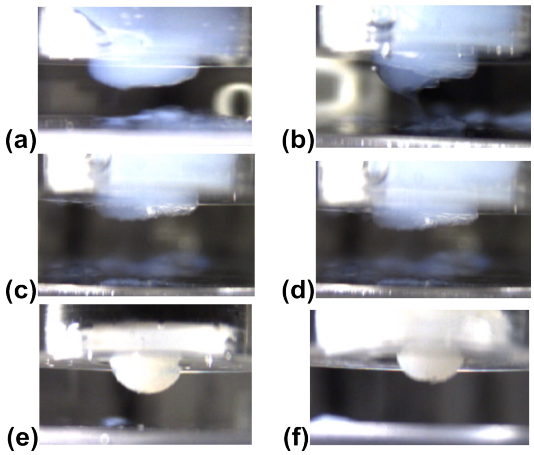

Figure 6.26: Post-detachment images were recoded by a side-view camera for the changes in the contact diameter, $2a$, of the SN gel at pH 1 after cycle 1 (a), cycle 3 (b), cycle 5 (c), and cycle 7 (d) in Figure 6.24. While the unchanged contact diameter of the DN gel is showing in (e) after cycle 1 and (f) cycle 7.

Figure 6.27 shows the changes in the contact diameter ($2a$) for both the SN and DN gels that were recorded from the adhesion tests in Figure 6.24 after the detachment cycle numbers 1, 3, 5 and 7 at pH 1. The measurements of the contact diameter of both the SN and DN gels were measured by ImageJ software after the gel was detached from the brush surface in cycle numbers 1, 3, 5 and 7.

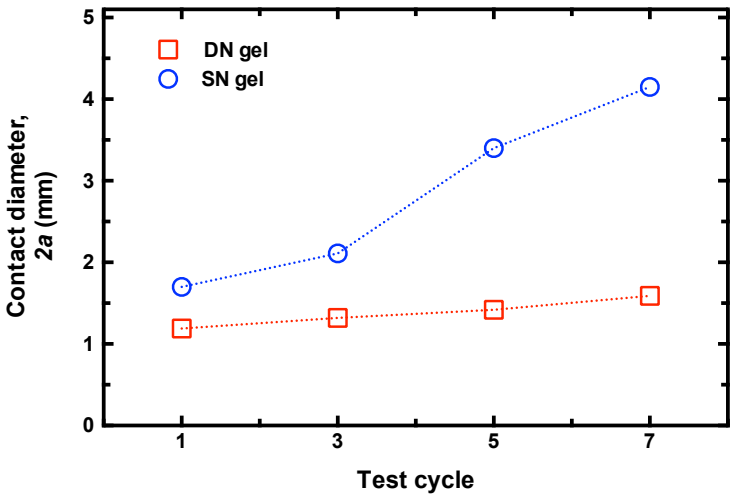

Figure 6.27: The measured contact diameter of the SN (blue symbols) and DN (red symbols) gels after detachment cycles 1, 3, 5 and 7 at pH 1.

It was found that the contact diameter of the soft PMAA (SN) hydrogel was significantly increased from 1.7 mm to 4.1 mm, which then led to an increase in the adhesion force in the final cycle number 9. Whereas, the contact diameter of the robust PMAA–POEGMA (DN) hydrogel was almost stable and not significantly affected by the detachment cycles.

6.11 Conclusion

The switchable adhesion experiments have shown that both the single-network (SN) and double-network (DN) hydrogels can adhere to the (oppositely charged) polybase brush surface in DI water at pH $\sim$ 6, but that their adhesion is very weak (switched off) at pH values below pH 4 or above pH 8. Since all the SN and DN hydrogels become uncharged below their pK_a value ($<$ pH 5), while the PDEAEMA brushes become uncharged above their pK_a value ($>$ pH 7), the adhesion interactions at the gel-brush interface disappeared at very high or low pH levels, i.e pH 1 or 12.

As a result of the larger elastic modulus (K) of the PMAA–POEGMA (DN) hydrogel, which was almost five times higher than the elastic modulus of the PMAA (SN) hydrogel, the adhesion force of the DN gel was five times stronger than the adhesion of the SN gel in DI water (pH $\sim$ 6). The PMAA–POEGMA (DN) hydrogel was also much tougher than the soft SN gel due to the higher crosslinker density of its first PMAA network. Therefore, the swelling ratio of the PMAA–POEGMA (DN) hydrogel was much lower than that of the PMAA (SN) hydrogel, especially at pH 1 and 12. The notable reduction in the swelling ratio of the PMAA–POEGMA (DN) hydrogel (at pH 1) was related to complex formations of strong hydrogen bonds between its two networks. These hydrogen bonds were disrupted, however, when the pH was increased above pH 5.8 and so the gel was free to swell to a limited extent due to the many crosslink points that tighten its chains [140].

The most remarkable result obtained in this gel-brush adhesion study was that DN hydrogel adhesion was not only switchable but was also repeatable up to four times inside DI water at pH $\sim$ 6 (without using HCl or NaOH). In contrast, the adhesion of the SN hydrogel could not to be repeated at the same place on the brush surface more than once. The reason for this was due to the cohesive failure that occurred after detaching the SN gel from the brush surface at pH 5.8. This cohesive failure caused a repulsive interaction between the same-charged surfaces

of the SN gel on the mechanical probe and the trace (cohesive failure) of the SN on the brush surface.

The adhesion of SN and DN hydrogels with the PDEAEMA brushes was controllable and switchable between sticking to non-sticking states by adding HCl into the surrounded water. After detaching the adhered SN and DN hydrogels from the PDEAEMA brush surface at pH 1, their adhesion was easily induced again at pH $\sim$ 6. It was therefore proven that both the SN and DN gels can follow a number of cycles of attachments–detachments with the brush surface at pH 6 and pH 1. The adhesion of the DN hydrogel was decreased from its initial adhesion measurements, which may be due to an increase in the roughness of the contact region of the hemispherical gel. In contrast, the adhesion of the SN gel was increased after seven attachment–detachment cycles of the adhesion tests due to the increase in its contact diameter with the brush surface as its shape changed from a hemispherical to flat gel due to the many cohesive failures that occurred within the previous detachment cycles.

Chapter 7

Switchable Adhesion in Salt Solutions

Abstract. The effect of adding sodium chloride solution at different concentrations into the water surrounding the hydrogel-brush adhesive interface was investigated. It was found that the adhesive force at the hydrogel-brush interface significantly increased after adding a very dilute salt solution (of 0.001 M) into the surrounding water. The work done in detaching the polyacid hydrogel from the polybase brush surface inside the 0.001 M sodium chloride solution was somewhat less than the work done inside deionised water, however, confirming that the adhesive interactions at the interface were affected and reduced. On the other hand, the hydrogel-brush adhesion was notably affected once the concentration of sodium chloride solution was raised above 0.5 M, as shown by the clear reduction obtained in respect to both the adhesive force and work done. This result confirmed that adhesion between the oppositely charged polyelectrolytes, a hydrogel and polymer brush, is switchable since it is eliminated by adding a high concentration of sodium chloride solution.

7.1 Introduction

It was previously shown that the adhesion between two oppositely charged polyelectrolytes, a hemispherical hydrogel and a polymer brush, was successfully switchable and repeatable a number of times by changing the pH value of the surrounding water. The adhesive interactions at the hydrogel-brush interface were strongly increased inside water at pH 5.8 due to the electrostatic interactions as well as by hydrogen bonding between the carboxylic groups of the PMAA gel and amine groups of the PDEAEMA brush. This adhesion was then easily

weakened, however, by changing the pH of water to pH 1 or pH 12. At these extreme pH values the adhesion interactions at the hydrogel-brush interface were weaker because the polymer chain collapses due to the dissipation of the electrostatic charges of either the hydrogel (carboxylic groups at pH 1) or the polymer brush (amino groups at pH 12).

The electrostatic charges of the weakly charged polyelectrolytes can also be affected by increasing the salt concentration in their surrounding water. This is because salt ions screen the electrostatic charges on the polymeric chains by shielding them, decreasing the osmotic pressure and causing the polymer chains to collapse or de-swell [58, 142, 152]. Various studies have shown that the weakly charged polyelectrolytes can undergo a de-swelling transition inside high ionic salt solutions by screening their charges. As an illustration of this, a single-network (SN) of the poly(methacrylic acid) (PMAA) and also an interpenetrating polymeric network (IPN) of the poly(methacrylic acid)–poly(*N*-isopropylacrylamide) (PMAA–PNIPAAm) hydrogels have each been shown to exhibit a salt-sensitive de-swelling behaviour when the ionic strength in their surrounded solutions is increased. The degree of swelling of these hydrogels was studied as a function of the salinity in their surroundings and it was found the de-swelling ratio was larger when the ionic strength approached 0.1 M of the NaCl solution [154, 161].

Furthermore, the extended and collapsed behaviour of the weak polyelectrolyte brushes has been studied as a function of the salt concentration. It was found that weak polyelectrolyte brushes remained extended at a low salt concentration but collapsed at a high ionic strength. For example, the thickness of polyelectrolyte brushes of poly(2-(methacryloyloxy)ethyltrimethylammonium chloride (PMETAC) was affected by NaCl concentration, being dramatically decreased at a concentration of 5.6 M. On the other hand, the extended brushes of dense PMETAC were not affected at a salt concentration lower than 5.6 M, since the balance between the high charge density and high osmotic pressure of the dense system meant that the brushes remained expanded [166].

In respect to the possibility of controlling and screening the charges of polyelectrolytes, another hypothesis has been proposed, namely to control the adhesion between the two oppositely charged polyelectrolytes in this study by using sodium chloride (NaCl) solutions (rather than using a strong acid or base). Screening the electrostatic charges of hydrogels and polymer brushes by adding salt solutions would therefore control attachment–detachment cycles

at the hydrogel-brush interface. The ability to control switchable adhesion process using environmentally friendly aqueous salt solutions opens the way for novel adhesive or self-healing systems in medical materials, since these materials can then come into contact with blood or other body fluids [39, 154].

In this chapter, a study of the switchable adhesion between a polyacid hydrogel and a polybase brush is reviewed as a function of the addition of NaCl solution (at fixed pH of DI water). Therefore, a single-network (SN) hydrogel of poly(methacrylic acid) (PMAA) and a double-network (DN) hydrogel of poly(methacrylic acid)–poly[oligo(ethylene glycol)methyl ether methacrylate] (PMAA–POEGMA) were used to test their adhesion with the poly[2-(diethyl amino)ethyl methacrylate] (PDEAEMA) brush as a function of increasing salt concentrations.

7.2 The Effect of Salt Solutions on Switchable Adhesion

7.2.1 Swelling Ratios of Hydrogels in Salt Solutions

Before presenting the results of the adhesion between a hydrogel and polymer brush as a function of increasing the concentration of NaCl solution in their surrounding water, the swelling ratio (Q) of the polyelectrolyte SN and DN hydrogels inside the NaCl solutions is first reviewed in order to understand their response to the increase in the ionic strength of salt ions. The influence of ionic strength on the swelling behaviour of polyelectrolyte SN and DN hydrogels was therefore studied using different concentrations of NaCl solution, with the pH value of the surrounding DI water being kept constant at pH 5.8. The concentrations of NaCl solutions were varied from a very low concentration of 0.001 M to a very high concentration of 5 M.

Many circular sheets of the PMAA (SN) and PMAA–POEGMA (DN) hydrogels were prepared with a diameter of 5 cm and a width of 5 mm to test their swelling ratios inside various NaCl solutions at different concentrations. After preparing these sheets, each hydrogel was dried in a vacuum oven at 50 °C for 5 h and then the weight of the dried gel (W_{dry}) was measured and recorded. Thereafter, the dried flat sheets of the SN and DN hydrogels were immersed inside NaCl solutions of different concentrations and left for 5 days. The weight of the swollen gel

(W_{swollen}) was then measured and recorded. Finally, the swelling ratios (Q) of both of the SN and DN hydrogels were calculated at different NaCl solutions.

Figure 7.1 shows the de-swelling behaviour of the PMAA (SN) and PMAA–POEGMA (DN) hydrogels inside salt solutions as a function of increasing the NaCl concentration. It was found that even a very small amount of NaCl (0.001 M) resulted in the swelling, Q, of both the SN and DN hydrogels decreasing to less than half of that inside DI water (without the addition of salt). Specifically, the swelling ratio of the PMAA (SN) hydrogel was 13.6 inside DI water (without adding salt) and 6.6 inside the 0.001 M NaCl solution. The swelling ratio of the PMAA–POEGMA (DN) hydrogel, meanwhile, was 6.5 inside DI water (without adding salt) and 2.7 inside the 0.001 M NaCl solution.

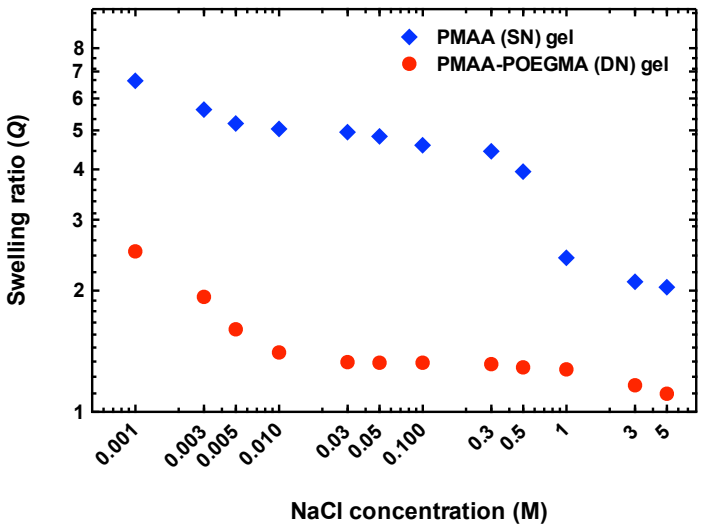

Figure 7.1: The swelling ratio (Q) of the PMAA (SN) hydrogel (blue symbols) and the PMAA–POEGMA (DN) hydrogel (red symbols) inside NaCl solutions of different concentrations between 0.001 M to $\sim$ 5 M.

The de-swelling behaviours of both the PMAA (SN) and PMAA–POEGMA (DN) hydrogels remained evident as the molarity of NaCl solutions was increased, until suddenly dropping once the NaCl solution reached a concentration higher than 1 M. The dramatic collapse in the hydrogel swelling ratio was due to the hydrated salt ions of the NaCl that served to disrupt the repulsive interactions between the chains in the gel, causing them to collapse and then shrink. Screening the electrostatic repulsions among the chains of the polyelectrolyte hydrogels was affected by replacing the counterions with the salt ions, leading to overall neutral hydrogels.

The intensive collapse of the hydrogels at highly concentrated NaCl solutions ($\sim$ 3 M and 5 M) was obtained upon an increase in the salt ions that shield that electrostatic charges, since the uncompensated charges of the hydrogels became more and more screened.

By comparing the de-swelling behaviours of the SN and DN hydrogels together inside highly concentrated salt solutions, it was found that the swelling ratio of the SN gel dropped remarkably as the ionic strength increased above 0.5 M. The size of the SN hydrogel continued to shrink until the ionic strength approached 5 M, due to counterions being shielded by salt ions. In contrast, the swelling ratio of the DN hydrogel was significantly smaller than that of the SN hydrogel inside all concentrations of NaCl solutions, for two reasons: firstly, the higher crosslinker degree of the first PMAA network of the DN gel, and secondly, the complex formation of strong hydrogen bonds at the interface between the two networks of the DN gel [140], which limited its swelling behaviour inside NaCl solutions.

As a result of the high degree of shrinkage in both networks of the SN and DN hydrogels, it was assumed that their adhesion at the interface with the polybase, PDEAEMA, brushes can be eliminated or weakened by adding a high concentration of the NaCl solution into the surrounding water. If the charges of either the hydrogel or the surface of the polymer brushes become neutral, the adhesive interactions at the gel-brush interface are likely to fail, resulting in a successful detachment for both polymers. The results of the salt-sensitive adhesion experiment are presented in the following section.

7.2.2 Switchable Adhesion Inside Salt Solutions

Increasing the NaCl concentration in the water surrounding the SN and DN hydrogels leads to a decrease in the polymeric network size as a result of the screening of their electrostatic charges among carboxylic groups [161]. Pull-off adhesion experiments at the gel-brush interface were therefore conducted between the polyacid hydrogel of both of the PMAA (SN) and PMAA–POEGMA (DN) with the polybase (PDEAEMA) brush (75 nm thick) underwater as a function of increasing salt concentrations using the mechanical tester (TA). The molarity of the NaCl solutions ranged from a very low concentration of 0.001 M to a very high concentration of 5 M. The experiments were carried out as follows:

1) The hydrogel was first brought into contact with and adhered to the surface of the PDEAEMA brush (with a thickness of $\sim$ 75 nm) inside DI water at pH 5.8 by applying a force of 0.5 N for 2 min (no salt was added at this step).

2) Next, the applied force on the adhered gel-brush interface was released without pulling the gel up from the brush surface. In other words, the gel remained in contact with the surface of the polymer brush inside water after removing the load.

3) A NaCl solution with a known concentration was then added into the water surrounding the gel-brush interface. A magnetic stirrer was used to stir the water very slowly so as to ensure that the NaCl solution spreads inside water.

4) The adhered gel-brush interface was then left inside the newly introduced NaCl solution for an hour.

5) After approaching the required time, the gel was pulled away from the brush surface, with the maximum adhesion force (F) and work done (W) being measured as a function of salt concentrations.

   Note: since the gel and brush were already adhered together inside DI water at pH 5.8 (step 1 above), the amount of this water was kept constant at 500 mL during all these experiments. As a consequence of that, the required molarities of the NaCl solutions were prepared in 500 mL of water. The amount of NaCl was doubled in the 500 mL solution, however, in order to dilute it later when it was subsequently added into the initial 500 mL of DI water that already surrounded the adhered gel-brush interface. For example, a 1 M NaCl solution was made by first dissolving 58.44 g from the NaCl in 500 mL of DI water and then diluted in the initial 500 mL of DI water that was used at the beginning of the experiment to adhere the hydrogel to the brush surface.

Figure 7.2 shows the results of (aqueous) pull-off adhesion experiments for the PMAA (SN) and PMAA–POEGMA (DN) hydrogels, with the PDEAEMA brush as a function of added NaCl concentration into their surrounding water. Interestingly, the adhesion force measurements of both SN and DN hydrogels unexpectedly increased after the addition of NaCl at

a very low concentration of 0.001 M. Specifically, the normal adhesion force at the SN gel-PDEAEMA brush interface was 0.09 N inside DI water at pH 5.8 (without adding salt), and this became much greater and reached 0.25 N inside the 0.001 M NaCl solution. In the same way, the normal value of the adhesion force at the DN gel-PDEAEMA brush interface inside water (at fixed pH and without adding salt) was 0.5 N, while it dramatically increased to 0.88 N after adding the 0.001 M NaCl solution. This result of the low salt concentration is not unique and had been previously observed to affect molecular diffusion inside a PMAA hydrogel [167]. It was found that the diffusion of fluorescein-tagged dextran (FDEX) within the PMAA network was unexpectedly greater in the presence of a low NaCl concentration (below 0.05 M) than that in the absence of the NaCl (in pure water). This was justified by the interaction between the additional charge from either the free charge released by the PMAA network or the ions of the salt solution with the dextran. The diffusion of dextran within the PMAA hydrogel did, however, decrease after increasing the NaCl concentration above 0.05 M.

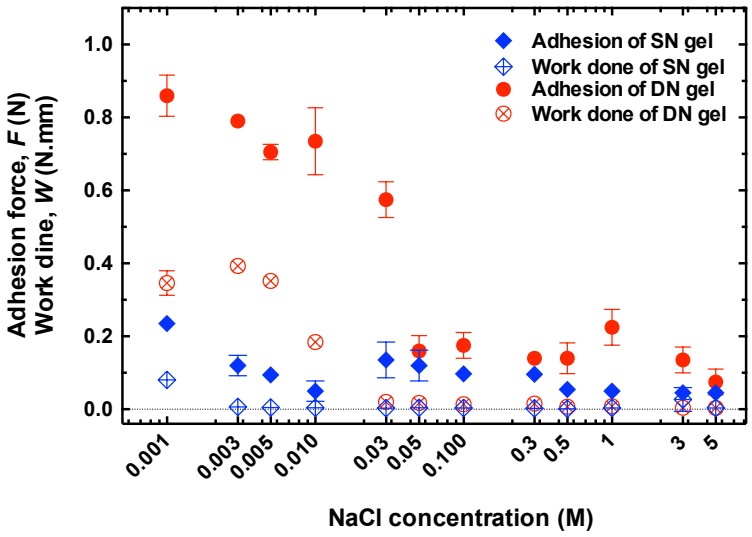

Figure 7.2: The adhesion experiments for the PMAA (SN) hydrogel (blue symbols) and the PMAA–POEGMA (DN) hydrogel (red symbols) after adding the NaCl solution into their surrounding water at different concentrations. The filled symbols are related to the maximum adhesion forces while the crossed symbols refer to the work done, which were collected from force-distance curves.

The reason why the maximum adhesion force increased after adding the NaCl solution at concentrations as low as 0.001 M is still not clear, but the decrease in the work done inside

the 0.001 M solution did serve to confirm a decrease in the adhesion at the gel-brush interface due to the effect of the salt ions. In other words, the work done in respect to both of the PMAA (SN) and PMAA–POEGMA (DN) hydrogels decreased, compared to the value inside DI water (at pH 5.8), after adding the 0.001 M NaCl salt solution. In the adhesion case of the PMAA (SN) hydrogel, the work done dropped slightly from 0.13 N.mm (in water) to 0.09 N.mm inside the 0.001 M salt solution. While the work done at the DN gel-PDEAEMA brushes interface reduced sharply from 1.4 N.mm (in water) to 0.38 N.mm after adding the 0.001 M NaCl solution to the surrounding DI water.

In the densely grafted brush of weakly charged polyelectrolytes, the conformation of the expanding chains is controlled by the balance between the osmotic pressure of the counterions and the electrostatic interactions between the similarly charged monomers on the chains. The structural conformation of the brush is not only controlled by the grafting density, however, but also depends on other parameters such as the charge fraction, chain length and the ionic strength of the surrounding solution. Since the degree of dissociation is decisive for the chain conformation of the weak polybase brush, the addition of a small amount of salt ions into a highly densely grafted and thick brush increases the osmotic pressure causing the chains to extend. The weak polybase brush, however, collapses and becomes like a quenched (strong polyelectrolyte) brush after adding a very high salt concentration [168].

Despite the fact that the presence of salt ions in a solution of weakly charged polyelectrolytes screens the electrostatic charges on the chain, the addition of a small amount of the salt induces the osmotic pressure and consequently makes the polymer chains more stretched. The process of screening all the electrostatic charges on the polymer chains by the salt solution is partially completed (only the charges at the top of the brush are screened by the salt ions) if the amount of the salt ions is very low. In other words, the salt ions cannot diffuse into the highly densely grafted brush because of the osmotic pressure, which forces the chain to be extended exceedingly [161, 166].

When the NaCl concentration was ≥ 0.001 M but ≤ 0.03 M, the adhesion force and work done at the interface between the SN/DN hydrogels with the polybase brush were still higher than their values inside DI water (without adding the salt). After increasing the NaCl concentrations to 0.05 M and above, however, the adhesion force and work done at the interface of the

oppositely charged polyelectrolytes dropped significantly and became very weak, especially inside 3 M and 5 M solutions. Here, both SN and DN hydrogels shrunk in highly concentrated NaCl solutions. The larger reduction in adhesion measurements was due to polymer chains collapsing as a results of the neutralisation of the electrostatic charges on the chains by substituting counterions with salt ions.

After increasing the concentration of the NaCl solution above 3 M, the adhesive forces decreased significantly for the SN and DN gels to below 0.05 N and 0.15 N, respectively. It is worth mentioning, however, that the adhesion of the DN hydrogel dropped more sharply inside the NaCl solution $>$ 3 M than the SN hydrogel, compared to their adhesion values inside DI water. On the other hand, the work done was very weak, below 0.005 N.mm, for both gels inside the NaCl solution $>$ 3 M, which is equivalent to their work done values inside very strong acidic (pH 1) solutions. The reason behind the decreasing adhesion at the hydrogel-brush interfaces inside the NaCl solution above $>$ 1 M was due to the hydrated salt ions diffusing into the adhesive gel-brush interface that eventually disrupted their hydrogen bonds and electrostatic interactions, resulting in a reduction in the adhesive force and thus the hydrogel was easily debonded from the brush surface inside the highly concentrated NaCl solutions.

Figure 7.3 shows the difference in the detaching process of the SN hydrogel and DN hydrogel from the PDEAEMA brush surface and also illustrates the failure type that occurred on the brush surface after detaching inside the 5 M NaCl solution. Although the adhesion measurements decreased significantly inside the highly concentrated NaCl solution of 5 M, it was found that a cohesive failure was still associated with the adhesion of the PMAA (SN) hydrogel (see Figure 7.3 (a)), while an adhesive failure was yet obtained with the PMAA–POEGMA (DN) (see Figure 7.3 (b)). These cohesive and adhesive failures resulted from the difference in the mechanical strength of the SN and DN hydrogels, since the soft SN gel had a much lower crosslinking density and a weaker mechanical strength compared to the highly crosslinked DN gel.

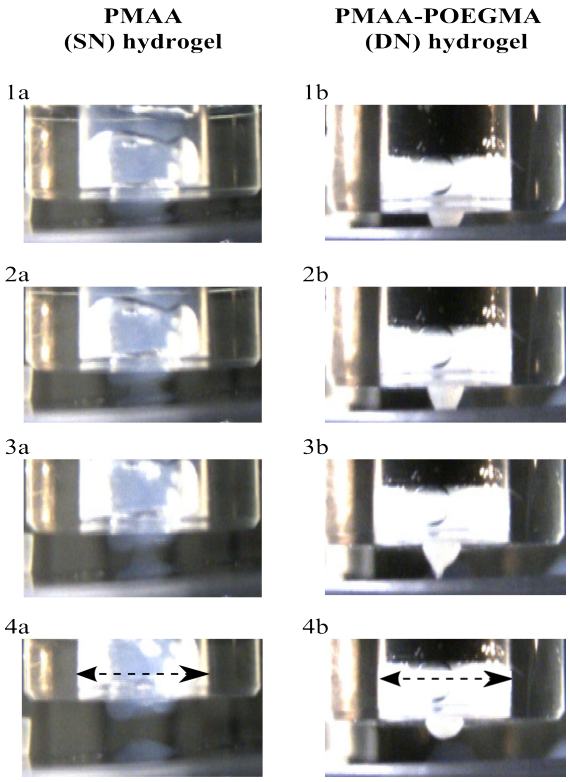

Figure 7.3: The detaching process for the hydrogel-brush interfaces after adding the 5 M NaCl solution into their surrounding water: (a) PMAA (SN) hydrogel and (b) PMAA–POEGMA (DN) hydrogel. A cohesive failure was still obtained with the SN hydrogel, while an adhesive failure occurred with the DN hydrogel. The black dashed arrow indicates the diameter length of the mechanical probe of 10 mm.

A study of a reversible adhesion was reported by Takahara and his co-workers [38] who successfully controlled a salt-sensitive adhesion between two surfaces of cationic and anionic polyelectrolyte brushes by using a 0.5 M NaCl solution. The thickness of both polyelectrolyte brushes was 100 nm. The two surfaces of the polymer brushes were adhered to each other after adding a few drops of DI water at their interface before pressing them together with a load of 4.9 N. The adhesion process was completed after 2 h, when the drops of the added water had dried. Eventually, the adhered surfaces of the two polymer brushes were easily detached after immersing them inside NaCl solution of 0.5 M at room temperature.

The repeatability of this salt-sensitive adhesion was partially achieved with the brush-brush interactions and was repeatable up to three times, although the adhesive strength had decreased sharply from 1.52 MPa to 0.30 MPa by the time of the third water-salt cycle. The reason for the reduction in the repeatable adhesion strength between the cationic and an-

ionic surfaces was unclear since both polymer brushes were retained on each substrate under AFM after completing their detaching process, although it could be due to the adsorption of contamination from the atmosphere into the brushes [38]. Using salt solutions to switch off the adhesion between the surfaces of two oppositely charged polyelectrolytes was later criticised by the same authors, however, due to the fact that inorganic salt layers formed at the adhesive interfaces, which negatively affected the repeated adhesion of the cationic and anionic surfaces [39].

7.3 Comparing the Effect of Salt and pH Solutions on Switchable Adhesion

Adding NaCl solutions to switch the adhesion off at the gel-brush interface is different from using a strong acidic or a strong basic solution in a number of respects. Figure 7.4 illustrates a comparison between the different effects of the salt and pH solutions on the adhesion of the PMAA (SN) and PMAA–POEGMA (DN) hydrogels with the PDEAEMA brush underwater. The data for the maximum adhesive force (F) and the work done (W) for both SN and DN hydrogels with the polybase brush at pH 1, 5.8 and 12, which are presented in Figure 7.4, were taken from Figure 6.23 in Chapter 6. Whereas, the data for the salt solutions at 1 M, 3 M and 5 M were taken from Figure 7.2 in Section 7.2.2.

Both the experimental adhesion studies for pH and salt solutions had the same experimental factors in terms of the applied force (0.5 N) at the gel-brush interface, contact time (2 min) and retraction speed at which the hydrogel was detached from the surface of the polymer brush (50 mm/min). In addition, the time for leaving the adhered gel-brush interface inside the newly introduced pH/salt solution was the same (1 h).

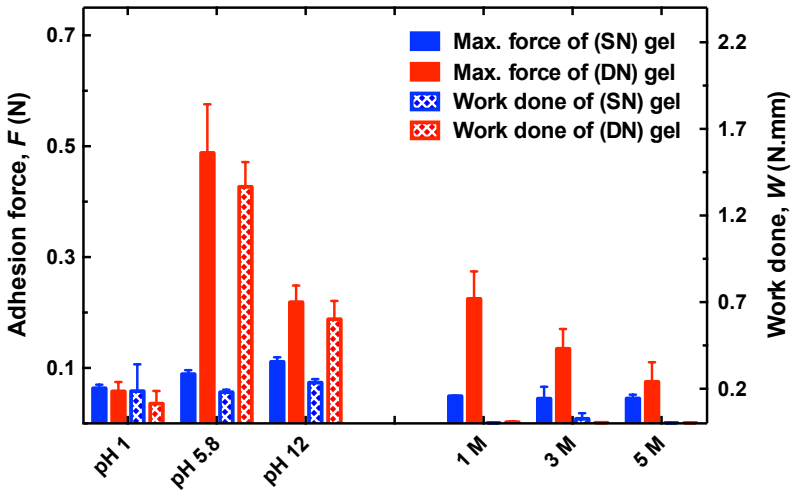

Figure 7.4: Maximum adhesion force and work done measurements at interfaces between the SN (blue columns) and DN (red columns) hydrogels and the polybase brushes inside pH solutions (on the left-hand side) and inside NaCl solutions (on the right-hand side). The filled columns indicate the measurement of the maximum adhesive force, while the dotted columns indicate the work done.

It can be clearly seen that the adhesion measurements for both SN and DN hydrogels (maximum adhesive force and the work done) decreased inside all these pH and NaCl solutions, compared to the adhesion value inside DI water at pH 5.8, where the adhesion is at its best. Apart from that, the adhesion of the SN hydrogel at pH 12 was slightly increased as a result of the intensive swelling behaviour of this gel inside this highly basic solution, which led to an increase in its contact diameter with the brush surface. The adhesion measurements inside the acidic solution at pH 1, however, were more significantly reduced due to the disruption of the hydrogen bonds and electrostatic interactions at the gel-brush interface. Both SN and DN hydrogels were neutral and had shrunk significantly at pH 1. Generally speaking, it was observed that the adhesion measurements inside the strong basic solution at pH 12, and also inside the NaCl salt solutions of 1 M, 3 M and 5 M, were distinctly higher than the adhesion measurements at pH 1 because both the adhesion force (F) and work done (W) were reduced.

These results suggest that the process of detaching the gel from the brush surface was more effective inside the acidic solution at pH 1, since both the adhesion force and work done were decreased. This was because the carboxylic acid groups of both the SN and DN hydrogels became completely non-ionized at pH 1 causing the gels to hydrophobically shrink, which

consequently decreased their interfacial adhesive interactions with the PDEAEMA brush. In contrast, the adhesion force was higher at the gel-brush interface after adding a highly concentrated aqueous NaCl solution, although the reason for this is unclear. The work done in detaching the hydrogels from the brush surface inside the NaCl solutions was almost zero, however, confirming that the interfacial adhesive interaction was reduced.

7.4 Conclusion

The aim of the work presented in this chapter was to investigate the effects of increasing salt concentrations on: i) the swelling ratios of the PMAA (SN) and PMAA–POEGMA (DN) hydrogels and also ii) on their adhesion measurements with the PDEAEMA brush. The switchable adhesion at the hydrogel-brush interface was examined as a function of increasing salt concentrations. The sodium chloride (NaCl) was used at concentrations ranging from a very low concentration of 0.001 M to a very high concentration of 5 M.

Firstly, the impact of the NaCl solution on the swelling ratio of both SN and DN hydrogels was examined as a function of salt concentration. It was found that both SN and DN hydrogels shrank directly inside a very dilute NaCl solution, decreasing to less than half the value of the swelling ratios that were measured inside DI water (at pH 5.8, without adding salts). As the concentration of the NaCl increased, the swelling ratio of SN and DN hydrogels decreased more. A significant de-swelling ratio, however, was obtained for both SN and DN hydrogels inside NaCl solutions with concentrations higher than 0.5 M.

Secondly, the impact of salt concentration on the adhesion of both SN and DN hydrogels with the polybase brush was investigated. It was found that the adhesive force at the gel-brush interface significantly increased after adding a very small amount of the NaCl salt (0.001 M) into the surrounding water. The work done in detaching the hydrogel from the brush surface was somewhat less than the work done inside DI water, however, confirming that the adhesive interactions at the interface were affected and reduced. On the other hand, the gel-brush adhesion was notably affected after raising the concentration of the NaCl solution above 0.5 M, as shown by the clear reduction obtained in respect of both the adhesive force and work done.

Overall, a cohesive failure was still obtained after detaching the PMAA (SN) hydrogel from the polybase brush surface, while an adhesive failure occurred with the adhesion of the PMAA–POEGMA (DN) hydrogel. This was because the mechanical strength of the robust DN gel was much stronger than that of the soft SN gel.

One major criticism of using highly concentrated salt solutions to switch the adhesion off at the gel-brush interface was that inorganic salts can precipitate on the polyelectrolyte surfaces, which affects the ability to repeat the '*on-off*' adhesion cycles. Since the repeatability of the adhesion was more likely to be disrupted after using salt solutions at high concentrations, it was suggested that the adhesion repeatability can be more efficiently applied and more easily controlled by using HCl to reduce the pH value of the surrounding water to pH $\sim$ 1.

Chapter 8

Summary and Future Work

8.1 Summary

'*Smart*' switchable adhesion is a promising technique for different potential applications, where two surfaces can be attached strongly and detach easily without causing damage to either surfaces. For example, switchable adhesives can be used for recycling and as a disassembly processes in the packaging and automotive industries. Moreover, repeatable and switchable adhesion can be utilised to develop self-healing adhesives in the medical field using environmentally friendly aqueous solvents.

This PhD thesis has presented a study into the development of switchable and repeatable adhesion underwater between two oppositely charged polyelectrolytes: a hydrogel with a polymer brush surface. The aims of this study were to: 1) evaluate the pH-sensitive adhesion at the hydrogel-brush interface by pull-off adhesion tests using a mechnical tester called the Stable Micro Systems TA.XT Plus Texture Analyser (TA) and 2) enhance the hydrogel-brush interfacial adhesion by improving the mechanical properties of the hydrogel and 3) prove the adhesion switchability at the hydrogel-brush interface either by changing the pH value or by increasing the salt concentration in the surrounding water.

Switchable adhesion is the ability to control the adhesion at the interface between polymer surfaces by switching their adhesion *on* or *off* on demand by means of an environmental trigger such as varying the pH level or adding salt. This study of switchable adhesion is based on testing the adhesion of the polymer brush with a hydrogel using two different types of the hydrogels: 1) a single-network (SN) hydrogel and 2) a double-network (DN) hydrogel. The

main difference between SN and DN hydrogels is that the DN hydrogel has a much stronger mechanical strength than the SN hydrogel. Both SN and DN hydrogels, however, have a high water content of 90 wt% and both are pH-stimuli responsive materials.

The SN hydrogel adhesion study was conducted between two gel-brush adhesive systems: i) the PMAA (SN) hydrogel–PDEAEMA brush and ii) the PDEAEMA (SN) hydrogel–PMAA brush, as a function of varying the pH of their surrounding water. It was found that the adhesion performance of adhesive structures of both i) the polyacid gel-polybase brush and ii) the polybase gel-polyacid brush are similar to each other in terms of their adhesion measurements at their interfaces, and also in respect to the cohesive failure that occurred after completing the detaching process. Furthermore, the results of the pH-sensitive adhesion prove that the SN gel-brush adhesion can be switchable depending on the introduced pH value of the surrounding water. In other words, the adhesion at the gel-brush interface is tuned and becomes stronger inside DI water at pH $\sim$ 6, while it becomes very low and weak inside strong basic or acidic solutions (i.e. at pH 12 or pH 1).

In general, the adhesion of SN hydrogels with the polymer brushes always ends with a cohesive failure, even after increasing their crosslinking densities. This is due to the increase in the brittleness of SN hydrogels when they are highly crosslinked, as the chains in their networks become unable to stretch while they are being retracted from the brush surface. Moreover, increasing the crosslinking density of SN hydrogels decreases the adhesion at the SN gel-brush interface inside DI water at pH $\sim$ 6, as a result of the increasing brittleness of the hydrogels. In contrast, the SN gel-brush adhesion increases when the SN hydrogel is loosely crosslinked due to the increase in the stretching process of the chains of the hydrogels when they are forced to detach from the oppositely charged surface of the polymer brush.

The major drawback of the cohesive failures evident in the adhesion of the SN hydrogels was successfully overcome by transforming the SN hydrogel into a double-network (DN) hydrogel. The DN gel is made by a two-step network formation, wherein the first network is a highly crosslinked PMAA network, which is responsible for the higher elastic modulus, and the second network is an extremely loosely crosslinked POEGMA, which is responsible for dissipating the stress and enhancing the mechanical strength of the DN hydrogel. The switchable adhesion of the DN hydrogels, therefore, is always associated with an adhesive failure, even when they

are detached inside DI water at pH $\sim$ 6 since the surface of the polymer brush is always clean and not damaged after they are detached from the DN gel.

By using DN hydrogels, this PhD thesis has therefore made a significant contribution and improvement to knowledge in the field of gel-brush switchable adhesion. The adhesion measurements at the hydrogel-brush interface have been dramatically enhanced by means of the PMAA–POEGMA (DN) hydrogel, since this DN hydrogel increases the adhesion with the polymer brush by five times more than the adhesion of the PMAA (SN) hydrogels. Another important contribution of the work presented in this thesis is that the adhesion at the DN gel-brush interface is repeatable up to four times inside DI water (without changing the pH value of the surrounding water). This is due to the adhesive failure that leaves the surface of the polybase brush clean after the detaching process. Atomic force microscopy (AFM) has confirmed that polymer brushes remain on the surface after being detached from the DN hydrogel for the first time inside DI water, because they are covalently bound onto the surface.

Since the adhesion at the gel-brush interface is much stronger underwater at pH $\sim$ 6 than it is at pH $\sim$ 1 and 12, the switchability of the already adhered gel-brush interface has been examined and reused a number of times. The adhesion at the hydrogel-brush interface, therefore, is weakened by reducing the pH value of water to pH 1, and then the adhesion is repeated by re-sticking the hydrogel and brush together inside DI water at pH $\sim$ 6. The results obtained during the pH 1–pH 6 cycles have shown that the adhesion of SN and DN hydrogels with the PDEAEMA brush can be switched *on* at pH 6 and then *off* at pH 1 on seven occasions. The confirmation of the switchability and repeatability of adhesion for both SN and DN hydrogels is demonstrated in the final adhesion cycle (i.e. after seven cycles of the attaching and detaching processes) which showed that both hydrogels are still capable of adhering efficiently and strongly to the brush surface inside DI water at pH 6. The cohesive failures of the SN hydrogel, which occurred during all seven test cycles, however, served to increase its adhesive contact diameter, leading to a slight increase in its adhesion compared to its initial adhesion value inside water at pH 6.

The switchable adhesion at the hydrogel-brush interface has also included an examination of the effect of increasing salt concentrations inside the surrounding water (at a fixed pH value of DI water) on their interfacial adhesion. Sodium chloride was used at concentrations ranging

from a very low molarity of 0.001 M to a very high molarity of 5 M. This is due to the fact that salt ions screen the electrostatic charges of the weakly charged polyelectrolytes causing them to become neutral. The adhesion results showed that the adhesion at the gel-brush interface is unexpectedly increased almost two-fold after adding a very dilute NaCl solution (of 0.001 M) into the surrounding water. This is because the addition of a small amount of the salt increases the osmotic pressure, making the polymer chains more stretched. The work done measurements at the gel-brush interface, however, have confirmed that the adhesion decreases after adding a very dilute NaCl solution into the surrounding water.

Eventually, the adhesion of both SN and DN hydrogels with the polybase brush became noticeably weaker after the concentration of the added NaCl solution increased above 0.5 M, and it became significantly weaker after raising the concentration of NaCl solutions to 3 M and 5 M. Even though the adhesion was reduced inside the most highly concentrated NaCl solutions, cohesive failure was still observed with the SN hydrogel while adhesive failure was obtained with the DN hydrogel. From the experiments in salt-sensitive adhesion, it can be concluded that the adhesion at the gel-brush interface becomes weaker inside salt solutions above 0.5 M. Using highly concentrated salt solutions has been criticised, however, on the basis that inorganic salts can form on these polymers that may affect the repeatability of the adhesion.

8.2 Future Work

This study of the adhesion between two oppositely charged polyelectrolytes has demonstrated switchable adhesion successfully underwater as a function of changing the pH value of the surrounding water and also by adding salt solutions into it. The adhesion process of attaching the hydrogel onto the surface of the polymer brush must be carried out in a wet environment (underwater) in order to stimulate the electrostatic charges on both polymers. There are still many unanswered questions about what would happen to the already adhered gel-brush interface if it was taken outside the surrounding water, as well as how long the adhesion will last. The SN hydrogel is more likely to become fragile when it is left outside water and allowed to dry, but the DN hydrogel is more likely to maintain its mechanical strength since this robust DN hydrogel has a lower swelling ratio inside water compared to the soft SN

hydrogel. It would be interesting, therefore, to assess the effects of dryness on the gel-brush interfacial adhesion. There are important implications for developing recycling techniques and as a disassembly processes in the packaging and automotive industries if the viability of the wet-dry adhesive cycles is confirmed.

In addition, the process of reducing the adhesion and eliminating adhesive interactions at the gel-brush interface has been conducted at a strong acidic pH value at pH $\sim$ 1, since this makes the DN hydrogel uncharged and hydrophobically shrunk. An opposite pH control of using a strong basic pH solution (at pH $\sim$ 12) can be achieved if the PMAA network in the DN hydrogel is substituted with a polybase network, such as the PDEAEMA gel, taking into consideration that the used polybase brush of the PDEAEMA must also be substituted with the polyacid, PMAA, brush. The study conducted here, could therefore be repeated using the cationic-based DN hydrogel with the polyacid brush in order to test their switchable adhesion at a strong basic pH solution.

Other stimuli are worth exploring, however, to achieve switchable and repeatable adhesion in circumstances where strong acid/base or salt solutions would be inappropriate. These include varying the temperature of the surrounding water at the gel-brush interface. To that end, a thermosensitive polymer would be required for either the hydrogel or polymer brush in order to switch its electrostatic charges *on* or *off* and to achieve a temperature-sensitive adhesion.

Bibliography

[1] S. J. Marshall, S. C. Bayne, R. Baier, A. P. Tomsia, and G. W. Marshall, "A review of adhesion science.," *Dental materials*, vol. 26, pp. e11–6, Feb. 2010.

[2] C. Onions, *The Oxford Dictionary on Enghish Etimology.* Clarendon Press, Oxford, 1966.

[3] A. J. Kinloch, *Adhesion and adhesives: science and technology.* Springer Science & Business Media, London, 2012.

[4] A. Lucas and J. Harris, *Ancient Egyptian materials and industries.* Courier Corporation, New York, 2012.

[5] R. D. Adams, *Adhesive Bonding: Science, Technology and Applications.* Elsevier, 2005.

[6] J. Comyn, *Adhesion science.* Royal Society of Chemistry, 1997.

[7] F. Awaja, M. Gilbert, G. Kelly, B. Fox, and P. J. Pigram, "Adhesion of polymers.," *Progress in Polymer Science*, vol. 34, no. 9, pp. 948–968, 2009.

[8] A. J. Kinloch, "The science of adhesion - Part 1 Surface and interfacial aspects.," *Journal of Materials Science*, vol. 15, no. 9, pp. 2141–2166, 1980.

[9] C. Creton and S. Gorb, "Sticky feet: from animals to materials.," *Mrs Bulletin*, vol. 32, no. 06, pp. 466–472, 2007.

[10] R. La Spina, M. Tomlinson, A. Chiche, and M. Geoghegan, "Development of a new underwater adhesive.," *Eur. Coat. J*, pp. 22–28, 2011.

[11] A. Schmid, L. R. Sutton, S. P. Armes, P. S. Bain, and G. Manfrè, "Synthesis and evaluation of polypyrrole-coated thermally-expandable microspheres: an improved approach to reversible adhesion.," *Soft Matter*, vol. 5, no. 2, p. 407, 2009.

[12] P. Flammang and R. Santos, "Biological adhesives: from biology to biomimetics.," *Interface Focus*, vol. 5, 2015.

[13] P. S. Shuttleworth, J. H. Clark, R. Mantle, and N. Stansfield, "Switchable adhesives for carpet tiles: a major breakthrough in sustainable flooring.," *Green Chemistry*, vol. 12, no. 5, pp. 798–803, 2010.

[14] S. k. Ahn, R. M. Kasi, S. C. Kim, N. Sharma, and Y. Zhou, "Stimuli-responsive polymer gels.," *Soft Matter*, vol. 4, no. 6, pp. 1151–1157, 2008.

[15] E. Wischerhoff, N. Badi, A. Laschewsky, and J. F. Lutz, "Smart Polymer Surfaces: Concepts and Applications in Biosciences.," in *Bioactive Surfaces*, vol. 240, pp. 1–33, Springer Berlin Heidelberg, 2010.

[16] C. de Las Heras Alarcón, S. Pennadam, and C. Alexander, "Stimuli responsive polymers for biomedical applications.," *Chemical Society reviews*, vol. 34, no. 3, pp. 276–285, 2005.

[17] P. M. Claesson, A. Dedinaite, and O. J. Rojas, "Polyelectrolytes as adhesion modifiers.," *Advances in Colloid and Interface Science*, vol. 104, pp. 53–74, July 2003.

[18] H. Gao, X. Wang, H. Yao, S. Gorb, and E. Arzt, "Mechanics of hierarchical adhesion structures of geckos.," *Mechanics of Materials*, vol. 37, no. 2, pp. 275–285, 2005.

[19] L. F. Boesel, C. Greiner, E. Arzt, and A. del Campo, "Gecko-inspired surfaces: a path to strong and reversible dry adhesives.," *Advanced materials*, vol. 22, no. 19, pp. 2125–2137, 2010.

[20] S. Reddy, E. Arzt, and A. del Campo, "Bioinspired Surfaces with Switchable Adhesion.," *Advanced Materials*, vol. 19, pp. 3833–3837, Nov. 2007.

[21] A. J. Crosby, M. Hageman, and A. Duncan, "Controlling polymer adhesion with "pancakes".," *Langmuir*, vol. 21, no. 25, pp. 11738–11743, 2005.

[22] M. Lamblet, E. Verneuil, T. Vilmin, A. Buguin, P. Silberzan, and L. Léger, "Adhesion enhancement through micropatterning at polydimethylsiloxane-acrylic adhesive interfaces.," *Langmuir*, vol. 23, no. 13, pp. 6966–74, 2007.

[23] J. A. Jofre-reche, J. Pulpytel, F. Arefi-khonsari, and J. M. Martín-Martínez, "Adhesion Improvement of Polydimethylsiloxane (PDMS) By Surface Treatment With Two Different Atmospheric Plasma.," *Adhesion Society*.

[24] H. Lee, B. P. Lee, and P. B. Messersmith, "A reversible wet/dry adhesive inspired by mussels and geckos.," *Nature*, vol. 448, no. 7151, pp. 338–341, 2007.

[25] H. Lee, N. F. Scherer, and P. B. Messersmith, "Single-molecule mechanics of mussel adhesion.," *Proceedings of the National Academy of Sciences of the United States of America*, vol. 103, no. 35, pp. 12999–13003, 2006.

[26] S. Förster and M. Schmidt, *Polyelectrolytes in solution*. Springer Berlin Heidelberg, 1995.

[27] A. Dobrynin and M. Rubinstein, "Theory of polyelectrolytes in solutions and at surfaces.," *Progress in Polymer Science*, vol. 30, no. 11, pp. 1049–1118, 2005.

[28] E. Cabane, X. Zhang, K. Langowska, C. G. Palivan, and W. Meier, "Stimuli-responsive polymers and their applications in nanomedicine.," *Biointerphases*, vol. 7, no. 1, 2012.

[29] G. Sudre, L. Olanier, Y. Tran, D. Hourdet, and C. Creton, "Reversible adhesion between a hydrogel and a polymer brush.," *Soft Matter*, vol. 8, no. 31, pp. 8184–8193, 2012.

[30] M. A. C. Stuart, W. T. S. Huck, J. Genzer, M. Müller, C. Ober, M. Stamm, G. B. Sukhorukov, I. Szleifer, V. V. Tsukruk, M. Urban, F. Winnik, S. Zauscher, I. Luzinov, and S. Minko, "Emerging applications of stimuli-responsive polymer materials.," *Nature materials*, vol. 9, no. 2, pp. 101–113, 2010.

[31] B. Zhao and W. Brittain, "Polymer brushes: surface-immobilized macromolecules.," *Progress in Polymer Science*, vol. 25, no. 5, pp. 677–710, 2000.

[32] P. Schexnailder and G. Schmidt, "Nanocomposite polymer hydrogels.," *Colloid and Polymer Science*, vol. 287, no. 1, pp. 1–11, 2009.

[33] J. Kopeček and J. Yang, "Hydrogels as smart biomaterials.," *Polymer international*, vol. 56, no. 9, pp. 1078–1098, 2007.

[34] R. La Spina, M. R. Tomlinson, L. Ruiz-Pérez, A. Chiche, S. Langridge, and M. Geoghegan, "Controlling network-brush interactions to achieve switchable adhesion.," *Angewandte Chemie International Edition*, vol. 46, no. 34, pp. 6460–6463, 2007.

[35] K. Johnson, R. Kendall, and A. Roberts, "Surface energy and the contact of elastic solids.," *Proceedings of the Royal Society of London. A. Mathematical and Physical Science*, vol. 324, no. 1558, pp. 301–313, 1971.

[36] G. S. Longo, M. Olvera de la Cruz, and I. Szleifer, "Molecular Theory of Weak Polyelectrolyte Gels: The Role of pH and Salt Concentration.," *Macromolecules*, vol. 44, no. 1, pp. 147–158, 2010.

[37] S. Uyaver and C. Seidel, "Effect of Varying Salt Concentration on the Behavior of Weak Polyelectrolytes in a Poor Solvent.," *Macromolecules*, vol. 42, no. 4, pp. 1352–1361, 2009.

[38] M. Kobayashi, M. Terada, and A. Takahara, "Reversible adhesive-free nanoscale adhesion utilizing oppositely charged polyelectrolyte brushes.," *Soft Matter*, vol. 7, no. 12, pp. 5717–5722, 2011.

[39] M. Kobayashi and A. Takahara, "Environmentally friendly repeatable adhesion using a sulfobetaine-type polyzwitterion brush.," *Polymer Chemistry*, vol. 4, no. 18, pp. 4987–4992, 2013.

[40] K.L. Mittal and A. Pizzi, *Adhesion Promotion Techniques: Technological Applications.* CRC Press, 1999.

[41] W. Wake, "Theories of adhesion and uses of adhesives: a review.," *Polymer*, vol. 19, no. 3, pp. 291–308, 1978.

[42] H. Hertz, "On the contact of elastic solids.," *J. reine angew. Math*, vol. 92, no. 110, pp. 156–171, 1881.

[43] K. Johnson, "Mechanics of adhesion.," *Tribology International*, vol. 31, no. 8, pp. 413–418, 1998.

[44] L. H. Lee, *Fundamentals of adhesion.* Springer Science & Business Media, 2013.

[45] R. A. L. Jones and R. W. Richards, *Polymers at Surfaces and Interfaces.* Cambridge University Press, 1999.

[46] K. R. Shull, "Contact mechanics and the adhesion of soft solids.," *Materials Science and Engineering: R: Reports*, vol. 36, no. 1, pp. 1–45, 2002.

[47] S. Xinghua and Z. Ya-Pu, "Comparison of various adhesion contact theories and the influence of dimensionless load parameter.," *Journal of Adhesion Science and Technology*, vol. 18, no. 1, pp. 55–68, 2004.

[48] D. Rimai, L. Demejo, and R. Bowen, "Mechanics of particle adhesion.," *Journal of Adhesion Science and Technology*, vol. 8, no. 11, pp. 1333–1355, 1994.

[49] V. Vaenkatesan, Z. Li, W. P. Vellinga, and W. H. de Jeu, "Adhesion and friction behaviours of polydimethylsiloxane- A fresh perspective on JKR measurements.," *Polymer*, vol. 47, pp. 8317–8325, nov 2006.

[50] S. T. Choi, "Extended JKR theory on adhesive contact of a spherical tip onto a film on a substrate.," *Journal of Materials Research*, vol. 27, no. 01, pp. 113–120, 2012.

[51] R. Horn, J. Israelachvili, and F. Pribac, "Measurement of the deformation and adhesion of solids in contact.," *Journal of Colloid and Interface Science*, vol. 115, pp. 480–492, Feb. 1987.

[52] P. Attard and J. Parker, "Deformation and adhesion of elastic bodies in contact.," *Physical review.*, vol. 46, no. 12, pp. 7959–7971, 1992.

[53] V. M. M. Derjaguin, Boris V. and Y. P. Toporov., "Effect of contact deformations on the adhesion of particles.," *Journal of Colloid and Interface Science*, vol. 53, no. 2, pp. 314–326, 1975.

[54] H. Zeng, *Polymer Adhesion, Friction, and Lubrication.* John Wiley & Sons, 2013.

[55] D. Tabor, "Surface forces and surface interactions.," *Journal of Colloid and Interface Science*, vol. 58, no. 1, pp. 2–13, 1977.

[56] F. Oosawa, *Polyelectrolytes.* Marcel-Dekker: New York, 1971.

[57] D. Roy, J. N. Cambre, and B. S. Sumerlin, "Future perspectives and recent advances in stimuli-responsive materials.," *Progress in Polymer Science*, vol. 35, no. 1, pp. 278–301, 2010.

[58] A. J. Ryan, C. J. Crook, J. R. Howse, P. Topham, R. A. L. Jones, M. Geoghegan, A. Parnell, L. Ruiz-Pérez, S. Martin, A. Cadby, A. Menelle, J. R. Webster, A. J. Gleeson, and W. Bras, "Responsive brushes and gels as components of soft nanotechnology.," *Faraday discussions*, vol. 128, pp. 55–74, 2005.

[59] Gert R. Strobl, *The Physics of Polymers.* Berlin: Springe, third edit ed., 1997.

[60] R. A. Jones, *Soft Condensed Matter.* Oxford University Press, 2002.

[61] M. Rubinstein and R. H. Colby, *polymer physics.* Oxford, UK: Oxford, 2003.

[62] P. M. Visakh, *Polyelectrolyte: Thermodynamics and Rheology.* Springer International Publishing, 2014.

[63] Y. Qiu and K. Park, "Environment-sensitive hydrogels for drug delivery.," *Advanced Drug Delivery Reviews*, vol. 64, pp. 49–60, 2012.

[64] I. Y. Galaev and B. Mattiasson, "Smart polymers and what they could do in biotechnology and medicine.," *Trends in Biotechnology*, vol. 17, no. 8, pp. 335–340, 1999.

[65] W. Brown, C. Foote, B. Iverson, and E. Anslyn, *Organic Chemistry.* Cengage Learning, 2012.

[66] W. Masterton, C. Hurley, and E. Neth, *Chemistry: Principles and Reactions.* Cengage Learning, the seventh ed., 2012.

[67] M. Clugston and R. Flemming, *Advanced Chemistry.* Oxford University Press, 2000.

[68] R. Myers, *The Basics of Chemistry*. Greenwood Publishing Group, 2003.

[69] J. Kenkel, *Analytical Chemistry for Technicians*. CRC Press, the third ed., 2010.

[70] M. Kumar Vyas, K. Schneider, B. Nandan, and M. Stamm, "Switching of friction by binary polymer brushes.," *Soft Matter*, vol. 4, no. 5, pp. 1024–1032, 2008.

[71] F. Liu and M. W. Urban, "Recent advances and challenges in designing stimuli-responsive polymers.," *Progress in Polymer Science*, vol. 35, no. 1, pp. 3–23, 2010.

[72] M. Van der Waarden, "Stabilization of carbon-black dispersions in hydrocarbons.," *Journal of Colloid Science*, vol. 5, no. 4, pp. 317–325, 1950.

[73] W. J. Brittain and S. Minko, "A structural definition of polymer brushes.," *Journal of Polymer Science, Part A: Polymer Chemistry*, vol. 45, no. 16, pp. 3505–3512, 2007.

[74] O. Azzaroni, "Polymer brushes here, there, and everywhere: Recent advances in their practical applications and emerging opportunities in multiple research fields.," *Journal of Polymer Science, Part A: Polymer Chemistry*, vol. 50, no. 16, pp. 3225–3258, 2012.

[75] R. Advincula, W. Brittain, K. Caster, and R. Jürgen, *Polymer brushes*. Weinheim: Wiley-vch, 2004.

[76] M. P. Weir and A. J. Parnell, "Water Soluble Responsive Polymer Brushes.," *Polymers*, vol. 3, no. 4, pp. 2107–2132, 2011.

[77] J. Rühe, M. Ballauff, M. Biesalski, P. Dziezok, F. Gröhn, D. Johannsmann, N. Houbenov, N. Hugenberg, R. Konradi, S. Minko, M. Michail, R. Netz, M. Schmidt, C. Seidel, M. Stamm, T. Stephan, D. Usov, and H. Zhang, "Polyelectrolyte brushes.," in *Polyelectrolytes with defined molecular architecture*, pp. 79–150, Springer Berlin Heidelberg, 2004.

[78] P. Pincus, "Colloid stabilization with grafted polyelectrolytes.," *Macromolecules*, vol. 24, no. 10, pp. 2912–2919, 1991.

[79] R. S. Ross and P. Pincus, "The Polyelectrolyte Brush: Poor Solvent.," *Macromolecules*, vol. 25, no. 8, pp. 2177–2183, 1992.

[80] E. B. Zhulina, T. M. Birshtein, and O. V. Borisov, "Theory of Ionizable Polymer Brushes.," *Macromolecules*, vol. 28, no. 5, pp. 1491–1499, 1995.

[81] R. Israels, F. A. M. Leermakers, and G. J. Fleer, "On the Theory of Grafted Weak Polyacids.," *Macromolecules*, vol. 27, no. 11, pp. 3087–3093, 1994.

[82] S. Milner, T. Witten, and M. Cates, "Theory of the grafted polymer brush.," *Macromolecules*, vol. 21, no. 8, pp. 2610–2619, 1988.

[83] A. C. Balazs, C. Singh, and E. Zhulina, "Modeling the Interactions between Polymers and Clay Surfaces through Self-Consistent Field Theory.," *Macromolecules*, vol. 31, no. 23, pp. 8370–8381, 1998.

[84] W. J. Brittain and S. Minko, "A structural definition of polymer brushes.," *Journal of Polymer Science Part A: Polymer Chemistry*, vol. 45, no. 16, pp. 3505–3512, 2007.

[85] S. Edmondson, V. L. Osborne, and W. T. S. Huck, "Polymer brushes via surface-initiated polymerizations.," *Chemical Society reviews*, vol. 33, pp. 14–22, Jan. 2004.

[86] M. Szwarc, "'Living' Polymers.," *Nature*, vol. 178, no. 4543, pp. 1168–1169, 1956.

[87] M. Szwarc, "Living Polymers and Mechanisms of Anionic Polymerization.," *Springer Berlin Heidelberg*, pp. 1–177, 1983.

[88] M. Szwarc, "Living polymers. Their discovery, characterization, and properties.," *Journal of Polymer Science Part A: Polymer Chemistry*, vol. 36, no. 1, pp. IX–XV, 1998.

[89] J. Chiefari, Y. K. Chong, F. Ercole, J. Krstina, J. Jeffery, T. P. Le, R. Mayadunne, G. F. Meijs, C. L. Moad, G. Moad, E. Rizzardo, and S. Thang, "Living Free-Radical Polymerization by Reversible Addition-Fragmentation Chain Transfer: The RAFT Process.," *Macromolecules*, vol. 31, no. 16, pp. 5559–5562, 1998.

[90] J. S. Wang and K. Matyjaszewski, "Controlled/"living" radical polymerization. Atom transfer radical polymerization in the presence of transition-metal complexes.," *Journal of the American Chemical Society*, vol. 117, no. 20, pp. 5614–5615, 1995.

[91] M. Kato, M. Kamigaito, M. Sawamoto, and T. Higashimuras, "Polymerization of Methyl Methacrylate with the Carbon TetrachloridelDichlorotris- (triphenylphosphine)ruthedum(II)/ Methylaluminum Bis(2,6-di-tert-butylphenoxide) Initiating System: Possibility of Living Radical Polymerization.," *Macromolecules*, vol. 28, no. 5, pp. 1721–1723, 1995.

[92] K. Matyjaszewski and J. Xia, "Atom transfer radical polymerization.," *Chemical reviews*, vol. 101, no. 9, pp. 2921–2990, 2001.

[93] P. Vana, *Controlled Radical Polymerization at and from Solid Surfaces*. Springer, 2015.

[94] K. Matyjaszewski, P. J. Miller, N. Shukla, B. Immaraporn, A. Gelman, B. B. Luokala, T. M. Siclovan, G. Kickelbick, T. Vallant, H. Hoffmann, and T. Pakula, "Polymers at Interfaces: Using Atom Transfer Radical Polymerization in the Controlled Growth of Homopolymers and Block Copolymers from Silicon Surfaces in the Absence of Untethered Sacrificial Initiator.," *Macromolecules*, vol. 32, no. 26, pp. 8716–8724, 1999.

[95] K. Matyjaszewski, D. Hongchen, W. Jakubowski, J. Pietrasik, and A. Kusumo, "Grafting from surfaces for "everyone": ARGET ATRP in the presence of air.," *Langmuir*, vol. 23, no. 8, pp. 4528–4531, 2007.

[96] R. Barbucci, *Hydrogels: Biological Properties and Applications*. Biological Properties and Applications. Springer, 2009.

[97] A. S. Hoffman, "Hydrogels for biomedical applications.," *Advanced drug delivery reviews*, vol. 64, pp. 18–23, 2012.

[98] T. Miyata, N. Asami, and T. Uragami, "A reversibly antigen-responsive hydrogel.," *Nature*, vol. 399, no. 6738, pp. 766–769, 1999.

[99] P. Gupta, K. Vermani, and S. Garg, "Hydrogels: from controlled release to pH-responsive drug delivery.," *Drug discovery today*, vol. 7, no. 10, pp. 569–579, 2002.

[100] J. M. Rosiak and F. Yoshii, "Hydrogels and their medical applications.," *Nuclear Instruments and Methods in Physics Research, Section B: Beam Interactions with Materials and Atoms*, vol. 151, no. 1, pp. 56–64, 1999.

[101] S. K. H. Gulrez, S. Al-Assaf, and G. O. Phillips, "Hydrogels: Methods of Preparation, Characterisation and Applications.," *INTECH Open Access Publisher*, 2011.

[102] L. L. Hench and J. K. West, "The sol-gel process.," *Chemical Reviews*, vol. 90, no. 1, pp. 33–72, 1990.

[103] C. Jeffrey, Brinker and G. W. Scherer, *Sol-gel science: the physics and chemistry of sol-gel processing*. Academic press, 2013.

[104] O. E. Philippova, "Responsive Polymer Gels 1.," *Polymer Science*, vol. 42, no. 2, pp. 208–228, 2000.

[105] D. J. Beebe, J. S. Moore, J. M. Bauer, Q. Yu, R. H. Liu, C. Devadoss, and B.-H. Jo, "Functional hydrogel structures for autonomous flow control inside microfluidic channels.," *Nature*, vol. 404, no. 6778, pp. 588–590, 2000.

[106] Y. J. Lee and P. Braun, "Tunable Inverse Opal Hydrogel pH Sensors.," *Advanced Materials*, vol. 15, no. 7-8, pp. 563–566, 2003.

[107] M. Hamidi, A. Azadi, and P. Rafiei, "Hydrogel nanoparticles in drug delivery.," *Advanced Drug Delivery Reviews*, vol. 60, no. 15, pp. 1638–1649, 2008.

[108] F. Ganji, S. Vasheghani-Farahani, and E. Vasheghani-Farahani, "Theoretical Description of Hydrogel Swelling: A Review.," *Iranian Polymer Journal*, vol. 19, no. 5, pp. 375–398, 2010.

[109] P. J. Flory and J. Rehner, "Effect of Deformation on the Swelling Capacity of Rubber.," *The Journal of Chemical Physics*, vol. 12, no. 10, pp. 412–414, 1944.

[110] P. J. Flory, "Statistical Thermodynamics of Semi-Flexible Chain Molecules.," *Proceedings of the Royal Society A: Mathematical, Physical and Engineering Sciences*, vol. 234, no. 1196, pp. 60–73, 1956.

[111] P. J. Flory, "Thermodynamics of High Polymer Solutions.," *The Journal of Chemical Physics*, vol. 10, no. 1, pp. 51–61, 1942.

[112] M. Ebara, Y. Kotsuchibashi, R. Narain, N. Idota, Y. J. Kim, J. M. Hoffman, K. Uto, and T. Aoyagi, *Smart Biomaterials*. Japan: Springer, 2014.

[113] P. J. Flory and J. Rehner, "Statistical mechanics of cross-linked polymer networks II. Swelling.," *The Journal of Adhesion*, vol. 11, no. 11, pp. 521–526, 1943.

[114] J. M. G. Cowie and V. Arrighi, *Polymers: chemistry and physics of modern materials*. Scotland, UK: CRC press, third edit ed., 2007.

[115] G. Moad and D. H. Solomon, *The Chemistry of Radical Polymerization*. Elsevier, 2005.

[116] M. Korolyov, Gennady V. Mogilevich, *Three-dimensional free-radical polymerization: cross-linked and hyper-branched polymers*. Springer Science & Business Media, 2008.

[117] J. F. E. Mano, *Biomimetic Approaches for Biomaterials Development*. John Wiley & Sons,, 2013.

[118] N. A. Peppas, J. Z. Hilt, A. Khademhosseini, and R. Langer, "Hydrogels in biology and medicine: From molecular principles to bionanotechnology.," *Advanced Materials*, vol. 18, no. 11, pp. 1345–1360, 2006.

[119] B. V. Slaughter, S. S. Khurshid, O. Z. Fisher, A. Khademhosseini, and N. A. Peppas, "Hydrogels in Regenerative Medicine.," *Advanced Materials*, vol. 21, no. 32-33, pp. 3307–3329, 2009.

[120] J. Elisseeff, "Hydrogels: structure starts to gel.," *Nature materials*, vol. 7, no. 4, pp. 271–273, 2008.

[121] B. D. Ratner, A. S. Hoffman, F. J. Schoen, and J. E. Lemons, *Biomaterials Science: An Introduction to Materials in Medicine.* Academic press, 2004.

[122] Y. L. Kuen and D. J. Mooney, "Hydrogels for Tissue Engineering.," *Chemical reviews*, vol. 101, no. 7, pp. 1869–1880, 2001.

[123] N. Peppas, P. Bures, W. Leobandung, and H. Ichikawa, "Hydrogels in pharmaceutical formulations.," *European Journal of Pharmaceutics and Biopharmaceutics*, vol. 50, no. 1, pp. 27–46, 2000.

[124] S. Dumitriu, *Polymeric Biomaterials, Revised and Expanded.* Quebec, Canada: CRC Press, second ed., 2001.

[125] Y. Tanaka, J. P. Gong, and Y. Osada, "Novel hydrogels with excellent mechanical performance.," *Progress in Polymer Science*, vol. 30, no. 1, pp. 1–9, 2005.

[126] A. Patel and K. Mequanint, *Hydrogel Biomaterials.* 2011.

[127] A. S. Hoffman, ""intelligent" polymers in medicine and biotechnology.," *Macromolecular Symposia*, vol. 98, no. 1, 1995.

[128] K. S. Soppimath, T. M. Aminabhavi, A. M. Dave, S. G. Kumbar, and W. E. Rudzinski, "Stimulus-Responsive "Smart" Hydrogels as Novel Drug Delivery Systems.," *Drug Development and Industrial Pharmacy*, vol. 28, no. 8, pp. 957–974, 2002.

[129] D. J. Waters, K. Engberg, R. Parke-Houben, C. N. Ta, A. J. Jackson, M. F. Toney, and C. W. Frank, "Structure and Mechanism of Strength Enhancement in Interpenetrating Polymer Network Hydrogels.," *Macromolecules*, vol. 44, no. 14, pp. 5776–5787, 2011.

[130] G. J. Calton, "Biotechnology and medicine.," *Cutis*, vol. 33, no. 4, pp. 375–378, 1984.

[131] J. Gong, Y. Katsuyama, T. Kurokawa, and Y. Osada, "Double-Network Hydrogels with Extremely High Mechanical Strength.," *Advanced Materials*, vol. 15, no. 14, pp. 1155–1158, 2003.

[132] J. A. Stammen, S. Williams, D. N. Ku, and R. E. Guldberg, "Mechanical properties of a novel PVA hydrogel in shear and unconfined compression.," *Biomaterials*, vol. 22, no. 8, pp. 799–806, 2001.

[133] M. Cloitre, *High Solid Dispersions.* Paris, France: Springer, 2010.

[134] K. Y. Lee, J. A. Rowley, P. Eiselt, E. M. Moy, K. H. Bouhadir, and D. J. Mooney, "Controlling mechanical and swelling properties of alginate hydrogels independently by cross-linker type and cross-linking density.," *Macromolecules*, vol. 33, no. 11, pp. 4291–4294, 2000.

[135] Y. Okumura and K. Ito, "The polyrotaxane gel: A topological gel by figure-of-eight cross-links.," *Advanced Materials*, vol. 13, no. 7, pp. 485–487, 2001.

[136] K. Haraguchi and T. Takehisa, "Nanocomposite Hydrogels: A Unique Organic-Inorganic Network Structure with Extraordinary Mechancal, Optical, and Swelling/De-swelling Properties.," *Advanced Materials*, vol. 14, no. 16, pp. 1120–1124, 2002.

[137] T. Nakajima, H. Sato, Y. Zhao, S. Kawahara, T. Kurokawa, K. Sugahara, and J. P. Gong, "A Universal Molecular Stent Method to Toughen any Hydrogels Based on Double Network Concept.," *Advanced Functional Materials*, vol. 22, no. 21, pp. 4426–4432, 2012.

[138] D. Myung, D. J. Waters, and M. E. A. Wiseman, "Progress in the development of interpenetrating network hydrogels.," *Polymer Advanced Technology*, vol. 19, no. 6, pp. 647–657, 2008.

[139] J. P. Gong, "Why are double network hydrogels so tough?.," *Soft Matter*, vol. 6, no. 12, p. 2583, 2010.

[140] S. Naficy, J. M. Razal, P. G. Whitten, G. G. Wallace, and G. M. Spinks, "A pH-sensitive, strong double-network hydrogel: Poly(ethylene glycol) methyl ether methacrylates-poly(acrylic acid).," *Journal of Polymer Science Part B: Polymer Physics*, vol. 50, no. 6, pp. 423–430, 2012.

[141] Y. Osada and A. Khokhlov, *Polymer Gels and Networks*. CRC Press, 2001.

[142] C. J. Crook, A. Smith, R. A. L. Jones, and A. J. Ryan, "Chemically induced oscillations in a pH-responsive hydrogel.," *Physical Chemistry.*, vol. 4, no. 8, pp. 1367–1369, 2002.

[143] K. Kato, E. Uchida, E. T. Kang, Y. Uyama, and Y. Ikada, "Polymer surface with graft chains.," *Progress in Polymer Science*, vol. 28, no. 2, pp. 209–259, 2003.

[144] T. Radeva, *Physical chemistry of polyelectrolytes*. Sofia, Bolgaria: CRC Press, 2001.

[145] W. Kern, "The Evolution of Silicon Wafer Cleaning Technology.," *Journal of The Electrochemical Society*, vol. 137, no. 6, pp. 1887–1892, 1990.

[146] P. D. Topham, J. R. Howse, C. J. Crook, A. J. Parnell, M. Geoghegan, R. A. Jones, and A. J. Ryan, "Controlled growth of poly (2-(diethylamino)ethyl methacrylate) brushes via atom transfer radical polymerisation on planar silicon surfaces.," *Polymer International*, vol. 7, no. 55, pp. 808–815, 2006.

[147] S. Alang Ahmad, A. Hucknall, A. Chilkoti, and G. J. Leggett, "Protein patterning by UV-induced photodegradation of poly(oligo(ethylene glycol) methacrylate) brushes.," *Langmuir*, vol. 26, no. 12, pp. 9937–9942, 2010.

[148] L. A. Fielding, S. Edmondson, and S. P. Armes, "Synthesis of pH-responsive tertiary amine methacrylate polymer brushes and their response to acidic vapour.," *Journal of Materials Chemistry*, vol. 21, no. 32, pp. 11773–11780, 2011.

[149] H. Fujiwara, *Spectroscopic ellipsometry: principles and applications*. Ibaraki, Japan: John Wiley & Sons, 2007.

[150] R. L. Spina, *"Switchable adhesion between oppositely charged polyelectrolytes"*. PhD thesis, Universty of Sheffield, Sheffield, 2010.

[151] M. Raftari, Z. J. Zhang, S. R. Carter, G. J. Leggett, and M. Geoghegan, "Nanoscale Contact Mechanics between Two Grafted Polyelectrolyte Surfaces.," *Macromolecules*, vol. 48, no. 17, pp. 6272–6279, 2015.

[152] A. J. Parnell, S. J. Martin, C. C. Dang, M. Geoghegan, R. A. Jones, C. J. Crook, J. R. Howse, and A. J. Ryan, "Synthesis, characterization and swelling behaviour of poly(methacrylic acid) brushes synthesized using atom transfer radical polymerization.," *Polymer.*, vol. 50, no. 4, pp. 1005–1014, 2009.

[153] S. A. Ahmad, G. J. Leggett, A. Hucknall, and A. Chilkoti, "Micro- and nanostructured poly[oligo(ethylene glycol)methacrylate] brushes grown from photopatterned halogen initiators by atom transfer radical polymerization.," *Biointerphases*, vol. 6, no. 1, pp. 8–15, 2011.

[154] J. Zhang and N. A. Peppas, "Synthesis and Characterization of pH- and Temperature-Sensitive Poly(methacrylic acid)/Poly(*N*-isopropylacrylamide) Interpenetrating Polymeric Networks.," *Macromolecules*, vol. 33, no. 1, pp. 102–107, 1999.

[155] A. Emileh, E. Vasheghani-Farahani, and M. Imani, "Swelling behavior, mechanical properties and network parameters of pH- and temperature-sensitive hydrogels of poly((2-dimethyl amino) ethyl methacrylate-co-butyl methacrylate).," *European Polymer Journal*, vol. 43, no. 5, pp. 1986–1995, 2007.

[156] W. Li, H. Kong, C. Gao, and D. Yan, "pH-responsive poly(2-diethylaminoethyl methacrylate)-functionalized multiwalled carbon nanotubes.," *Chinese Science Bulletin*, vol. 50, no. 20, pp. 2276–2280, 2005.

[157] O. Okay, "General Properties of Hydrogels.," in *Hydrogel Sensors and Actuators*, pp. 1–15, Springer Berlin Heidelberg, 2009.

[158] M. Tokita and K. Nishinari, "Gels: Structures, Properties, and Functions.," in *Progress in Colloid and Polymer Science*, Springer, 2004.

[159] K. Mittal, "Adhesion measurement of thin films.," *Active and Passive Electronic Components*, vol. 3, no. 1, pp. 21–42, 1976.

[160] J. Hurler, A. Engesland, B. Poorahmary Kermany, and N. Skalko-Basnet, "Improved Texture Analysis for Hydrogel Characterization: Gel Cohesiveness, Adhesiveness, and Hardness.," *Journal of Applied Polymer Science*, vol. 125, no. 1, pp. 180–188, 2012.

[161] J. Ostroha, M. Pong, A. Lowman, and N. Dan, "Controlling the collapse/swelling transition in charged hydrogels.," *Biomaterials*, vol. 25, no. 18, pp. 4345–4353, 2004.

[162] J. E. Elliott, M. MacDonald, J. Nie, and C. N. Bowman, "Structure and swelling of poly(acrylic acid) hydrogels: Effect of pH, ionic strength, and dilution on the crosslinked polymer structure.," *polymer.*, vol. 45, no. 5, pp. 1503–1510, 2004.

[163] N. Rikkert, P. Gong, and S. Igal, "Weak Polyelectrolytes Tethered to Surfaces: Effect of Geometry, Acid-Base Equilibrium and Electrical Permittivity.," *Journal of Polymer Science Part B: Polymer Physics*, vol. 44, no. 18, pp. 2638–2662., 2006.

[164] N. A. Peppas, K. B. Keys, M. Torres-Lugo, and A. M. Lowman, "Poly (ethylene glycol)-containing hydrogels in drug delivery.," *Journal of Controlled Release*, vol. 62, no. 1, pp. 81–87, 1999.

[165] L. Ruiz-Pérez, A. Pryke, M. Sommer, G. Battaglia, I. Soutar, L. Swanson, and M. Geoghegan, "Conformation of Poly(methacrylic acid) Chains in Dilute Aqueous Solution.," *Macromolecules*, vol. 41, no. 6, pp. 2203–2211, 2008.

[166] M. Kobayashi, Y. Terayama, M. Hino, K. Ishihara, and A. Takahara, "Characterization of swollen structure of high-density polyelectrolyte brushes in salt solution by neutron reflectivity.," *Journal of Physics: Conference Series*, vol. 184, no. 1, 2009.

[167] A. M. Al-Baradi, M. Mears, R. A. L. Jones, and M. Geoghegan, "Diffusion of dextran within poly(methacrylic acid) hydrogels.," *Journal of Polymer Science, Part B: Polymer Physics*, vol. 50, no. 18, pp. 1286–1292, 2012.

[168] S. Sanjuan, P. Perrin, N. Pantoustier, and Y. Tran, "Synthesis and swelling behavior of pH-responsive polybase brushes.," *Langmuir*, vol. 23, no. 10, pp. 5769–5778, 2007.